UNIVERSITA' DEGLI STUDI DI VERONA

DEPARTMENT OF

NEUROSCIENCES, BIOMEDICINE AND MOVEMENT SCIENCES

GRADUATE SCHOOL OF

LIFE AND HEALTH SCIENCES

DOCTORAL PROGRAM IN

NEUROSCIENCE, PSYCHOLOGICAL AND PSYCHIATRIC SCIENCES, AND MOVEMENT SCIENCES

XXXIII Cycle / Starting Academic Year 2017-2018

CLINICOGENETIC CORRELATIONS IN RARE COMPLEX MOVEMENT DISORDERS

Focus on combined and complex dystonia phenotypes

S.S.D. MED/26

Coordinator: Prof. Gianluigi Zanusso

Tutor: Prof. Michele Tinazzi

Doctoral Student: Dr. Francesca Magrinelli

CLINICOGENETIC CORRELATIONS IN RARE COMPLEX MOVEMENT DISORDERS
Focus on combined and complex dystonia phenotypes
Francesca Magrinelli
Doctoral Thesis
Verona, Italy, 30 June 2021

Abstract

Movement disorders is relatively unique among neurology subspecialties in its reliance on clinical judgement to accurately define disease phenotypes which are often complex. Progress in genetics – particularly the advent of next-generation sequencing (NGS) – has enabled an unparalleled gene discovery and revealed unmatched intricacy of genotype-phenotype correlations in the field of movement disorders and neurodegeneration. "Deep phenotyping", with detailed characterization and continual updating of movement disorder phenotypes, and the active involvement of movement disorder specialists in the multidisciplinary process to establish clinicogenetic correlations are the cornerstone of precision medicine and will have increasingly more crucial implications for the diagnosis, treatment and counseling of movement disorders in the advanced NGS era.

This thesis summarizes the 18-month clinical and research experience of the PhD candidate in a hub center for the diagnosis and treatment of movement disorders (National Hospital for Neurology and Neurosurgery) and its neurogenetic research laboratory (UCL Queen Square Institute of Neurology) in the United Kingdom. It investigates clinicogenetic correlations of rare complex movement disorders, with particular focus on combined and complex dystonia phenotypes, including neurodegeneration with brain iron accumulation (NBIA) syndromes.

General objectives of the projects herein reported were: 1) to characterize phenotypically a large cohort of patients with combined and complex dystonia syndromes; 2) to explore genetic causes of dystonia phenotypes through NGS techniques, including whole-exome (WES) and whole-genome sequencing (WGS); 3) to expand the phenotypic and genotypic spectrum of known genetic movement disorders; and 4) to investigate new possible candidate disease genes.

This thesis consists of six chapters. After a general introduction (chapter I) and summary of aims (chapter II), chapter III reports on the retrospective clinical review and analysis of WES data of a large cohort of patients with complex movement disorder phenotypes, in particular dystonia and NBIA syndromes. Chapter IV describes preliminary results of an ongoing study on WGS to explore the genetic basis of dystonia, including the first association of a dystonia phenotype with the peroxisomal gene *AMACR*. Chapter V dissects the phenotype and genotype of *PLA2G6*-related parkinsonism based on data from 14 unpublished cases and a systematic literature review. Chapters VI provides final remarks and future directions.

Table of contents

Chapter I
Introduction

1. Preamble

The present thesis summarizes the 18-month clinical and research experience of the PhD candidate in a hub center for the diagnosis and treatment of movement disorders (National Hospital for Neurology and Neurosurgery) and its neurogenetic research laboratory (UCL Queen Square Institute of Neurology) in the United Kingdom. The PhD candidate is a neurologist by training and has had the opportunity to deepen her clinical knowledge in movement disorders as well as to acquire laboratory and analytical skills in neurogenetics of movement disorders from the ground up, including wet lab techniques, analysis and validation of next-generation sequencing (NGS) data, and interpretation of genetic findings in the clinical context (clinicogenetic correlations), with the ultimate goal to develop a bridging expertise between bedside and bench and *vice versa*.

2. Genetics of movement disorders in the next-generation sequencing era

Parts of this paragraph have been published by the PhD candidate as a Review article in Movement Disorder Clinical Practice.[1]

"Phenotype" is the observable or quantifiable characteristics of an individual – including findings of nongenetic investigations – which result from the interaction of its gene makeup with environmental factors. However, in a narrower sense, geneticists refer to phenotype as the set of specific features arising from the expression of one or few genes. In keeping with this, “genotype” is the genetic constitution of an individual, overall or at a specific locus, that is responsible of a given phenotype.[1, 2]

Movement disorders is relatively unique among neurology subspecialities in its reliance on clinical assessment as well as clinicians' expertise and experience to accurately define disease phenotypes for several reasons.[1, 3] First, movement disorders are highly heterogeneous clinical entities with an aberrant motor output as the unifying presentation, and their classification has universally been based on motor phenomenology over the past decade.[3-6] Briefly, they reflect the abnormal execution of motor programs (parkinsonism or dystonia), the overgeneration of oscillatory muscle activity (tremor), the spontaneous occurrence of muscle jerks (myoclonus), or the excessive or inappropriate appearance of otherwise well-executed movement patterns (chorea, tics, and stereotypies).[7] In addition, movement disorders can manifest alone, in various combination, or in the context of complex clinical pictures, where they are associated with other neurological features (e.g., seizures, cognitive impairment, peripheral neuropathy, myopathy), psychiatric comorbidity, and systemic manifestations. Finally, movement disorders most often lack diagnostic biomarkers.[3]

Genetic underpinnings of movement disorders have systematically been explored since the last decades of the 20th century, when a CAG repeat expansion in the previously mapped locus for Huntington's disease was identified as its molecular etiology,[8, 9] and homozygous mutations in the *ATP7B* gene were first linked to Wilson's disease.[10] Hence, two strategies have mainly contributed to unravel causative variants and risk alleles in Parkinson's disease and other movement disorders, either alone or in combination.[11] These include the hypothesis-driven "candidate-gene approach", applied for example to linkage analysis,[12, 13] homozygosity mapping,[14-17] and case-control association studies,[18] and "large-scale approaches", such as genome-wide scan linkage analysis,[19] genome-wide scan association analysis,[20, 21] and the most recent massive parallel sequencing,[22, 23] which on the contrary do not require *a priori* hypotheses on genes or biological pathways associated with the disease under investigation.[11]

Massive parallel sequencing refers collectively to NGS technologies which have become available in the past few decades, that is methods enabling high-throughput

genomic (DNA) and transcriptomic (RNA) sequencing.[24] The rapid evolution and growing availability of these technologies have radically changed the scenario of both medical genetic research and clinical practice. In particular, landmark steps from first-generation sequencing (e.g., Sanger sequencing, which allows one-at-a-time sequencing reactions for amplified DNA fragments of 500-1000 base pairs; Figure I-1, left) to massive sequencing or NGS (which enables millions of simultaneous sequencing reactions of amplified DNA fragments of 50-500 base pairs; Figure I-1, middle) occurred in parallel with the evolution of movement disorder nosology from an anatomical-centered ("*extrapyramidal* disorders") to a phenomenological-centered classification.[5, 6]

Figure I-1. Evolution of sequencing technologies

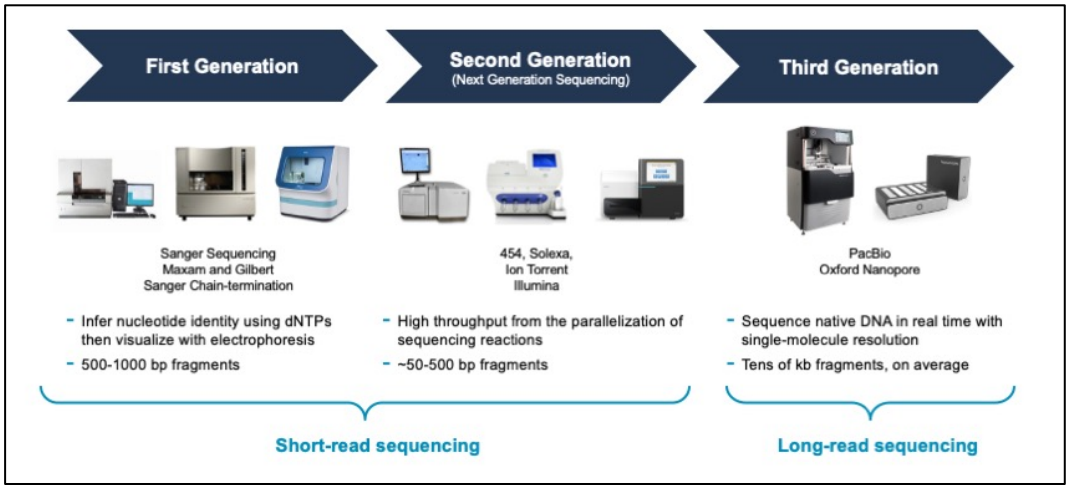

Legend: bp = base pairs; dNTP = deoxyribonucleotide triphosphate. Reproduced from the website https://www.pacb.com.

Interestingly, NGS technologies have enabled an unparalleled discovery of disease-causing or disease-predisposing genes and revealed unmatched complexity of genotype-phenotype correlations in the movement disorder field,[23] which has resulted in revolutionizing the nomenclature and taxonomy of genetic movement disorders[23, 25] as well as posing new challenges for movement disorder specialists in terms of diagnosis, treatment, and counseling.[1, 26]

This landscape is set to get even more complex with the advent of long-read sequencing (PacBio Single Molecule Real-Time Sequencing and Oxford Nanopore Technology)[27-30] and other technologies (e.g., electronic nano-device sequencing, BioNano nanochannel-based genome optical mapping) which promise to overcome intrinsic limitations of "short-read" NGS (which "reads" PCR-derived DNA fragments; Figure I-1, middle) outlined below. Short-read NGS technologies are ideal for identifying single nucleotide polymorphisms or short insertions/deletions but are not optimized to identify structural variations and large repeat expansions.[27, 28] Furthermore, many genomic regions cannot be accurately sequenced using short-read technologies, including homologous elements, highly GC-rich sequences, and large repetitive sequences (e.g., human endogenous retroviruses (HERV)-K retrotransposons), which are implicated in the pathogenesis of neurological disorders.[27, 28] Other genomic regions that cannot be adequately resolved using short-read technologies include gene duplications, multiple copies, and the major histocompatibility complex. All these loci (sometimes referred to as "camouflaged regions") are potential drivers of neurological disorders, and yet our knowledge of the genetic sequences in these regions in dystonia is unknown. Finally, contrary to long-read sequencing, short-read technologies allow to directly phase only a limited number of detected variants without resorting to parental genotypes or statistical imputation.[22,23] The post-NGS technological advances also shed light to the relatively unexplored non-coding regions of the genome in the etiopathogenesis of human diseases. Over the past few years, a number of genetic discoveries in the movement disorder field were made possible by the advent of this "third-generation sequencing" (Figure I-1, right).[29] First, a SINE-VNTR-Alu (SVA) retrotransposon insertion in the *TAF1* gene has been recognized as possible molecular underpinning of X-linked dystonia-parkinsonism, with a hexameric repeat expansion within the SVA insertion acting as a genetic modifier of disease expressivity.[31, 32] In addition, intronic pentanucleotide repeat expansions in four different genes have been linked to familial cortical myoclonic tremor syndromes (*SAMD12*, *STARD7*, *MARCH6*, *YEATS2*).[33-36] Finally, a trinucleotide repeat expansion in the *NOTCH2NLC* gene has been associated with neuronal intranuclear inclusion disease.[37]

In this rapidly evolving scenario, challenges in research and medical genetics have progressively shifted from the technical capability to generate massive amount of DNA or RNA sequences rapidly and at affordable cost towards issues with data storage and, most importantly, data analysis and data interpretation in a clinical context.

To trace an outline of data analysis complexity, it is noteworthy that NGS techniques such as whole-exome sequencing (WES) and whole-genome sequencing (WGS) detect several thousand and a few million sequence variants that differ from the human genome reference per sequenced individual, respectively. For instance, WES in a single patient generates on average 20,000-25,000 variants.[38] Among them, only one variant (in the case of heterozygous or hemizygous variants associated with autosomal or X-linked dominant inheritance or *de novo* occurrence) or two variants (in the case of compound heterozygous or homozygous variants associated with recessive inheritance) are causally related to the disease under investigation, provided that the latter is monogenic. Therefore, in the process of filtering and prioritize variants for analysis, excluding variants which are benign, neutral, and/or common in the general healthy population ("primary filtering") represents a first crucial step for increasing the likelihood to identify disease-causing variants in Mendelian disorders (Figure I-2).[38, 39, 40] This process is essentially performed by filtering out variants with an insufficient read depth (quality control) and synonymous variants as well as by excluding variants by minor allele frequency (i.e., the frequency at which the second most common allele occurs in a given population) after comparing them against publicly available population databases, such as 1000 Genomes Project (www.internationalgenome.org), dbSNP (www.ncbi.nlm.nih.gov/projects/SNP), ExAC and gnomAD (www.gnomad.broadinstitute.org). The rare complex movement disorders explored in the present thesis are caused by mutations that are expected to be absent from population datasets or present at a very low frequency. In addition to primary filtering, "second filtering" consists of strategies to prioritize remaining candidate variants by consideration, among others, of the gene (mode of inheritance, expression and function) and *in silico* pathogenicity prediction tools.[38]

Figure I-2. Workflow for filtering and functional analysis of WES data

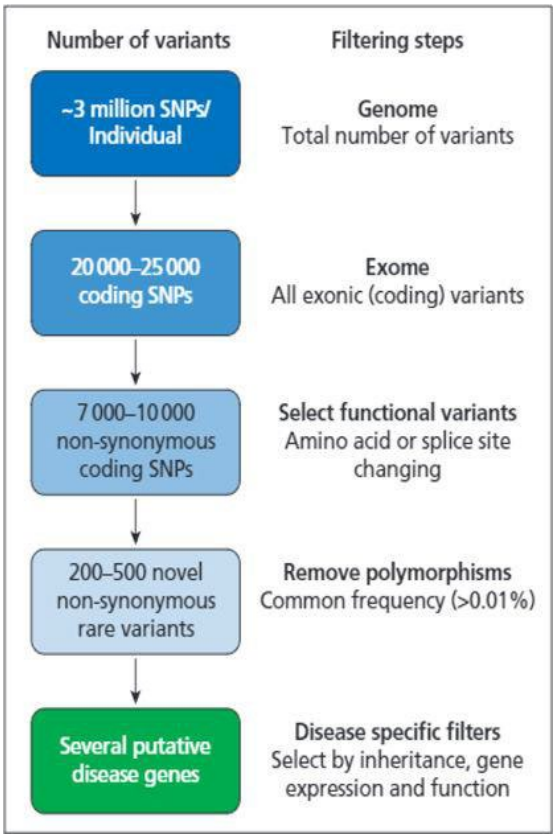

Legend: SNP = single-nucleotide polymorphism. Reproduced from Efthymiou et al., 2016[41]

Another major challenge in analyzing NGS data is the frequent occurrence of sequencing artifacts, which are usually not specific to individual exomes and are determined by abnormal chemical reactions affecting the coverage and amplification of genomic regions.[42] These phenomena are estimated to occur in more than 1% of exomes. It is therefore critical to exclude variants present in >1% of internal exome database to reduce the possibility of artifacts as well as to confirm NGS findings by Sanger sequencing. Querying in-house exome datasets is also an additional strategy to exclude low-frequency variants.

As for challenges in data interpretation in the clinical context, numerous examples are offered by the movement disorder field, where the advent and widespread availability of NGS technologies have led to the identification of an exponential number of disease-causing genes and fueled the complexity of genotype–phenotype

correlations.[23] Among other aspects, it has emerged that mutations in different genes may account for the same "core" movement disorder (genetic heterogeneity).[26] For instance, variants in *NKX2-1*, *ADCY5* and *PDE10A* can all manifest with early-onset chorea,[43] mutations in *PRRT2*, *MR-1*, *SCN8A* and *SLC16A2* with paroxysmal kinesigenic dyskinesia,[44] and defects in *GLRA1*, *GLRB* and *SLC6A5* with hyperekplexia.[45] On the other hand, mutations in one and the same gene can cause multiple, often markedly different movement disorder phenotypes (phenotypic heterogeneity) as a consequence of biological phenomena such as incomplete penetrance, variable expressivity, pleiotropy, and stochastic events (Figures I-3, I-4).[1]

Figure I-3. Schematic of biological phenomena contributing to phenotypic heterogeneity in monogenic disorders

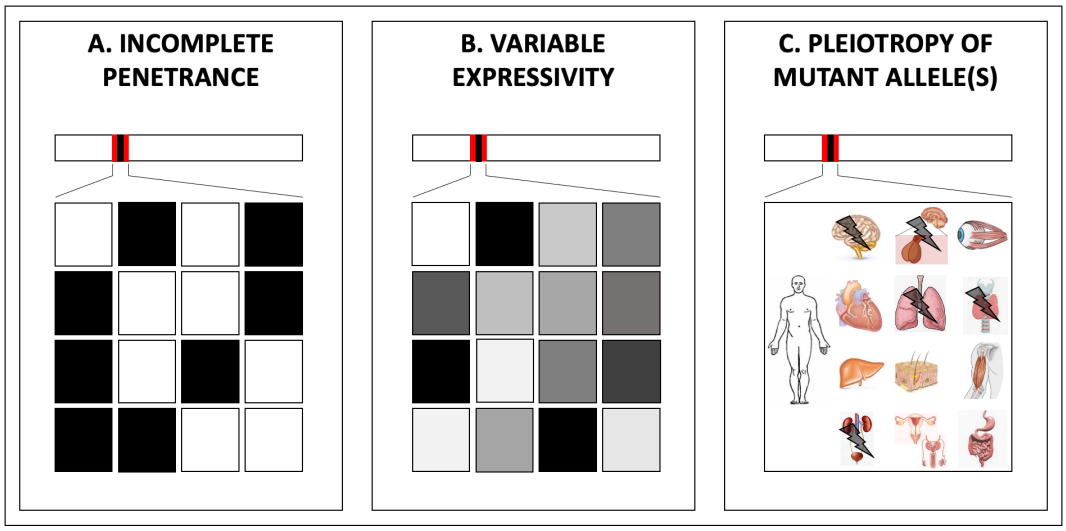

(A-B) Squares represent individuals carrying the same variant in a gene. (A) Shaded square means the individual manifests the disease phenotype. Non-shaded square means the individual does not manifest the disease phenotype (non-penetrance). (B) Shaded square means the individual manifests the disease phenotype with different degree of severity. Non-penetrance (non-shaded squares) can be viewed as an extreme endpoint of variable expression. (C) Individual carrying a variant in a pleiotropic gene with multisystemic effects. In the example, a variant in the *NKX2-1* gene encoding the thyroid transcription factor 1, with involvement (grey thunderbolt) of the nervous system (chorea, choreoathetosis), pituitary gland (cystic mass), thyroid (congenital hypothyroidism), lung (neonatal respiratory distress, chronic interstitial lung diseases), and urinary system (megabladder). Modified from Magrinelli et al., 2021[1]

Figure I-4. Overview of genetic and nongenetic determinants of incomplete penetrance, variable expressivity, and pleiotropy of mutant alleles

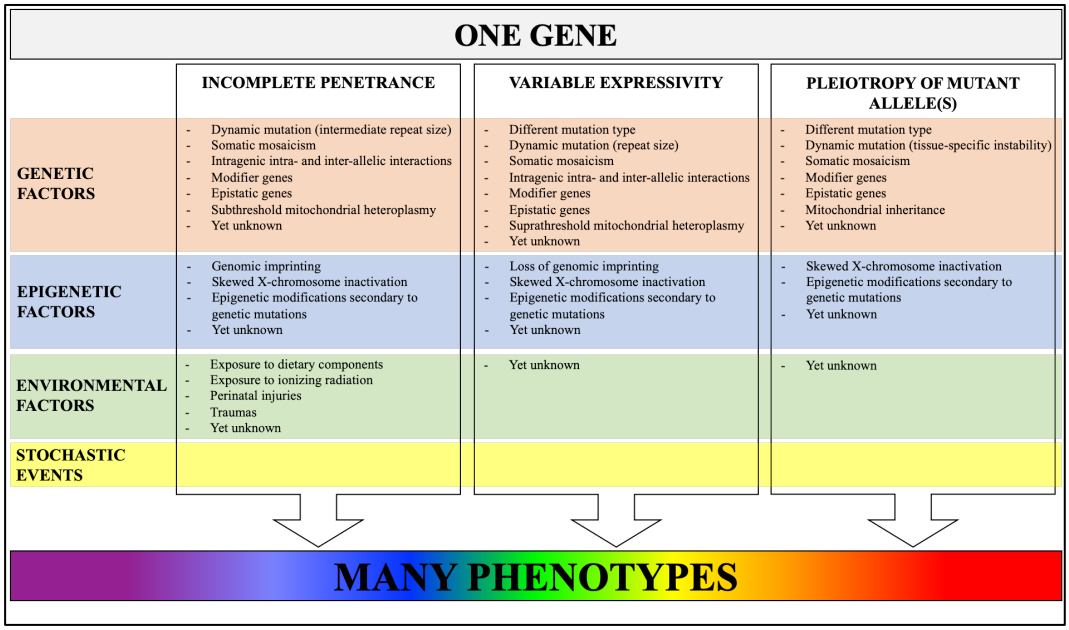

Stochastic (i.e., random) events might act at all levels and further contribute to phenotypic heterogeneity. Reproduced from Magrinelli et al., 2021[1]

Variant pathogenicity prediction (i.e., the probabilistic assertion of the likelihood that an identified genetic variant is disease-causing)[46] and integration of genetic findings with detailed phenotypic features and family history of affected individuals under investigation are steps of a complex, multidisciplinary process to establish a genetic diagnosis involving bioinformaticians, geneticists and clinicians. Always more often movement disorder specialists will be required to formulate challenging pathogenicity assertions by matching data collected in the clinical arena with genetic findings.

Understanding the relationship between genotype and phenotype is the cornerstone of precision medicine and an essential requirement for clinicians in the advanced NGS era. Indeed, automated processes and machine learning algorithms have hitherto failed to provide accurate genotype-to-phenotype predictions, which limits their use in clinical diagnostics and neurogenetic research at present. Despite their expected refinement in the next future, it is unlikely these tools will ever fully

replace the role of clinicians and geneticists, especially in the movement disorder field, which strongly relies on fine-grained clinical judgement for phenotype definition without parallel in neurology. As a consequence, the exponential growth of genetic knowledge driven by NGS has reaffirmed the central role of meticulous clinical phenotyping. More specifically, it has promoted individual-oriented "deep phenotyping",[47] namely the detailed and comprehensive analysis of discrete components of a phenotype that goes beyond what is typically recorded in clinical charts (e.g., nuanced phenotypic traits, such as "short stature" or "mild dysmorphic features"), generally in a way which is computationally accessible and enables to integrate the resulting wealth of data with non-clinical information. In other words, a transition from the "definition" to the "holistic characterization" of phenotypes has been promoted by the NGS revolution. In clinical practice, deep phenotyping can further guide clinicians through differential diagnosis, selection of genetic tests and interpretation of their results, targeted therapeutic interventions and genetic counseling. In the research setting, it enables to expand the knowledge on established genotype-phenotype correlations or to determine novel ones.

The following introductory paragraphs prepare the reader for the main topics addressed in chapters III, IV, and V, providing an overview on dystonia and its associated genes and biological pathways.

3. Dystonia: definition and consensus classification

"*Dystonia is a movement disorder characterized by sustained or intermittent muscle contractions causing abnormal, often repetitive, movements, postures, or both. Dystonic movements are typically patterned, twisting, and may be tremulous. Dystonia is often initiated or worsened by voluntary action and associated with overflow muscle activation*."[48]

The term "dystonia" is used to refer to either an isolated neurological sign or a plethora of syndromes in which dystonia can be the prominent or a minor clinical

feature.[48, 49] Although the overall epidemiology of dystonia remains undetermined, patients with dystonia represent approximately 20% of cases in movement disorder clinics.[49, 50] Definitions, nomenclature, and taxonomy of dystonia have repeatedly been refined over the past decades in order to absorb advances in the knowledge of clinical, physiopathological, and etiological aspects of dystonia.[25, 48] Besides formulating the definition which opens this paragraph, the 2013 consensus update on the phenomenology and classification of dystonia suggested to categorize dystonia according to two axes (Figure I-5) and aimed to harmonize and systematize the basis for future research in this field.[48]

Figure I-5. Classification of dystonia according to clinical characteristics (axis 1) and etiology (axis 2)

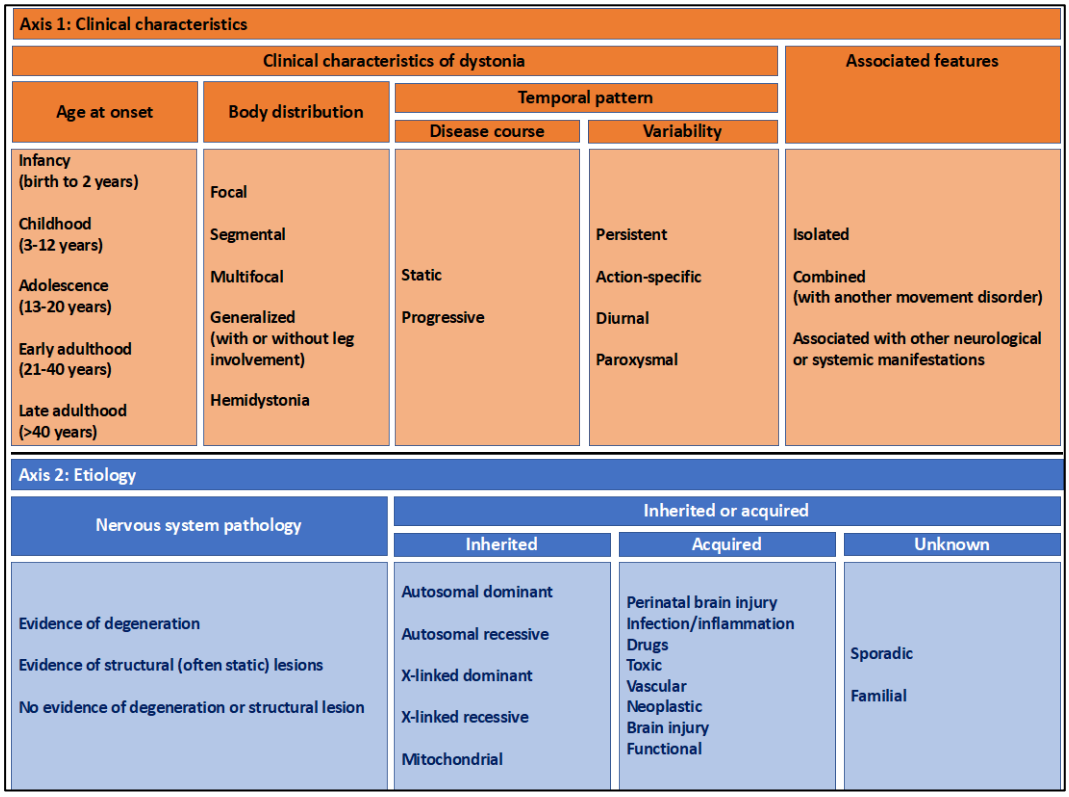

Modified from Albanese et al., 2013[48]

The first axis focuses on the clinical characterization of dystonia in terms of age at onset, body distribution, temporal pattern and associated features (Figure I-5,

orange boxes).[48] In terms of age at onset, Albanese et al. have proposed a categorization of dystonia into five clusters, including infancy-onset (birth to 2 years), childhood-onset (3-12 years), adolescence-onset (13–20 years), early-adulthood-onset (21–40 years), and late-adulthood-onset (>40 years).[48] Furthermore, based on its pattern of distribution, which may evolve and therefore needs repetitive assessments over time, dystonia has been classified into "focal" (if only one body region is affected), "segmental" (when two or more contiguous body regions or both arms are affected), "multifocal" (if two noncontiguous or multiple body regions are affected), "generalized" (when the trunk and at least two other body regions are affected, with or without leg involvement), and "hemidystonia" (when body regions affected are restricted to one hemi-body).[48] Depending on whether dystonia evolves in terms of severity and distribution over time, it is distinguished into "progressive" or "static".[48] Moreover, clinical manifestations of dystonia may be present throughout the day ("persistent" dystonia), follow a circadian rhythm (dystonia with "diurnal fluctuations", as typically observed in levodopa-responsive dystonia), occur only during specific tasks or actions, or be induced by different triggers ("paroxysmal" dystonia).[48] Finally, by looking for the presence of associated features, dystonia can be classified into "isolated" (if it is the sole manifesting clinical feature, with the exception of tremor) or "combined" (if it is associated with other neurological or systemic signs).[48] Nevertheless, in the most recent literature on the topic, dystonia is classified in three subgroups, i.e. "isolated", "combined", and "complex", where "combined" refers to the combination of dystonia with other movement disorders, whereas "complex" refers to the coexistence of dystonia and other neurological (non-motor) or systemic signs.[51-53] In particular, "complex" dystonia syndromes encompass a heterogeneous group of neurological syndromes including, among others, mitochondrial disorders, organic acidurias, syndromes with brain calcification or brain iron accumulation, lipid storage disorders, and disorders of thiamine metabolism.[51]

The second axis of the 2013 consensus classification deconstructs the etiology of dystonia by discriminating neuropathological findings (if available) and by defining whether dystonia is inherited, secondary to non-genetic causes (acquired), or

idiopathic (Figure I-5, blue boxes). Dystonia of undetermined etiology can be further classified into "sporadic" and "familial" forms. Despite enormous advances in our understanding of the pathophysiology of dystonia,[49] the majority of patients with suspected genetic dystonia remain undiagnosed after maximal investigation, implying that a number of causative genes have not yet been recognized. A growing percentage of the so-called idiopathic forms will likely be allocated to the group of inherited dystonia with the evolution of our knowledge about genetics of dystonia.[51]

For the purposes of the present thesis, the following paragraph will focus on genetics and biological pathways of dystonia.[48, 50]

4. Dystonia genes and biological pathways

Parts of this paragraph have been published by the PhD candidate as a Video NeuroImage in Neurology[54] and as a Review article in Parkinsonism and Related Disorders.[55]

The pathophysiological basis of dystonia is controversial[49, 56] but likely a combination of acquired precipitant with a genetic predisposition.[57] The genetic contribution to many forms of dystonia has emerged since the 1990s (Figure I-6),[49] when mutations in *GCH1* and a GAG deletion in *TOR1A* were identified as the first cause of autosomal dominant dopa-responsive dystonia and early-onset generalized dystonia, respectively.[58, 59] Many factors initially hampered the unraveling of genetic underpinnings of dystonia. First, the paucity of pedigrees with multiple members affected.[49] Second, the wide phenotypic heterogeneity and the lack of biomarkers for dystonia phenotypes, which prevented the identification of homogenous patient cohorts for genetic studies.[49, 60] Third, the reduced penetrance of some forms of dystonia, which limited the selection of sporadic cases with actual inherited forms for molecular testing for either diagnostic or research purposes.[61]
On the contrary, advances in the field have occurred over the past two decades with the advent of NGS technologies, which have enabled the rapid identification of hundreds of novel dystonia-associated genes, the majority of which account for

childhood-onset complex phenotypes, in which dystonia may not represent a prominent clinical manifestation (Figure I-6).[61-64] Overall, monogenic inheritance is most often confirmed in early-onset dystonia, either isolated or combined, where a family history is sometimes elicited.[49, 61] However, some monogenic forms of dystonia, such as DYT-*TOR1A* and DYT-*THAP1*,[25, 59, 65] may present as sporadic cases due to reduced penetrance.[61] On the other hand, in adult-onset focal dystonia (e.g., cervical dystonia, blepharospasm, spasmodic dysphonia, task-specific dystonia), which represents by far the highest proportion of dystonia cases, the etiology remains almost invariably unknown although there is suggestion of a strong genetic basis.[61] Indeed, 20-30% of patients with cervical dystonia have at least another family member with either cervical or another form of dystonia and up to almost 35% of patients with blepharospasm have a family history of focal dystonia.[66-69]

Figure I-6. Timeline of the major discoveries in the field of isolated dystonia

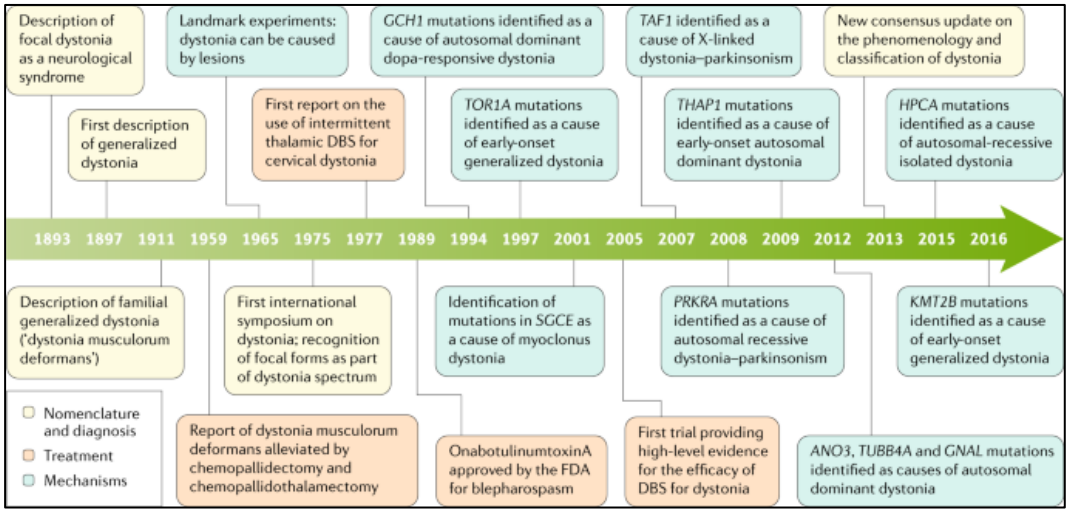

Genetic discoveries appear in green boxes. Reproduced from Balint et al., 2018[49]

In addition to the rapid increase in dystonia-related genes, the NGS revolution has favoured the development of a new nomenclature system for inherited dystonias.[25] The old designation of genetic forms reflecting the progressive numbering of dystonia-associated loci identified initially by linkage analysis studies (e.g., DYT1,

DYT6, DYT11) has been replaced by a more rational naming system indicating the main movement disorder phenotype and its causative gene (e.g., DYT-*TOR1A*, DYT-*THAP1*, and DYT-*SGCE*)[23, 25, 48] Finally, *in vivo* and *in vitro* evidence from molecular mechanisms linked to old and recent genetic findings has brought to light that the protein products of dystonia-associated genes are involved in a few shared, non-mutually exclusive, biological pathways, including dopamine signaling and presynaptic neurotransmitter release, gene transcription during neuroregulation, mitochondrial function and cell energy homeostasis, endo-lysosomal and autophagic functions, cell transport and homeostasis of calcium and heavy metals, as outlined below.[64, 70]

Dopamine signaling

A causal association between impaired dopamine signaling and inherited dystonia has been recognized since the discovery of the first gene linked to dopa-responsive dystonia, namely *GCH1*, in 1994.[59, 71] *GCH1* codes for the enzyme GTP-cyclohydrolase, which is involved in the synthesis of tetrahydropterin, an essential cofactor for the conversion of tyrosine into DOPA by the enzyme tyrosine hydroxylase.[59, 71] After *GCH1*, which has been linked to both autosomal dominant and recessive dystonia,[71] other genes encoding enzymes which play a role in the dopamine synthesis or metabolic pathways have been associated with different forms of infancy- or childhood-onset generalized dystonia, including *TH* (tyrosine hydroxylase),[72] *SPR* (sepiapterin reductase),[73] *PTS* (6-pyruvoyl-tetrahydropterin synthase),[74] *DDC* (aromatic amino acid decarboxylase),[75] *SLC18A2* (intracellular vesicular monoamine transporter 2),[76] and *SLC6A3* (cell surface monoamine transporter),[77] with loss-of-function mutations resulting in reduced levels of dopamine and its metabolites. In addition, evidence of altered dopamine signaling comes from the most prevalent monogenic forms of dystonia, such as reduced expression of D2 receptors in the striatal neurons of *TOR1A* and *THAP1* mutation carriers[78] and in the cerebrospinal fluid of patients with *KMT2B*-related dystonia[79] Furthermore, several dystonia-associated genes which were discovered more recently are robustly expressed in the striatum and modulate responses to

dopaminergic stimulation. For example, *GNAL* encodes the α subunit of the enzyme guanine nucleotide binding protein G(olf),[80] which is involved in the transduction of dopamine and adenosine signaling and is functionally coupled with the enzyme adenylate cyclase type 5, which is encoded by *ADCY5*, the latter being associated with an early-onset choreo-dystonia phenotype.[81] Finally, genes linked to much rarer forms of dystonia, including *KCTD17* (potassium channel tetramerization domain containing 17)[82, 83] and *HPCA* (hippocalcin),[84, 85] have been demonstrated to modulate postsynaptic dopaminergic responses in fly models, although the exact mechanisms have not been clarified so far.[64]

Figure I-7. Main dystonia-associated genes involved in dopamine signaling

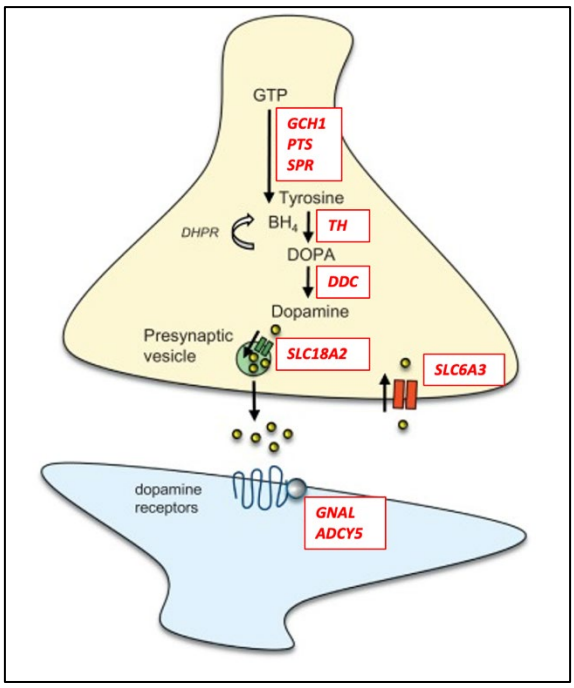

Modified from Jinnah et al., 2019.[70]

Presynaptic neurotransmitter release

Defects of the presynaptic terminal function are also increasingly recognized in the etiopathogenesis of dystonia. As an example, *PRRT2*, the gene whose monoallelic mutations represent the most frequent cause of paroxysmal kinesigenic

dyskinesia/dystonia (PKD), encodes a protein which blocks the trans-SNARE complex assembly at the presynaptic level.[86, 87] Loss-of-function mutations in this gene affect neurotransmitter release and reduce the likelihood of vesicle release upon depolarization.[88] In addition, *PRRT2* has been proven to downregulate the activity of sodium channels Nav1.6, which are encoded by *SCN8A,* another established gene linked to PKD.[89] Other genes closely linked to presynaptic terminal function, such as *CACNA1A* and *CACNA1B* (encoding the VGCCs Cav2.1 and Cav2.2) and *KCNMA1* (encoding the calcium-activated potassium BK channels), have been associated with a wide spectrum of paroxysmal dystonic and ataxic manifestations or epileptic encephalopathy.[64, 90] Finally, the protein product of *PNKD*, the gene responsible for paroxysmal non-kinesigenic dyskinesia/dystonia, modulates neurotransmitter release at the presynaptic region.[91]

Gene transcription during neuroregulation

Impaired gene transcription during neuroregulation has been identified as another unifying pathomechanism in some monogenic forms of dystonia.[64] Examples are offered by *THAP1*, which codes for a zinc finger protein with a DNA-binding domain regulating gene transcription,[65] and *KMT2B*, which encodes a histone lysine N-methyltransferase with a role in chromatin modeling and epigenetic regulation of gene expression.[79] Loss-of-function mutations in the aforementioned genes are thought to cause (generalized) dystonia by reducing the pro-transcriptional activity of the normal gene products.[64] Intriguingly, both genes are highly expressed in the cerebellum,[64] possibly indicating their major role in the correct development of cerebellar neurons and motor pathways, which have increasingly been recognized in the pathophysiology of dystonia.[92]

Mitochondrial function and cell energy homeostasis

Defects in the mitochondrial function or, more broadly, in neuronal energy homeostasis are another well-recognizable theme in the pathophysiology of focal, multifocal and complex forms of dystonia.[70] Dystonia is a frequent and often

prominent manifestation of Leigh syndrome, a necrotizing mitochondrial encephalopathy which has hitherto been linked to mutations in more than 100 different genes (both nuclear and mitochondrial).[93-95] In addition, dystonia can be associated with optic neuropathy in the so-called "Leber's plus" syndromes, which are caused by mutations in the genes encoding the subunits of the enzyme NADH dehydrogenase.[96] In these cases, dystonia is usually secondary to an overt histopathological damage of the basal ganglia. In other cases, dystonia is due to perturbations of neuronal energy homeostasis (energy shortage) without any evidence of brain lesions.[70] A paradigmatic example is offered by exercise-induced dystonia associated with mutations in the *SLC2A1* gene, which encodes the glucose transporter type 1.[97] An overview of the phenotype and pathophysiological mechanism underlying this disorder is provided in Figure I-8.[54]

Figure I-8. Overview of the clinical picture and pathogenesis of glucose transporter type 1 deficiency syndrome

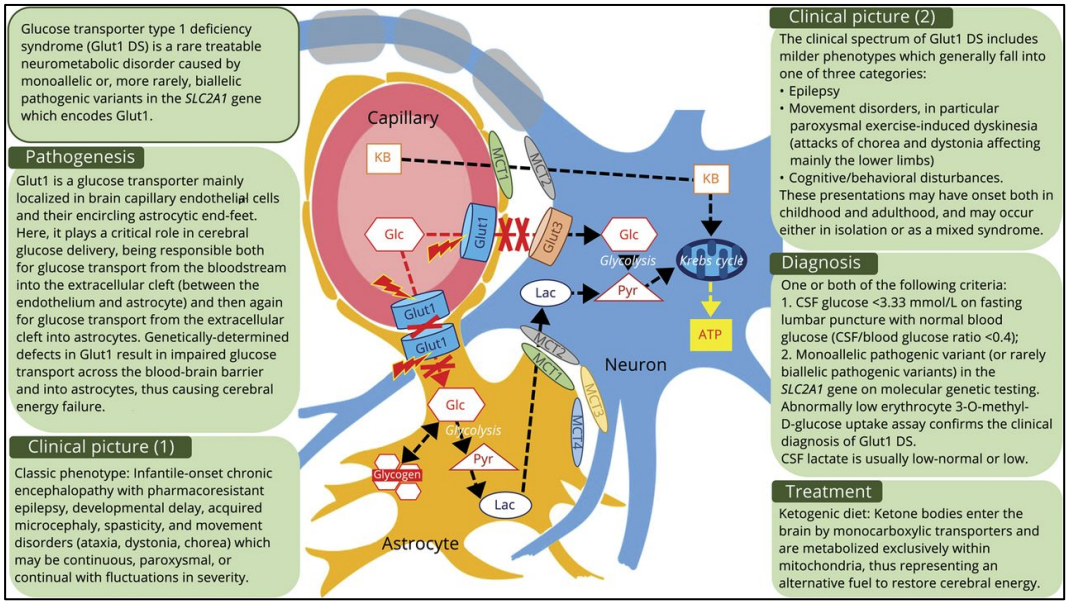

Legend. Red dashed lines indicate defective pathways in Glut1 DS. ATP = adenosine triphosphate; Glc = glucose; Glut = glucose transporter; KB = ketone bodies; Lac = lactate; MCT = monocarboxylic transporter; Pyr = pyruvate. Reproduced from Magrinelli et al., 2020.[54]

Endo-lysosomal and autophagic functions

Dystonia is a well-documented clinical feature in a number of lysosomal storage disorders (e.g., GM1 gangliosidosis, Niemann-Pick type C, fucosidosis) which usually manifest as childhood-onset complex syndromes in which dystonia can be the prominent or a minor feature.[98-104] These disorders most often show typical neuroimaging and neuropathological changes mainly affecting the basal ganglia. More recently, dystonia phenotypes have also been associated with defects of the endo-lysosomal compartment, in particular subunits of the homotypic fusion and vacuole protein sorting (HOPS) complex, a highly conserved multiprotein complex which mediates autophagosome-lysosome fusion through interaction with syntaxin 17. Mono- or bi-allelic loss-of-function mutations in the HOPS subunit *VPS16* account for generalized dystonia, and bi-allelic loss-of-function mutations in the HOPS subunit *VPS41* (bi-allelic) have been linked to a severe infancy-onset dystonia syndrome.[105, 106] In addition, bi-allelic loss-of-function variants in *SQSTM1*, which encodes a component of an autophagy receptor with a role in selective autophagy, have been associated with a complex phenotype characterized by progressive dystonia, chorea, ataxia, and vertical gaze palsy.[107] Finally, variants in the gene encoding the interferon regulatory factor 2-binding protein-like protein (*IRF2BPL*) have recently been related to a complex neurodevelopmental syndrome characterized by generalized dystonia, anarthria, and seizures,[108-110] and a skin biopsy from an affected subject revealed enlarged lysosomes containing osmiophilic material, which suggests lysosomal dysfunction.[111]

Cell transport and homeostasis of calcium and heavy metals

Another unifying theme in the pathophysiology of dystonia syndromes is represented by neurological or systemic disorders characterized by brain deposition of calcium, copper, iron, or manganese, mostly in the basal ganglia.[10, 70, 112-114]
Primary brain calcification syndromes, historically known as Fahr's disease, are heterogeneous disorders characterized by pathological peri-microvascular calcium deposition in the basal ganglia, subcortical white matter, thalamus and

cerebellum.[112] Clinical manifestations are protean. Some affected individuals remain asymptomatic throughout their life despite demonstrable brain calcinosis, though most experience progressive neurological deterioration. Psychiatric symptoms (depression, anxiety, psychosis), movement disorders (dystonia, parkinsonism), and cognitive impairment are typical manifestations.[112] Five genes have hitherto been linked to adult-onset movement disorder phenotypes with brain calcium deposition, including *SLC20A2*, *PDGFRB*, *PDGFB*, *XPR1*, and *MYORG* (Table I-1).[112, 113]

Dystonia is a major phenotypic feature in Wilson's disease, a multisystem disorder characterized by defective copper excretion into the biliary tract, and subsequent toxic accumulation of free copper in different organs, primarily the liver and brain. Bi-allelic mutations in the copper transporter encoded by *ATP7B* gene account for the disease (Table I-1).[10]

Neurodegeneration with brain iron accumulation (NBIA) syndromes are a group of clinically and genetically heterogeneous neurodegenerative disorders characterized by a combination of extrapyramidal (dystonia, parkinsonism, chorea), pyramidal (hyperreflexia, spasticity), cerebellar, psychiatric and cognitive manifestations, along with regression, optic atrophy, and peripheral neuropathy in some cases (Figure I-9; Table I-1).[115-117] They have been clustered under the diagnostic label "NBIA" due to the historical recognition of iron deposition in the basal ganglia, substantia nigra and, in some cases, dentate nucleus, which is now recognized as an inconstant and anyway not pathognomonic neuroradiological feature of these disorders. Ten genes have hitherto been strongly associated with the NBIA syndromes, including *PANK2*, *PLA2G6*, *FA2H*, *ATP13A2*, *FTL*, *CP*, *WDR45*, *COASY*, *DCAF17*, *C19orf12*. Among them, *FTL* (ferritin light chain) and *CP* (ceruloplasmin) are only linked to adult-onset phenotypes and directly involved in iron homeostasis regulation. *COASY* (CoA synthase) and *PANK2* (pantothenate kinase type 2) are involved in coenzyme A biosynthesis. *PLA2G6* (phospholipase A2), *FA2H* (fatty acid hydroxylase 2), and *C19orf12* (protein of the outer mitochondrial membrane) encode proteins acting in the metabolism of membrane lipids (phospho- and sphingolipids). *ATP13A2* (P-type cation pump of lysosomes) and *WDR45* (a member of the WD scaffold protein family) are linked to the

autophagosome pathway. Finally, *DCAF17* codes for a protein whose function remains unknown, and which localizes to nucleoli.[114]

Figure I-9. Relative frequency of genetically determined NBIA subtypes

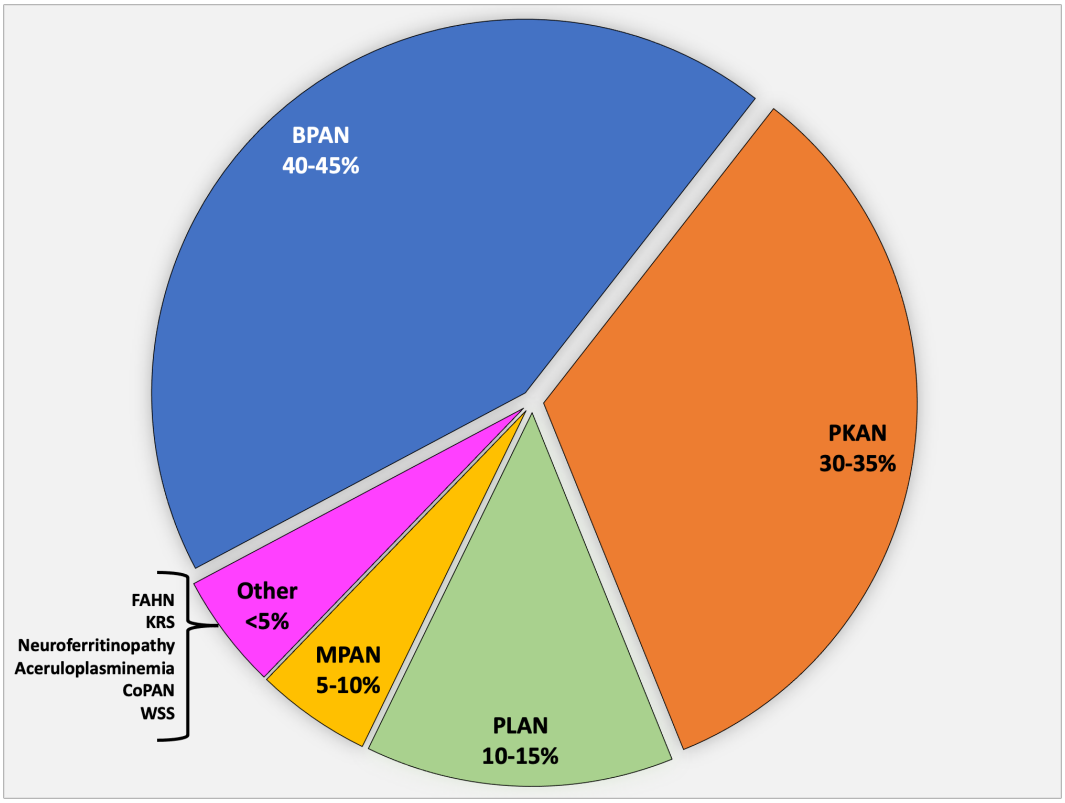

Based on prevalence of NBIA subtypes in the *International Registry for NBIA and Related Disorders* from the Hayflick laboratory.[114] Legend: BPAN = beta-propeller protein-associated neurodegeneration (*WDR45*); CoPAN = *COASY* protein-associated neurodegeneration; FAHN = fatty acid hydroxylase-associated neurodegeneration (*FA2H*); KRS = Kufor-Rakeb syndrome (*ATP13A2*); MPAN = mitochondrial membrane-protein associated neurodegeneration; PLAN = *PLA2G6*-associated neurodegeneration; PKAN = pantothenate kinase-associated neurodegeneration (*PANK2*); WSS = Woodhouse-Sakati syndrome (*DCAF17*).

Table I-1. Dystonia syndromes associated with brain calcifications, Wilson's disease, NBIA, and manganese transportopathies

DYSTONIA SYNDROMES	OMIM®	Chromosome	Gene	Mode of inheritance	Age of onset	Main phenotype	Laboratory and imaging findings
DISORDERS WITH BRAIN CALCIFICATIONS							
Primary familial brain calcification (Fahr's disease)	213600	8p11.21	*SLC20A2*	AD	Third-fourth decade	Progressive parkinsonism, **dystonia**, action tremor, psychiatric features, headache, seizures.	Brain CT/MRI: basal ganglia and dentate calcification. In *MYORG*, possible intrapontine calcifications.
	615007	5q32	*PDGFRB*	AD			
	615483	22q13.1	*PDGFB*	AD			
	616413	1q25.3	*XPR1*	AD			
	618317	9p13.3	*MYORG*	AR			
DISORDERS OF COPPER METABOLISM							
Wilson's disease	277900	13q14.3	*ATP7B*	AR	Adolescence or early adulthood	Complex **dystonia** phenotype with tremor (action tremor, wing-beating tremor), parkinsonism, cerebellar signs, neuropsychiatric and cognitive features, sunflower cataracts, Kayser-Fleischer ring, chronic liver disease.	Blood tests: low serum copper and ceruloplasmin, abnormal liver function. Urine tests: high urinary copper. MRI: high T2 signal in the basal ganglia, "face of the giant panda" or "double panda" signs.
NEURODEGENERATION WITH BRAIN IRON ACCUMULATION							
NBIA/DYT-*PANK2* (PKAN)	234200	20p13	*PANK2*	AR	Childhood (late onset reported)	Parkinsonism, **dystonia** (mostly oromandibular), behavioral changes, pigmentary retinopathy in 50% of cases.	Brain MRI: iron deposition in the basal ganglia with "eye of the tiger" sign.
NBIA/DYT/PARK-*PLA2G6* (PLAN)	256600	22q13.1	*PLA2G6*	AR	Childhood (late onset reported)	Parkinsonism, **dystonia**, pyramidal signs, psychiatric features, cognitive decline, cerebellar ataxia.	Brain MRI: usually iron deposition in the globus pallidus and substantia nigra; cerebellar atrophy in late-onset forms.
HSP/NBIA-*C19orf12* (HSP43, MPAN)	614298	19q12	*C19orf12*	AR, AD	Childhood	Spastic paraparesis, dysarthria, **dystonia**, parkinsonism, neuropathy, psychiatric features, optic atrophy.	Brain MRI: iron deposition in the globus pallidus and substantia nigra.
COASY-protein associated neurodegeneration (CoPAN)	615643	17q21.2	*COASY*	AR	Childhood	Global developmental delay, ataxia, pyramidal signs, **dystonia**, parkinsonism.	Brain MRI: iron deposition in the globus pallidus and substantia nigra.
HSP/NBIA-*FA2H* (HSP35, FAHN)	234200	20p13	*FA2H*	AR	First-second decade	Spastic paraparesis, ataxia, **dystonia**.	Brain MRI: iron deposition in the basal ganglia (not constant), pontocerebellar

								atrophy, white matter hyperintensities.
	Kufor-Rakeb disease (PARK-*ATP13A2*)	606693	1p36.13	*ATP13A2*	AR	Second-third decade	Early-onset levodopa-responsive parkinsonism, **dystonia**, pyramidal features, supranuclear upgaze palsy, cognitive impairment.	Brain MRI: generalized atrophy, putaminal and caudate iron deposition.
	NBIA/CHOREA-*FTL* (Neuroferritinopathy)	606159	19q13.33	*FTL*	AD	Usually adulthood (second to sixth decade)	Progressive chorea and **dystonia** (mainly affecting the orofacial region), palatal tremor, cognitive decline, psychiatric features.	Blood tests: low ferritin, liver function tests may be abnormal. Brain MRI: iron deposition in the basal ganglia and dentate; cystic degeneration of putamen and globus pallidus; cortical lining sign.
	NBIA/DYT/PARK-*CP* (Aceruloplasminemia)	604290	3q24-q25	*CP*	AR	Middle adulthood	Retinal degeneration, diabetes, neurological features (**dystonia**, parkinsonism including rest tremor, ataxia).	Blood tests: absent serum ceruloplasmin, high serum ferritin. Brain MRI: iron deposition in the basal ganglia and dentate.
	Woodhouse-Sakati syndrome	241080	2q31.1	*DCAF17*	AR	Usually adolescence	Facial dysmorphic features (e.g., long triangular face, prominent nasal bridge, hypertelorism), hypogonadism, endocrinological issues (e.g., diabetes mellitus, hypothyroidism, reduced level of insulin-like growth factor 1, alopecia), sensorineural hearing loss, intellectual disability, ECG abnormalities, neurological manifestations (**dystonic spasms with dystonic posturing**, dysarthria and dysphagia).	Blood tests: abnormalities consistent with endocrinological manifestations. Brain MRI: progressive fronto-parietal white matter changes; iron deposition in the basal ganglia; small pituitary gland
	NBIA/PARK-*WDR45* (BPAN)	300894	Xp11.23	*WDR45*	XLD	Early childhood	First stage (early childhood): developmental delay, intellectual disability, epilepsy, stereotypies, dysfunctional sleep, ocular defects. Second stage (adolescence or early adulthood): rapidly progressive **dystonia**-parkinsonism and cognitive decline. Both males and females present with a similar phenotype.	Brain MRI: iron deposition in the basal ganglia; hyperintense halo surrounding the substantia nigra with a central hypointense band on T1-weighted images.
MANGANESE TRANSPORTOPATHIES								
	SLC30A10 deficiency	613280	1q41	*SLC30A10*	AR	Childhood or adulthood	Liver disease, polycythemia. Childhood: **limb dystonia**, dysarthria, fine tremor, bradykinesia, spastic paraparesis. Adulthood: parkinsonism, including rest tremor.	Blood tests: abnormal liver function, polycythemia. Brain MRI: T1 hyperintensities of the basal ganglia.
	SLC39A14 deficiency	617013	8p21.3	*SLC39A14*	AR	Infancy	Loss of developmental milestones, **dystonia**, bulbar signs, spasticity.	Brain MRI: T1 hyperintensities of the basal ganglia.
	SLC39A8 deficiency	616721	4q24	*SLC39A8*	AR	Infancy	Cranial synostoses with lacunar skull, severe psychomotor disability, **dystonia**, seizures, and vision and hearing impairment.	Brain MRI: T1 hyperintensities of the basal ganglia; cerebral and cerebellar atrophy,

Finally, since 2012 three genes involved in manganese transport and homeostatic regulation (i.e., *SLC30A10, SLC39A14* and *SLC39A8*)[118-121] have been linked with combined or complex dystonia syndromes, where dystonia is frequently associated with parkinsonism, other neurological features, and, as for *SLC30A10*, with polycythemia and chronic liver disease. Hyperintensity of the basal ganglia in T1-weighted MRI sequences is the radiological hallmark of these disorders, in which dystonia typically emerges during childhood, often accompanied by parkinsonism and other neurological manifestations (Table I-1).[118-121]

To date, treatment of dystonia syndromes remains largely symptomatic.[49] The development of target-specific disease-modifying pharmacological agents will depend upon the complete understanding of molecular pathomechanisms of dystonia. In this scenario, the landmark observation that dystonia-associated genes converge on a limited number of biological pathways has several implications. On the one hand, exploring dystonia gene and their biological pathways may contribute to re-classify patients with heterogeneous dystonia phenotypes into biologically meaningful groups. This could facilitate research on disease-modifying strategies and optimize clinical trial designs. On the other hand, some of the emerging biological pathways in the field of dystonia (e.g., endo-lysosomal compartment and autophagy), are currently extensively investigated in other movement disorders, including Parkinson's disease (e.g., *GBA*). This suggests that improving our knowledge of the crosstalk between dystonia and other movement disorders at the molecular level may contribute to unravel the pathophysiology and develop specific treatment not only for dystonia syndromes but also for other neurological disorders. Finally, disruption of the aforementioned molecular pathways of dystonia may play a role in the pathogenesis of symptoms commonly associated with dystonia in complex dystonia phenotypes, including epilepsy and psychiatric features. Therefore, further elucidate the molecular basis of dystonia may contribute to a better comprehension of the pathophysiology of these symptoms and the risk of developing them.

Chapter II
Objectives

General objectives of the study projects presented in the following chapters were:

1) to deeply characterize the phenotype of a large cohort of patients with complex movement disorders ("deep phenotyping"), in particular combined and complex dystonia, referred to a UK hub center for the diagnosis and treatment of movement disorders (National Hospital for Neurology and Neurosurgery, London) and its neurogenetic research laboratory (UCL Queen Square Institute of Neurology, University College London);

2) to investigate genetic underpinnings of complex movement disorders in the aforementioned clinical cohort through next-generation sequencing techniques (whole-exome and whole-genome sequencing) as well as the selection, execution and interpretation of proper ancillary genetic (e.g., Sanger sequencing, homozygosity mapping) and, in few cases where it was possible, functional tests;

3) to expand the phenotypic and genotypic spectrum of known genetic disorders;

4) to investigate new possible disease-causing genes.

Chapter III

Retrospective clinical review and analysis of whole-exome sequencing data of a cohort of patients with complex movement disorders (mainly combined and complex dystonia)

1. Preamble

The study presented in this chapter aimed to clinically and genetically review a historical cohort of patients with complex movement disorders, in particular combined and complex dystonia syndromes, who had whole-exome sequencing (WES) performed on a research basis at the UCL Queen Square Institute of Neurology, London, UK, between 2014 and 2020. For this study, exomes available were re-annotated and re-analyzed in one step and at once in order to absorb improvements in bioinformatics pipelines as well as recent updates in neurogenetics of movement disorders.

The role of PhD candidate in this study consisted of reviewing clinical records, analyzing WES data through both an extended "candidate-gene approach" and a "hypothesis-free approach", validating promising WES findings by Sanger sequencing and, if probands' family members were available for genetic testing, performing segregation analysis.

2. Introduction and specific aims

Dystonia syndromes are characterized by a high level of phenotypic heterogeneity, including the combination of dystonia with other movement disorders (combined dystonia) and/or other neurological, psychiatric, or systemic manifestations (complex dystonia).[26, 48] The advent and widespread availability of next-generation sequencing (NGS) technologies have enabled an unparalleled discovery of dystonia-related genes, thus revealing dystonia is also underlain by a high degree of genetic heterogeneity.[26, 63, 64] Against this rapidly evolving background, the

interpretation of NGS findings and their correlation with phenotypic features in genetic dystonia syndromes have become increasingly challenging. Genetic testing relying on targeted NGS panels for dystonia showed low diagnostic yield (<25%) in early-onset and/or familial dystonia syndromes.[122-124] Few studies have hitherto explored the use of WES for the molecular diagnosis of dystonia syndromes, reporting inconsistent diagnostic rates ranging from 20.2% to 69.2%, which mainly reflects discrepancies in phenotype-related inclusion criteria and genetic testing performed before the inclusion in the study as well as whether the availability of DNA from probands' relatives was required.[122, 125-128] An overview of previous studies on NGS in dystonia is provided in Table III-1.

This project, which was designed before the majority of WES studies mentioned above were published, aimed to:

- explore genetic underpinnings of complex movement disorders, in particular combined and complex dystonia phenotypes, including neurodegeneration with brain iron accumulation (NBIA) syndromes;
- expand the phenotypic and genotypic spectrum of the aforementioned movement disorders linked to known disease-causing genes;
- investigate new candidate disease-causing genes;
- establish the diagnostic yield of WES in a large cohort of patients with heterogeneous complex movement disorders.

3. Subjects and methods

Subjects

I retrieved a pool of 139 exomes belonging to patients who were referred to the UCL Queen Square Institute of Neurology, London, UK, to have WES performed on a research basis for complex movement disorders between 2014 and 2020. The cohort was enriched with cases of combined and complex dystonia and/or suspected NBIA syndromes based on their clinical and/or neuroradiological characteristics. In particular, inclusion criteria for undergoing WES were: 1) presenting with

complex movement disorder phenotypes with dystonia as the prominent phenomenological feature; and/or 2) presenting with MRI evidence of brain iron deposition; and/or 3) presenting with clinical features highly suggestive of an NBIA syndrome. The latter included early-onset dystonia (particularly with involvement of the oromandibular region and/or the trunk) or complex parkinsonism, and/or history of neurodevelopmental delay or regression of definitely acquired neurodevelopmental milestones, and/or presence of psychiatric issues associated with a movement disorder phenotype. Patients with a positive family history and/or those who had been tested negative for pathogenic variants in the most common genes associated with Parkinson's disease and dystonia genes were included preferentially.

Generation of WES data

WES data analyzed in this project were generated according to standardized protocols and reflected the evolution of Illumina NGS technologies (Illumina, San Diego, CA, USA) over the 6-year time interval of cases' recruitment. Samples were prepared according to the most recent techniques/technologies available from time to time, including Nextera Rapid Capture Enrichment and Agilent SureSelect Target Enrichment systems to capture genomic regions of interest (coding regions) by enriching them out of an NGS genomic fragment library, and Illumina HiSeq 2000, X, and 4000 platforms for sequencing. An overview of the 4-step Illumina NGS workflow is provided in Figure III-1. Technical details on the evolution of Illumina enrichment systems and sequencing platforms are beyond the scope of this chapter and can be found elsewhere (https://support.illumina.com).

DNA sample retrieval

Blood samples for DNA extraction had been collected by consultants working at the National Hospital for Neurology and Neurosurgery (NHNN), London, UK, and by clinical collaborators based in other hospitals in the UK and other countries (mainly in South-East Asia). DNA had been extracted from peripheral white blood

Table III-1. Overview of studies exploring genetics of dystonia by NGS techniques

NGS technique	Inclusion criteria	Number of patients included	Genetic tests performed prior to inclusion in the study	Diagnostic yield	Reference
NGS gene panel (148 dystonia-associated genes)	Dystonia as prominent phenotypic feature	65	-	24.6%	[124]
NGS gene panel (127 MD-associated genes, including 69 dystonia-associated genes)	Early-onset (<40 years) or familial MD (including dystonia)	135	38% of included patients had previous genetic testing	15.6%	[129]
NGS gene panel (65 MD-associated genes, including 30 dystonia-associated genes)	Dystonia as part of the phenotype	114	*TOR1A* GAG deletion, *PANK2* and *PLA2G6*	8.8%	[130]
NGS gene panel (94 dystonia-associated genes)	Onset of dystonia before the age of 40 years or positive family history or dystonia combined with another MD or co-occurrence of other unexplained neurological or systemic manifestations or paroxysmal dystonia or laryngeal dystonia	61	-	14.8%	[123]
WES	Childhood-onset dystonia (<18 years)	65	NGS gene panel including 67 dystonia-associated genes	24.6%	[126]
WES	Dystonia as part of the phenotype	189	12.7% of included patients had previous tests for dystonia-associated genes	20.2%	[125]
WES	Early-onset (<40 years) or familial dystonia. Required availability of DNA from probands' relatives.	32	NGS gene panel including 69 dystonia-associated genes	34.4%	[122]
WES	Early-onset generalized dystonia (before 30 years of age). Required availability of DNA from probands' relatives.	16	-	37.5%	[127]
WES	Combined or complex dystonia	13	Different NGS gene panels	69.2%	[128]
WGS	Dystonia as prominent phenotypic feature	111	-	11.7%	[131]

Legend: MD = movement disorders; NGS = next-generation sequencing; WES = whole-exome sequencing; WGS = whole-genome sequencing.

cells according to standard procedures in the neurogenetic diagnostic or research laboratories at the NHNN or the UCL Queen Square Institute of Neurology, respectively. I retrieved DNA samples corresponding to available exomes for possible validation of WES findings. All patients had given their consent prior to the study, which was approved by the Queen Square Ethics Committee and conducted according to the Declaration of Helsinki.

Figure III-1. Illumina NGS workflow overview

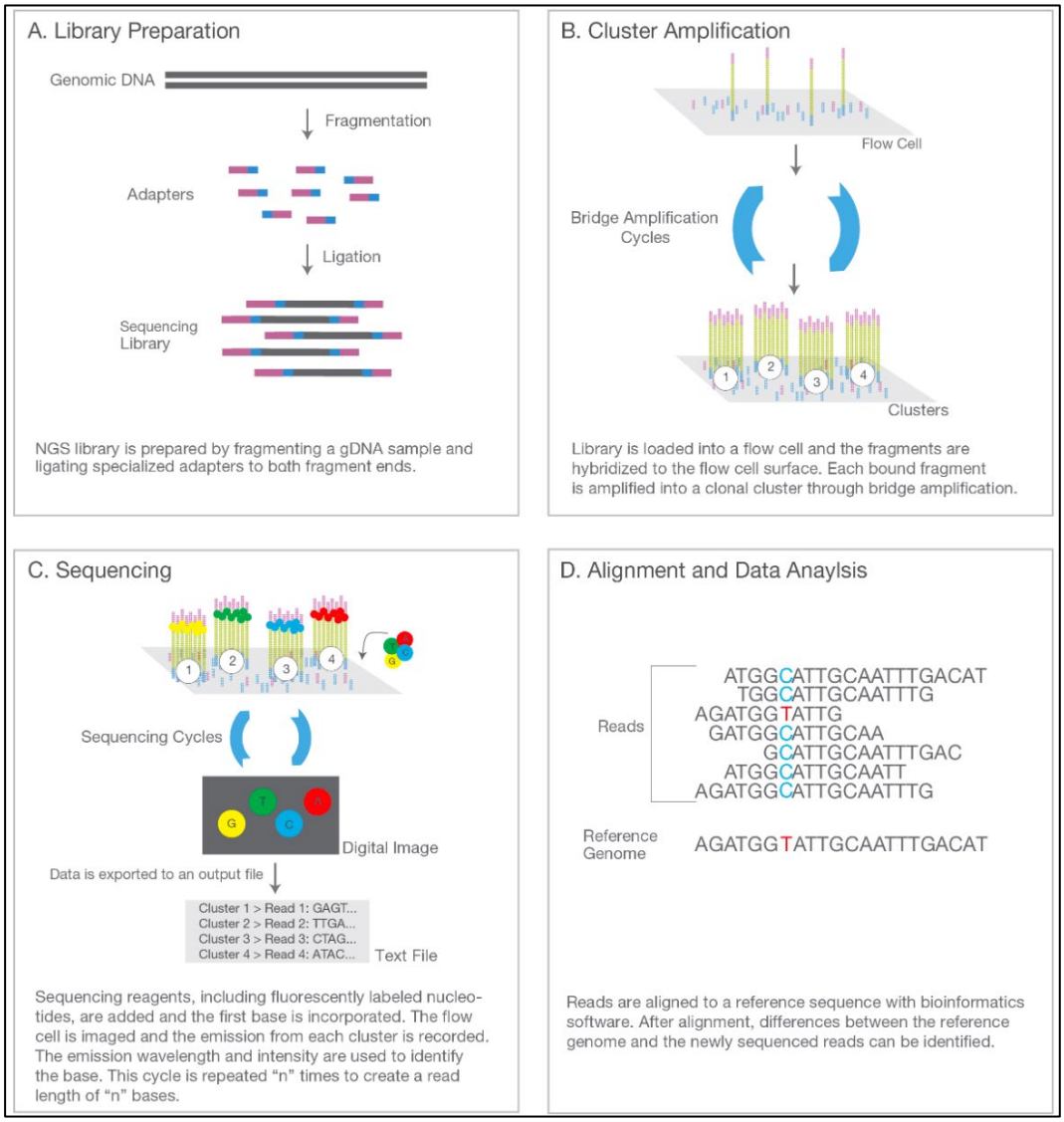

Illumina NGS workflow consists of four stages: (A) library preparation, (B) cluster generation, (C) sequencing, and (D) alignment and data analysis. NGS = next-generation sequencing. Reproduced from www.illumina.com.

Review of clinical data

Clinical records available at the NHNN as well as clinical information provided by external collaborators were extensively reviewed. Predefined data were extracted and tabulated, including gender, ethnicity, age at symptom onset, symptom(s) at onset, age at first assessment, age at last assessment, prominent movement disorder characterizing the phenotype, presence of different neurological and psychiatric symptoms/signs, history of developmental delay and/or regression, findings from laboratory, neuroimaging and other investigations, past medical and surgical history, pharmacological history, family history of neurological and/or psychiatric disorders, history of parental consanguinity, negative results of previous genetic tests, response to treatment. Phenotypic features were recorded as non-missing only if they were explicitly stated to be present or absent. For patients with long-term follow-up available, the likelihood that their disorder had a genetic etiology was re-assessed in view of the evolution of their clinical picture, response to treatment, and re-collection of anamnestic information or results of investigations which were not available at the time of recruitment for WES. Finally, for deceased patients, I recorded age of death and calculated disease duration according to the formula (age at death *minus* age at symptom onset).

Bioinformatic pipeline

WES data available were re-annotated and re-analyzed in one step and at once in order to absorb improvements in bioinformatics pipelines as well as the most recent updates in neurogenetics of movement disorders. Paired-end reads were aligned to the GRCh38 human reference using the Burrows-Wheeler Aligner BWA-MEM[132] and processed using the GATK best-practices to create BAM files.[133] Variants were called using GATK 4.1.4.0. Variants were annotated using Variant Effect Predictor.[134]

Variant filtering and functional analysis

WES data were analyzed according to an extended candidate-gene approach and, for cases with no promising findings after this stage, according to a hypothesis-free approach.

Candidate-gene approach

Based on main clinical diagnostic categories and main movement disorder phenotypes I identified in the study cohort by reviewing clinical data, I first analyzed WES data through an extended candidate-gene approach which aimed to prioritized variants in a large number of preselected genes (see Box III-1). Candidate genes included those linked to the historically so-called "NBIA syndromes" (10 genes) and "Fahr's disease" (currently "primary familial brain calcification" syndromes; 5 genes) as well as genes included in comprehensive and updated panels for early-onset dystonia (114 genes), Parkinson's disease and complex parkinsonism (66 genes), hereditary spastic paraplegia (107 genes), hereditary ataxia (254 genes), and mitochondrial disorders (473 genes) provided by the *Genomics England PanelApp* (https://panelapp.genomicsengland.co.uk). With the support of a bioinformatician (Prasanth Sivakumar), group-csv files containing protein-coding variants in the candidate genes which were non-synonymous and had a maximum allele frequency (MAX_AF) between 0.05 and 0.5 from the whole pool of exomes were created.

Box III-1. Candidate genes analyzed

Neurodegeneration with brain iron accumulation (NBIA): 10 genes
ATP13A2; C19orf12; COASY; CP; DCAF17; FA2H; FLT; PANK2; PLA2G6; WDR45.
Familial primary brain calcification (formerly Fahr's disease): 5 genes
SLC20A2; MYORG; PDGFB; PDGFRB; SPR.
Early onset dystonia (version: 1.86)*: 114 genes
ADAR; ADCY5; ANO3; APTX; ATM; ATP13A2; ATP1A3; ATP7B; BCAP31; C19orf12; CHMP2B; COASY; CP; CSTB; DCAF17; DDC; DLAT; FA2H; FBXO7; FTL; GCH1; GNAO1; HPCA; HTRA2; KMT2B; MECR; NKX6-2; PANK2; PINK1; PLA2G6; PNKD; PRKN; PRKRA; PRRT2; SERAC1; SGCE; SLC2A1; SLC30A10; SLC6A3; SPR; SYNJ1; TH; THAP1; TOR1A;

TUBB4A; VAC14; VPS13A; WDR45; WDR73; XK; YY1; CIZ1; GNAL; TAF1; ACTB; AFG3L2; AP1S2; ARSA; ARX; ATP1A2; AUH; CACNA1A; CYP27A1; DCTN1; DRD2; DRD5; EARS2; ERCC6; FASTKD2; FOXG1; FOXRED1; GAMT; GCDH; HPRT1; KCNQ2; L2HGDH; MAT1A; MCOLN1; MMADHC; MPV17; MR1; MT-ND6; NDUFA12; NPC2; PARK7; PCDH12; PDGFRB; PDHX; PLP1; PNPT1; PSEN1; PTEN; PTS; QDPR; RNASEH2A; RNASEH2B; RNASEH2C; SAMHD1; SCP2; SDHAF1; SLC19A3; SLC20A2; SLC39A14; SLC46A1; SUCLA2; SUOX; TIMM8A; TPK1; TREM2; TREX1; VPS37A; ATXN2_CAG; ATXN3_CAG; JPH3_CTG.
Parkinson disease and complex parkinsonism (version; 1.69)*: 66 genes
ATP13A2; ATP1A3; C19orf12; CSF1R; DCTN1; DNAJC6; FBXO7; FTL; GBA; GCH1; GRN; LRRK2; LYST; MAPT; OPA3; PANK2; PARK7; PINK1; PLA2G6; PRKN; PRKRA; PTRHD1; RAB39B; SLC30A10; SLC39A14; SLC6A3; SNCA; SPG11; SPR; SYNJ1; TH; TUBB4A; VPS13A; VPS35; WDR45; CHCHD2; TAF1; ANO3; ATP6AP2; ATXN2; ATXN3; C9orf72; EIF4G1; GIGYF2; GNAL; HTRA2; HTT; IPPK; JPH3; NR4A2; SGCE; SLC41A1; SNCAIP; TBP; THAP1; TOR1A; UCHL1; ATN1; ATXN1; ATXN2; ATXN3; C9orf72; HTT; JPH3; PPP2R2B; TBP.
Hereditary spastic paraplegia (version 1.219)*: 107 genes
ABCD1; ADAR; AFG3L2; AIMP1; ALDH18A1; ALS2; AP4B1; AP4E1; AP4M1; AP4S1; ARG1; ATL1; ATP13A2; B4GALNT1; BSCL2; C12orf65; C19orf12; CAPN1; CYP27A1; CYP2U1; CYP7B1; DDHD1; DDHD2; ERLIN1; ERLIN2; FA2H; FARS2; GBA2; HACE1; HSPD1; KIDINS220; KIF1A; KIF5A; L1CAM; NIPA1; NKX6-2; NT5C2; OPA3; PCYT2; PLP1; PNPLA6; POLR3A; REEP1; RNASEH2B; RTN2; SACS; SERAC1; SLC16A2; SLC1A4; SLC25A46; SLC2A1; SPART; SPAST; SPG11; SPG21; SPG7; TFG; TUBB4A; UBAP1; WASHC5; WDR45B; ZFYVE26; CDK16; DARS; GCH1; IBA57; KDM5C; KIF1C; LYST; MAG; MARS2; MTPAP; REEP2; SARS2; SLC33A1; AMPD2; AP5Z1; ARL6IP1; ARSI; CCT5; DSTYK; ENTPD1; GAD1; GJC2; KLC4; MARS; PCDH12; PGAP1; PSEN1; RAB3GAP2; TECPR2; USP8; VAMP1; VPS37A; WDR48; ZEB2; ZFYVE27; ATXN10_ATTCT; ATXN1_CAG; ATXN2_CAG; ATXN3_CAG; ATXN7_CAG; CACNA1A_CAG; FXN_GAA; HTT_CAG; PPP2R2B_CAG; TBP_CAG.
Hereditary ataxia – adult onset (version 2.42)*: 254 genes
AAAS; ABCB7; ABHD12; ADCY5; ADGRG1; ADPRHL2; AFG3L2; AMPD2; ANO10; AP1S2; APTX; ARMC9; ARSA; ATCAY; ATM; ATP1A2; ATP1A3; ATP7B; ATP8A2; B3GALNT2; B4GAT1; BRF1; CA8; CACNA1A; CACNA1G; CAMTA1; CAPN1; CASK; CHMP1A; CLCN2; CLN6; CLP; 1; COA7; COASY; COG5; COQ8A; COX20; CP; CSTB; CWF19L1; CYP27A1; CYP2U1; DARS2; DDHD2; DNAJC19; DNAJC5; DNMT1; EBF3; EIF2B1; EIF2B2; EIF2B3; EIF2B4; EIF2B5; ELOVL4; EPM2A; EXOSC3; EXOSC8; EXOSC9; FGF14; FLVCR1; FOLR1; FXN; GBA2; GFAP; GJC2; GLRA1; GLRB; GOSR2; GPAA1; GRID2; GRM1; HEXA; HEXB; IRF2BPL; ITPR1; KCNA1; KCNA2; KCNC3; KCND3; KCNJ10; KCNQ2; KIF1C; MAPK8IP3;

MARS2; MFN2; MMACHC; MRE11; MSTO1; MT-ATP6; MTTP; NHLRC1; NKX2-1; NKX6-2; NPC1; NPC2; OPA1; OPA3; OPHN1; PACS2; PEX16; PEX6; PLA2G6; PMPCA; PMPCB; PNKD; PNKP; PNPLA6; POLG; POLR3A; PRICKLE1; PRKCG; PRNP; PRRT2; PTRH2; PUM1; RARS2; RNF170; RNF216; ROBO3; RORA; SACS; SAMD9L; SCN1A; SCN8A; SCYL1; SEPSECS; SETX; SIL1; SLC1A3; SLC25A46; SLC2A1; SLC39A8; SLC52A2; SLC9A1; SLC9A6; SNX14; SPG7; SPR; SPTBN2; SQSTM1; SRD5A3; STUB1; SYNE1; SYNGAP1; TBC1D23; TERT; TMEM106B; TMEM240; TOE1; TPP1; TSEN15; TSEN2; TSEN54; TTBK2; TTPA; TUBA1A; TUBB2B; TUBB3; TUBB4A; TWNK; UBA5; UCHL1; VLDLR; VPS13D; VPS53; WDR73; WDR81; WFS1; WWOX; ZFYVE26; AARS; ATP2B3; DYNC1H1; EEF2; ELOVL5; GALC; GDAP2; KCNQ3; LNPK; MORC2; MTPAP; PEX2; SAR1B; VAMP1; VRK1; XRCC1; ALAS2; ATN1; ATXN1; ATXN10; ATXN2; ATXN3; ATXN7; ATXN8; BEAN1; CACNB4; CCDC88C; CDK5; DAB1; DCC; DMXL2; FMR1; FRMD4A; GLI3; HTT; KCNK18; MME; MVK; NAGLU; NOP56; PAX2; PAX6; PCLO; PDYN; PI4KA; PIK3R5; POLG2; PPP2R2B; RELN; RUBCN; SCN9A; SLC25A32; SLC6A5; SMPD4; SYT14; TBP; TDP1; TGM6; THG1L; TINF2; TSEN34; TTC19; TUBA8; TUBB; TUBB2A; UBR4; ZNF592; ATN1_CAG; ATXN10_ATTCT; ATXN1_CAG; ATXN2_CAG; ATXN3_CAG; ATXN7_CAG; CACNA1A_CAG; CSTB_CCCCGCCCCGCG; FMR1_CGG; FXN_GAA; NOP56_GGCCTG; PPP2R2B_CAG; TBP_CAG; ISCA-37404-Loss; ISCA-37478-Gain; ISCA-37478-Loss; ISCA-37468-Loss.

Mitochondrial disorders (version 2.34)*: 473 genes

AARS2; ABAT; ABCB7; ACAD9; ACO2; AFG3L2; AGK; AIFM1; ANO10; APOPT1; APTX; ATAD3A; ATP5D; ATPAF2; BCS1L; BOLA3; BTD; C12orf65; C19orf70; C1QBP; CA5A; CARS2; CHCHD10; CLPB; CLPP; COA6; COA7; COQ2; COQ4; COQ6; COQ7; COQ8A; COQ8B; COQ9; COX10; COX14; COX15; COX20; COX6A1; COX6B1; COX7B; CYC1; DARS2; DGUOK; DLAT; DLD; DNA2; DNAJC19; DNM1L; DNM2; EARS2; ECHS1; ELAC2; ETFDH; ETHE1; FARS2; FASTKD2; FBXL4; FDX2; FDXR; FH; FLAD1; FOXRED1; GARS; GDAP1; GFER; GFM1; GFM2; GLRX5; GTPBP3; HARS2; HCCS; HIBCH; HLCS; HSD17B10; HSPD1; HTRA2; IARS2; IBA57; ISCA1; ISCA2; ISCU; KARS; LARS2; LIAS; LIPT1; LIPT2; LONP1; LRPPRC; LYRM7; MARS2; MDH2; MECR; MFF; MFN2; MGME1; MICU1; MIPEP; MPC1; MPV17; MRPL3; MRPL44; MRPS2; MRPS22; MRPS34; MSTO1; MT-ATP6; MT-ATP8; MT-CO1; MT-CO2; MT-CO3; MT-CYB; MTFMT; MT-ND1; MT-ND2; MT-ND3; MT-ND4; MT-ND4L; MT-ND5; MT-ND6; MTO1; MTPAP; MT-RNR1; MT-TA; MT-TC; MT-TD; MT-TE; MT-TF; MT-TG; MT-TH; MT-TI; MT-TK; MT-TL1; MT-TL2; MT-TM; MT-TN; MT-TP; MT-TQ; MT-TR; MT-TS1; MT-TS2; MT-TV; MT-TW; MT-TY; NADK2; NARS2; NAXE; NDUFA1; NDUFA10; NDUFA11; NDUFA2; NDUFA4; NDUFA6; NDUFA9; NDUFAF1; NDUFAF2; NDUFAF3; NDUFAF4; NDUFAF5; NDUFAF6; NDUFAF8; NDUFB11; NDUFB3; NDUFB8; NDUFS1; NDUFS2; NDUFS3; NDUFS4; NDUFS6; NDUFS7; NDUFS8; NDUFV1; NDUFV2; NFU1; NUBPL; OPA1; OPA3; PARS2; PC; PDHA1; PDHB; PDHX; PDP1; PDSS1; PDSS2; PET100; PMPCA; PMPCB; PNPLA8; PNPT1; POLG;

POLG2; PPA2; PUS1; QRSL1; RARS2; RMND1; RNASEH1; RRM2B; RTN4IP1; SACS; SARS2; SCO1; SCO2; SDHA; SDHAF1; SDHD; SERAC1; SFXN4; SLC19A2; SLC19A3; SLC25A1; SLC25A12; SLC25A19; SLC25A26; SLC25A3; SLC25A32; SLC25A38; SLC25A4; SLC25A42; SLC25A46; SPG7; SUCLA2; SUCLG1; SURF1; TACO1; TAZ; TIMM50; TIMM8A; TK2; TMEM126B; TMEM70; TOP3A; TPK1; TRIT1; TRMT10C; TRMT5; TRMU; TRNT1; TSFM; TTC19; TUFM; TWNK; TYMP; UQCC2; UQCRB; VARS2; WARS2; YARS2; ATP5A1; ATP5F1; ATP5H; ATP5J2; ATP5L; ATP5L2; ATPAF1; COA3; COA4; COQ5; COX11; COX16; COX17; COX18; COX19; COX6A2; COX6B2; CYCS; DCC; ERAL1; G6PC; GATB; GATC; HPDL; IDH3A; IDH3B; MRM2; MRPS14; MRPS16; MT-RNR2; MT-TT; NDUFA12; NDUFAF7; NDUFB7; NDUFB9; NFS1; NSUN3; PITRM1; POLRMT; PTCD3; QARS; SDHAF3; SDHAF4; SDHB; SLC25A21; SPATA5; TARS2; TFAM; TIMM22; TIMMDC1; TMEM65; TOMM70; UQCC1; UQCC3; UQCR10; UQCR11; UQCRC2; UQCRQ; XPNPEP3; YME1L1; ABCB6; ACADM; ACADS; ACADSB; ACADVL; ACAT1; AK2; ALAS2; ALDH18A1; ALDH1B1; APOO; ATAD3B; ATP5B; ATP5C1; ATP5E; ATP5G1; ATP5G2; ATP5G3; ATP5I; ATP5J; ATP5O; BDH1; BOLA1; BOLA2; C19orf12; CEP89; CHKB; CISD2; CLPX; COA1; COA5; COASY; COX4I1; COX4I2; COX5A; COX5B; COX6C; COX7A1; COX7A2; COX7B2; COX7C; COX8A; CPT1A; CPT2; CRAT; CTBP1; CYP24A1; D2HGDH; DARS; DHTKD1; DIABLO; DIAPH1; DLST; DTD1; DYM; ECSIT; ERCC6L2; ETFA; ETFB; FA2H; FBP2; FGF12; FXN; GATM; GLUD1; GUF1; HADH; HADHA; HADHB; HMGCL; HMGCS2; HSPA9; HSPE1; HTT; IARS; IER3IP1; KIF5A; L2HGDH; LACTB; LARS; LETM1; LYRM4; MICU2; MRPL12; MRPL40; MRPS23; MRPS7; NAXD; NDUFA13; NDUFA3; NDUFA5; NDUFA7; NDUFA8; NDUFAB1; NDUFB1; NDUFB10; NDUFB2; NDUFB4; NDUFB5; NDUFB6; NDUFC1; NDUFC2; NDUFS5; NDUFV3; NNT; OGDH; OXA1L; OXCT1; PAM16; PANK2; PDE12; PDK1; PDK2; PDK3; PDK4; PDP2; PDPR; PET117; PLA2G6; PNPLA4; POP1; PPOX; PTCD1; PTRH2; PYCR1; ROBO3; SAMHD1; SDHAF2; SDHC; SECISBP2; SEPSECS; SLC22A5; SLC25A10; SLC25A13; SLC25A20; SLC25A22; SLC25A24; SLC25A40; SLC33A1; SLC39A8; SLC44A1; SLC52A2; SLC52A3; SRRT; SSBP1; STAT2; STXBP1; SUCLG2; TANGO2; TIMM44; TMEM126A; TRAK1; TRAP1; TXN2; UQCRC1; UQCRFS1; UQCRH; USMG5; VPS13C; WFS1; XRCC4; DMPK_CTG; FXN_GAA; ISCA-37440-Loss.

* Information on the process for gene inclusions in these panels is provided by the *Genomics England PanelApp* website (https://panelapp.genomicsengland.co.uk).

Variants obtained were manually looked through and further filtered to prioritize their functional analysis according to previous descriptions in the literature, frequency against the annotated control database gnomAD (version v3.1.1; http://gnomad.broadinstitute.org/) and the internal database of 17,701 exomes, and variant pathogenicity prediction according to *in silico* tools, including PolyPhen-2

(http://genetics.bwh.harvard.edu/pph2/), SIFT (http://sift.bii.a-star.edu.sg), and MutationTaster (http://www.mutationtaster.org/). The Combined Annotation Dependent Depletion (CADD) score (https://cadd.gs.washington.edu/snv) was also integrated to the prioritization criteria, with a conservative cut-off of 15 to determine deleteriousness. I referred to OMIM (https://omim.org/) and GeneCards (https://www.genecards.org/) as well as to Varsome (https://varsome.com/), ClinVar (https://www.ncbi.nlm.nih.gov/clinvar/) and the public version of HGMD (http://www.hgmd.cf.ac.uk/ac/index.php) for an overview of genes and variants, respectively. Variants were considered to have a causal association with the phenotype under investigation if they fulfilled the following criteria: 1) high sequencing quality (i.e., high number of reads), 2) known pathogenic or likely pathogenic variant reported in ClinVar and/or HGMD, 3) loss of function (LoF) variants occurring in known LoF-intolerant genes according to the ExAC database (now available for consultation at http://gnomad.broadinstitute.org/), or 4) missense variants predicted to be deleterious by at least 2 of the aforementioned *in silico* prediction tools and absent or very rare in the aforementioned population databases. Fitting with the model of inheritance known for the gene was required to confirm pathogenicity. Variants were finally interpreted according to the guidelines by the American College of Medical Genetics and Genomics (ACMG).[46]

Hypothesis-free approach

For cases with no promising findings from analysis of WES data according to the candidate-gene approach, I analyzed single exomes annotated as reported above following a hypothesis-free approach. Where an autosomal dominant mode of inheritance was suspected, heterozygous variants with minimum allele frequency (MAF) <0.001 (shared among affected individuals, if DNA from proband's relatives was available) were considered. *De novo* variants (i.e., variants detected in the proband but not detected in both proband's parents) were investigated through trio-WES and/or Sanger sequencing, where possible. If a recessive fashion of inheritance was suspected, homozygous, hemizygous or heterozygous (for compound heterozygosity) variants with MAF <0.005 were included. Variants were

further filtered and classified according to the criteria detailed in the previous subparagraph (see also chapter I, paragraph I-2).

Validation of NGS findings

I performed bi-directional Sanger sequencing to confirm promising findings from WES. Target-specific primers for the amplification of DNA regions of interest were designed and blasted using Primer3[135] and NCBI Primer-BLAST, respectively.[136] The protocol I used for Sanger sequencing is detailed in Box III-2. Briefly, Sanger sequencing consists of a first polymerase chain reaction (PCR) where, per sample, Fast-start Master Mix, H_2O, forward and reverse target-specific primers, and DNA are mixed in a standard 96-well plate or individual tubes, centrifuged and put on a thermal cycler. In a second step, the PCR product is checked for its expected size by running it on agarose gel using the principle of gel electrophoresis, which makes PCR fragments move at different speeds according to their size. The obtained gel is then visualized using UV light. If the correct size of the amplicon is confirmed, the remaining PCR product is cleaned up using the ExoSap method. The cleaned PCR product undergoes sequencing PCR followed by cleaning via the Sephadex method and sequencing on a 3730 DNA analyzer. Electropherograms were analyzed using Sequencher 4.1.4, Gene Codes Corporation, Ann Arbor, MI, USA, or FinchTV 1.4.0, Geospiza, Inc., Seattle, WA, USA.

If DNA from probands' family members was available, I performed segregation analysis. This step was unfortunately limited by the retrospective nature of the project, with several included participants deceased or not traceable at the time I performed analysis, and by ethical concerns about active recruitment of subjects for research purposes during the COVID-19 pandemic.

Finally, I critically analyzed results in the context of previous literature in order to identify possible phenotypic and genotypic elements of novelty, and I reviewed the in-house exome database and contacted external collaborators in order to replicate novel promising findings.

Box III-2. Sanger sequencing workflow

1. PCR

For each amplification reaction (total volume: 15ul):

- 7.5ul Fast-start Master Mix
- 5ul H_2O
- 0.75ul forward primer
- 0.75ul reverse primer
- 1ul DNA (concentration around 50ng/ul).

1. Make a master mix with the aforementioned products in an Eppendorf tube and divide into wells (14ul into each), except DNA (1ul) which is added last.
2. Centrifuge briefly to mix contents.
3. Run on thermal cycler at usually a touchdown (TD) program from 65° to 55°.

Thermal cycler program				
94°C - 10mins	8 cycles of: 94°C - 30sec 65°C - 30sec 72°C - 45sec	16 cycles of: 94°C - 30sec 65°C - 30sec* (TD -0.7°C) 72°C - 45sec	16 cycles of: 94°C - 30sec 55°C - 30sec 72°C - 45sec	72°C 5-10mins (final extension) 4°C - forever

Troubleshoot:
For difficult or G-C rich templates:
- add 20% of solution Q or 5-10% of DMSO
- more stringent TD program depending on melting temperature of primers.

2. Check PCR products on agarose gel (gel electrophoresis)

1. Prepare 2% agarose gel (mix 2g of agarose powder in 100mL of TBE 1x and heat in a microwave for roughly 2mins).
2. Add 6ul of Gel Red.
3. Pour into gel casting tray, add the combs, and let it set for 30mins.
4. Mix 3ul of loading dye with 7ul of PCR product and load onto gel.
5. Run at 100 V for 30mins.

3. Enzymatic PCR clean up

1. Transfer 5µl of PCR product to a clean plate.
2. Add 2µl ExoSAP-IT™ into each product, and pipette-mix.
3. Apply sticky lid, seal firmly.
4. Run on thermal cycler.

Thermal cycler program	
37°C - 15mins	80°C - 15mins

Box III-2 (continued). Sanger sequencing workflow

4. Preparing Sequencing reaction

In each sequencing reaction:

- 4.5ul H_2O
- 2ul sequencing buffer
- 1 ul primer (forward or reverse)
- 0.5ul Big Dye
- 2ul cleaned PCR product.

1. Make a mix with the aforementioned products in an Eppendorf tube and divide into wells (8ul into each), except cleaned PCR product (2ul) which is added last.
2. Centrifuge briefly to mix contents.
3. Run on thermal cycler.

Thermal cycler program	
94ºC - 1min	25 cycles of: 94ºC - 30sec 50ºC - 15sec 60ºC - 4mins

5. Sequencing clean-up with user-prepared Sephadex plates

1. Prepare Sephadex for each plate in a 50mL tube, with:
   - 40ml distilled water (autoclaved)
   - 2.9g Sephadex G-50 Bioreagent, DNA grade, fine
   - Mix well and allow the Sephadex to hydrate for at least 30mins at room temperature.
2. Prepare the purification plate by adding 350µl of the well-mixed Sephadex to each well of a Corning® FiltrEX™ 96-well filter plate, 0.66mm glass fiber filter, polystyrene.
3. Place the glass plate on an empty collection plate (prepare a balancing plate of equal mass) and centrifuge both for 3mins at 750xg.
4. Place glass plate onto a new plate (which will go to the sequencer) and pipette the entire volume of the sequencing reaction (10µl) from the sequencing plate onto the Sephadex columns.
5. Centrifuge for 5mins at 910xg (final volume after spinning is ~10µl).
6. Make sure you have liquid in all wells.
7. Put your sequencing plate is ready to go to the sequencer.

Statistical analysis

Descriptive statistics were performed using IBM SPSS Statistics for Macintosh (version 21). Results are presented as valid percentages (i.e., counts divided by the total number of non-missing observations) for dichotomous variables and median with interquartile range (IQR, weighted average) for continuous variables.
The diagnostic yield was calculated as the ratio of the number of patients fitting the inclusion criteria and having a confirmed or highly likely genetic diagnosis on the number of all patients included in the final clinical study cohort.

4. Results

Cohort description

The initial pool of exomes which were selected and included in the bioinformatic pipeline and generation of group-csv files corresponded to 139 individual cases. However, 11 cases were excluded from the clinical cohort results after the extensive review of clinical records since the etiology of their disorders appeared to be most likely nongenetic in view of additional clinical information and follow-up which become available since recruitment for WES (e.g., clinical picture most likely secondary to prolonged exposure to antipsychotic medications or brain lesions due to pre- or peri-natal complications, cerebrovascular disease, central nervous system infectious or inflammatory diseases).

Distribution of gender, ethnicity, and age of symptom onset is summarized in Figure III-2. Among the finally included 128 cases, gender (Figure III-2A) was unfortunately not reported in 9 cases (7.0%), and exact ethnicity (Figure III-2B) was missing in 39 cases (30.5%). Birth and perinatal history were unremarkable in 65/67 (97.0%) cases, whereas one patient was born premature, and one patient had prolonged jaundice in the neonatal period. Congenital nystagmus was observed in one case.

Figure III-2 – Gender, ethnicity, and age of onset distribution in the study clinical cohort

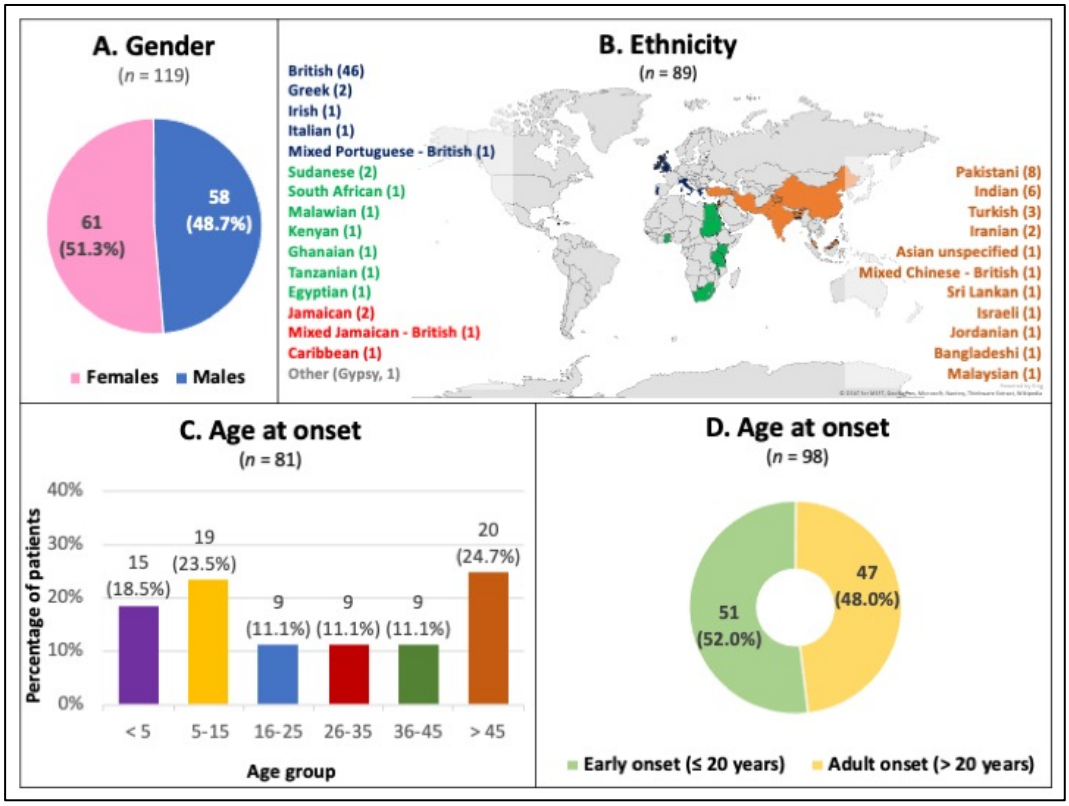

In the 81 cases (63.3%) where the exact information was specified, median age of symptom onset was 22.0 years (IQR 40.5), with the distribution into age groups of symptom onset detailed in Figure III-2C. Categorization of age at symptom onset into the two macro-groups “early-onset” (≤20 years) or “late-onset” (>20 years) was possible in a higher percentage of cases (98 out of 128, 76.6%; Figure III-2D), with early-onset (51 cases, 52.0%) and adult-onset (47 cases, 48.0%) phenotypes being almost equally represented. Presenting manifestations were trackable in 102 cases (79.7%) and are summarized in Figure III-3, with isolated dystonia (46 cases, 45.1%), isolated parkinsonism (14 cases, 13.7%), and neurodevelopmental delay (9 cases, 8.8%) being the most frequent clinical features at disease onset.

Figure III-3. Presenting phenotypic features in the study clinical cohort

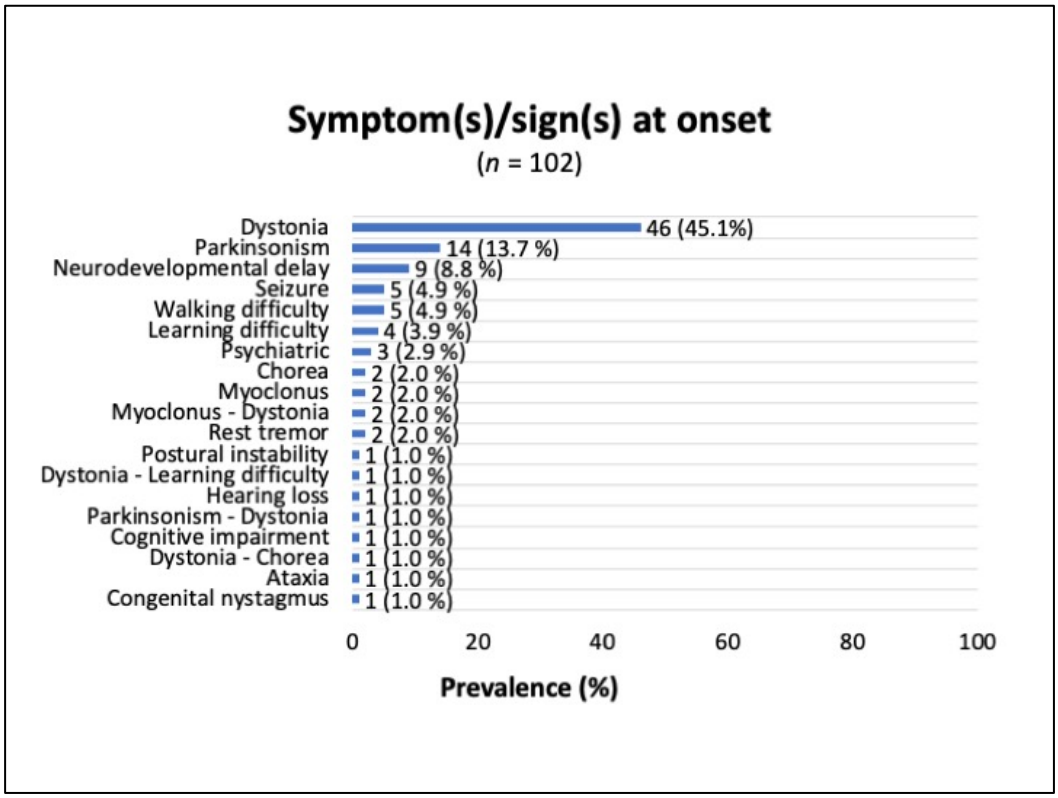

By reviewing descriptions or, where available, videos of the neurological examination, I could define the prominent movement disorder which characterized the phenotype in 113 cases (88.3%), with overt dystonia or dystonic tremor (58 cases, 51.3%), parkinsonism (20 cases, 17.7%), or an association of both dystonia and parkinsonism (8 cases, 7.1%) being the most represented (Figure III-4).

Figure III-5 plots the frequency of neurological and psychiatric symptoms present in the investigated cohort as absolute symptom count calculated out the total count of non-missing information regarding predetermined symptom categories reported on the Y-axis. Among 56 cases where the distribution was specified, dystonia was generalized in 30 (53.6%), focal in 12 (21.4%), segmental in 10 (17.8%), multifocal in 3 (5.4%), and affected one hemi-body only (hemi-dystonia) in one (1.8%). In the same sub-group, as expected in view of the inclusion criteria, the presence of (prominent) oromandibular dystonia was highlighted in 15 cases (26.8%).

Figure III-4. Main movement disorder phenotype in the study clinical cohort

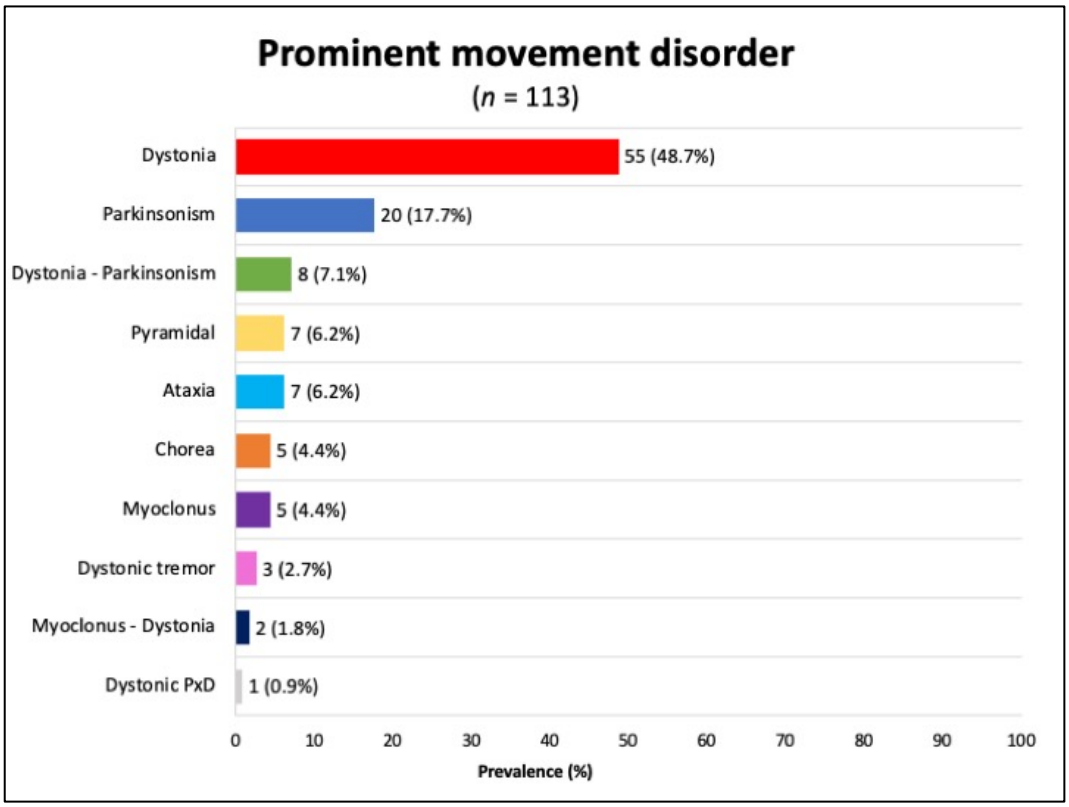

Legend: PxD = paroxysmal dyskinesia.

Figure III-5. Clinical symptoms in the study clinical cohort

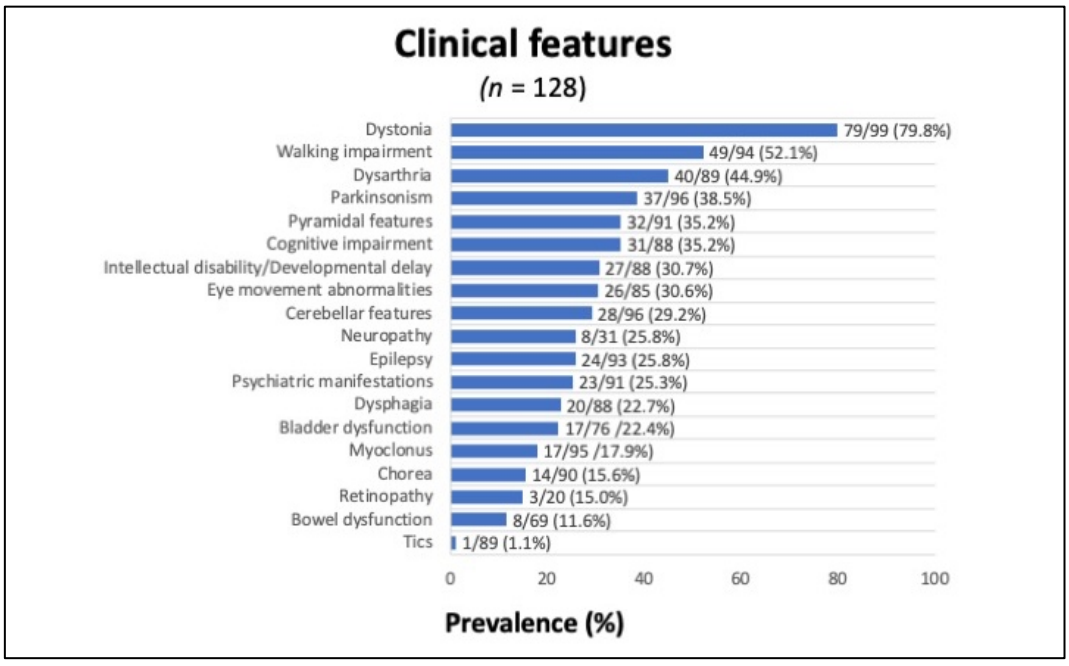

Brain MRI (Figure III-6) was available in 86/128 (67.2%) patients and unremarkable in 17 (19.8%) of them. Among abnormal brain MRI scans, 27 (31.4%) showed cerebral atrophy, 22 (25.6%) cerebellar atrophy, 30 (34.9%) evidence of mineralization of the basal ganglia, 23 (26.7%) T2-weighted hyperintensity of the white matter, and 14 (16.3%) other findings.

Figure III-6. Brain MRI features in the clinical study cohort

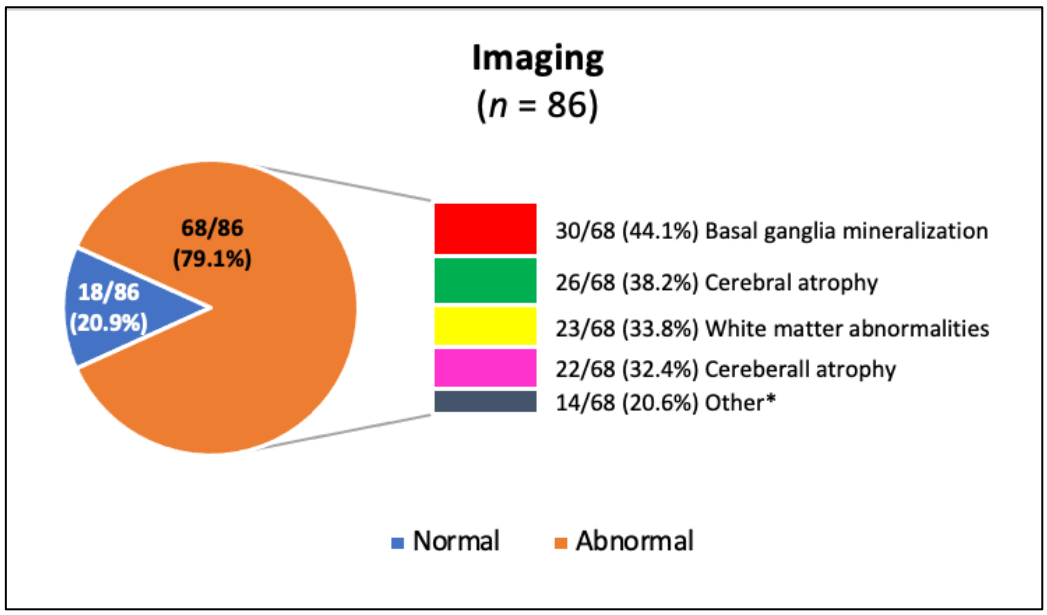

* Please refer to the main text for further details.

In particular, five cases displayed thin corpus callosum, one subject T2 hyperintensity of the dentate nuclei and surrounding cerebellar white matter, one patient pachygyria with perisylvian polymicrogyria and thickened cranial nerves (with clinical exclusion of leprosy), one case widespread microhaemorrhages, one subject focal T2 hyperintensity of the caudate head unilaterally, one patient a large developmental cortical malformation with polymicrogyria and cortical dysplasia, midsagittal plane abnormalities with absence of septum pellucidum, and abnormal olfactory bulb on one side, one case signal alteration within the pre-chiasmatic optic

nerve unilaterally, one subject findings "consistent with post-hypoxic changes" in the basal ganglia, one patient ventriculomegaly, and one case cystic areas in the basal ganglia on T1-weighted sequences corresponding to hyperintense signal on T2-weighted images. In 15/128 (11.7%) cases with a brain CT scan available, there was no evidence of intracranial calcifications. A DaTscan was performed in 25/128 (19.5%) cases and abnormal in 21.

A positive family history for neurological disorders was reported in 38 out of 98 cases (38.8) where information about the pedigree was available. There was a clear history of parental consanguinity in 12/128 (16.2%) and uncertain consanguinity in other 2/128 cases (2.7%).

Previous negative genetic testing was reported in 67/128 cases (52.3%) at the time of recruitment for WES, although this information was missing for several cases from external collaborator.

Median age at last assessment available was determined for 89/128 (69.5%) cases, being 46.0 years (IQR 24.5), and median disease duration at last assessment for cases with both age of onset and age at last assessment available (72/128, 56.3%) was 14.5 years (IQR 20.2). Eighteen patients were certainly deceased at the time clinical records were reviewed, with a median age at death of 60.0 years (IQR 27.7).

Genetic findings

Genetic cohort results refer to the initial pool of 139 exomes as the bioinformatic pipeline and generation of group-csv files were carried out before the extensive review of clinical records which led to the exclusion of 11 cases (see above). Coverage metrics were generated with the support of a bioinformatician (David Murphy) using GATK CollectWgsMetrics after a joint discussion.[137] Figure III-7 plots the percentage of the exome covered 10 (blue), 30 (orange), 60 (grey), and 90 (yellow) times (Y-axis, 0-0.9=0-90%) for each exome (X-axis). Since metrics were generated against the "padded" exome file also used for alignment (exons plus 100 bp on either side), it has to be acknowledged that the output shown slightly underestimates the actual coverage.

Figure III-7. Coverage metrics of the whole pool of exomes (n = 139)

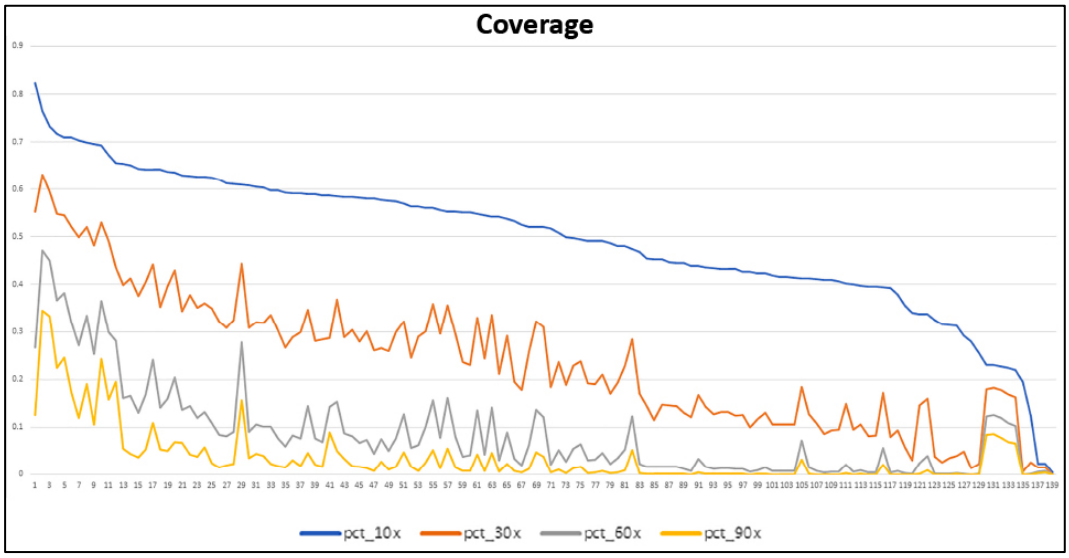

Figure generated by bioinformatician David Murphy after a joint discussion. Y-axis represents the percentage of exome covered 10 (blue), 30 (orange), 60 (grey), and 90 (yellow) times (Y-axis, 0-0.9=0-90%) based on the SureSelect V7 padded exome intervals, whereas single exomes are represented on X-axis.

Figure III-8 summarizes the variant filtering and functional analysis workflow. Following the candidate-gene approach for 139 analyzed samples, 2,027,294 coding variants were listed in the group-csv files, of which 319,686 were nonsynonymous, had maximum AF between 0.005 and 0.5 and were stop-gain, stop-loss, frameshift, nonsense or splice site variants. Of these, 42,602 lay within the predetermined candidate genes (see Box III-1). Manual curation was performed, including filtering for frequency, mode of inheritance, consistency between phenotype under investigation and gene under question, validation of promising findings by Sanger sequencing, and segregation analysis (where possible). This led to the identification of a confirmed or highly likely genetic etiology in 26 out of 128 cases included in the clinical study cohort (20.3%). A likely genetic cause was determined in additional three cases (2.3%), where no further genetic or functional tests in the proband or pedigree nor evidence from previous literature allowed to strengthen probabilistic assertions on variants' pathogenicity. Another three cases (2.3%) were solved by analyzing WES data through the hypothesis-free approach. Relevant genetic findings are detailed in the following sub-paragraphs. Thanks to

the availability of DNA from probands' relatives, segregation analysis was performed to confirm findings in *DRD2*, *ENSG00000165714*, *FA2H*, *NDUFA12, PLA2G6*, and *WARS2* mutation carriers. In summary, at least likely genetic causes were identified in 25.0% of patients (32 cases) included in the final clinical study cohort (n = 128) by analyzing WES results by a combination of candidate-gene and hypothesis-free approaches (see Methods).

In three "WES-negative" cases, alternative genetic tests performed simultaneously to the present study revealed the conclusive diagnosis. In one 59-year-old White British male presenting with a one-year history of severe anxiety, behavioral changes, and parkinsonism, Southern blotting revealed the presence of 20 CAG repeats on allele 1 and 44 ± 2 CAG repeats on allele 2 of the *HTT* gene, thus confirming the diagnosis of Huntington's disease. In one 37-year-old Pakistani female, who was the product of a consanguineous marriage and presented with a recent history of dystonia-parkinsonism and anxiety, multiplex ligation-dependent probe amplification (MLPA) revealed a known pathogenic homozygous deletion of exon 3 of the *PRKN* gene, thus leading to the diagnosis of *PRKN*-associated Parkinson's disease. Finally, a 22-year-old female of unspecified Asian origin, who presented with a history of global developmental delay, generalized dystonia, and emotional lability, and showed signal abnormality and volume loss in the striatum bilaterally with a little right caudate head focal hyperintense lesion, mild generalized cerebro/cerebellar atrophy, was found to carry the mutation m.627G>A in the *MT-TF* gene by mitochondrial DNA sequencing.

In 12 cases matching the inclusion criteria at the time of recruitment for WES and extensive review of clinical records, an analysis of the evolution of clinico-radiological picture at the end of this study revealed the likelihood of a genetic aetiology was very low. These mainly included patients with atypical parkinsonism (multiple system atrophy or progressive supranuclear palsy), some of whom with MRI evidence of iron deposition in the basal ganglia. By exclusion of these cases *a posteriori*, WES resulted to detect an at least likely genetic etiology in 27.6% of cases (32/116).

Figure III-8. Workflow of variant filtering and functional analysis

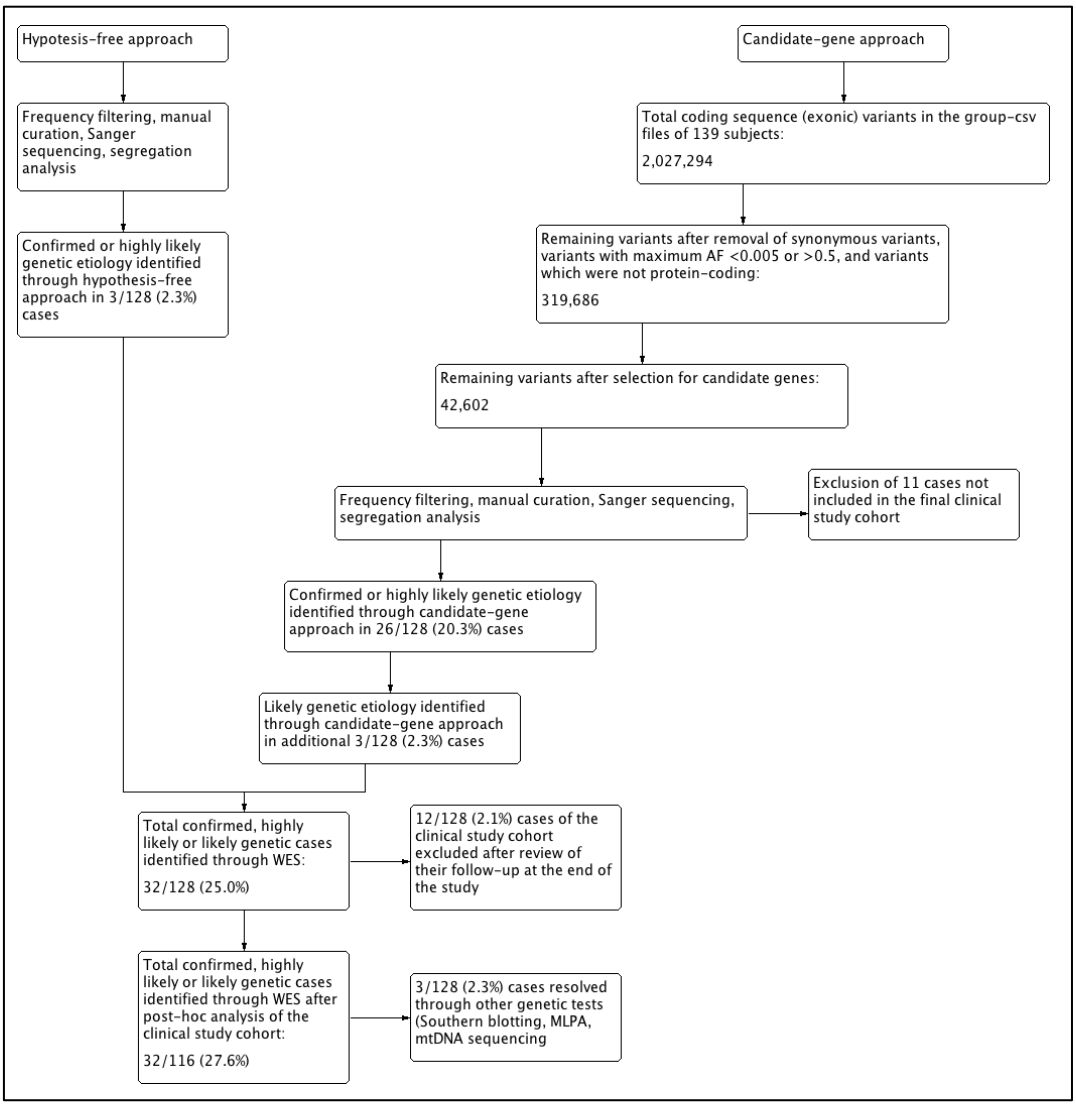

Legend: AF = allele frequency; MLPA = multiplex ligation-dependent probe amplification; mtDNA = mitochondrial DNA; WES = whole-exome sequencing.

Main genetic findings in single cases/pedigrees

Most relevant findings in single cases/pedigrees are detailed below in alphabetical order of their respective genes along with an overview of genes and previous evidence from the literature. Whenever findings from the present study gave me the opportunity to expand research to other internal cases and/or to cases from collaborators, this has been discussed in the relative sub-paragraphs.

C19orf12

One male of likely Brazilian origin was referred with the clinical suspicion of NBIA and found to carry the heterozygous nonsense variant NM_001256047:c.205C>T (p.Gln69Ter) in the *C19orf12* gene (Figure III-9), which has been linked to mitochondrial membrane protein-associated neurodegeneration (MPAN; OMIM #614297).

Figure III-9. Sanger sequencing in the heterozygous carrier of a nonsense *C19orf12* variant

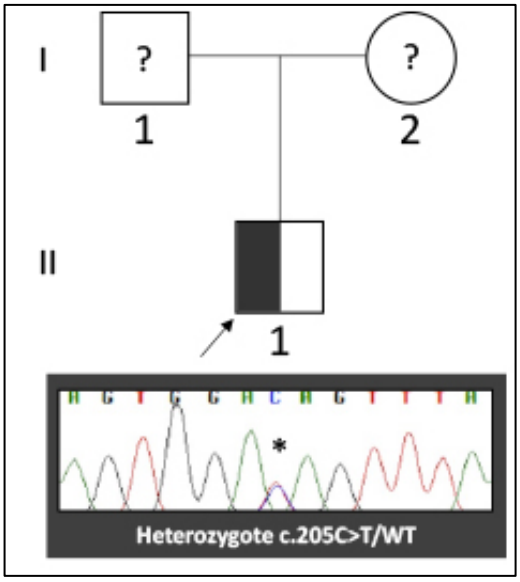

Sanger sequencing confirmed the proband was heterozygote for the variant NM_001256047:c.205C>T (p.Gln69Ter) in the *C19orf12* gene. The region was amplified using the following primers (5'→3'): F-ctcatggtgatggtggtgtg, R-ATCATACTGGATCTCGGCCC, with an amplicon size of 354 base pairs. The electropherogram was analyzed using the Sequencher software package. The mutation is highlighted by an asterisk. WT = wild type.

Unfortunately, further information on the proband's clinicoradiological features and family history was not trackable. Similarly, parents' DNA was not available for segregation analysis to establish if the transmission was autosomal dominant, or the variant occurred *de novo* in the proband.

The mutation detected is absent in gnomAD, has a CADD score of 45, and is predicted disease causing by MutationTaster. It is recorded pathogenic/likely pathogenic by multiple submitters in ClinVar and has previously been reported in three cases from two pedigrees by the Authors who have recently proposed an autosomal dominant mode of inheritance for MPAN, including one pedigree where *de novo* occurrence of this mutation was demonstrated in the proband.[138] As observed in their paper, this variant as well as other mutations described with an autosomal dominant or *de novo* occurrence affect nucleotides in the last (fourth) exon of the *C19orf12* gene. For this reason, the mutant transcript might escape nonsense mediated mRNA decay and cause disease through a toxic gain-of-function mechanism, which provides a possible explanation for the different fashion of inheritance in their cases compared to previous reports on MPAN.[138]

CACNA1A

A 60-year-old White British female presented with a longstanding history of head tremor since early childhood. She had a strong family history of dystonic tremor, including head tremor in her mother and tremor affecting the head and/or the upper limbs in her six siblings, which highly suggests a disorder with an autosomal dominant mode of inheritance. The proband had previously been tested negative for DYT-*TOR1A*, DYT-*SGCE* and expansions in the genes associated with the most common spinocerebellar ataxias (i.e., SCA1, SCA2, SCA3, SCA6, SCA7). On WES, I found the proband carried the missense variant NM_001127222:c.325A>T (p.Ile109Leu) in the *CACNA1A* gene. This mutation is absent in gnomAD, has a CADD score of 27.8, and is predicted pathogenic by all *in silico* prediction tools. Different types of monoallelic mutations in *CACNA1A*, which encodes the voltage-gated P/Q-type calcium channel subunit alpha-1A, are associated with a number of different phenotypes, including SCA6 (OMIM# 183086),[139] episodic ataxia type 2 (EA2; OMIM# 108500),[140] familial hemiplegic migraine type 1 (FHM1; OMIM# 141500)[141] with or without progressive cerebellar ataxia, benign paroxysmal torticollis of the infancy,[142] early infantile epileptic encephalopathy,[143] and paroxysmal head tremor.[144] Of the first three allelic disorders mentioned, SCA6 is

a polyglutamine disorder caused by a 20-to-33 CAG triplet expansion in exon 47 of *CACNA1A*,[139] whereas EA2 and FHM1 are due to *CACNA1A* loss-of-function mutations and gain-of-function missense mutations, respectively.[140, 141] *CACNA1A*-related disease phenotypes described more recently have revealed that there is a wide phenotypic overlap between hemiplegic migraine, diverse forms of cerebellar dysfunction and epilepsy, and that genotype-phenotype correlation might be not as strict as initially reported. For example, both loss-of-function and gain-of-function *CACNA1A* mutations cause severe developmental epileptic encephalopathies in the spectrum of Lennox-Gastaut syndrome and congenital ataxia.[143]

Unfortunately, no family members were available to test segregation, and the variant has therefore to be considered of unknown clinical significance. Nevertheless, the absence of the variant in the population database gnomAD, its pathogenicity predictions by *in silico* tools, the phenotype herein described, and the consistency between the suggested transmission in this pedigree and the known mode of inheritance of *CACNA1A*-related disorders suggest this finding is at least worthy of consideration should any evidence emerge from future cases/literature.

COASY

In one female patient referred by an external collaborator for early-onset severe generalized dystonia with prominent involvement of the lower limbs and clinicoradiological suspicion of NBIA, I detected the heterozygous variant NM_025233:c.1357C>T (p.Arg453Ter) in the *COASY* gene, which was confirmed by Sanger sequencing (Figure III-10). This nonsense variant has two heterozygous entries in gnomAD, has a CADD score of 36, and is predicted disease causing by MutationTaster. The variant has not been reported in the literature so far. Extensive review of the proband's WES data by removing all applied filters (see Methods) failed to identify a second mutation in this gene, which has hitherto been reported with an autosomal recessive mode of inheritance only. Therefore, the possibility of COASY protein-associated neurodegeneration (CoPAN), albeit being possibly consistent with the phenotype, remains purely speculative at present and will be further explored through non-NGS-based genetic testing.

Figure III-10. Sanger sequencing in the heterozygous carrier of a nonsense *COASY* variant

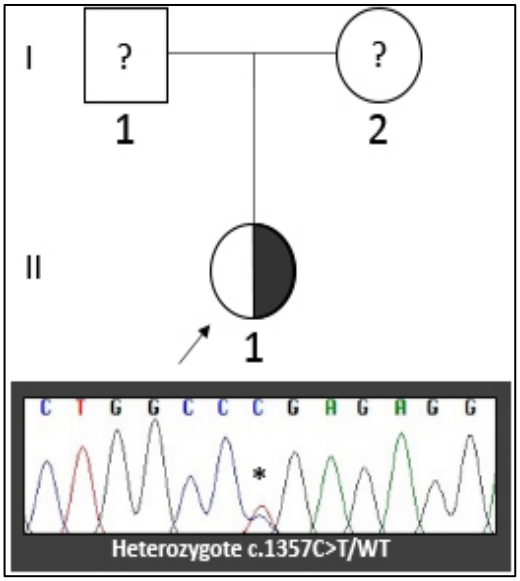

Sanger sequencing confirmed the proband carried the variant NM_025233:c.1357C>T (p.Arg453Ter) in the *COASY* gene in the heterozygous state. The region was amplified using the following primers (5'→3'): F-cctaagccgctactagaccc, R-tgaacagacagtcccacgtt, with an amplicon size of 333 base pairs. The electropherogram was analyzed using the Sequencher software package. The mutation is highlighted by an asterisk. WT = wild type.

DCTN1

One middle-aged White British female presented with a history of premature birth, mild intellectual disability, epilepsy since childhood, along with a complex neuropsychiatric syndrome characterized by parkinsonism, pyramidal signs, stimulus-sensitive myoclonus, central apnea (for which she had tracheostomy), severe anxiety, and "poor communication". Deep phenotyping and family history collection were limited since the patient was lost to follow-up at the time of this study. Interestingly, her brother was reported to have a similar phenotype, including parkinsonism with prominent axial involvement, pyramidal signs, stimulus-sensitive myoclonus, and central apnea. The proband's brain MRI showed global atrophy, with no signal abnormalities in the basal ganglia or cerebral white matter, and her DaTscan showed evidence of nigrostriatal degeneration. Her EMG revealed myopathic changes, whereas plasma amino acids, urine organic acids, and plasma

and CSF lactate were unremarkable. She had normal karyotype, and her mitochondrial DNA sequencing was negative.

By analyzing the proband's WES data, I detected the missense variant NM_001190837:c.211G>A (p.Gly71Arg) in the *DCTN1* gene, which was confirmed by Sanger sequencing (Figure III-11). Unfortunately, no DNA samples from family members were available for segregation analysis.

Figure III-11. Pedigree and Sanger sequencing of the *DCTN1* variant carrier

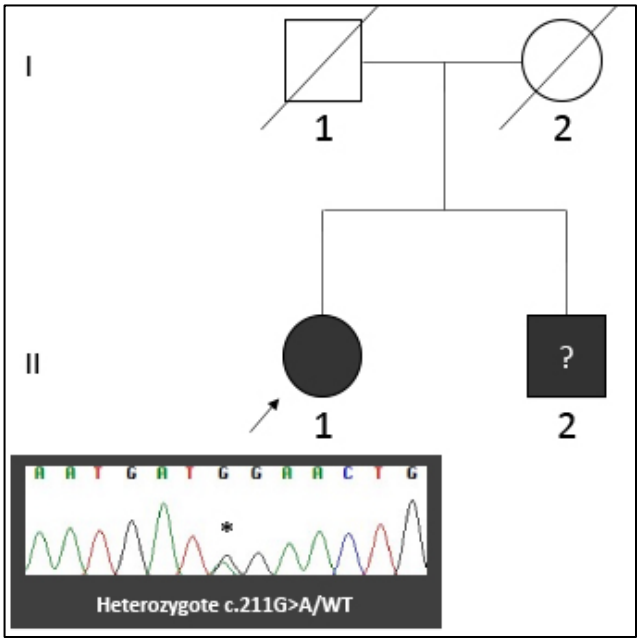

Sanger sequencing confirmed the proband was heterozygote for the variant NM_001190837(*DCTN1*):c.211G>A (p.Gly71Arg). The region was amplified using the following primers (5'→3'): F-tctgaggcctctaactgtctg, R-gacacaaaagaagggcgtga, with an amplicon size of 311 base pairs. The electropherogram was analyzed using the Sequencher software package. The mutation is highlighted by an asterisk. WT = wild type.

The *DCTN1* gene maps on chromosome 2p13.1, encodes the largest subunit of the dynactin complex, which binds directly to microtubules and to cytoplasmic dynein, a microtubule-based biologic motor protein, and has hitherto been linked to Perry syndrome (OMIM# 168605), as well as other neurological phenotypes with first and/or second motor neuron involvement.[145] Perry syndrome is a rare autosomal

dominant disorder whose main phenotypic features are parkinsonism, central hypoventilation, weight loss, and depression or other psychiatric symptoms. Its penetrance is about 50%.[146] TDP-43 pathology has been documented in Perry syndrome, thus indicating a pathological overlap with amyotrophic lateral sclerosis and some forms of frontotemporal lobar degeneration.[146-148]

The *DCTN1* variant herein detected is absent in gnomAD, is predicted pathogenic by all *in silico* prediction tools, including a CADD score of 29.4, and is recorded as pathogenic in ClinVar. It affects a highly conserved amino acid residue within the GKNDG binding motif of the CAP-Gly domain. This mutation was originally reported in two pedigrees of Canadian and Turkish ancestry, respectively, and then described worldwide.[147, 149] Different mutations in the same codon (Gly71Glu, Gly71Ala) of the *DCTN1* gene have been described in several families with Perry syndrome, thus suggesting exon 2 of the gene might represent a mutational hotspot.[146]

Although missing information about the proband's follow-up and family history as well as the lack of segregation analysis limit the strength of the finding, the coexistence of atypical parkinsonism and central respiratory involvement in two siblings suggest an autosomal dominant mode of inheritance and make the genetic finding in the *DCTN1* gene herein reported at least likely associated with the phenotype under investigation.

DRD2

This 27-year-old Greek male, second child from non-consanguineous parents, presented with a history of difficulty in sitting still and generalized choreiform movements and myoclonic jerks since the age of six months. During early childhood, he was diagnosed with attention deficit hyperactivity disorder, mild intellectual disability, learning difficulties, anxiety, and social withdrawal. During teenage years, he developed walking difficulties with recurrent falls, as well as behavioral issues with occasional aggressiveness. His birth, perinatal history and past medical history were otherwise unremarkable. He did not have any family history of neurological or psychiatric disorders. Neurological examination at age

20 revealed oculomotor apraxia, generalized chorea, intermittent myoclonus involving the neck and upper limbs, and a broad-based gait with left foot dystonia. There were no pyramidal nor parkinsonian signs. His serum ceruloplasmin, lysosomal enzymes, plasma amino acids, urine organic acids, brain MRI, EEG, metabolic screening, CSF analysis (including pterins and neurotransmitter metabolites) were normal. Formal neuropsychometry revealed severe cognitive dysfunction, although his cooperation was suboptimal during the assessment.

Trio-WES (proband, parents) detected the proband carried the *de novo* missense variant NM_000795:c.1121T>G (p.Met374Arg) in the *DRD2* gene, which I confirmed by Sanger sequencing (Figure III-12, pedigree A).

The *DRD2* gene encodes the dopamine receptor 2 (D2R).[150] The aforementioned *DRD2* variant is absent in gnomAD, is predicted pathogenic by all *in silico* prediction tools, including a CADD score of 29.4, and affects an amino acid residue completely conserved across species down to invertebrates (Figure III-12, lower part).

Prior to this finding, the *de novo* variant NM_000795:c.634A>T (p.Ile212Phe) in *DRD2* was reported in a single Dutch pedigree with an early-onset complex movement disorder featuring chorea and dystonia by van der Weijden et al.[151] However, no additional *DRD2* variants were detected by the Authors in a cohort of 121 chorea cases of undetermined genetic etiology, thus leaving the causal association between the variant and phenotype unconfirmed.

By reviewing the in-house exome database and contacting external collaborators, we found an unrelated subject carrying the heterozygous variant NM_000795:c.1121T>G (p.Met374Arg) in *DRD2*, which was confirmed to be *de novo* by trio-WES followed and confirmed by Sanger sequencing (Figure III-12, pedigree B). The carrier was a 3-year-old Chilean girl who presented at the age of four months with chorea involving the upper limbs, trunk and tongue. She had global developmental delay, with independent sitting achieved at 15 months and walking at two years. She did not have any expressive language but understood some words. Neurological examination at age three showed generalized choreiform movements, which also involved her tongue, and axial hypotonia. Her brain MRI,

EEG, metabolic screening, CSF neurotransmitters, serum ceruloplasmin, plasma amino acids, urine organic acids, and lysosomal enzymes were unremarkable.

Figure III-12. Segregation analysis of a novel *DRD2* variant in two pedigrees with chorea/choreo-dystonia

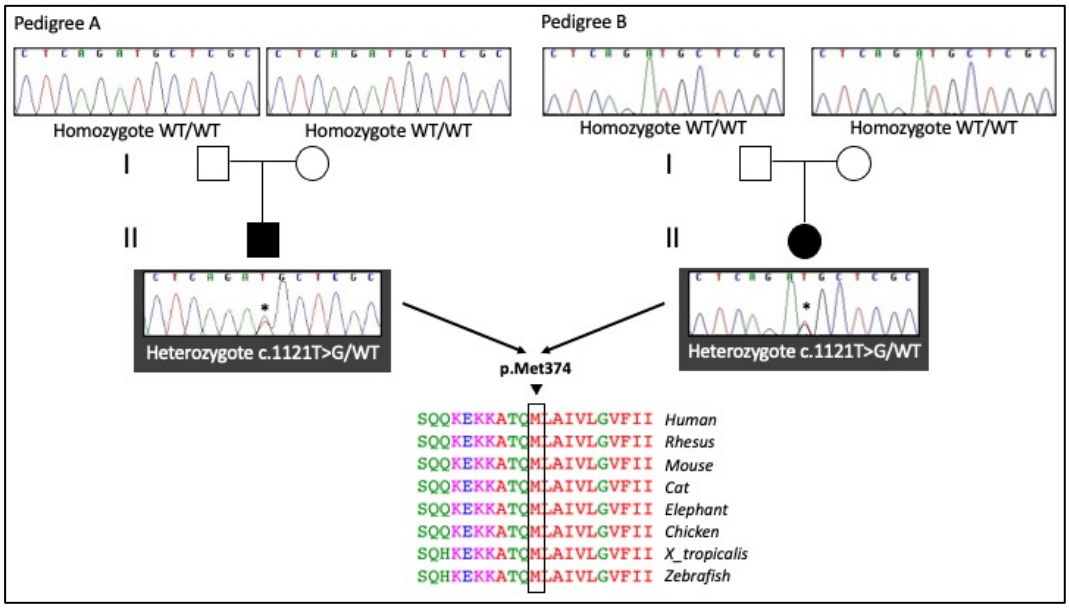

Upper part. Segregation analysis confirmed the proband in both families carried the *de novo* variant NM_000795:c.1121T>G (p.Met374Arg) in the *DRD2* gene. The region of interest was amplified using the following primers (5'→3'): F-AGCCACCACCAGCTGACTCT, R-CTGTGCCTGAGGAAATGCTA, with an amplicon size of 352 base pairs. Electropherograms were analyzed using the Sequencher software package. The mutation is highlighted by an asterisk. WT = wild type. *Lower part.* The *DRD2* variant affects an amino acid residue completely conserved across species down to invertebrates. Multiple sequence alignment was analyzed using Clustal Omega.[152]

Analysis of WES data from both our family trios did not detect any other potential candidate mutations, including other *de novo* or bi-allelic likely pathogenic variants or variants in known genes linked to monogenic movement disorders.

In support of its pathogenic role, the amino acid substitution p.Met374Arg is located in the protein sixth transmembrane domain, which forms part of the binding pocket core for D2R agonists. A missense mutation at the same residue

(p.Met374Leu) was previously demonstrated to shift the ligand-free D2R towards its active conformation,[153] therefore suggesting that a similar activation mechanism might occur for p.Met374Arg. The p.Ile212Phe variant was also shown to determine increased agonist potency and constitutive activation,[151] thus supporting that heterozygous *DRD2* variants are pathogenic through a gain-of-function mechanism.

Overall, our two cases have provided definitive evidence to support the pathogenic role of monoallelic *DRD2* variants in early-onset chorea and choreo-dystonia, thus justifying the inclusion of *DRD2* in the diagnostic workup of idiopathic early-onset hyperkinetic movement disorders. In addition, compared to the Dutch cases previously reported,[151] the new *DRD2* cases herein described have expanded the age of symptom onset to as early as four months and showed that developmental delay, myoclonus and cognitive and neuropsychiatric dysfunction can be part of the phenotype associated with *DRD2*.

Findings on DRD2 have been reported as a Letter: Published Article in Movement Disorders (Reference: Mencacci NE, Steel D, ***Magrinelli F****, Hsu J, Keller Sarmiento IJ, Troncoso Schifferli M, Muñoz D, Stefanis L, Lubbe SJ, Wood NW, Kurian MA, Stamelou M. Childhood-onset chorea caused by a recurrent de novo DRD2 variant; accepted on March 19, 2021).*

ENSG00000165714

A 23-year-old Pakistani male, product of a non-consanguineous marriage, presented with a history of global developmental delay, regression of acquired babbling, epilepsy since the age of three, and early-onset generalized dystonia with superimposed dystonic spasms since teenage years. On neurological examination (age 18) he showed dysmorphic features (short stature, strabismus, short forehead, and scoliosis). He was anarthric and PEG-fed. There was upgaze restriction, severe generalized dystonia with intermittent superimposed extensor spasms, and hyperreflexia. His birth was unremarkable. He had an elder sister with a similar, albeit more severe, clinical picture. His brain MRI revealed widespread white matter changes (images not available), whereas metabolic screening, CSF analysis (including pterins and neurotransmitter metabolites), serum ceruloplasmin, plasma

amino acids, and lysosomal enzymes were unremarkable. His sister's brain MRI showed dolichocephaly and severe generalized neuroparenchymal volume loss, marked reduction of white matter bulk, marked thinning of the corpus callosum and brainstem (Figure III-13A), T2/FLAIR hyperintensity in the white matter of the cerebral hemispheres (Figure III-13B), but no evidence of iron deposition on SWI sequences. His sister's electroretinogram and flash visual evoked potentials were reported to be normal during childhood, thus likely excluding retinal and optic nerve involvement.

Figure III-13. Brain MRI findings in the proband's affected sister

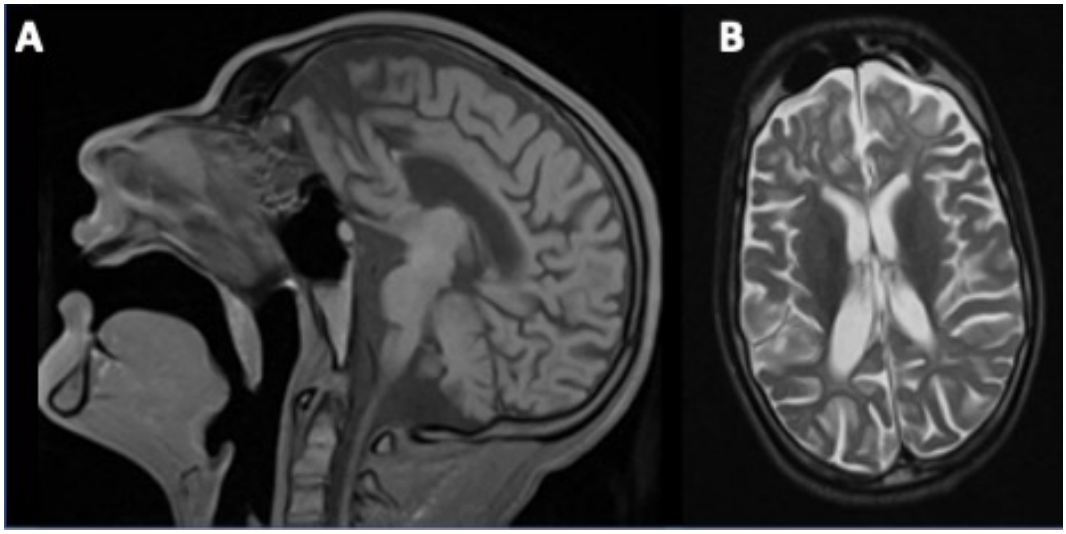

Brain MRI: (A) T1-weighted image showing cerebro/cerebellar atrophy, including the brainstem, reduction of white matter bulk, and thin corpus callosum; (B) diffuse T2 hyperintensity of the white matter of both hemispheres.

In the proband, a hypothesis-free approach for WES data analysis revealed two heterozygous variants (one missense, one nonsense) in a promising candidate gene (*ENSG00000165714*) which encodes one subunit of a protein complex involved in regulating lysosome positioning[154] and has not been hitherto linked to any human disease. The missense variant is absent in gnomAD, has a CADD score of 27.3, and is predicted pathogenic by all *in silico* prediction tools. The frameshift variant resulting in a premature stop codon has only one heterozygous entry in gnomAD,

has a CADD score of 32, and is not present in ClinVar. Sanger sequencing in the proband's similarly affected sister and their unaffected parents confirmed that both affected siblings were compound heterozygotes for the two variants mentioned above.

In two other British pedigrees, genetic testing on aborted fetuses with evidence of severe contractures of the extremities revealed different variants in the same gene. Functional tests to support the pathogenicity of these findings are ongoing. This collaborative project is led by Dr Niccolo Mencacci. For the sake of confidentiality and embargo policy, no other information on this gene is reported in the present thesis. Nevertheless, these preliminary findings were overall worth mentioning since they potentially confirm the endo-lysosomal compartment as one of the emerging biological pathways of monogenic dystonia (see chapter I).

FA2H

A 33-year-old White British male, who was born to non-consanguineous parents, had normal delivery and neurodevelopmental milestones till the age of 2 years, when he was first noticed to run on his tiptoes. At age 4, when he started going to school and doing gymnastics, his walking was reported having subtle abnormalities. Gait difficulties gradually progressed to an over spastic paraparesis, and he was still able to walk independently until the age of 8 when he needed bilateral Achilles tendon lengthening. He lost his independent gait at the age of 12. His upper limbs were affected to a lesser degree starting from the second decade. His past medical history also included generalized epilepsy since the age of 9. His younger sister was affected with spastic paraparesis but had no history of seizures. The proband's brain MRI revealed cerebellar atrophy and diffuse white matter T2 hyperintensity.

On WES, I found the proband carried two heterozygous variants in the *FA2H* gene, i.e. the nonsense variant NM_024306:c.782dupA (p.His261GlnfsTer52) and the missense variant NM_024306:c.798C>G (p.Asp266Glu). To verify whether the variants were in *trans* configuration, I performed segregation analysis in the two family members for whom DNA was available, that is his father and affected sister.

The proband's affected sister carried both the above-mentioned mutations, whereas their father only carried the missense mutation (Figure III-14).

Figure III-14. Segregation analysis in the *FA2H* pedigree

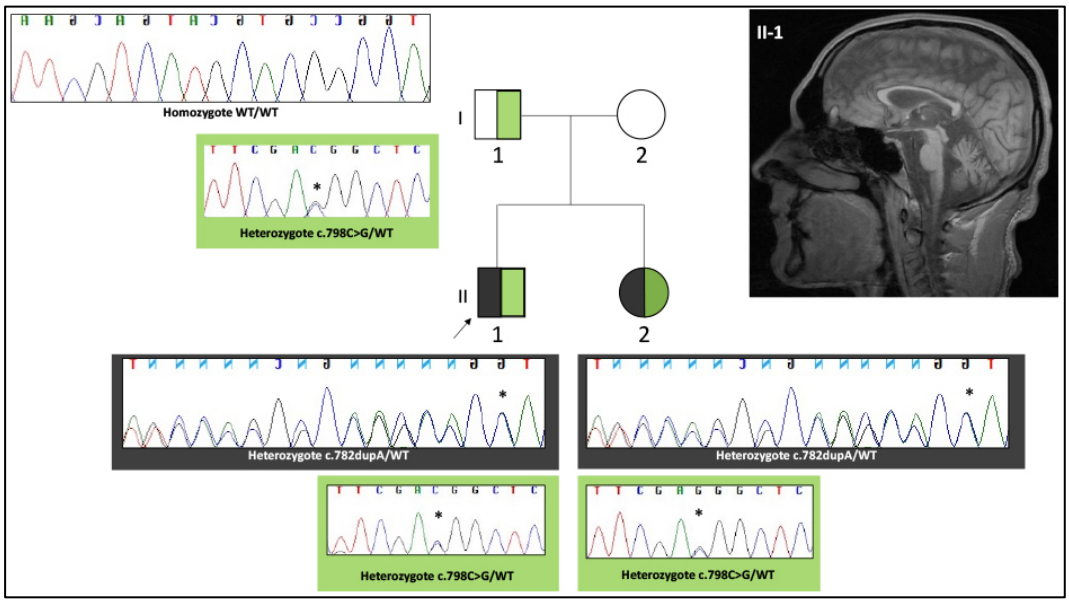

Segregation analysis confirmed the proband (II-1) and his affected sister were compound heterozygote for two variants in the *FA2H* gene, i.e. NM_024306:c.782dupA (p.His261GlnfsTer52; grey) and NM_024306:c.798C>G (p.Asp266Glu; green), the latter being inherited from their father. The region of the missense variant was amplified using the following primers (5'→3'): F-cccatcccatgttcctttgc, R-aaccctctgtatatgccccg, with an amplicon size of 617 base pairs, whereas the region of the nonsense variant was amplified using a different primer set (5'→3'): F-GGAGCCTCATCGAGTACCTC, R-gagtcacatcaaacgtcccg, with an amplicon size of 249 base pairs. Electropherograms were analyzed using the Sequencher software package. Mutations are highlighted by asterisks. Arrow = proband; WT = wild type.

In humans, biallelic mutations in the *FA2H* have been associated with a phenotypic spectrum including neurodegeneration with brain iron accumulation (fatty acid hydroxylase-associated neurodegeneration, FAHN), hereditary spastic paraplegia (HSP) type 35, and leukodystrophy with spasticity and dystonia.[155] Phenotypic features in the proband were consistent with previous reports on *FA2H*-related disorders, including the association of spastic paraparesis and epilepsy as well as MRI evidence of white matter abnormalities and lack of iron deposition in the basal

ganglia.[155] The variant NM_024306:c.782dupA p.(His261GlnfsTer52) results in a truncated mRNA transcript which is likely to undergo nonsense mediated mRNA decay. It is absent from gnomAD and can be classified as pathogenic. The missense variant NM_024306:c.798C>G (p.Asp266Glu; green) is likely pathogenic. It is absent from gnomAD and is predicted pathogenic by all *in silico* prediction tools, including a CADD score of 17.6. It alters a highly conserved amino acid residue in a functional domain of the FA2H protein.

FASTKD2

One 27-year-old male born to a consanguineous couple of South-East Asian origin presented with recent-onset oromandibular dystonia and dysarthria. He complained of difficulty chewing and swallowing. He had a history of obsessive-compulsive disorder and depression, without any exposure to antipsychotic medications, and had had a singular seizure in his 20s. His brain MRI was reported to be unremarkable, although it was not clear if T2*/SWI sequences had been performed. On WES, the proband was found to be homozygote for the variant ENST00000236980:c.712G>C (p.Ala238Pro) in the *FASTKD2* gene (Figure III-15). I could not find any promising variants in other genes related to early-onset dystonia or NBIA (*ANO3, ATP13A2, ATP1A3, C19orf12, DCTN1, FBXO7, GCH1, GNAL, PANK2, PLA2G6, SGCE, SLC6A3, SPR, TAF1, TH, THAP1, TOR1A, TUBB4A, WDR45*) nor NBIA. The variant has three heterozygous but no homozygous entries in gnomAD, is predicted pathogenic by SIFT and MutationTaster, has a CADD score of 17.4, and can be classified as of unknown significance. *FASTKD2* encodes a FAS-activated serum-threonine kinase domain 2 which locates in the mitochondrial inner compartment and has been associated with combined oxidative phosphorylation deficiency-44. Bi-allelic nonsense mutations in *FASTKD2* gene have hitherto been associated with childhood-onset mitochondrial encephalopathy, but it has been suggested that missense mutations might account for adult-onset milder phenotypes. The history of adult-onset dystonia and isolated seizure makes this finding at least intriguing and worthy of consideration should further evidence emerge from additional cases.

Figure III-15. Functional analysis of a missense VUS in *FASTKD2*

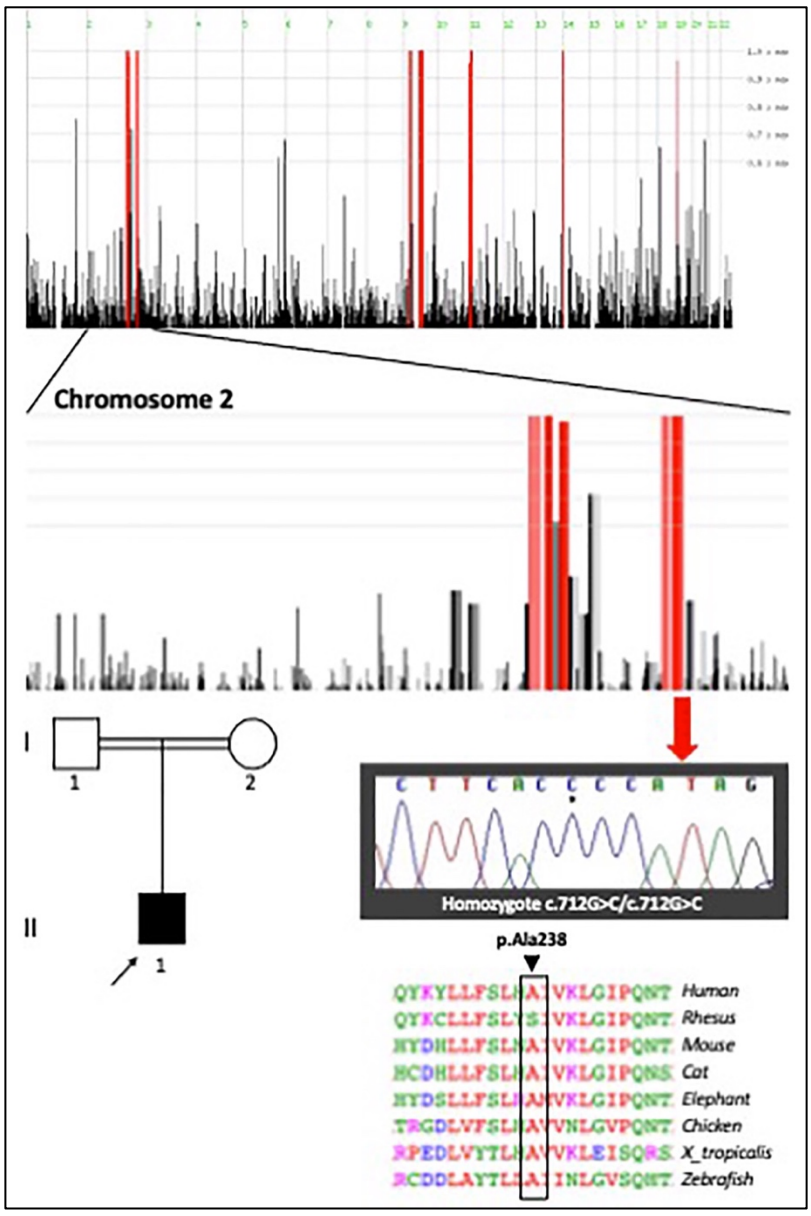

Homozygosity mapping on the proband (upper part) performed with Homozygosity Mapper (www.homozygositymapper.org) revealed a peak on chromosome 2 (middle part) whose genomic coordinates included those of *FASTKD2*. Lower part: Sanger sequencing confirmed the proband was homozygote for the variant ENST00000236980:c.712G>C (p.Ala238Pro) in the *FASTDK2* gene. The region was amplified using the following primers (5'→3'): F-CTGATGTTTAGCCACCCTGC, R-tctactgggcctgaattcca, with an amplicon size of 530 base pairs. The electropherogram was analyzed using the Sequencher software package. The mutation is highlighted by an asterisk. The *FASTKD2* variant affects an amino acid residue highly conserved across species down to invertebrates. Multiple sequence alignment was analyzed using Clustal Omega.[152] VUS = variant of unknown significance.

FTL

In two unrelated White British females, I detected the pathogenic variant ENST00000331825.11:c.460dupA (p.Arg154LysfsTer27) in the heterozygous state in the *FTL* gene (Figure III-16), which has been linked to neuroferritinopathy. This is an autosomal dominant NBIA syndrome caused by mutations in the ferritin light chain gene (*FTL*; chromosome 19q13.33).[156] It was originally described in families from Northern England, but later also in France, Italy, Japan, and India. Neuroferritinopathy usually begins between the fourth and sixth decade of life with either prominent dystonia, chorea, pyramidal signs, or a bradykinetic-rigid syndrome. Laboratory investigations reveal low to low-normal serum ferritin levels, with normal iron, hemoglobin and transferrin. Neuroradiological clues include cortical iron deposition (pencil lining sign),[157] bilateral pallidal necrosis, and cystic cavitation of the basal ganglia in advanced stages.[158]

Both individuals belong to White British pedigrees from North England (Cumbria region), where this variant has been first reported and demonstrated to have a founder origin. The first patient gene (Figure III-16, pedigree A) is currently 48 years old and had onset of symptoms at age 35, when she was pregnant with her fourth child. She developed dysarthria, jaw-closing dystonia, and action tremor of her left arm. She denied gait, balance, urinary and cognitive issues. She was the only child of her biological father and had four half-siblings from her mother and four children who were all in good health. On examination, she presented with severe oromandibular dystonia, with jaw closing spasms and side to side jaw movements. Her neurological assessment was otherwise unremarkable. Her brain MRI showed symmetrical signal abnormalities and some volume changes in the lentiform nuclei, T1 hyperintense and T2 hypointense signal in the globus pallidus bilaterally, and further are of increased susceptibility in the red nuclei, dentate nuclei (Figure III-16, middle black box) and, to a lesser extent, the thalamic nuclei and putamina.

Figure III-16. Sanger sequencing of two patients with neuroferritinopathy

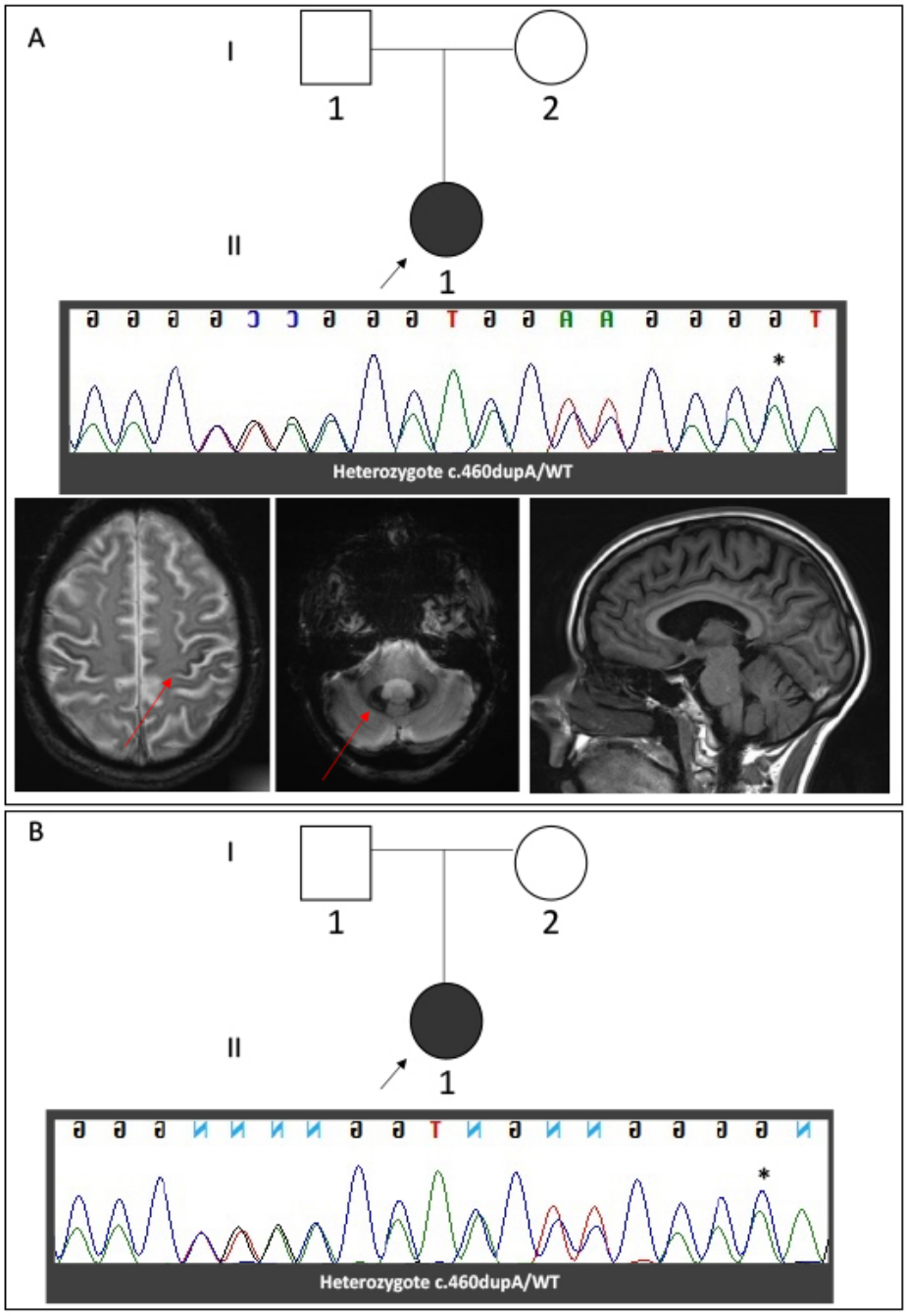

Sanger sequencing confirmed the probands of both families from the Cumbria region (North England) were heterozygotes for the variant ENST00000331825.11(*FTL*):c.460dupA (p.Arg154LysfsTer27). The region was amplified using the following primers (5'→3'): F-ccctcttctctctcagCTCTG, R-CCATTTGGTCCAAGGCTTGT, with an amplicon size of 293 base pairs. The electropherogram was analyzed using the Sequencher software package. The mutation is highlighted by an asterisk. WT = wild type.

On SWI sequences, increased susceptibility was also observed in the cortical outline of both cerebral hemispheres (Figure III-16, left black box), particularly in the bilateral motor, insular and visual cortices. Mild generalized cerebral atrophy was also observed (Figure III-16, right black box). Formal neuropsychometry at age 37 revealed a mild-moderate degree of cognitive dysfunction predominantly affecting frontal-subcortical systems. There was no evidence of peripheral nerve involvement on neurophysiology. Routine blood tests, including ferritin, and CSF analysis were normal. Her clinical picture deteriorated rapidly, with dystonia affecting the upper and, subsequently, the lower limbs, onset of balance difficulties, progression of dysarthria and dysphagia (which led to PEG tube insertion at age 40), and onset of depression and severe anxiety.

The second *FTL* patient (Figure III-16, pedigree B) was referred from external collaborators for choreo-dystonia with onset in early-middle adulthood and MRI evidence of T2 hypointensity in the basal ganglia bilaterally. She had a positive family history, with her mother diagnosed with parkinsonism in mid-adulthood. Further details on her clinical picture and disease course were not available.

FUCA1

One patient referred by an external collaborator with the clinical suspicion of NBIA was found to carry the homozygous nonsense variant NM_000147.4:c.1138G>T (p.Glu380Ter) in the *FUCA1* gene (Figure III-17). No clinicoradiological details nor information about the proband's pedigree were available. However, this nonsense mutation has previously been reported in association with the lysosomal storage disorder fucosidosis[159] and is recorded in ClinVar as pathogenic, thus being likely to be the cause of the disease in the index case.

Figure III-17. Sanger sequencing of a patient carrying a homozygous *FUCA1* variant

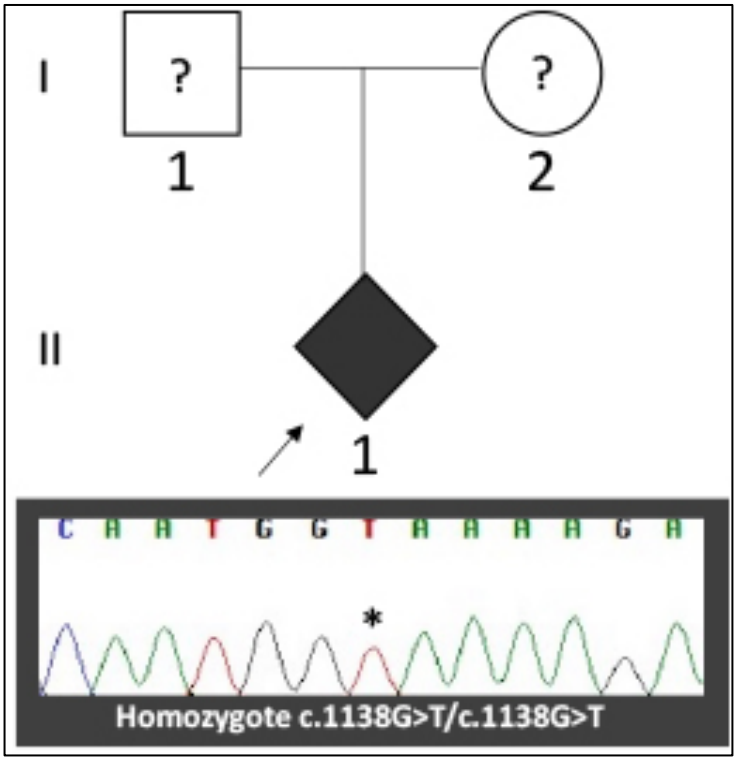

Sanger sequencing confirmed the proband (II-1) carried the homozygous variant c.1138G>T (p.Glu380Ter) in the *FUCA1* gene. The region of interest was amplified using the following primers (5'→3'): F-acagagtgtgccctagattct, R-tggcttgtgacattgtggac, with an amplicon size of 378 base pairs. Electropherograms were analyzed using the Sequencher software package. The mutation is highlighted by an asterisk. Arrow = proband.

GJC2

One Pakistani male, product of a consanguineous marriage, developed a progressive spastic paraparesis and ataxia. He had a history of congenital nystagmus, epilepsy and mild cognitive impairment. Brain MRI revealed thin corpus callosum and diffuse white matter hyperintensity in T2/FLAIR sequences. NCS/EMG did not detect signs of peripheral neuropathy nor myopathy. His muscle biopsy and respiratory chain enzymes were normal. He was tested negative for the commonest SCA expansions (SCA1-2-3-6-7). On WES, I detected the homozygous variant NM_020435:c.970_971dupGC (p.Ala325ProfsTer147) in the *GJC2* gene, which was confirmed by Sanger sequencing in the proband. No samples from

family members were available for segregation analysis. The proband died at age 40.

Biallelic mutations in the *GJC2* gene, which encodes the gap junction protein connexin47, account for an early onset dysmyelinating disorders of the central nervous system characterized by nystagmus, psychomotor delay, progressive spasticity, and cerebellar signs. This has first been described as Pelizaeus-Merzbacher-like disease. The variant herein reported creates a frameshift starting at codon Ala325 and introduces a premature stop codon. It is absent in gnomAD, and ClinVar classifies it as pathogenic/likely pathogenic. It has previously been reported in the literature in male born from consanguineous Turkish parents presenting with psychomotor regression since age 3, dysarthria, spastic tetraplegia, and ataxia.[160]

GLB1

In one Sri Lankan male who was referred for early-onset generalized dystonia, WES revealed two heterozygous variants in the *GLB1* gene, i.e. the intronic variant ENST00000307363.10(*GLB1*):c.915-1G>A and the missense variant ENST00000307363.10(*GLB1*):c.1325G>A (p.Arg490Gln). The patient was born to non-consanguineous healthy parents and had two elder sisters who were reported to be similarly affected since childhood. This case was referred from an external collaborator. Unfortunately, no clinical or neuroradiological details about the proband and his affected siblings were available. Segregation analysis (Figure III-18) revealed that the proband's father was heterozygote for the intronic *GLB1* variant only, his mother was heterozygote for the missense variant only, and his affected sisters were heterozygotes for both variants, which were therefore in *trans* configuration in the three affected siblings.

The intronic variant ENST00000307363.10(*GLB1*):c.915-1G>A is absent from gnomAD, is predicted pathogenic by all *in silico* prediction tools, and most probably affects splicing by alteration of the wild-type acceptor site according to Human Splicing Finder. It has not been reported before. The missense variant ENST00000307363.10(*GLB1*):c.1325G>A (p.Arg490Gln) has 13 heterozygous

and no homozygous entries, is predicted pathogenic by all *in silico* tools, and is reported pathogenic/likely pathogenic in ClinVar. It was not possible to obtain samples for RNA extraction in order to perform functional tests.

Figure III-18. Segregation analysis in a *GLB1* pedigree

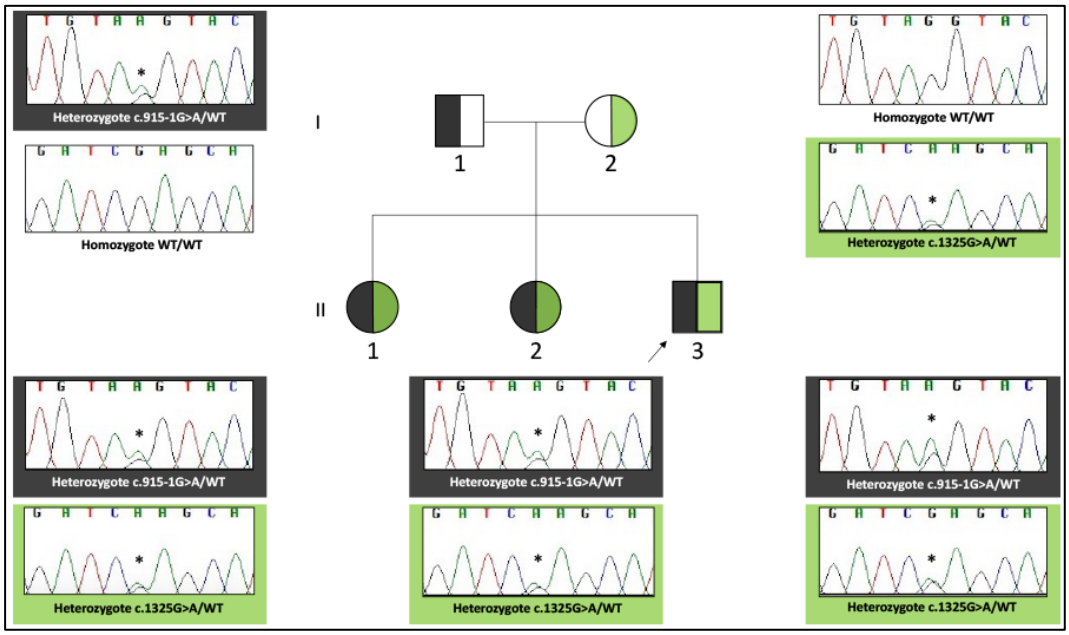

Segregation analysis confirmed the proband (II-3) and his two elder siblings were compound heterozygotes for the paternally inherited variant ENST00000307363:c.915-1G>A (grey) and the maternally inherited variant ENST00000307363:c.1325G>A (p.Arg490Gln) (green) in the *GLB1* gene. The region of the intronic variant was amplified using the following primers (5'→3'): F-ACTGGCTGGCTAGATCACTG, R-ggcacacccctcctcaaatt, with an amplicon size of 302 base pairs. The region of the missense variant was amplified using a different set of primers (5'→3'): F-cgggaggtggaggaagattt, R-cagagcaaaaccctgtctca, with an amplicon size of 424 base pairs. Electropherograms were analyzed using the Sequencher software package. Mutations are highlighted by an asterisk. Arrow = proband; WT = wild type.

GLB1 encodes the enzyme beta-galactosidase-1, a lysosomal hydrolase that cleaves the terminal beta-galactose from ganglioside substrates and other glycoconjugates.[161] Biallelic loss-of-function variants in *GLB1* account for GM1-gangliosidosis, a rare lysosomal storage disorder which occurs due to beta-D-galactosidase deficiency. Three phenotypes of GM1-gangliosidosis have been

described (infantile, juvenile and adult onset). Type 3 disease (adult onset) usually manifests in the first decade but can occur as late as 4th decade, and the majority of these patients survive beyond the second decade.[162] The most common presentation of type 3 GM1-gangliosidosis is with generalized dystonia (with prominent cranial involvement) and severe dysarthria often progressing to anarthria. Bone abnormalities are mild ranging from flattened vertebral bodies, short stature and scoliosis.[163] Brain MRI usually shows symmetrical hyperintensity in the posterior putamen corresponding to neuronal loss and gliosis in the striatum.[163] Bone marrow examination can demonstrate foam cells with wrinkled tissue appearance of the cytoplasm.

GNAO1

A 57-year-old White British female with a longstanding history of clumsiness since early childhood (age: 4-5 year) and onset of choreo-dystonia since age 25 was found to carry the heterozygous variant ENST00000262493.12:c.951A>C (p.Lys317Asn) in the *GNAO1* gene. She had a history of migraine and peripheral neuropathy. She also had a number of autoimmune conditions, such as rheumatoid arthritis and Raynaud's phenomenon. She was diagnosed with heart failure and had a pacemaker for heart conductive problems (tachy-brady syndrome with episodes of complete heart block. Due to the latter, she did not have any brain available. She had a negative muscle biopsy at the age of 30. Her family history was unremarkable. The variant is not present in GnomAD, is predicted pathogenic by all *in silico* prediction tools, and affect an amino acid residue which is highly conserved across species. Further research is ongoing in order to establish whether this variant occurred *de novo* in the proband. The relationship between this finding and the clinical picture remains uncertain.

KCNC3

One case referred by an external collaborator was found to carry the heterozygous nonsense variant c.1007del (p.Asn336ThrfsTer13) in the *KCNC3* gene, which has

been associated with spinocerebellar ataxia type 13. The variant was absent from GnomAD and have not been hitherto reported. No clinico-radiological information was traceable, and no residual DNA was available after WES, so that the variant could not be confirmed by Sanger sequencing. The variant was however detected in numerous reads by looking at the BAM file associated with WES.

KIAA1840

One Pakistani male, who was the youngest of four siblings born to a second-cousin marriage, presented with a history of learning difficulties and gait impairment since the age of 15 due to lower limb spasticity. His eldest brother was reported to be similarly affected. His brain MRI revealed thin corpus callosum, cerebral and cerebellar atrophy, and periventricular white matter T2 hyperintensity. His eldest brother was similarly affected. The proband was found to carry a homozygous 4 base pair (bp) deletion and a homozygous 8 bp insertion at the same position NM_025137.4:c.5399-407delAGATinsTGGAGGAG) in the *KIAA1840* gene, which has been related to spastic paraplegia type 11. These nucleotide changes lead to a frameshift that causes a stop codon at 1830 amino acid position (p.Gln1800LeufsTer1830). This variant is predicted to induce a frameshift which would create a premature stop codon and therefore result in targeting of the mRNA for nonsense-mediated decay or the production of a truncated protein

Figure III-19. Neuroimaging, family tree, Sanger sequencing, and BAM file of one SPG11 case

Brain MRI of the *KIAA1840* case showing (A) conspicuous thinning of the corpus callosum and mild cerebellar atrophy in a sagittal T1 sequence, and (B) confluent periventricular T2/FLAIR hyperintensities with symmetrical and white matter predominant volume loss in a coronal section. Sanger sequencing confirmed the proband (II-4) was homozygote for the variant NM_025137.4:c.5399_5402delAGATinsTGGAGGAG (grey) in the *SPG11* gene, with a 4-basis deletion highlighted in blue on the reference sequence (yellow box) and the 8-basis insertion showed in the red box on the electropherogram. The region of the variant was amplified using the following primers (5'→3'): F-TTTTCTCAACCCAGGCCCAT, R-CAGTAGGCGCCCAATCAAAA, with an amplicon size of 407 base pairs. DNA from other family members was not available for segregation analysis. Electropherograms were analysed using the Sequencher

software package. The mutation is highlighted by an asterisk. Arrow = proband; WT = wild type. (C) Due to difficulty in interpreting WES annotation and chromatogram in this case, the BAM file was reviewed and the 13 reads for this position extracted, actual data consistent with the aforementioned mutation.

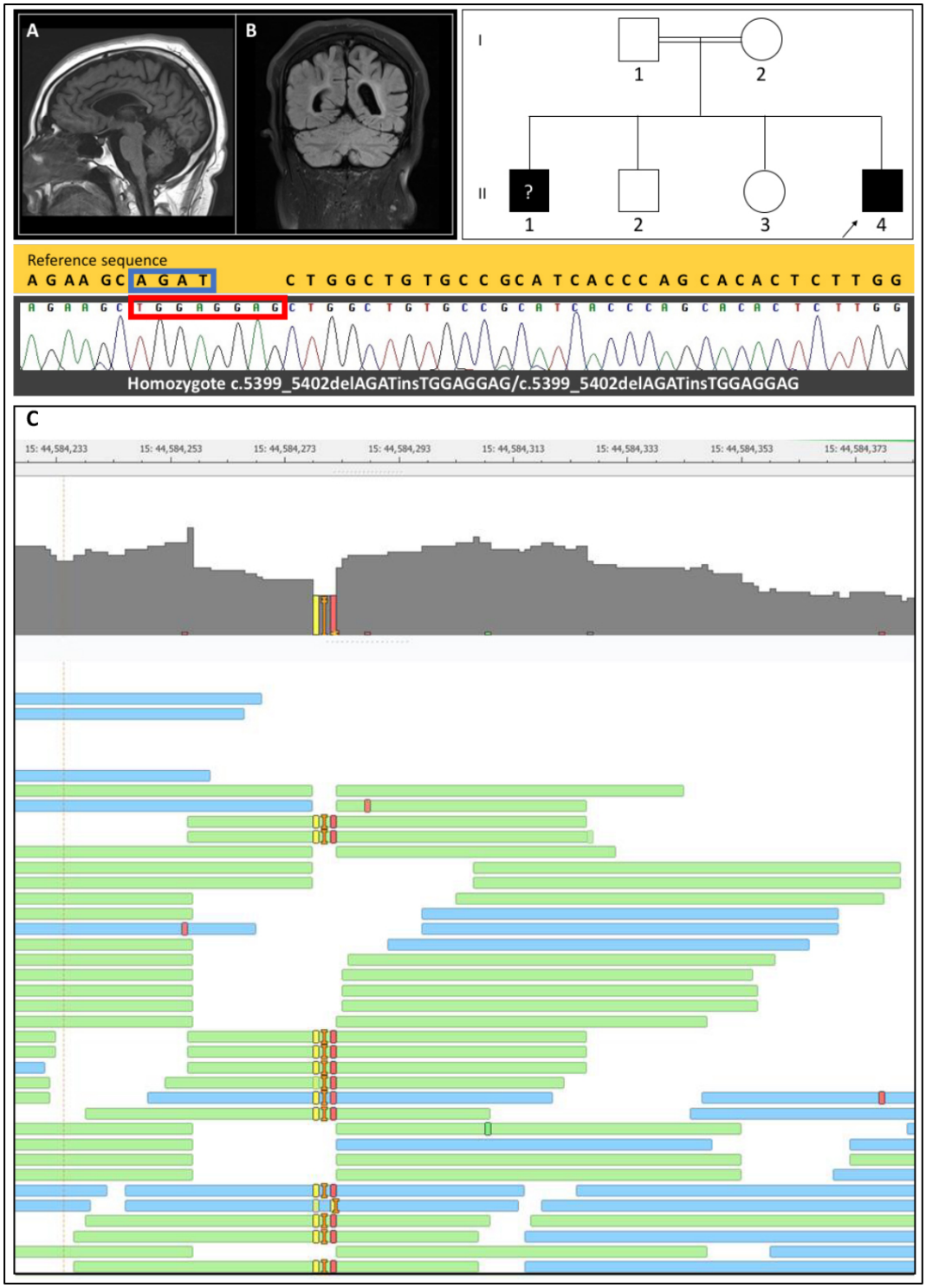

KMT2B

Figure III-20. Sanger sequencing of four *KMT2B* singletons

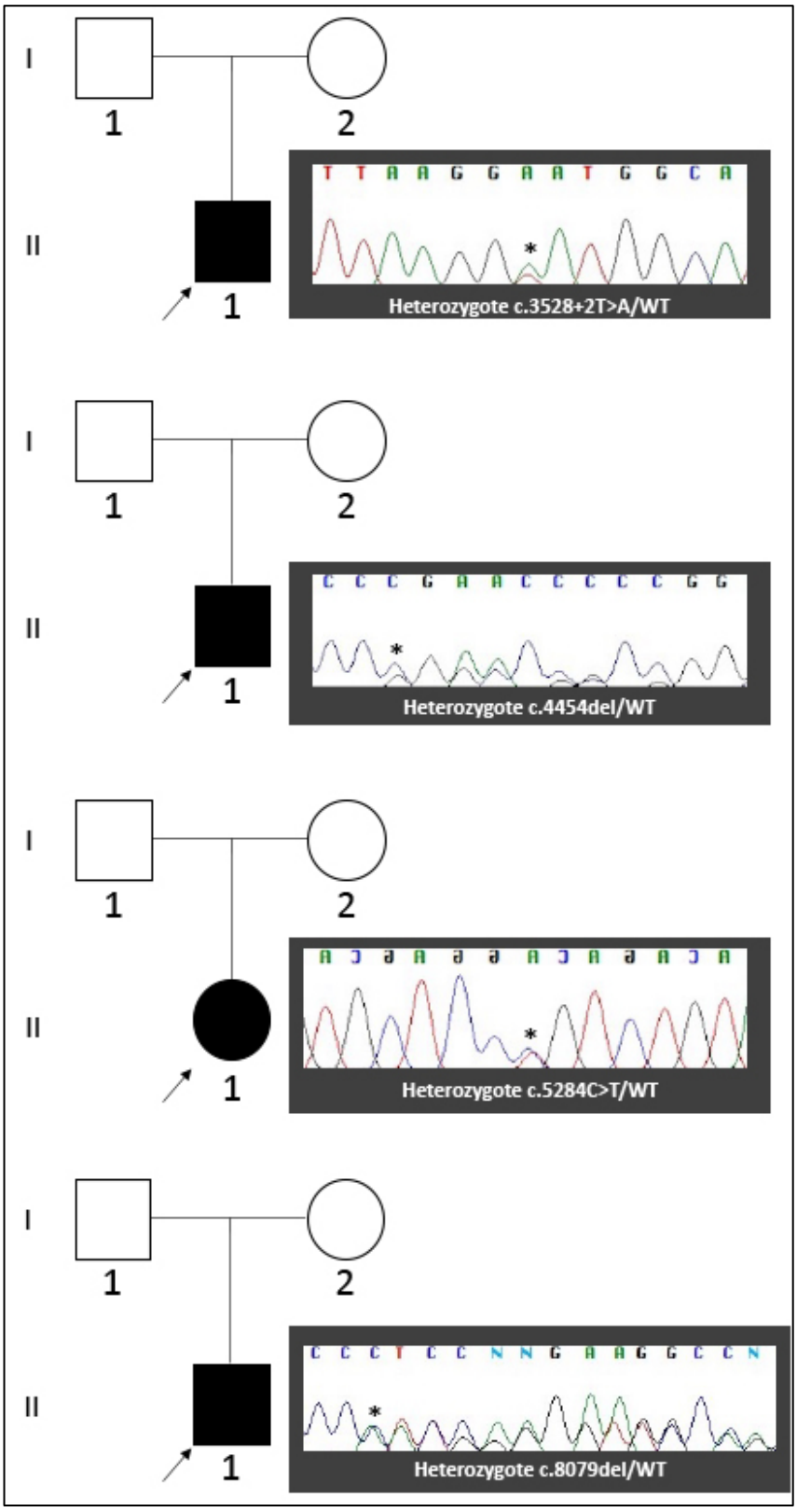

Four cases (three males, one female) presented with generalized dystonia with prominent oromandibular and/or laryngeal involvement and onset of symptoms constantly by the age of 6 years. They all had normal brain MRI. They did not have any family history of neurological disorders. Each carried a heterozygous variant in the *KMT2B* gene, which was previously reported in the literature (Figure III-20) associated with the same isolated dystonia phenotype.[79, 164] These included the intronic variant NM_014727.3:c.3528+2T>A, the nonsense variants c.4454del (p.Pro1485ArgfsTer9) and c.8079del (p.Ile2694SerfsTer44), and the missense variant c.5284C>T (p.Arg1762Cys). Two cases underwent deep brain stimulation of the globus pallidus, but only one had some improvement from functional neurosurgery.

MIEF2

A 27-year-old White British male born to a first-cousin couple presented with childhood-onset levodopa-responsive generalized dystonia with laryngeal involvement, limb spasticity, learning difficulties, and kyphoscoliosis. He had four sisters and two brothers, who were all in good health. There were two cousins with cerebral palsy on the paternal side. His brain MRI showed possible basal ganglia mineralization. His DaTscan revealed bilateral nigrostriatal degeneration. His muscle biopsy showed COX-negative fibers. WES and subsequent Sanger sequencing revealed the homozygous nonsense variant ENST00000323019.8:c.607G>T (p.Glu203Ter) in the candidate gene *MIEF2* gene, which encodes the mitochondrial elongation factor 2 and is associated with a combined oxidative phosphorylation deficiency.[165]

Figure III-21. Sanger sequencing confirming the *MIEF2* variant (next page)

Sanger sequencing confirmed the proband (II-2) carried the homozygous variant ENST00000323019.8(*MIEF2*):c.607G>T (p.Glu203Ter). The region of interest was amplified using the following primers (5'→3'): F-AGGCCTACTTTCGGAGCAAG, R-AGAACTCAAGCTGCGTCCT, with an amplicon size of 216 base pairs. Electropherograms were analyzed using the Sequencher software package. The mutation is highlighted by an asterisk. Arrow = proband.

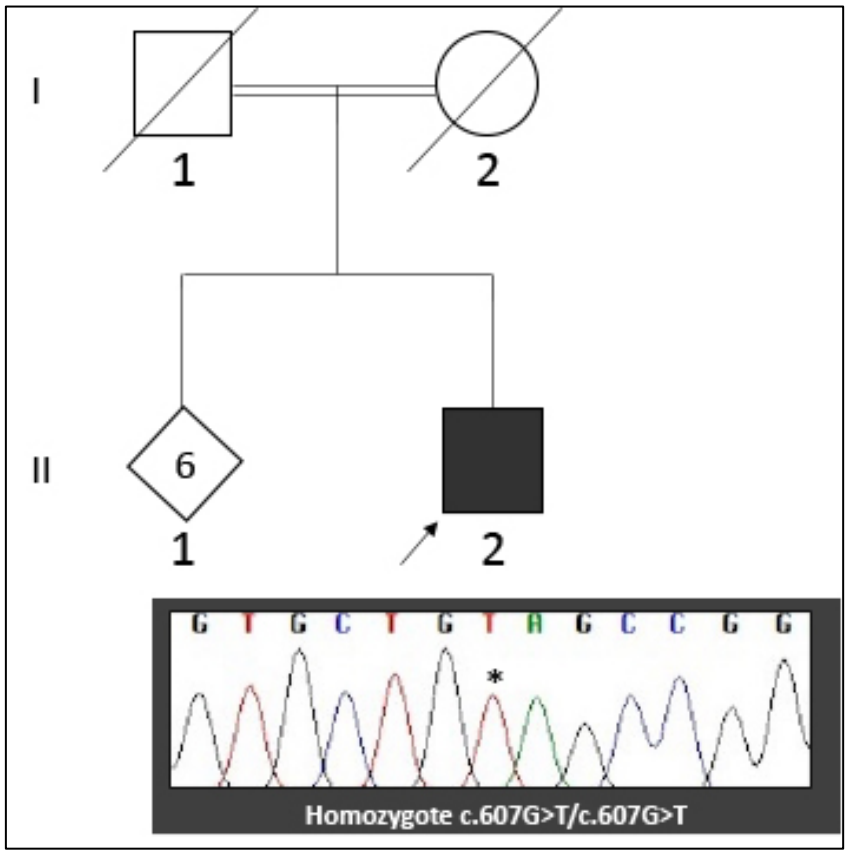

NDUFA12

A 19-year-old Egyptian male, born to first cousins, had normal neurodevelopment until age 2, when he started walking on his tiptoes (right>left) and falling frequently. Achilles tenotomy surgery provided transient improvement. After age 4, he developed right hand tremor, scoliosis, and progressive stiffness in his lower limbs, with loss of independent walking. On examination, he showed kyphoscoliosis, dystonia of the extremities with dystonic tremor of his right hand, and lower limb spasticity. There was no cognitive impairment. Serum ceruloplasmin, creatine kinase and aminoacid/acylcarnitine were normal. He had increased urine lactate and decreased urine 3-methylglutaric acid. Brain MRI revealed T2/FLAIR hyperintensity and T1 hypointensity with cystic areas in the BG bilaterally (Figure III-22). One of his elder sisters developed dystonic tremor and muscle weakness of her right hand since age 16 (Figure III-22, pedigree A). Brain MRI showed bilateral T2/FLAIR hyperintensity of the GP bilaterally. On

WES, I identified both siblings carried the homozygous variant NM_018838.5(*NDUFA12*):c.178C>T (p.Arg60Ter).

The nuclear gene *NDUFA12* encodes the supernumerary subunit A12 of mitochondrial complex I (CI; NADH:ubiquinone oxidoreductase), the first multimeric enzyme of the respiratory chain which contributes ~40% of the proton driving force for ATP synthesis. Subunit A12 was suggested to contribute to the assembly and stabilization of CI extramembrane arm.[166] Biallelic loss-of-function mutations in *NDUFA12* were initially associated with Leigh syndrome in a Pakistani female presenting with early motor developmental delay, motor regression since age 2, scoliosis, progressive dystonia, and T2 hyperintensities in the globus pallidus and elevated lactate on brain MRI and MR spectroscopy, respectively.[167] Since then few other cases have been reported, with clinical manifestations ranging from a complex neurological syndrome characterized by prominent dystonia to isolated optic atrophy.[168, 169]

To better characterize the clinical spectrum and course of *NDUFA12*-related disorders, I reviewed the in-house database of exomes and contacted external collaborators. I collected pheno-genotypic data from cases identified by retrieving databases of several diagnostic and research genetic laboratories worldwide and performed a systematic literature review (Table III-2). Seven additional *NDUFA12* cases were identified (Figure III-22, pedigrees B-F)

A 21-year-old Turkish male, product of a third-degree consanguineous marriage, was healthy until age 7, when he developed progressive scoliosis and gait difficulty with left foot in-turning. Dystonia did not respond to levodopa or anticholinergics and became generalized over a two-year period. The patient was wheelchair bound at age 11 and experienced focal seizures since age 12. On examination, he showed generalized dystonia with dysarthria and feeding difficulty secondary to oromandibular involvement, kyphoscoliosis, left hand clenching, lower limb hyperreflexia, and diffuse muscle atrophy. His cognitive functions were intact. His 25-year-old brother had a 15-year history of tip-toe walking on the left foot, with eversion aggravated by walking. Lower limb hyperreflexia and kyphoscoliosis were also detected on assessment. Metabolic workup, including blood lactate and pyruvate, ammonia, Tandem Mass Spectrometry, urinary organic acids, serum and urine amino acids, and very long chain fatty acids, was

unremarkable in both siblings. Their brain MRI showed symmetrical T2 hyperintensity and atrophy of the lentiform nuclei, with corresponding neuronal loss on MR spectroscopy. Whole-exome sequencing (WES) revealed they carried the homozygous variant NM_018838.5(*NDUFA12*):c.121dupG (p.Glu41GlyfsTer10).

A 16-year-old Saudi male, product of a first-cousin couple, had a history of motor developmental delay and experienced progressive gait unsteadiness since age 2, with frequent falls during school years. He developed fixed flexion of the right hand which progressed to right hemiplegia. He had severe visual impairment (hand motion). Brain MRI detected symmetrical T2 hyperintensity of the BG, with cystic degeneration on the left. Neurological examination revealed dysarthria and limb spasticity (right>left), with normal reflexes and downgoing plantar responses. Ophthalmological assessment revealed optic nerve atrophy. His 12-year-old brother had a history of severe global neurodevelopmental delay, with balance difficulties and recurrent falls since early childhood. He had a history of recurrent urinary tract infections since birth. On examination, he was dysarthric and wheelchair bound due to spastic quadriplegia. His visual function was normal. Brain MRI detected symmetrical T2 hyperintensity of the BG. Plasma lactate was 4.9mmol/L.

On WES, both siblings were found to carry the homozygous variant NM_018838.5(*NDUFA12*):c.4G>T (p.Glu2Ter).

A 10-year-old Pakistani female, born to a consanguineous marriage, was delivered at 37 weeks following labor induction due to intrauterine growth restriction (birth weight: 1.9kg). She had a febrile seizure at age 4 and developed progressive gait and posture impairment as well as left arm weakness since age 6.5, when brain MRI revealed symmetrical T2 hyperintensity of the posterior putamen, with cytotoxic oedema and chronic gliosis. She experienced status dystonicus at age 8. One year later, she was admitted due to an episode of prolonged lethargy which was attributed to accidental baclofen overdosing. Muscle biopsy revealed non-specific mild predominance of slow fibers, and assessment of respiratory chain enzymes showed low CI activity (0.034; reference range (r.r.): 0.104-0.268). Paired lactate values in CSF and blood were 2.2mmol/L and 1.9mmol/L, respectively. NCS/EMG was unremarkable. She was started on coenzyme Q10, thiamine, biotin, and anticholinergics. On examination (age 10), she was wheelchair bound with scoliosis and truncal hypotonia, limb flexor spasticity and dystonic posturing of the

extremities. Deterioration of her visual function led to an ophthalmological assessment which revealed severe optic atrophy (Figure). An extended next-generation sequencing (NGS) panel for nuclear mitochondrial genes revealed the homozygous variant NM_018838.5(*NDUFA12*):c.178C>T p.(Arg60Ter).

A 16-year-old Pakistani male, product of consanguineous parents, presented with a one-year history of progressive bilateral visual loss. His past medical history included depression treated with escitalopram. He had an asymptomatic sibling. On examination, visual acuity (VA) was 5/400 bilaterally, with normal intraocular pressure and anterior segment US biomicroscopy. Direct and consensual pupillary light reflexes were absent. Fundoscopy disclosed mild optic disc pallor bilaterally, with cup-to-disc ratios 0.2 (right eye) and 0.4 (left eye), narrow temporal rim of the left optic disc, and retinal arterial tortuosity bilaterally. Fundus autofluorescence was normal. His neurological assessment was otherwise unremarkable. Serological testing for HIV, syphilis and HTLV was negative. Paraneoplastic antibodies and rheumatological workup including serum anti-AQP4, anti-MOG, and anti-CRMP5 antibodies were unremarkable, as well as serum thiamin, cyanocobalamin and folate levels. He had normal brain and orbit MRI, and slightly increased CSF protein levels (63.9mg/dL; r.r.: <45). WES revealed the homozygous variant NM_018838.5(*NDUFA12*):c.253G>T (p.Glu85Ter). Mitochondrial DNA sequence was unremarkable.

A 33-year-old Turkish male born to consanguineous parents presented at age 28 with sudden bilateral painless visual loss (VA 20/40), which slowly progressed over the following years. His VA was 20/200 bilaterally at age 30 and remained relatively stable ever since. Perimetry revealed central scotomas spanning most of the central 30 degrees of the visual field bilaterally, more pronounced in the left eye. Intraocular pressure was normal, and anterior segment US biomicroscopy unremarkable aside from mild cataract. Pupils were isocor, with the left one showing relative afferent deficit. Fundoscopy revealed pale optic discs with cup-to-disc ratios 0.7 (right eye) and 0.8 (left eye), whereas macula, peripheral retina, and vessels were unremarkable. Bilateral optical coherence tomography detected markedly reduced thickness of the peripapillary retinal nerve fiber layer and microcystic macular edema (left>right). Neurological assessment was otherwise

unremarkable. MRI brain orbits detected optic chiasm atrophy. Screening for cardiovascular risk factors, including sleep apnea, was unremarkable. An NGS panel for nuclear and mitochondrial genes linked to optic atrophy detected the heterozygous variant ENST00000304511.2(*TMEM126A*):c.314G>A (p.Arg105Gln), whose causal relationship was excluded based on high frequency in population databases and *in silico* prediction tools. Whole-genome sequencing revealed he carried the homozygous variant NM_018838.5(*NDUFA12*):c.83del (p.Phe28SerfsTer11).

Demographic, phenotypic and genetic features of *NDUFA12* cases identified are detailed in Table III-2.

Three novel *NDUFA12* mutations are herein reported. The p.Glu2Ter variant is absent in gnomAD, affects an amino acid residue highly conserved across species, and is consistently predicted pathogenic by *in silico* tools, including a CADD score of 40. The p.Phe28SerfsTer11 and p.Glu41GlyfsTer10 variants are absent in gnomAD and predicted to result in premature stop codons.

This series expands the pheno-genotypic spectrum of *NDUFA12*-associated disorders and provides evidence of inter- and intra-familial clinical heterogeneity associated with the same mutation. It also supports the inclusion of *NDUFA12* variants in the diagnostic workup of not only Leigh/Leigh-like syndromes but also isolated optic atrophy.

Figure III-22. Pedigrees, phenotypic features, and mutations reported so far with the *NDUFA12* gene (next page)

First line. Pedigrees with *NDUFA12* mutations herein reported. Second line. Phenotypic spectrum linked to biallelic mutations in the *NDUFA12* gene. Third line. Evidence of dystonia, as well as basal ganglia abnormalities on brain MRI and optic nerve atrophy on ophthalmological assessment. Fourth line. Schematic of *NDUFA12* mutations reported so far.

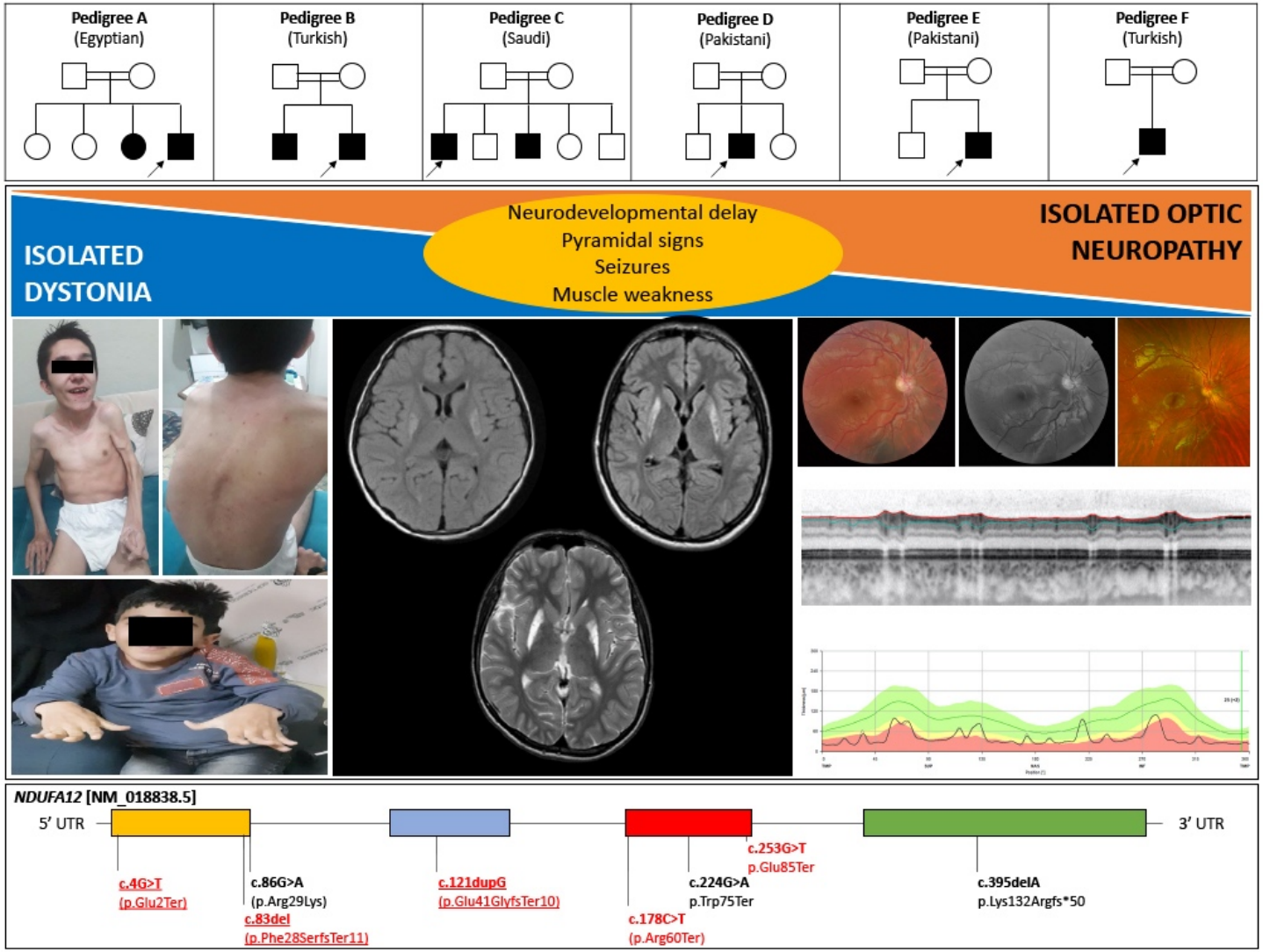
Pedigree A
(Egyptian)
Pedigree B
(Turkish)
Pedigree C
(Saudi)
Pedigree D
(Pakistani)
Pedigree E
(Pakistani)
Pedigree F
(Turkish)
ISOLATED DYSTONIA
Neurodevelopmental delay
Pyramidal signs
Seizures
Muscle weakness
ISOLATED OPTIC NEUROPATHY
NDUFA12 [NM_018838.5]
5' UTR
3' UTR
c.4G>T
(p.Glu2Ter)
c.86G>A
(p.Arg29Lys)
c.83del
(p.Phe28SerfsTer11)
c.121dupG
(p.Glu41GlyfsTer10)
c.178C>T
(p.Arg60Ter)
c.224G>A
p.Trp75Ter
c.253G>T
p.Glu85Ter
c.395delA
p.Lys132Argfs*50

Table III-2. Demographic, phenotypic and genetic features of 9 new and 9 previously reported *NDUFA12* cases

Family	Case	Sex/ AE (y)	Ethnicity	Consanguinity	FH	Perinatal history/NDM	AO (y)	Symptom at onset	Clinical manifestations			Brain MRI	Other investigations	*NDUFA12* variants (NM_018838.5)
									Neurological	Ophthalmological	Other			
This case series														
A	3	M/19	Egyptian	Yes	Yes	Normal birth. Normal NDM.	2	Unilateral tip-toe walking, recurrent falls	Right hand tremor; spasticity; dystonia of extremities.	None	Scoliosis	T2/FLAIR hyperintensity and T1 hypointensity of BG, with some cystic areas	Aminoacid/acylcarnitine and TANDEM mass spectrometry: normal. Urine organic acid: increased lactate and decreased 3 methyl glutaric acid. CK and cerulopasmin: normal.	Hom c.178C>T (p.Arg60Ter)
A	4	F/N.A.	Egyptian	Yes	Yes	Normal birth. Normal NDM.	16	Clumsiness and tremor of the right hand	Hand weakness and right hand tremor	None	-	T2 hyperintensity of GP	-	Hom c.178C>T (p.Arg60Ter)
B	1	M/25	Turkish	Yes	Yes	Normal birth. Normal NDM.	10	Gait disturbance with unilateral intoeing	Left foot dystonia, which worsens with exercise; hyperreflexia lower limbs.	None	None	Atrophy and T2 hyperintensity of lentiform nucleus bilaterally	None	Hom c.121dupG (p.Glu41GlyfsTer10)
B	2	M/21	Turkish	Yes	Yes	Normal birth. Normal NDM.	7	Gait disturbance with unilateral intoeing	Generalized dystonia, including oromandibular and left foot dystonia which worsens with exercise; focal seizures (since age 12).	None	Scoliosis	Atrophy and T2 hyperintensity of lentiform nucleus	Plasma lactate and pyruvate, ammonia, TANDEM mass spectrometry, urinary organic acids, serum and urine aminoacids and VLCFA: normal. MRS: neuronal loss in lentiform nucleus.	Hom c.121dupG (p.Glu41GlyfsTer10)
C	5	M/16	Saudi	Yes	Yes	Global delay of NDM	2	Gait unsteadiness and falls Spastic-dystonic tetraparesis	Right hand dystonia	Visual impairment	-	Bilateral symmetrical T2 hyperintensity of BG along with left BG encephalomalacia	-	Hom c.4G>T (p.Glu2Ter)
C	6	M/12	Saudi	Yes	Yes	Global delay of NDM	N.A.	Gait unsteadiness and falls	Spastic quadriplegia	None	Recurrent UTI	Bilateral symmetrical T2 hyperintensity of BG	Optic nerve atrophy Plasma lactate: 4.9	Hom c.4G>T (p.Glu2Ter)
D	7	F/10	Pakistani	Yes	No	Premature induced birth for poor intrauterine growth. Normal NDM.	6.5	Gait abnormality and left arm weakness	Trunk hypotonia; dystonic posturing; episode of status dystonicus.	Visual impairment	Febrile convulsion Scoliosis	T2 hyperintensities in the posterior putamen bilaterally (chronic gliotic scarring and acute cytotoxic oedema).	Optic atrophy Plasma lactate: 1.9 CSF lactate: 2.2 NCS/EMG: no evidence of peripheral neuropathy MB: mild predominance of slow fibers. RCE: low complex I, normal complexes 2-3-4.	Hom c.178C>T (p.Arg60Ter)
E	8	M/16	Pakistani	Yes	No	Normal birth. Normal NDM.	15	Subacute visual loss	Absent direct and consensual pupillary light reflexes	Visual impairment	Depression	Normal	V.A. 5/400 bilaterally Optic atrophy	Hom c.253G>T (p.Glu85Ter)

													Serology for HIV, syphilis, HTLV: negative. Autoimmune screening: negative. CSF: mildly elevated proteins (63.9 mg/dL; r.i. <45 mg/dl).	
F	9	M/33	Turkish	Yes	No	Normal birth. Normal NDM.	28	Acute visual loss	None	Visual impairment		Optic chiasm atrophy	Optic atrophy OCT: markedly thickness of peripapillary nerve fiber layer. NGS gene panel for optic atrophy: negative.	Hom c.83del (p.Phe28SerfrTer11)
Previously reported cases														
G[167]	10	F/10	Pakistani	Yes	No	Delayed early motor NDM.	2	Regression of motor abilities	Generalized dystonia Muscle atrophy	Visual impairment (detected on follow-up)	Scoliosis Growth retardation Hypertrichosis	T2 hyperintensity of GP	MB: type 1 fibre atrophy and fibre type disproportion. Brain MRS: elevated lactate in the whole cerebrum. Plasma lactate: 4.9 mmol/l (r.i. <2.1). CSF lactate: 2.4 mmol/l (r.i. 1.1-1.8). Optic atrophy.	Hom c.178C>T (p.Arg60Ter)
H*[169]	11*	F/Birth*	Mennonite	No	No	Symmetric intrauterine growth restriction*	Birth	Facial dysmorphisms, short limbs, persistent thrombocytopenia, direct hyperbilirubinemia, and poor feeding*	-		Facial dysmorphisms (large ears with increased folding anteriorly, long philtrum, small mouth with prominent alveolar ridge, epicanthal folds), short upper and lower extremities with bowing of the tibia and fibula bilaterally, supinated ankles, and mild generalized hypertonia. Flexion wrist contractures, clenched fists.	-	Elevated ALP; low serum vitamin D 25-OH; direct hyperbilirubinemia. US abdomen: normal. Thrombocytopenia. Congenital infection screen: negative. US head: normal. Echocardiogram: patent ductus arteriosus and patent foramen ovale. Chest X-ray: hypoinflated lungs, dysplastic bones throughout the thorax and visualized upper extremities. Skeletal survey: marked osteopenia, foreshortened long bones with thickened diaphyses, irregular "raggedy" metaphyses, and no wormian bones.*	Hom c.178C>T (p.Arg60Ter)*

											Thumbs were held between the second and third fingers, bilaterally.*			
I[168]	12	M/9	Italian	Yes	No	Birth: poor sucking, hypotonia. Mild global delay of NDM.	4	Sudden-onset convergent strabismus	Strabismus, nystagmus, minimal ptosis in the left eye	None	None	Age 5: T2 hyperintensity of the brainstem (red nuclei and tegmental tract) Follow-up MRIs: normal.	Brain MRS: normal. VEP: increased latency in both eyes. ERG: normal. BAEPs: normal. ECG/Ecocardiography: normal. Plasma lactate: 2.85 mmol/l (r.i. 0.5-2.2) on one occasion only.	Hom c.86G>A (p.Arg29Lys)
L[168]	13	F/15	Italian	Yes	No	Birth: respiratory distress. Normal NDM.	6	Dystonia right arm	Generalized dystonia Spastic-dystonic gait evolving to spastic-dystonic tetraparesis Oromandibular dystonia	None	Scoliosis	Typical Leigh syndrome pattern. Follow-up MRI: lesions in the basal ganglia (putamen), partial agenesis of septum pellucidum, and mild enhancement of left optic nerve after gadolinium	Brain MRS: normal. VEP: abnormal in amplitude in both eyes. Cardiological evaluation: normal. Plasma lactate: 3.62 mmol/l (r.i. 0.5-2.2). Urine lactate: >400 mmol/l creatinine (r.i. <200). Plasma amino acids: increased alanine (852 mmol/l; r.i. 150-400).	Hom c.395delA (p.Lys132ArgfsTer50)
M[168]	14	F/13	Moroccan	Yes	Yes	Birth: respiratory distress. Normal NDM.	4	Sudden-onset nystagmus, right hemiparesis	Generalized dystonia Trunk hypotonia Extrapyramidal syndrome Peripheral neuropathy	None	None	T2 hyperintensity of lentiform nucleus and brainstem	Brain MRS: lactate peak. Plasma lactate: 2.4 mmol/l (r.i. 0.5-1.95). CSF lactate: 2.8 mmol/l (r.i. 1-1.9). NCS: peripheral neuropathy	Hom c.224G>A (p.Trp75Ter)
M[168]	15	F/9	Moroccan	Yes	Yes	Normal NDM.	9	Sudden-onset visual impairment	Extrapyramidal syndrome	Visual impairment	None	T2 hyperintensity of lentiform nucleus	Hyperlactatorachia (lactate 2.8 mmol/L; r.i. 1–1.90, with normal plasma lactate	Hom c.224G>A (p.Trp75Ter)
M[168]	16	F/7	Moroccan	Yes	Yes	Normal NDM.	7	Visual impairment	None	Visual impairment	None	Normal	Optic atrophy. Hyperlactatorachia (2.4 mmol/L; r.i. 1–1.90)	Hom c.224G>A (p.Trp75Ter)
N[168]	17	M/11	Syrian	Yes	Yes	Normal NDM.	5	Limb dystonia	Limb dystonia	None	Episodes of vomiting	T2/T2-FLAIR hyperintensity of lentiform nucleus and red nucleus	FO, VEP, ERG, BAEPs: normal. Serum lactate: 2.6 mmol/L (r.i. 0.5-2.20) Brain MRS: normal.	Hom c.253G>T (p.Glu85Ter)
N[168]	18	F/4	Syrian	Yes	Yes	Normal birth. Normal NDM.	3.5	Limb dystonia	Limb and oromandibular dystonia. Rigidity. Tip-toe walking.	None		N.A.	Serum lactate: 2.2 mmol/L (r.i. 0.5-2.20). Acylcarnitine profile and urinary organic acids: normal.	Hom c.253G>T (p.Glu85Ter)

Legend. AE = age at last evaluation; ALP = alkaline phosphatase; AO = age of onset; BG = basal ganglia; CSF = cerebrospinal fluid; F = female; FH = family history; FO = fundus oculi; GP = globus pallidus; Hom = homozygote; M = male; MB = muscle biopsy; MRI = magnetic resonance imaging; MRS = magnetic resonance spectroscopy; N.A. = not available; NDM = neurodevelopmental milestones; OCT = optical coherence tomography. Ref = reference; r.i. = reference interval; UTI = urinary tract infections; V.A. = visual acuity. VLCFA = very long chain fatty acids. Y = years. * Co-occurrence of biallelic mutations in *NDUFA12* and biallelic mutations in *GNPTAB* (mucolipidosis II alpha/beta).

NIPA1

A novel *NIPA1* missense variant, c.661C>A, p.P221T (NM_144599), was identified in a female in her mid-50s. This patient was reported to have suffered from a mild Rubella infection at age 4, after which she developed hearing impairment, myoclonus epilepsy and cerebellar signs (ataxia, dysmetria). Brain MRI revealed cerebellar degeneration without further abnormalities. Her paternal grandmother was thought to be clumsy from her sixties on and the patient's own 10- year-old son has some hearing impairment and clumsiness. Unfortunately, none of the family members were available for further clinical or genetic testing.

NPC1

One Indian subject referred for early-onset generalized dystonia was found to carry two heterozygous variants in the *NPC1* gene, namely c.1990G>A (p.Val664Met) and c.346C>T (p.Arg116Ter), which I confirmed by Sanger sequencing (Figure III-23). Unfortunately, no clinical details nor family members for further genetic testing were available, and the diagnosis remains therefore speculative.

Figure III-23. Sanger sequencing of one *NPC1* case

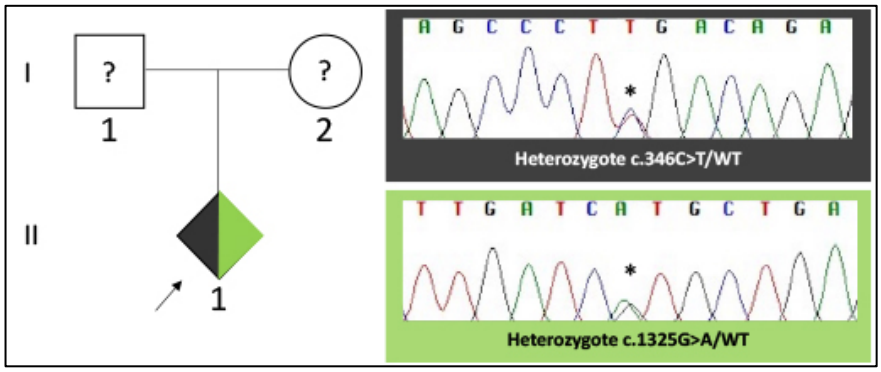

Segregation analysis confirmed the proband (II-1) and both her siblings were homozygotes for the variant NM_003560.4:c.2222G>A (blue) in the *PLA2G6* gene, whereas their parents, who were first cousins, carried the variant in the heterozygous state. The region was amplified using the following primers (5'→3'): F-gctcagcctgactcgaaag, R-aacagagcagacccttggg, with an amplicon size of 315 base pairs. Electropherograms were analysed using the Sequencher software package. The mutation is highlighted by an asterisk. Arrow = proband; WT = wild type.

PANK2

Two putatively compound heterozygous, previously published mutations in *PANK2* (see Figure 3-8) were identified in a female Caucasian patient with early-onset dystonia-parkinsonism and MRI evidence of iron deposition in the basal ganglia. These were the nonsense variant c.1441C>T (p.Arg481Ter) and the missense variant c.1561G>A (p.Gly521Arg). Unfortunately, this sample was from a collaborator and no additional family members could be contacted, nor the original MRI with further clinical details received.

A second case of Italian ancestors presenting with young-onset dystonia with prominent oromandibular involvement and MRI evidence of mineralization of the basal ganglia was found to carry the PANK2 variants c.823_824del (p.Leu275ValfsTer16) and c.966G>T (p.Glu322Asp).

PLA2G6

One female with early-onset dystonia-parkinsonism born to consanguineous parents of Pakistani origin was found to be homozygote for the previously reported pathogenic variant NM_003560.4:c.2222G>A (p.Arg741Gln) in the *PLA2G6* gene (Figure III-24). Her affected sister was included in the study cohort reported in chapter IV and also found to be homozygote for this *PLA2G6* variant. Both affected sisters are extensively discussed in chapter V (see Cases 10 and 11), where I dissected the phenotype and genotype of *PLA2G6*-related parkinsonism by reviewing data from 14 unpublished cases and 72 cases from a systematic literature review. Intriguingly, both cases did not show evidence brain iron accumulation on MRI.

Figure III-24. Segregation analysis in the *PLA2G6* pedigree

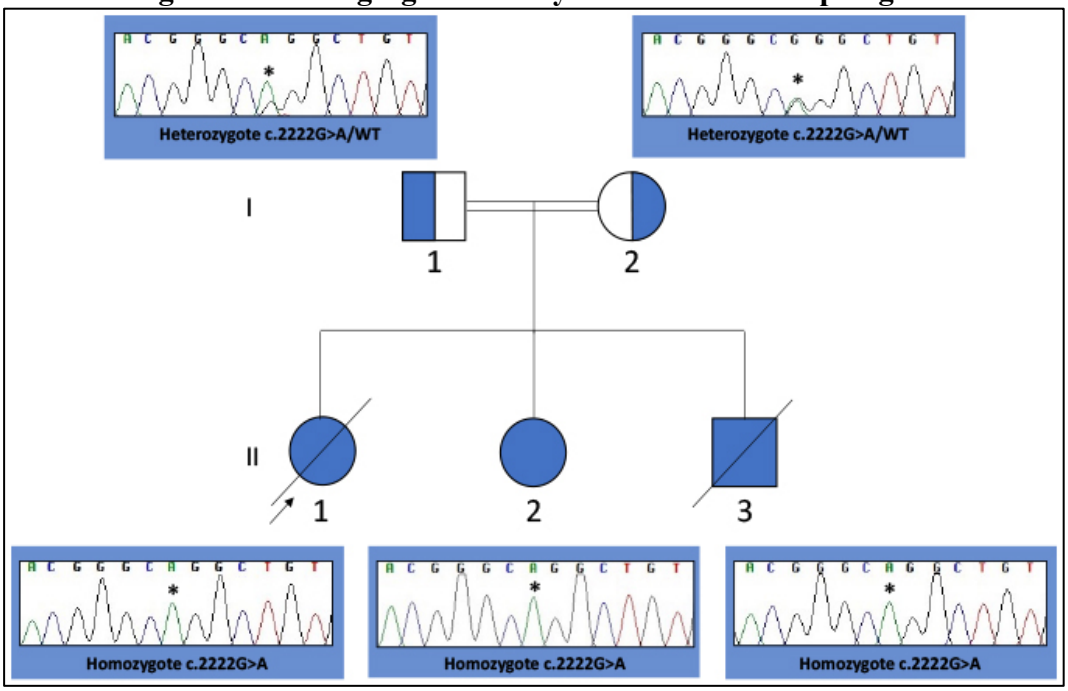

Segregation analysis confirmed the proband (II-1) and both her siblings were homozygotes for the variant NM_003560.4:c.2222G>A (blue) in the *PLA2G6* gene, whereas their parents, who were first cousins, carried the variant in the heterozygous state. The region was amplified using the following primers (5'→3'): F-gctcagcctgactcgaaag, R-aacagagcagacccttggg, with an amplicon size of 315 base pairs. Electropherograms were analysed using the Sequencher software package. The mutation is highlighted by an asterisk. Arrow = proband; WT = wild type.

THAP1

In one 33-year-old male patient of Arabic unspecified ethnicity referred for early-onset dystonia with prominent bulbar involvement, I detected on WES the heterozygous variant NM_018105.3:c.211_212insG. This variant led to a premature stop codon and has not previously been reported which is predicted to cause a frameshift with premature termination (p.Leu71CysfsTer15). No further details on his clinicoradiological features nor family history were available. The frequent involvement of the larynx, oromandibular region, and face and the common occurrence of speech problems in *THAP1*-associated dystonia suggest that this group of patients will be a particularly important group to target for genetic screening.[65]

TSPOAP1

One pedigree was blindly identified to carry the homozygous variant NM_004758.3:c.538delG (p.Ala180ProfsTer8) in the *TSPOAP1* gene. This pedigree was found to cross match with Family A of the discovery gene paper by Mencacci et al. Since details on the functional consequences of this mutation and a detailed clinical description can be found in this publication, this pedigree will not be further discussed here.[170]

WARS2

One 47-year-old Iranian male, who was the only child of a non-consanguineous marriage, presented with a history of mild intellectual disability, rest tremor since middle childhood, and tremulous cervical dystonia since late adolescence. The course of his neurological symptoms had been quite static since his late 20s. His brain MRI showed cerebellar atrophy, and SWI sequences shows brain iron deposition. There was no family history of neurological disorders. In this patient, WES revealed two heterozygous variants in the *WARS2* gene, i.e. NM_015836.4:c.37T>G (p.Trp13Gly) and NM_015836.4:c.408dupA (p.Gln137ThrfsTer86). The latter was also found in the proband's mother, who was the only family member available for segregation analysis. This observation increased the likelihood that the variants were in *trans* configuration in the proband. Interestingly, the proband's brain MRI showed mineralization of the globus pallidus bilaterally on SWI sequences (Figure III-25). This is the first report describing MRI evidence of basal ganglia mineralization, thus expanding the phenotypic spectrum of *WARS*-related neurodegeneration.

Aminoacyl-tRNA synthetases catalyze the aminoacylation of tRNA by their cognate amino acid. Because of their central role in linking amino acids with nucleotide triplets contained in tRNAs, aminoacyl-tRNA synthetases are thought to be among the first proteins that appeared in evolution. Two forms of tryptophanyl-tRNA synthetase exist, a cytoplasmic form, named WARS, and a mitochondrial form, named WARS2. This gene encodes the mitochondrial tryptophanyl-tRNA

synthetase. Two alternative transcripts encoding different isoforms have been described.

Figure III-25. Neuroimaging and segregation analysis of the *WARS* case

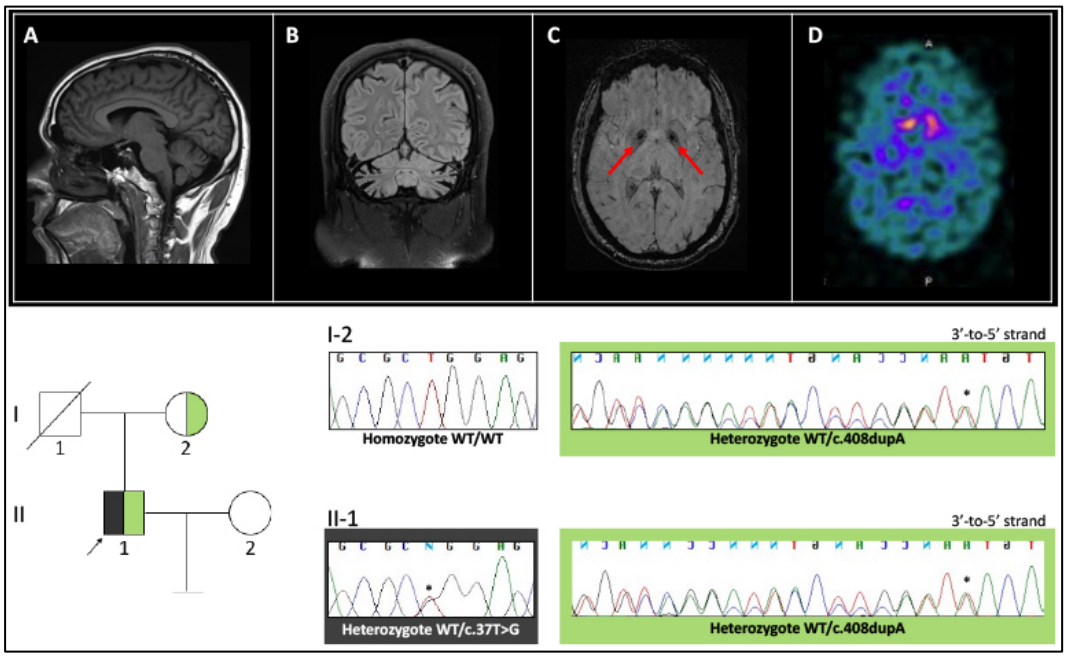

Upper part. Brain MRI of the proband revealed cerebellar atrophy (A-B) and symmetrical mineralization of the globus pallidus (C) on SWI sequences. DaTscan showing reduced tracer uptake in the basal ganglia bilaterally (D). Lower part. Segregation analysis confirmed the proband (II-1) carried two heterozygous variants in the *WARS2* gene, namely NM_015836.4:c.37T>G (p.Trp13Gly) and NM_015836.4:c.408dupA (p.Gln137ThrfsTer86), the latter being inherited from his mother. The regions of interest were amplified using the primer set (5'→3'): F-attccaaacaagacggctcc, R-cctaagaagcgggaggagag (amplicon size 219 base pairs) for the missense variant and the primer set (5'→3'): F-caagaaaacactggccacct, R-ccattagtgagtggcagacc (amplicon size 240 base pairs) for the frameshift variant. Electropherograms were analysed using the Sequencher software package. The mutations are highlighted by an asterisk. Arrow = proband; WT = wild type.

WDR45

In two female subjects of the clinical study cohort, I identified heterozygous variants in the *WDR45* gene.

One patient was a 53-year-old White British female with a history of motor developmental delay since the age of 7 months, learning difficulties, generalized

epilepsy presenting with absences since the age of 15 months and tonic-clonic seizures later in life. She developed dystonia with superimposed dystonic spasms, parkinsonism, and chorea from around the second-third decade. Brain MRI revealed global cerebro/cerebellar atrophy, severe dilatation of the lateral and third ventricles, and T2* hypointensity in the globus pallidus and substantia nigra bilaterally, with no calcification in CT scan, thus being consistent with severe and mineralization of the globus pallidus (Figure III-25). In this case, I identified the variant ENST00000322995:c.1006+5G>A in the *WDR45* gene. This variant has not previously been reported and is predicted to affect splicing by activation of a cryptic donor site according to Human Splicing Finder.

Figure III-25. Neuroimaging and segregation analysis of one WDR45 case

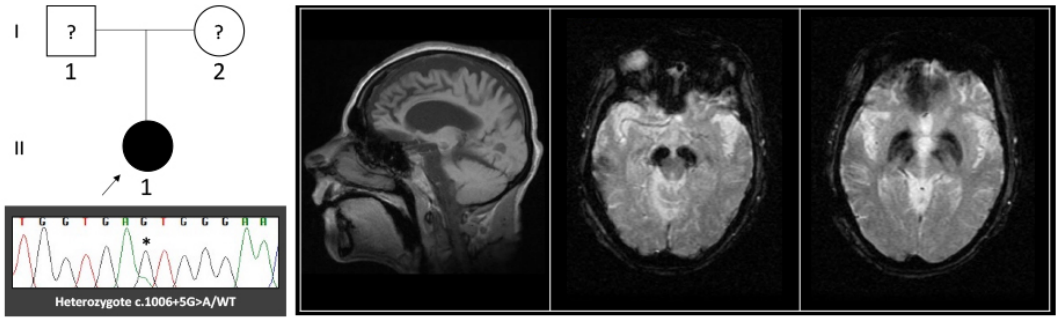

The second WDR45 mutation carrier was a 35-year-old British female born to healthy unrelated parents after a normal pregnancy and died at age 39. Her developmental milestones were delayed, she never acquired language, did not learn to walk independently and suffered from severe learning disability and progressive spastic quadriplegia from birth. At age 3, she developed seizures with predominantly absent episodes and occasional tonic convulsions that are complicated by dystonic posturing, dysarthria and dysphagia and myoclonic jerks from age 15 onwards. Her slowly progressive movement disorder and her cognitive abilities deteriorated significantly in her twenties. The patient was wheelchair-bound since her early teens and fully dependent on her carers in the activities of daily living. Brain MRI at age 27 showed global atrophy and signal changes in the

globus pallidus and substantia nigra consistent with iron accumulation. Her family history was unremarkable. On WES, I detected the heterozygous insertion of three base pairs (ATA) at position c.1035_1037dup (p.Lys345_Tyr346insTer) of the *WDR45* gene (Figure III-26).

Figure III-26. Sanger sequencing of the second WDR45 case

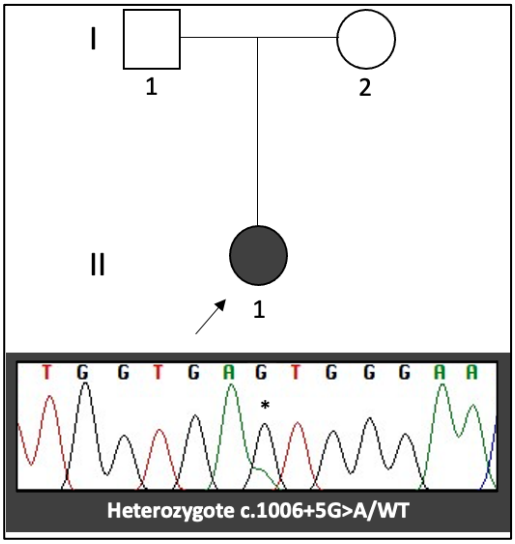

WDR45 mutations have been established as the causal link in static encephalopathy of childhood with neurodegeneration in adulthood and NBIA, more specifically BPAN.[171] BPAN is an X-linked dominant disorder and was first linked to the *WDR45* gene in 2012. Beta-propeller protein-associated neurodegeneration (BPAN, OMIM# 300894), historically known as static encephalopathy of childhood with neurodegeneration in adulthood (SENDA), is a rare neurological disorder characterized by a bi-phasic course.[171] During early childhood affected individuals present with global neurodevelopmental delay, seizures, pyramidal signs in the lower limbs and behavioral issues which remain quite stable. In the second phase, which usually occurs between the second and fourth decade and hints at the diagnosis, patients develop rapidly progressive dystonia-parkinsonism.[171] The prevalence of BPAN is unknown, with less than 100 cases reported so far. The majority of patients are female, although few male cases have been reported (F:M

ratio ≅ 6:1). BPAN is characterized by a two-stage disease course. Although symptom onset is in childhood, the mean age at diagnosis is in early adulthood. The first phase of the disease, in childhood, is characterized by developmental delay of variable degree, followed by intellectual disability with predominant verbal impairment but also poor coordination, both in fine and gross motor skills. Epilepsy with seizures triggered by fever is also common. It is often initially drug-resistant but tends to become less difficult to treat or even to completely resolve after puberty. Abnormal behaviours may resemble those observed in Rett syndrome are also described. Other features include abnormal sleep patterns and ophthalmological findings, such as bilateral partial retinal colobomas, myopia, spontaneous retinal detachment, and bilateral optic atrophy. During adolescence or early adulthood, patients experience a neurologic deterioration with movement disorders and cognitive decline. Subjects usually show a rigid–akinetic parkinsonism with gait and postural impairment along with upper limb dystonia.[171] The severity of the clinical manifestations can vary. Factors such as a skewed X-inactivation in females, a somatic mosaicism or the variable pathogenic impact of the carried variant are thought to play a major role.[171]

5. Discussion

This project reviewed both phenotypically and genotypically a large cohort of patients presenting with complex movement disorders (particularly combined or complex dystonia phenotypes), for whom exome sequencing data had been made available over the previous 6 years.

From a phenotypic perspective, the cohort was highly heterogeneous in terms of ethnicity, age of symptom onset, clinicoradiological features, and disease course, especially when compared to previous studies exploring genetic underpinnings of dystonia through WES.[122, 125-128] In particular, two groups were identified according to the age of onset, with early-onset (≤20 years) and late-onset (>20 years) phenotypes being equally represented (52.0% vs 48.0%, respectively). The prominent movement disorder in these complex syndromes was dystonia or

dystonic tremor, either alone or associated with parkinsonism, in nearly 60% of the study cohort. Body distribution of dystonia was equally highly heterogeneous, being generalized in only 55% of cases. Brain MRI was characterized by different combinations of, among others, cerebro/cerebellar atrophy, mineralization of the basal ganglia, and white matter abnormalities in above 80% of the patients for whom neuroradiological data were available. Although recruitment of cases followed the stringent inclusion criteria mentioned above as for clinico-radiological features, the interpretation of this cohort as representative of different phenotypes and genetic etiologies in complex and combined dystonic syndromes should be cautious. Indeed, since the majority of cases were recruited by adult neurologists, this study might have mainly included patients with less severe phenotypes and survival into adulthood.

Overall, the combination of an extended candidate gene approach and a hypothesis free approach led to a confirmed or highly likely genetic etiology in 20.3% of the clinical study cohort. Moreover, a likely genetic cause was determined in further three cases (2.3%), where probabilistic assertions on variants' pathogenicity could not be strengthen by segregation analysis, additional genetic and/or functional tests in the proband or their pedigree, or evidence from previous literature. In 12 cases who initially matched the inclusion criteria, clinical features recorded during their follow-up (i.e., the evolution of their clinical picture and response to treatment till the end of this study) excluded a genetic aetiology of their disorders or made it very unlikely. These were mainly patients with atypical parkinsonism (multiple system atrophy or progressive supranuclear palsy), some of whom were initially recruited due to MRI evidence of iron deposition in the basal ganglia. By exclusion of these cases *a posteriori*, WES resulted to detect an at least likely genetic etiology in 27.6% of cases, which is consistent with the majority of recently published studies on dystonia cohorts analyzed through WES.[122, 125-128] The main findings from the present study have been discussed in the relative sub-paragraphs of the results. The final diagnostic yield suggests the presence of several causal dystonia genes yet to be identified. In addition, given that the overall exome coverage was not 100% (for none of the depths, see Figure III-7), it is even more likely that more disease-

causing mutations in known and novel dystonia-associated genes were simply not covered by this approach and missed. This might depend on the large variation in sequencing coverage between exomes obtained over a 6-year period, which reflects the evolution of Illumina platforms and technologies. In addition, this adds to bioinformatics-related "data loss" due to misannotation and subsequent misfiltering. Finally, limitations of both next-generation (and exome) sequencing should be considered when reflecting on the frequency of confirmed genetic etiologies in the present dystonia cohort. In this regard, it is worth mentioning that alternative genetic tests performed simultaneously to WES revealed the conclusive diagnosis in three "WES-negative" cases, who were diagnosed with Huntington disease (Southern blotting), *PRKN*-associated Parkinson's disease (MLPA), and Leigh-like syndrome associated to the *MT-TF* gene (mitochondrial DNA sequencing).

This study has several limitations, which are mostly attributable to its retrospective design and intrinsic limitations of NGS techniques. For instance, it was not possible to collect precise history and family history as well as detailed clinicoradiological features in several patients, for whom a generic referral to the neurogenetic research laboratory for complex dystonia or NBIA was the only information available. For the same reason, the extension of genetic testing to probands' family members to perform segregation analysis was possible in a very limited number of cases, including six patients for whom a confirmed molecular diagnosis was formulated. WES is a fast, reliable, and affordable technique that permits screening of known genes and identification of new genes in singletons, pedigrees and disease cohorts. However, it is not able to detect large deletion/expansion, repeats, and copy number variants, which are increasingly recognized as molecular underpinnings of neurodegenerative disorders. In this study, WES was not complemented with CGH array for each of the samples, or even for those with unknown genetic etiology. This is a limitation of this study, since especially copy number variations are often enriched in patients with developmental delay, mental retardation and psychiatric phenotypes as present in the cohort investigated here. In addition, genes harbouring disease-causing mutations for an individual may not (or not sufficiently) be covered

in the exome capture target kit definition (see Chapter I). For the present study cohort, 100% exome coverage was not available and therefore the approach is likely to have missed more variants. Finally, the sample size may be too small to detect either novel pathogenic variants or disease genes reliably or to conduct case-control studies and check for enrichment of pathogenic variants in the disease cohort.

In conclusion, this study has analyzed both phenotipically and genotypically a cohort of 128 patients presenting with complex movement disorders (particularly combined or complex dystonia phenotypes) and exome data available. The *post-hoc* diagnostic yield of WES in the present cohort was 27.6%. Besides expanding the phenotypic and genotypic spectrum of several genetic dystonic syndromes, this study has replicated the association between the *DRD2* gene and a choreo-dystonia phenotype and identified one recently confirmed dystonia-associated gene (*TSPOAP1*) and one new candidate gene (*ENSG00000165714*), for which further research is ongoing.

Chapter IV

Exploring combined and complex dystonia syndromes through whole-genome sequencing – Preliminary results from an ongoing clinicogenetic study

1. Preamble.

The ongoing study presented in this chapter aims to characterize phenotypically and genotypically a large cohort of patients with dystonia syndromes who are actively enrolled in the 100,000 Genomes Project after recruitment at the National Hospital for Neurology and Neurosurgery, London, UK. The 100,000 Genomes Project is a national sequencing project led by the UK Department of Health. It aimed to sequence and analyze 100,000 genomes from patients with rare diseases, including neurological and neurodevelopmental disorders, and cancer between 2013 and 2019. The present study planned to analyze whole-genome sequencing (WGS) data through both an extended "candidate-gene approach" and a "hypothesis-free approach", in agreement with the methods followed in the study on whole-exome sequencing presented in the previous chapter. However, this study has been delayed by the COVID-19 pandemic and is currently ongoing. I will therefore present here only general information about subjects and methods as well as relevant findings from WGS data analysis through the candidate-gene approach in the first 30 subjects analyzed. Due to this selection bias and the limited WGS data analysis, I will not report on any statistics about the study cohort nor considerations about the diagnostic yield of WGS for dystonia phenotypes.

My role in this study consisted of reviewing clinical records, analyzing WGS data through an extended "candidate-gene approach", validating promising WGS findings by Sanger sequencing, perform segregation analysis (if probands' family members were available for genetic testing). By selecting patients recruited under Human Phenotype Ontology terms "dystonia", "tremor" and "parkinsonism", I obtained a list of 486 cases with annotated genomes, of which approximately 300 had confirmed dystonic features.

2. Subjects and methods

Subjects

I analyzed a pool of 50 genomes belonging to patients who were enrolled in the 100,000 Genomes Project at the National Hospital for Neurology and Neurosurgery. Inclusion criteria for selected available genome was an enrolment using the Human Phenotype Ontology terms including in their string the words "dystonia", "tremor", or "parkinsonism". These aimed to include

DNA sample retrieval

WGS-associated DNA samples previously collected at the National Hospital for Neurology and Neurosurgery (NHNN), London, UK, were retrieved for possible further testing to validate NGS findings. DNA was previously extracted from peripheral white blood cells according to standard procedures in the neurogenetic diagnostic laboratory at the NHNN. The ethics committee of Queen Square had approved the study. All patients had given their consent prior to the study, which was conducted according to the Declaration of Helsinki.

Review of clinical data

Clinical records available at the NHNN were extensively reviewed and integrated with information from face-to-face assessment. Predefined categories for which data were extracted were sex, ethnicity, history of developmental delay and/or regression, characteristics of dystonia (isolated/combined, presence of tremor, age at symptom onset, symptom(s) at onset), age at first assessment, age at last assessment, associated neurological, psychiatric, and systemic symptoms/signs, findings from laboratory, neuroimaging (in particular, brain MRI and DaTscan) and other investigations, past medical and surgical history, pharmacological history, family history of neurological and/or psychiatric disorders, history of parental consanguinity, negative results of previous genetic tests, response to treatment.

Generation of WGS data and bioinformatic pipeline

DNA was extracted from whole blood at a central DNA extraction and QC laboratory. Samples were tested for adequate concentration (Picogreen), DNA degradation (gel electrophoresis) and purity (OD 260/280 quality control (Trinean)) before selection for WGS. DNA samples were prepared at a minimum concentration of 30 ng/µl in 110 µl, visually inspected for degradation and had to have an OD 260/280 between 1.75 and 2.04. They were then prepared in batches of 96 and shipped on dry ice to the sequencing provider (Illumina Inc, Great Chesterford, UK). Further sample QC was performed by Illumina Inc to ensure that the concentration of the DNA was > 30 ng/ul and that every sample generated high quality genotyping results (Illumina Infinium Human Core Exome microarray). 0.5 µg of the DNA sample was fragmented using Covaris LE220 (Covaris Inc., Woburn, MA, USA) to obtain an average size of 450 base pair (bp) DNA fragments. DNA samples were processed using the certified Illumina TruSeq DNA PCR-Free Sample Preparation kit (Illumina Inc., San Diego, CA, USA) on the Hamilton Microlab Star (Hamilton Robotics, Inc, Reno, NV, USA). The final libraries were checked using the Roche LightCycler 480 II (Roche Diagnostics Corporation, Indianapolis, IN, USA) with KAPA Library Quantification Kit (Kapa Biosystems, Inc, Wilmington, MA, USA) for concentration. From February 2014 to June 2017 three read lengths were used: 100bp (377 samples), 125bp (3,154 samples) and 150bp (9,656 samples). Samples sequenced with 100bp and 125bp reads utilised three and two lanes of an Illumina HiSeq 2500 instrument, respectively. Samples sequenced with 150bp reads utilised a single lane of a HiSeq X instrument. At least 95% of the autosomal genome had to be covered at 15X and a maximum of 5% of insert sizes had to be less than twice the read length. Following sample and data QC at Illumina, 13,187 sets of WGS data files were received at the University of Cambridge High Performance Computing Service (HPC) for further QC. An overview of the 4-step Illumina NGS workflow is provided in Figure III-1.

Variant filtering and analysis through a “candidate-gene” approach

Based on the clinical diagnoses of cases included and evidence from the study reported in chapter III, I selected as candidate genes (see Box IV-1) those included in panels for early-onset dystonia (114 genes), Parkinson's disease and complex parkinsonism (66 genes), hereditary spastic paraplegia (107 genes), hereditary ataxia (254 genes), mitochondrial disorders (473 genes), and undiagnosed metabolic disorders (649 genes) in the *Genomics England PanelApp* (https://panelapp.genomicsengland.co.uk).

Box IV-1. Candidate genes analyzed

Early onset dystonia (Version: 1.86): 114 genes
ADAR; ADCY5; ANO3; APTX; ATM; ATP13A2; ATP1A3; ATP7B; BCAP31; C19orf12; CHMP2B; COASY; CP; CSTB; DCAF17; DDC; DLAT; FA2H; FBXO7; FTL; GCH1; GNAO1; HPCA; HTRA2; KMT2B; MECR; NKX6-2; PANK2; PINK1; PLA2G6; PNKD; PRKN; PRKRA; PRRT2; SERAC1; SGCE; SLC2A1; SLC30A10; SLC6A3; SPR; SYNJ1; TH; THAP1; TOR1A; TUBB4A; VAC14; VPS13A; WDR45; WDR73; XK; YY1; CIZ1; GNAL; TAF1; ACTB; AFG3L2; AP1S2; ARSA; ARX; ATP1A2; AUH; CACNA1A; CYP27A1; DCTN1; DRD2; DRD5; EARS2; ERCC6; FASTKD2; FOXG1; FOXRED1; GAMT; GCDH; HPRT1; KCNQ2; L2HGDH; MAT1A; MCOLN1; MMADHC; MPV17; MR1; MT-ND6; NDUFA12; NPC2; PARK7; PCDH12; PDGFRB; PDHX; PLP1; PNPT1; PSEN1; PTEN; PTS; QDPR; RNASEH2A; RNASEH2B; RNASEH2C; SAMHD1; SCP2; SDHAF1; SLC19A3; SLC20A2; SLC39A14; SLC46A1; SUCLA2; SUOX; TIMM8A; TPK1; TREM2; TREX1; VPS37A; ATXN2_CAG; ATXN3_CAG; JPH3_CTG.
Parkinson Disease and Complex Parkinsonism (Version; 1.69): 66 genes
ATP13A2; ATP1A3; C19orf12; CSF1R; DCTN1; DNAJC6; FBXO7; FTL; GBA; GCH1; GRN; LRRK2; LYST; MAPT; OPA3; PANK2; PARK7; PINK1; PLA2G6; PRKN; PRKRA; PTRHD1; RAB39B; SLC30A10; SLC39A14; SLC6A3; SNCA; SPG11; SPR; SYNJ1; TH; TUBB4A; VPS13A; VPS35; WDR45; CHCHD2; TAF1; ANO3; ATP6AP2; ATXN2; ATXN3; C9orf72; EIF4G1; GIGYF2; GNAL; HTRA2; HTT; IPPK; JPH3; NR4A2; SGCE; SLC41A1; SNCAIP; TBP; THAP1; TOR1A; UCHL1; ATN1; ATXN1; ATXN2; ATXN3; C9orf72; HTT; JPH3; PPP2R2B; TBP.
Hereditary spastic paraplegia (Version 1.219): 107 genes
ABCD1; ADAR; AFG3L2; AIMP1; ALDH18A1; ALS2; AP4B1; AP4E1; AP4M1; AP4S1; ARG1; ATL1; ATP13A2; B4GALNT1; BSCL2; C12orf65; C19orf12; CAPN1; CYP27A1; CYP2U1; CYP7B1; DDHD1; DDHD2; ERLIN1; ERLIN2; FA2H; FARS2; GBA2; HACE1; HSPD1; KIDINS220; KIF1A; KIF5A; L1CAM; NIPA1; NKX6-2; NT5C2; OPA3; PCYT2; PLP1; PNPLA6; POLR3A; REEP1; RNASEH2B; RTN2; SACS; SERAC1; SLC16A2; SLC1A4;

SLC25A46; SLC2A1; SPART; SPAST; SPG11; SPG21; SPG7; TFG; TUBB4A; UBAP1; WASHC5; WDR45B; ZFYVE26; CDK16; DARS; GCH1; IBA57; KDM5C; KIF1C; LYST; MAG; MARS2; MTPAP; REEP2; SARS2; SLC33A1; AMPD2; AP5Z1; ARL6IP1; ARSI; CCT5; DSTYK; ENTPD1; GAD1; GJC2; KLC4; MARS; PCDH12; PGAP1; PSEN1; RAB3GAP2; TECPR2; USP8; VAMP1; VPS37A; WDR48; ZEB2; ZFYVE27; ATXN10_ATTCT; ATXN1_CAG; ATXN2_CAG; ATXN3_CAG; ATXN7_CAG; CACNA1A_CAG; FXN_GAA; HTT_CAG; PPP2R2B_CAG; TBP_CAG.
Hereditary ataxia – adult onset (Version 2.42): 254 genes
AAAS; ABCB7; ABHD12; ADCY5; ADGRG1; ADPRHL2; AFG3L2; AMPD2; ANO10; AP1S2; APTX; ARMC9; ARSA; ATCAY; ATM; ATP1A2; ATP1A3; ATP7B; ATP8A2; B3GALNT2; B4GAT1; BRF1; CA8; CACNA1A; CACNA1G; CAMTA1; CAPN1; CASK; CHMP1A; CLCN2; CLN6; CLP; 1; COA7; COASY; COG5; COQ8A; COX20; CP; CSTB; CWF19L1; CYP27A1; CYP2U1; DARS2; DDHD2; DNAJC19; DNAJC5; DNMT1; EBF3; EIF2B1; EIF2B2; EIF2B3; EIF2B4; EIF2B5; ELOVL4; EPM2A; EXOSC3; EXOSC8; EXOSC9; FGF14; FLVCR1; FOLR1; FXN; GBA2; GFAP; GJC2; GLRA1; GLRB; GOSR2; GPAA1; GRID2; GRM1; HEXA; HEXB; IRF2BPL; ITPR1; KCNA1; KCNA2; KCNC3; KCND3; KCNJ10; KCNQ2; KIF1C; MAPK8IP3; MARS2; MFN2; MMACHC; MRE11; MSTO1; MT-ATP6; MTTP; NHLRC1; NKX2-1; NKX6-2; NPC1; NPC2; OPA1; OPA3; OPHN1; PACS2; PEX16; PEX6; PLA2G6; PMPCA; PMPCB; PNKD; PNKP; PNPLA6; POLG; POLR3A; PRICKLE1; PRKCG; PRNP; PRRT2; PTRH2; PUM1; RARS2; RNF170; RNF216; ROBO3; RORA; SACS; SAMD9L; SCN1A; SCN8A; SCYL1; SEPSECS; SETX; SIL1; SLC1A3; SLC25A46; SLC2A1; SLC39A8; SLC52A2; SLC9A1; SLC9A6; SNX14; SPG7; SPR; SPTBN2; SQSTM1; SRD5A3; STUB1; SYNE1; SYNGAP1; TBC1D23; TERT; TMEM106B; TMEM240; TOE1; TPP1; TSEN15; TSEN2; TSEN54; TTBK2; TTPA; TUBA1A; TUBB2B; TUBB3; TUBB4A; TWNK; UBA5; UCHL1; VLDLR; VPS13D; VPS53; WDR73; WDR81; WFS1; WWOX; ZFYVE26; AARS; ATP2B3; DYNC1H1; EEF2; ELOVL5; GALC; GDAP2; KCNQ3; LNPK; MORC2; MTPAP; PEX2; SAR1B; VAMP1; VRK1; XRCC1; ALAS2; ATN1; ATXN1; ATXN10; ATXN2; ATXN3; ATXN7; ATXN8; BEAN1; CACNB4; CCDC88C; CDK5; DAB1; DCC; DMXL2; FMR1; FRMD4A; GLI3; HTT; KCNK18; MME; MVK; NAGLU; NOP56; PAX2; PAX6; PCLO; PDYN; PI4KA; PIK3R5; POLG2; PPP2R2B; RELN; RUBCN; SCN9A; SLC25A32; SLC6A5; SMPD4; SYT14; TBP; TDP1; TGM6; THG1L; TINF2; TSEN34; TTC19; TUBA8; TUBB; TUBB2A; UBR4; ZNF592; ATN1_CAG; ATXN10_ATTCT; ATXN1_CAG; ATXN2_CAG; ATXN3_CAG; ATXN7_CAG; CACNA1A_CAG; CSTB_CCCCGCCCCGCG; FMR1_CGG; FXN_GAA; NOP56_GGCCTG; PPP2R2B_CAG; TBP_CAG; ISCA-37404-Loss; ISCA-37478-Gain; ISCA-37478-Loss; ISCA-37468-Loss.
Mitochondrial disorders (Version 2.34): 473 genes
AARS2; ABAT; ABCB7; ACAD9; ACO2; AFG3L2; AGK; AIFM1; ANO10; APOPT1; APTX; ATAD3A; ATP5D; ATPAF2; BCS1L; BOLA3; BTD; C12orf65; C19orf70; C1QBP; CA5A; CARS2; CHCHD10; CLPB; CLPP; COA6; COA7; COQ2; COQ4; COQ6; COQ7; COQ8A;

COQ8B; COQ9; COX10; COX14; COX15; COX20; COX6A1; COX6B1; COX7B; CYC1; DARS2; DGUOK; DLAT; DLD; DNA2; DNAJC19; DNM1L; DNM2; EARS2; ECHS1; ELAC2; ETFDH; ETHE1; FARS2; FASTKD2; FBXL4; FDX2; FDXR; FH; FLAD1; FOXRED1; GARS; GDAP1; GFER; GFM1; GFM2; GLRX5; GTPBP3; HARS2; HCCS; HIBCH; HLCS; HSD17B10; HSPD1; HTRA2; IARS2; IBA57; ISCA1; ISCA2; ISCU; KARS; LARS2; LIAS; LIPT1; LIPT2; LONP1; LRPPRC; LYRM7; MARS2; MDH2; MECR; MFF; MFN2; MGME1; MICU1; MIPEP; MPC1; MPV17; MRPL3; MRPL44; MRPS2; MRPS22; MRPS34; MSTO1; MT-ATP6; MT-ATP8; MT-CO1; MT-CO2; MT-CO3; MT-CYB; MTFMT; MT-ND1; MT-ND2; MT-ND3; MT-ND4; MT-ND4L; MT-ND5; MT-ND6; MTO1; MTPAP; MT-RNR1; MT-TA; MT-TC; MT-TD; MT-TE; MT-TF; MT-TG; MT-TH; MT-TI; MT-TK; MT-TL1; MT-TL2; MT-TM; MT-TN; MT-TP; MT-TQ; MT-TR; MT-TS1; MT-TS2; MT-TV; MT-TW; MT-TY; NADK2; NARS2; NAXE; NDUFA1; NDUFA10; NDUFA11; NDUFA2; NDUFA4; NDUFA6; NDUFA9; NDUFAF1; NDUFAF2; NDUFAF3; NDUFAF4; NDUFAF5; NDUFAF6; NDUFAF8; NDUFB11; NDUFB3; NDUFB8; NDUFS1; NDUFS2; NDUFS3; NDUFS4; NDUFS6; NDUFS7; NDUFS8; NDUFV1; NDUFV2; NFU1; NUBPL; OPA1; OPA3; PARS2; PC; PDHA1; PDHB; PDHX; PDP1; PDSS1; PDSS2; PET100; PMPCA; PMPCB; PNPLA8; PNPT1; POLG; POLG2; PPA2; PUS1; QRSL1; RARS2; RMND1; RNASEH1; RRM2B; RTN4IP1; SACS; SARS2; SCO1; SCO2; SDHA; SDHAF1; SDHD; SERAC1; SFXN4; SLC19A2; SLC19A3; SLC25A1; SLC25A12; SLC25A19; SLC25A26; SLC25A3; SLC25A32; SLC25A38; SLC25A4; SLC25A42; SLC25A46; SPG7; SUCLA2; SUCLG1; SURF1; TACO1; TAZ; TIMM50; TIMM8A; TK2; TMEM126B; TMEM70; TOP3A; TPK1; TRIT1; TRMT10C; TRMT5; TRMU; TRNT1; TSFM; TTC19; TUFM; TWNK; TYMP; UQCC2; UQCRB; VARS2; WARS2; YARS2; ATP5A1; ATP5F1; ATP5H; ATP5J2; ATP5L; ATP5L2; ATPAF1; COA3; COA4; COQ5; COX11; COX16; COX17; COX18; COX19; COX6A2; COX6B2; CYCS; DCC; ERAL1; G6PC; GATB; GATC; HPDL; IDH3A; IDH3B; MRM2; MRPS14; MRPS16; MT-RNR2; MT-TT; NDUFA12; NDUFAF7; NDUFB7; NDUFB9; NFS1; NSUN3; PITRM1; POLRMT; PTCD3; QARS; SDHAF3; SDHAF4; SDHB; SLC25A21; SPATA5; TARS2; TFAM; TIMM22; TIMMDC1; TMEM65; TOMM70; UQCC1; UQCC3; UQCR10; UQCR11; UQCRC2; UQCRQ; XPNPEP3; YME1L1; ABCB6; ACADM; ACADS; ACADSB; ACADVL; ACAT1; AK2; ALAS2; ALDH18A1; ALDH1B1; APOO; ATAD3B; ATP5B; ATP5C1; ATP5E; ATP5G1; ATP5G2; ATP5G3; ATP5I; ATP5J; ATP5O; BDH1; BOLA1; BOLA2; C19orf12; CEP89; CHKB; CISD2; CLPX; COA1; COA5; COASY; COX4I1; COX4I2; COX5A; COX5B; COX6C; COX7A1; COX7A2; COX7B2; COX7C; COX8A; CPT1A; CPT2; CRAT; CTBP1; CYP24A1; D2HGDH; DARS; DHTKD1; DIABLO; DIAPH1; DLST; DTD1; DYM; ECSIT; ERCC6L2; ETFA; ETFB; FA2H; FBP2; FGF12; FXN; GATM; GLUD1; GUF1; HADH; HADHA; HADHB; HMGCL; HMGCS2; HSPA9; HSPE1; HTT; IARS; IER3IP1; KIF5A; L2HGDH; LACTB; LARS; LETM1; LYRM4; MICU2; MRPL12; MRPL40; MRPS23; MRPS7; NAXD; NDUFA13; NDUFA3; NDUFA5; NDUFA7; NDUFA8; NDUFAB1; NDUFB1; NDUFB10; NDUFB2; NDUFB4; NDUFB5;

NDUFB6; NDUFC1; NDUFC2; NDUFS5; NDUFV3; NNT; OGDH; OXA1L; OXCT1; PAM16; PANK2; PDE12; PDK1; PDK2; PDK3; PDK4; PDP2; PDPR; PET117; PLA2G6; PNPLA4; POP1; PPOX; PTCD1; PTRH2; PYCR1; ROBO3; SAMHD1; SDHAF2; SDHC; SECISBP2; SEPSECS; SLC22A5; SLC25A10; SLC25A13; SLC25A20; SLC25A22; SLC25A24; SLC25A40; SLC33A1; SLC39A8; SLC44A1; SLC52A2; SLC52A3; SRRT; SSBP1; STAT2; STXBP1; SUCLG2; TANGO2; TIMM44; TMEM126A; TRAK1; TRAP1; TXN2; UQCRC1; UQCRFS1; UQCRH; USMG5; VPS13C; WFS1; XRCC4; DMPK_CTG; FXN_GAA; ISCA-37440-Loss.
Undiagnosed metabolic disorders (Version 1.457): 649 genes
AARS2; AASS; ABAT; ABCA1; ABCB11; ABCB4; ABCB7; ABCD1; ABCD4; ABCG5; ABCG8; ABHD12; ABHD5; ACAD8; ACAD9; ACADM; ACADS; ACADSB; ACADVL; ACAT1; ACO2; ACOX1; ACSF3; ACY1; ADA; ADAR; ADSL; AFG3L2; AGA; AGK; AGL; AGPS; AGXT; AHCY; AIFM1; AKR1D1; ALAD; ALAS2; ALDH18A1; ALDH3A2; ALDH4A1; ALDH5A1; ALDH6A1; ALDH7A1; ALDOA; ALDOB; ALG1; ALG11; ALG12; ALG14; ALG3; ALG6; ALG8; ALG9; ALPL; AMACR; AMN; AMT; ANO10; APOA1; APOA5; APOB; APOC2; APOE; APOPT1; APRT; APTX; ARG1; ARSA; ARSB; ARSE; ASAH1; ASL; ASPA; ASS1; ATAD3A; ATIC; ATP13A2; ATP6AP1; ATP6V0A2; ATP7A; ATP7B; ATP8B1; ATPAF2; AUH; B3GALNT2; B3GALT6; B3GAT3; B3GLCT; B4GALT1; B4GALT7; BAAT; BCKDHA; BCKDHB; BCKDK; BCS1L; BOLA3; BTD; C12orf65; C19orf12; CA5A; CAT; CBS; CCDC115; CHCHD10; CHKB; CHST14; CHST3; CHST6; CHSY1; CISD2; CLDN16; CLDN19; CLN3; CLN5; CLN6; CLN8; CLPB; CLPP; CNNM2; COG1; COG4; COG5; COG6; COG7; COG8; COQ2; COQ4; COQ6; COQ7; COQ8A; COQ8B; COQ9; COX10; COX14; COX15; COX20; COX6A1; COX6B1; COX7B; CP; CPOX; CPS1; CPT1A; CPT2; CTH; CTNS; CTSA; CTSC; CTSD; CTSK; CUBN; CYC1; CYP27A1; CYP7B1; D2HGDH; DARS; DARS2; DBH; DBT; DCXR; DDC; DGUOK; DHCR24; DHCR7; DHFR; DHODH; DHTKD1; DLAT; DLD; DNA2; DNAJC12; DNAJC19; DNAJC5; DNM1L; DNM2; DOLK; DPAGT1; DPM1; DPM2; DPM3; DPYD; DPYS; DYM; EARS2; EBP; ECHS1; ELAC2; ENO3; EPG5; EPM2A; ETFA; ETFB; ETFDH; ETHE1; EXT1; EXT2; FA2H; FAH; FAR1; FARS2; FASTKD2; FBP1; FBXL4; FDX2; FECH; FGFR2; FH; FKRP; FKTN; FMO3; FOLR1; FOXRED1; FTCD; FUCA1; FUT8; FXN; G6PC; G6PC3; GAA; GABRG2; GALC; GALE; GALK1; GALNS; GALNT3; GALT; GAMT; GARS; GATM; GBA; GBE1; GCDH; GCH1.GCLC; GDAP1; GFER; GFM1; GFPT1; GIF; GK; GLA; GLB1; GLDC; GLRA1; GLRX5; GLUD1; GLUL; GLYCTK; GM2A; GMPPB; GNE; GNMT; GNPAT; GNPTAB; GNPTG; GNS; GPD1; GPHN; GRHPR; GSS; GTPBP3; GUSB; GYG1; GYS1; GYS2; HAAO; HADH; HADHA; HADHB; HAMP; HARS2; HCCS; HCFC1; HEXA; HEXB; HFE; HFE2; HGD; HGSNAT; HIBCH; HLCS; HMBS; HMGCL; HMGCS2; HOGA1; HPD; HPRT1; HPS1; HS2ST1; HSD17B10; HSD17B4; HSD3B7; HSPD1; HTRA2; HYAL1; IARS2; IBA57; IDH2; IDS; IDUA; IER3IP1; ISCA2; ISCU; ISPD; ITPA; IVD; KARS; KYNU; L2HGDH; LAMP2; LARGE1; LARS; LARS2; LBR; LCAT; LCT; LDHA; LDLR; LDLRAP1; LIAS; LIPA; LIPT1; LMBRD1; LONP1; LPIN1; LPL; LRPPRC; MAGT1; MAN1B1;

MAN2B1; MANBA; MAOA; MARS2; MAT1A; MCCC1; MCCC2; MCEE; MCOLN1; MFF; MFN2; MFSD8; MGAT2; MGME1; MLYCD; MMAA; MMAB; MMACHC; MMADHC; MOCS1; MOCS2; MOGS; MPDU1; MPI; MPV17; MRPL3; MRPS22; MSMO1; MT-ATP6; MT-ATP8; MT-CO1; MT-CO2; MT-CO3; MT-CYB; MTFMT; MTHFR; MT-ND1; MT-ND2; MT-ND3; MT-ND4; MT-ND4L; MT-ND5; MT-ND6; MTO1; MTPAP; MTR; MT-RNR1; MTRR; MT-TA; MT-TC; MT-TD; MT-TE; MT-TF; MT-TG; MT-TH; MT-TI; MT-TK; MT-TL1; MT-TL2; MT-TM; MT-TN; MTTP; MT-TP; MT-TQ; MT-TR; MT-TS1; MT-TS2; MT-TV; MT-TW; MT-TY; MUT; MVK; NAGA; NAGLU; NAGS; NARS2; NDUFA1; NDUFA10; NDUFA11; NDUFA2; NDUFAF1; NDUFAF2; NDUFAF3; NDUFAF4; NDUFAF5; NDUFAF6; NDUFB11; NDUFB3; NDUFS1; NDUFS2; NDUFS3; NDUFS4; NDUFS6; NDUFS7; NDUFS8; NDUFV1; NDUFV2; NEU1; NFU1; NGLY1; NHLRC1; NNT; NPC1; NPC2; NSDHL; NT5C3A; NUBPL; OAT; OCRL; OPA1; OPA3; OTC; OXCT1; PAH; PANK2; PC; PCBD1; PCCA; PCCB; PCK1; PCSK9; PDHA1; PDHB; PDHX; PDP1; PDSS1; PDSS2; PEPD; PET100; PEX1; PEX10; PEX11B; PEX12; PEX13; PEX14; PEX16; PEX19; PEX2; PEX26; PEX3; PEX5; PEX6; PEX7; PFKM; PGAM2; PGAP2; PGAP3; PGK; 1.00; PGM1; PGM3; PHGDH; PHKA1; PHKA2; PHKB; PHKG2; PHYH; PIGA; PIGL; PIGN; PIGO; PIGT; PIGV; PINK1; PLA2G6; PMM2; PMPCA; PNP; PNPO; PNPT1; POLG; POLG2; POMGNT1; POMGNT2; POMT1; POMT2; POR; PPA2; PPOX; PPT1; PRKAG2; PRODH; PRPS1; PSAP; PSAT1; PTS; PUS1; PYCR1; PYGL; PYGM; QDPR; RARS2; RBCK1; RBP4; RFT1; RMND1; RNASEH1; RPIA; RPL10; RRM2B; SACS; SAMHD1; SAR1B; SARS2; SC5D; SCO1; SCO2; SCP2; SDHA; SDHAF1; SDHB; SDHD; SEC23B; SERAC1; SETX; SGSH; SI; SKIV2L; SLC12A3; SLC16A1; SLC17A5; SLC18A2; SLC19A2; SLC19A3; SLC22A5; SLC25A1; SLC25A12; SLC25A13; SLC25A15; SLC25A19; SLC25A20; SLC25A22; SLC25A26; SLC25A3; SLC25A38; SLC25A4; SLC25A46; SLC2A1; SLC2A2; SLC30A10; SLC35A1; SLC35A2; SLC35C1; SLC35D1; SLC37A4; SLC39A14; SLC39A4; SLC39A8; SLC3A1; SLC40A1; SLC46A1; SLC52A2; SLC52A3; SLC5A1; SLC6A19; SLC6A20; SLC6A3; SLC6A8; SLC7A7; SLC7A9; SMPD1; SPG7; SPR; SPTLC1; SPTLC2; SRD5A3; SSR4; ST3GAL3; ST3GAL5; STS; SUCLA2; SUCLG1; SUMF1; SUOX; SURF1; TACO1; TALDO1; TANGO2; TAT; TAZ; TCN2; TFR2; TIMM8A; TK2; TMEM165; TMEM5; TMEM70; TPK1; TPP1; TRAP1; TREX1; TRIM37; TRMU; TRNT1; TRPM6; TSFM; TTC19; TTC37; TTPA; TUFM; TUSC3; TWNK; TYMP; UGT1A1; UMOD; UMPS; UQCRB; UROD; UROS; VARS2; VIPAS39; VKORC1; VPS33B; WDR45; WFS1; XDH; XYLT1; XYLT2; YARS2; ALG13; ATP5A1; ATP5E; COX4I2; CSTB; DHDDS; GLS; HSPA9; LIPC; MRPS16; NDUFA12; NDUFB9; NDUFC2; OPLAH; PDK3; PIGM; PSPH; RANBP2; RNASET2; RYR1; SDHAF2; SDHC; STAT2; TH; UQCRQ; UROC1; ABCG2; ALG2; AMPD1; AOX1; ARSG; ATXN7; BCAT1; BCAT2; C1GALT1C1; CD320; CETP; CLPS; CNDP1; COA5; COX8A; CYP7A1; DHFR2; DLST; DMGDH; DPEP1; EGF; FOLR2; FOLR3; FXYD2; GALNT12; GCSH; GGT1; HAL; HYKK; KHK; LFNG; LIPI; LYRM4; MRPL12; MTHFD1; NAT8L; NDUFA9; NT5C; NUP62; OGDH; PDK1; PDK2; PDK4; PDP2; PDPR; PDXK; PEX11A;

PHKG1; PHYKPL; PNLIP; PPM1B; PPM1K; PREPL; PTPRZ1; RNASEH2A; RNASEH2B; RNASEH2C; SARDH; SCARB1; SHPK; SLC22A4; SLC25A2; SLC27A5; SLC36A2; SLC52A1; SLCO1B1; SLCO1B3; SUCLG2; SUGCT; TCN1; TDO2; TM6SF2; TMEM126A; TPMT; TREH; UPB1; USF1; ISCA-37440-Loss.

Analysis of variants were initially conducted using the Opal platform by Fabric Genomics in the research environment, the access to which was provided to researchers with authorized study protocol in the context of the 100,000 Genomes Project. An example of the output for variant analysis in the Opal platform is provided in Figure IV-1.

Variants resulting from call of Tier 1, Tier 2, and Tier 3 variants (Figure IV-1) were manually looked through, and further filtered to prioritize their analysis according to previous description in the literature, frequency against annotated control databases (ExAC, http://exac.broadinstitute.org/; gnomAD, http://gnomad.broadinstitute.org/), and variant pathogenicity prediction according to *in silico* tools, including PolyPhen-2 (http://genetics.bwh.harvard.edu/pph2/), SIFT (http://sift.bii.a-star.edu.sg), and MutationTaster (http://www.mutationtaster.org/). The CADD score (https://cadd.gs.washington.edu/snv) was also integrated to the prioritization criteria, with a cut-off of 15 to determine deleteriousness. I also referred to OMIM (https://omim.org/) and Varsome (https://varsome.com/) for an overview of genes and variants, respectively.

Figure IV-1. Output variant analysis in the Opal platform/100,000 Genomes Project with their classification in Tier 1, Tier 2, and Tier 3

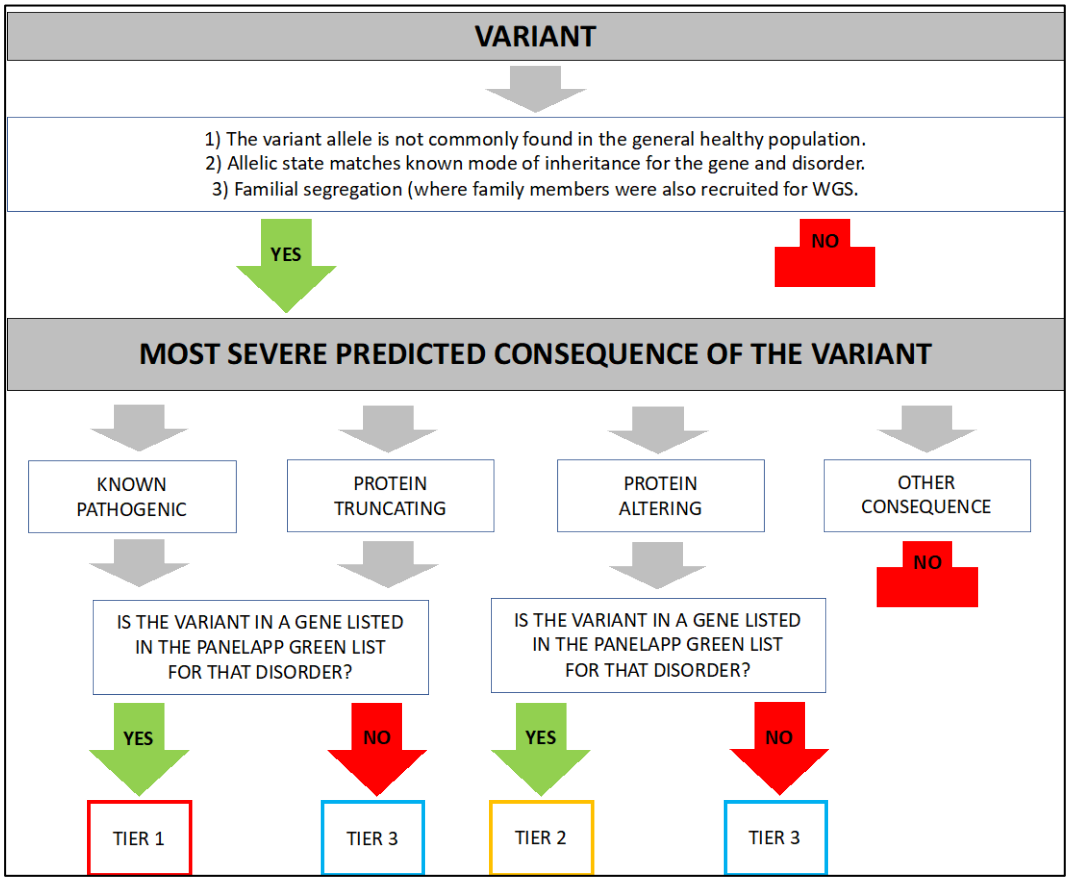

Variants were considered as having a causal association with the phenotype under investigation if they fulfilled the following criteria: 1) known likely pathogenic/pathogenic variant reported in ClinVar and/or HGMD, 3) loss of function (LoF) variants occurring in genes known to be intolerant to LoF according to the ExAC database, or 4) missense variants predicted to be deleterious by at least 2 of the aforementioned *in silico* prediction tools and absent or very rare in the aforementioned population databases. Fitting with the model of inheritance known for the gene was also required to confirm pathogenicity. Variants were finally interpreted according to the guidelines by the American College of Medical Genetics and Genomics (ACMG).[46]

Validation of NGS findings

I designed and blasted target-specific primers for the amplification of DNA regions carrying promising variants and performed Sanger sequencing to confirm

promising findings as reported in chapter III (see Methods and Box III-2). Electropherograms were analyzed using Sequencher 4.1.4, Gene Codes Corporation, Ann Arbor, MI, USA, or FinchTV 1.4.0, Geospiza, Inc., Seattle, WA, USA. If DNA from probands' family members was available, I performed segregation analysis. Finally, I reviewed the in-house database of exomes and contacted external collaborators to replicate novel promising findings.

3. Main preliminary results and related discussion

AMACR

A 46-year-old right-handed White British was first referred to the Movement Disorder clinic for a slowly progressive tremor in her arms and voice starting in her early-mid 30s. She reported intermittent head tremor and occasionally leg tremor when lying in bed. The patient was in good health until her teenage years, when she started to suffer from longstanding severe migraine. At age 17, she experienced an episode of left arm weakness which solved over a 6-month period. At age 23, she had an episode of severe right-side headache with documented left homonymous hemianopia and impaired left arm function, with slow but full recovery. At age 27, she was admitted to the ITU due to impaired consciousness after a tonic-clonic seizure. She remained in coma for one month. Then, she had a slow recovery over months, with residual mild cognitive impairment and emotional lability. The patient is an only child. Her father was diagnosed with primary progressive multiple sclerosis in late adulthood. Her family history was otherwise unremarkable as for neurological disorders. On examination, she presented with generalised dystonia, mainly affecting her neck, larynx, and arms. She had brisk reflexes throughout, mild limb dysmetria, and mild frontal disinhibition.

Blood tests revealed slightly elevated alanine transaminase on repetitive occasions. At the time of her first admission (when she was 23 years old), a brain MRI showed abnormalities suggestive of cerebral vasculitis. A muscle biopsy came back to be normal. She improved after a cycle of intravenous methylprednisolone. During her second admission at age 27, she underwent a brain CT scan which was normal, an

EEG which showed bilateral slow waves. Three consecutive brain MRI revealed symmetrical T2 hyperintensities in the pons, midbrain and bilateral posterior thalamus. On one occasion, after partial seizures, some swelling of the left hemisphere was detected. A lumbar puncture revealed mild inflammatory changes with increased lactate. At age 35, she was tested for serum anti-NMDR and anti-VGKC with negative results. An EEG at age 38 showed generalised excess of slow and theta activities. A follow-up brain MRI revealed T2/FLAIR hyperintensities in the midbrain, pons and both thalami, with involvement of the middle cerebellar peduncles (Figure IV-2, arrows). MR spectroscopy on the brainstem did not show any detectable lactate levels. There was neuronal loss within the leukoencephalopathy tissue in this region without increase in the choline levels, but with total creatine amount significantly increased. Whole sequencing of mitochondrial DNA was normal. The patient was finally enrolled in the 100,000 Genomes Project.

Figure IV-2. Neuroimaging of the first *AMACR* case

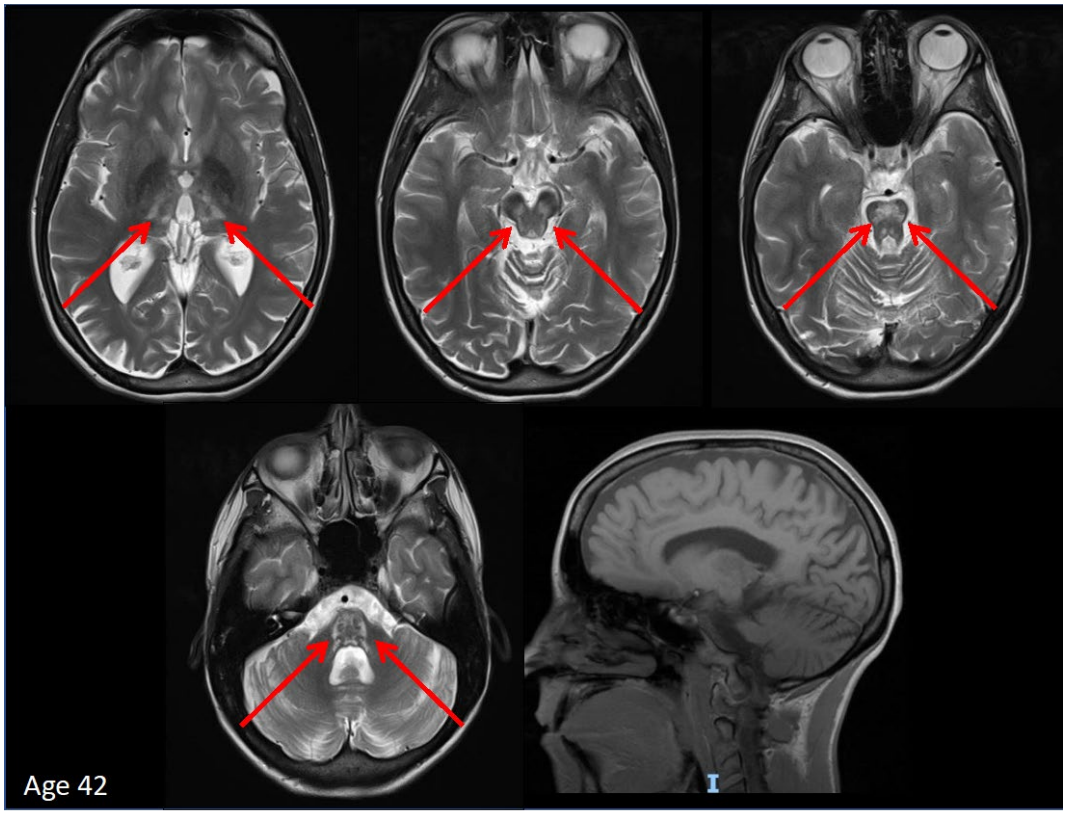

Whole genome sequencing and subsequent Sanger sequencing revealed that the patient was heterozygote for two novel variants in the *AMACR* gene. Segregation analysis revealed the presence of the missense variant also in her father and detect the deletion also in her daughter, thus confirming the variants were in *trans* configuration.

The missense variant has 2 heterozygous and no homozygous entries in the population database, affects an amino acid residue completely conserved across species down to invertebrates (Figure IV-3), and is consistently predicted pathogenic by in silico prediction tools, including a Combined Annotation Dependent Depletion (CADD) of 26.9.

The deletion variant has 5 heterozygous and no homozygous entries in gnomAD, is predicted to result in a frameshift mutant with the stop codon after 9 codons and a potential null allele. RNA was extracted from the proband's skin fibroblasts in the proband, and cDNA synthetized. Quantitative PCR confirmed statistically significant reduction of the AMACR transcript in the proband compared to healthy controls (Figure IV-3).

Figure VI-3. Segregation analysis in the first *AMACR* pedigree

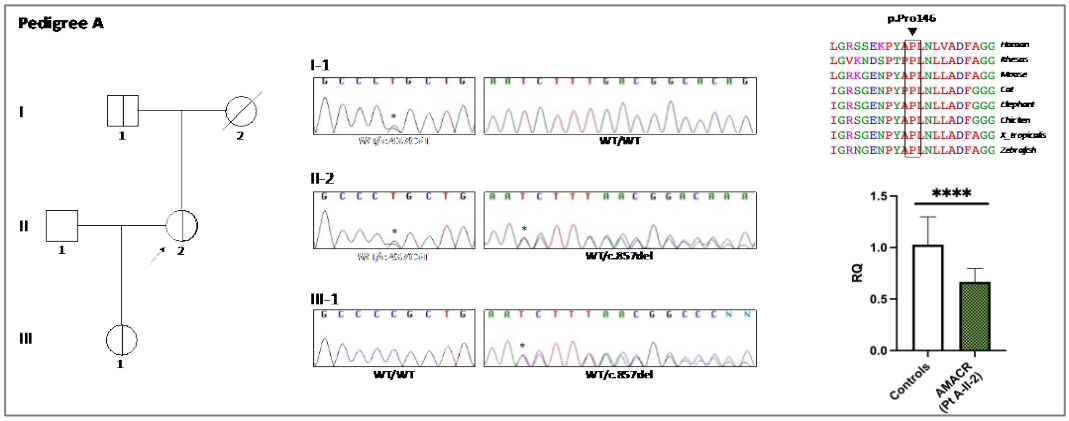

Sanger sequencing confirmed the proband was compound heterozygote for the variant NM_014324.5:c.437C>T (grey) in the *AMACR* gene, which was also detected in the proband's father, and the variant NM_014324.5:c.857delT (green) in the *AMACR* gene, which was also found in the proband's daughter. Electropherograms were analysed using the Sequencher software package. Arrow = proband; WT = wild type.

The diagnosis was further confirmed by Very Long Chain Fatty Acids. Her phytanic acid levels were normal. Her pristanic acid level was markedly elevated at 112.40 umol/L (range <2). Nerve conduction studies did not detect neuropathy. An ophthalmological revealed drusenoid material within the vascular arcades with localised retinal pigment epithelium loss. Finally, enzymatic activity tests for peroxisomal beta oxidation in the patient's fibroblasts showed a reduced peroxisomal beta-oxidation activity of the branched-chain fatty acid pristanic acid, but normal phytanic acid alpha-oxidation and normal very long-chain fatty acid metabolism. These results were in agreement with the diagnosis of the peroxisomal disorder AMACR deficiency.

Peroxisomes are dynamic organelles involved in a number of cellular catabolic and anabolic processes, including fatty acid alpha- and beta-oxidation, bile acid synthesis, and the early steps of plasmalogen production. Defects in human genes encoding peroxisomal proteins account for a group of heterogenous metabolic disorders with variable degree of severity ranging from early lethality to subtle neurological impairment. These disorders can be classified into three main groups, including peroxisome biogenesis disorders, single peroxisomal enzyme deficiencies, and single peroxisomal substrate transport deficiencies (Table IV-1).

Alpha-methylacyl-coenzyme A racemase deficiency is a rare peroxisomal disorder caused by bAi-allelic mutations in the *AMACR* gene. The gene product in an enzyme which catalyzes the conversion of (R)-stereoisomers of α-methyl-branched-chain fatty acids, including pristanic acid and C27-bile acid intermediates into their corresponding (S)-stereoisomers, which are the only substrates entering peroxisomal β-oxidation. In keeping with this, AMACR deficiency results in the accumulation of (R)-stereoisomers of pristanic acid, THCA, and DHCA, which can be measured in plasma, cells, and tissues. The disorder was first described in three subjects with adult-onset sensory motor neuropathy with or without pigmentary retinopathy in 2000. Since the discovery paper,[172] a few reports have expanded the phenotypic spectrum of the disease, including isolated transaminasemia, epilepsy, recurrent encephalopathic episodes, tremor, cerebellar ataxia. In infants, the clinical

presentation differs to that seen in adults, including abnormal bile acid synthesis, coagulopathy and neonatal cholestasis.

Figure IV-4. Overview of peroxisomal catabolic and anabolic processes

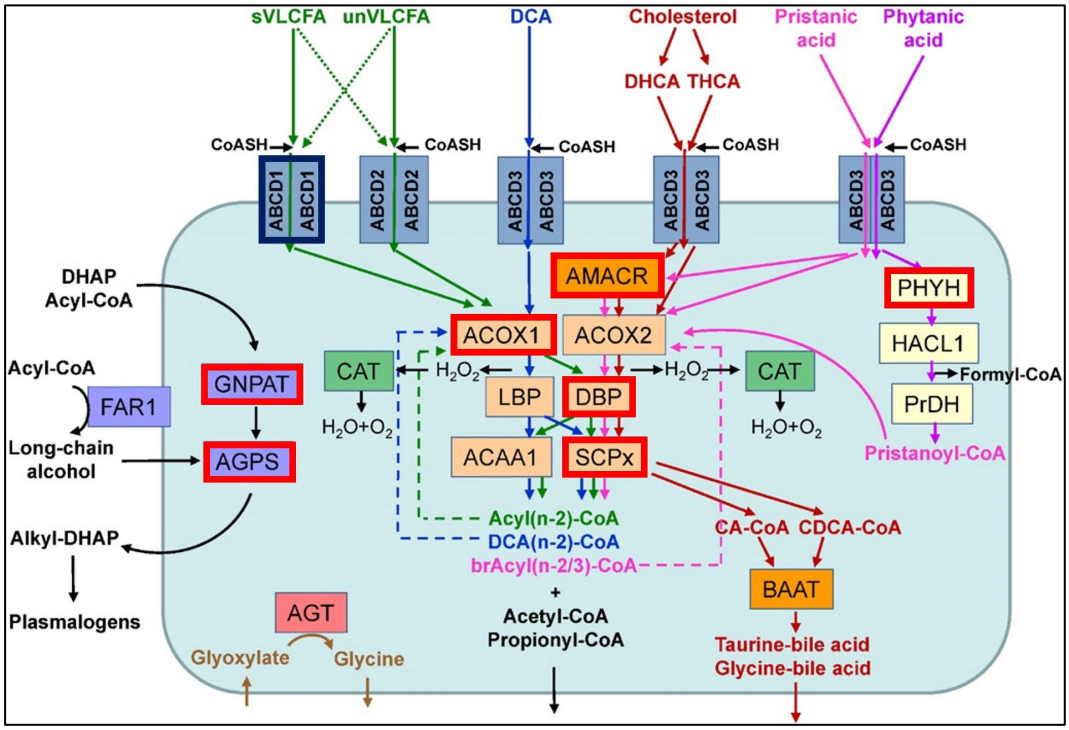

Table V-1. Peroxisomal disorders

Peroxisome biogenesis disorders	• Zellweger syndrome • Neonatal adrenoleukodystrophy • Infantile Refsum disease • Rhizomelic chondrodysplasia punctata type 1
Single peroxisomal enzyme deficiencies	• Acyl-CoA oxidase 1 (ACOX1) • D-bifunctional protein (DBP) • 2-methylacyl-CoA racemase (AMACR) • Sterol carrier protein X (SCPx) • Phytanoyl-CoA hydroxylase (adult Refsum disease; PHYH) • Acyl-CoA-dihydroxyacetonephosphate acyltransferase (GNPAT) • Alkyl-dihydroxyacetonephosphate synthase deficiency (AGPS)
Single peroxisomal substrate transport deficiencies	• X-linked adrenoleukodystrophy (ABCD1)

Figure IV-5. Phenotypic spectrum of AMACR deficiency hitherto reported

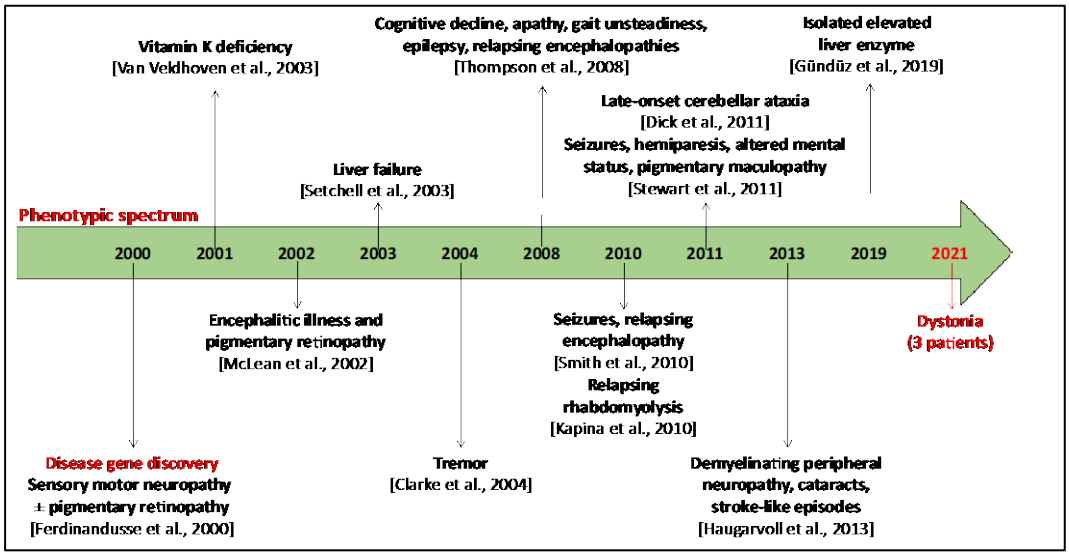

In order to establish whether dystonia might represent an expansion of the phenotypic spectrum of AMACR deficiency described so far, I searched for similar cases by reviewing the in-house cohort of 17,701 exomes at the UCL Queen Square Institute of Neurology, London, UK, and by contacting the Adult Neurometabolic Unit at the National Hospital for Neurology and Neurosurgery, London, UK (Dr Elaine Murphy) and the leading European center for peroxisomal disorders (Amsterdam University Medical Centre, Amsterdam, The Netherlands; Dr Sacha Ferdinandusse). I found an additional two siblings showing generalized dystonia in the context of AMACR deficiency.

Pedigree B. Two Pakistani sisters who were born to consanguineous parents and presented with generalised dystonia with prominent cervico-brachial involvement in the context of biochemically determined AMACR deficiency. The eldest sister's past medical history included a stroke like episode with confusion and right homonymous hemianopia in adulthood, whereas the youngest sister has no history of acute neurological events. In both cases, brain MRI detected T2/FLAIR hyperintensities in the midbrain, pons and both thalami. They showed increased levels of plasma pristanic acid. One of them underwent neurophysiology with exclusion of peripheral nerve involvement, and an ophtalmological assessment revealing Refsum-like retinopathy. In both siblings, enzymatic activity tests for

peroxisomal beta oxidation in cultured skin fibroblasts were consistent with AMACR deficiency (Figure IV-6).

Figure IV-6. Neuroimaging in the second pedigree with dystonia associated with AMACR deficiency

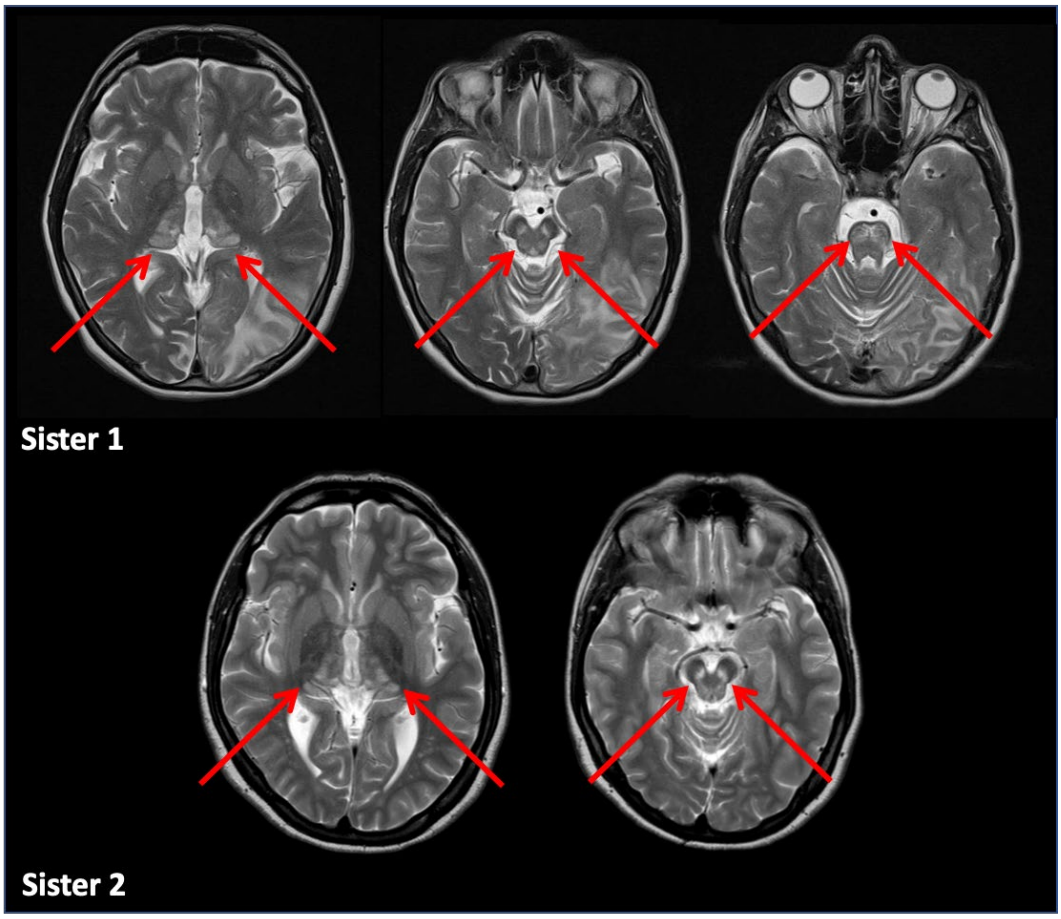

In pedigree B, Sanger sequencing was performed to analyse the five exons of *AMACR* and exon-intron boundaries. I used the following sets of primers in the proband (pedigree B, II-1). Only one variant (c.146G>T) was detected in AMACR.

Exon 1	Fw	5'-gattgggagggcttcttgca-3'
	Rv	5'-ggtgcagcctcgatcgaac-3'
Exon 2	Fw	5'-tttatgtttgtctcagagaaggga-3'
	Rv	tgaacacccatgctctcttga
Exon 3	Fw	tgattattcctctaagatgctcaca
	Rv	cttagggacaagtggcaggc
Exon 4	Fw	tgctttgacacttgagttatctgg
	Rv	aagccatggaaaatgcccca

Exon 5	Fw	cagtgggctcagcattcatttt
	Rv	CTGTTCCTCCATGTTTCCATGC

Figure VI-7. Segregation analysis in the second *AMACR* pedigree

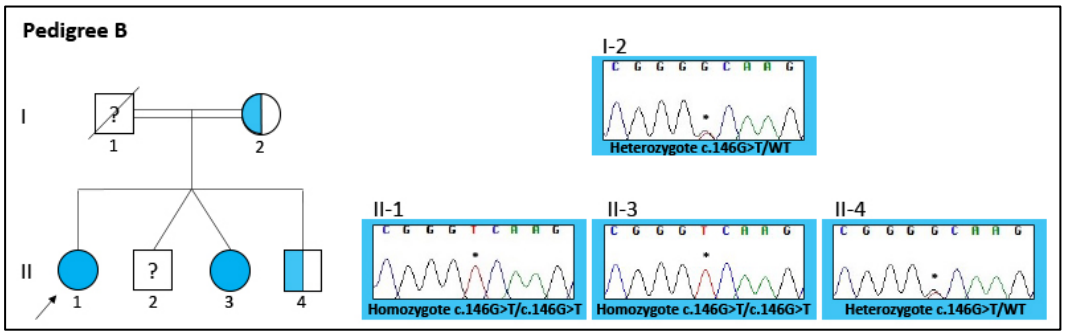

Sanger sequencing confirmed the proband and her affected sister were homozygote for the variant NM_014324.5:c.146G>T (light blue) in the *AMACR* gene, which was detected in the heterozygous state in their mother and one of their unaffected brothers. The region was amplified using the following primers (5'→3'): F-gattgggagggcttcttgca, R-ggtgcagcctcgatcgaac, with an amplicon size of 406 base pairs. Electropherograms were analysed using the Sequencher software package. Arrow = proband; WT = wild type.

These cases expanded the phenotypic and genotypic spectrum of AMACR deficiency, in particular by demonstrating that dystonia represents a new adult-onset clinical feature. Dietary exclusion of phytanic and pristanic acid offers a potential treatment for AMACR deficiency, as described successfully in Refsum disease. Long-term follow ups of patients with AMACR deficiency are missing. Recognition of the spectrum of presentation of AMACR deficiency phenotypes and careful follow up of patients prescribed a restrictive diet is crucial to establish whether lowering pristanic acid modifies the disease natural history.

Interestingly, dystonia with a similar pattern of leukoencephalopathy has been reported in sterol carrier protein 2a deficiency of sterol carrier protein X (SCPx), another enzymatic disorder which affect the same metabolic pathway.[173]

ATP13A2

One 18-year-old male was born to a consanguineous Pakistani couple and had normal ante- and peri-natal history. He had delayed neurodevelopmental milestones (walking at 3 years, talking at 5 years of age). He showed progressive gait and balance difficulties since age 11 and lost his ability to walk independently at age 13. The patient had a history of learning difficulties, with further deterioration of his cognitive performance since teenage years, but he did not undergo formal psychometry. In addition to his neurological symptoms, he was investigated and diagnosed in infancy with laryngomalacia, gastro-oesophageal reflux, and hypospadia. Symptomatic treatment consisted of trihexyphenidyl, baclofen and L-dopa. He had been intensely investigated, including normal brain and spine MRI, without any conclusive diagnosis when he presented in our clinic. Prominent phenotypic features were stereotypies, which included body rocking and finger pointing, with autistic-like behaviour, such as avoiding eye contact and a tendency to be reclusive. Although he did not speak in whole sentences, he was responsive and followed simply commands. He had hyperreflexia, and a spastic gait with toe-walking. There was dystonic posturing of the hands. He was a bit slow on finger tapping but did not display clear bradykinesia. Additionally, there was a mild vertical gaze palsy. A syndromic diagnosis of pallidopyramidal syndrome with cognitive difficulties and vertical gaze palsy prompted genetic testing for *ATP13A2* mutations.

On WGS, I detected the proband was homozygote for the variant NM_022089:c.2218C>T (p.Arg740Ter) in the *ATP13A2* gene. This variant is predicted pathogenic by almost all *in silico* prediction tools, including a CADD score of 37. It has no homozygous entries and only one heterozygous entry in the population database GnomAD. It is classified as pathogenic according to the ACMG guidelines. A DaTscan showed bilaterally reduced availability of the presynaptic dopamine transporters (Figure IV-8). He was started on Levodopa with good response but also the development of dyskinesia. Formal neuropsychometry showed prominent behavioural frontal signs and impaired executive functioning, memory performance and praxis.

Figure IV-8. Sanger sequencing and DatScan of one patient with Kufor-Rakeb syndrome.

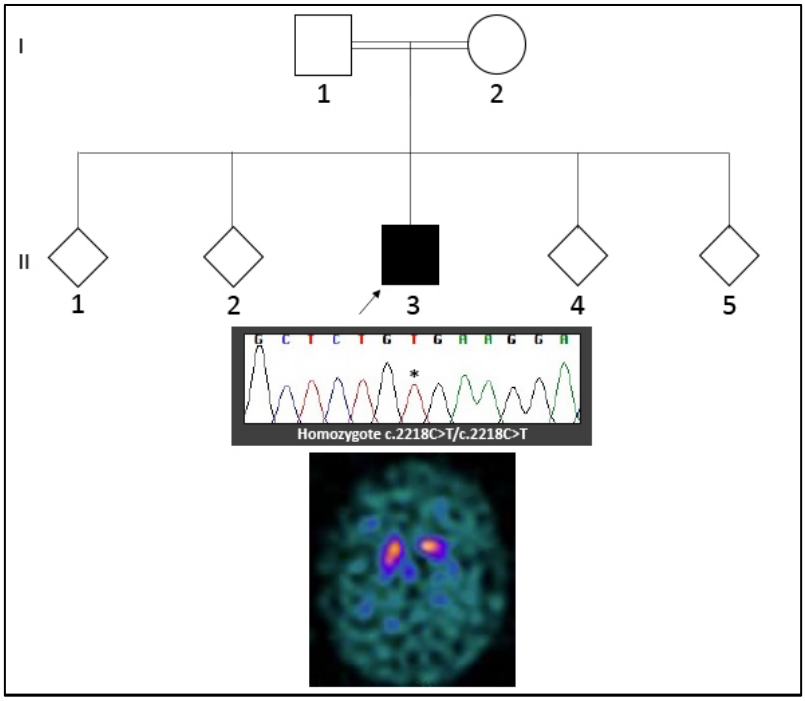

This patient with Kufor-Rakeb disease has been reported in a Case Series in Movement Disorders Clinical Practice (Reference: Balint B, Damasio J, ***Magrinelli F****, Guerreiro R, Bras J, Bhatia KP. Psychiatric manifestations of ATP13A2 mutations).*[174]

The gene *ATP13A2* maps on chromosome 1 and encodes a member of the P5 subfamily of ATPases which transports inorganic cations as well as other substrates, with a prevalent expression at the lysosomal membrane. ATP13A2 reduced intracellular Mn(2+) concentrations and protected cells from Mn(2+)-induced cytochrome c release and apoptosis. In addition, it is involved in Zn transport, and Zn(2+) dyshomeostasis caused by loss of *ATP13A2*/PARK9 leads to lysosomal dysfunction, alpha-synuclein accumulation, and neurotoxicity, thus further strengthen the evidence of defects of the lysosomal pathway in the pathogenesis of parkinsonism. Finally, its protein product acts as lysosomal polyamine exporter. At high concentrations polyamines induce cell toxicity, which was exacerbated by *ATP13A2* loss due to lysosomal dysfunction, lysosomal rupture, and cathepsin B activation. defective lysosomal polyamine export as a mechanism for lysosome-dependent cell death that may be implicated in

neurodegeneration, and shed light on the molecular identity of the mammalian polyamine transport system.

DDC

Two 32-year-old identical male twins born to a consanguineous couple from Jordan presented during infancy with extreme hypotonia and oculogyric crises and developed slowly progressive dystonia-parkinsonism along with neuropsychiatric issues from some years later. On WGS, they were found to carry the homozygous pathogenic variant c.749C>T (p.Ser250Phe) in the *DDC* gene, which is linked to

PLA2G6

Two cases with PLA2G6-related dystonia-parkinsonism were identified in this cohort through WGS.

A 33-year-old white British female with a history of dystonia-parkinsonism presented complaining of her head and trunk pulling backwards. These symptoms appeared over few months during her first cycle of in vitro fertilization. Her perinatal and developmental history was unremarkable. She had polycystic ovary syndrome with anovulatory infertility, and an ovarian dermoid cyst removed at age 25 with negative serum anti-NMDAR (N-methyl-D-aspartate receptor) antibody testing. She reported difficulty in holding a pen and a tightening feeling in her right hand (not entirely task-specific) since age 27. There was a history of sleep disturbances suggestive of REM sleep behavior disorder (RBD). Her parents and two youngest siblings were in good health. Dystonia slowly became generalized (facial grimacing, limb involvement). She experienced balance difficulties with occasional falls and developed anxiety and depression with suicidal ideation. On examination at age 36, she showed retrocollis and extensor truncal dystonia, parkinsonism (rest tremor in her limbs, bradykinesia and rigidity), brisk reflexes, and mild limb dysmetria. She used a walking stick. Laboratory tests and initial brain MRI were unremarkable, and genetic tests of TOR1A, LRRK2, PRKN and PINK1

negative. Her follow-up brain MRI with susceptibility-weighted imaging (SWI) sequences (Figure V-1A) showed only cerebellar atrophy (Figure V-1B), and a DaTscan detected bilaterally reduced tracer uptake in the striatum (Figure V-1C). Neuropsychological tests at age 37 revealed attentional dysfunction with associated memory difficulty. She had no benefit from trihexyphenidyl and a mild response to ropinirole, whereas low-dose levodopa resulted in worsening of dystonia and tremor as well as early dyskinesias. She had a good, albeit unsustained, response to apomorphine. At age 38, she underwent bilateral deep brain stimulation (DBS) of the GP internus (GPi), with improvement of her truncal dystonia and abrupt cessation of dyskinesias, which allowed to increase her levodopa daily dose. Trio whole-genome sequencing (WGS) and targeted resequencing (Figure V-2) demonstrated she was a compound heterozygote for the maternally inherited variant NM_003560.4:c.956C>T (p.Thr319Met) and the paternally inherited variant NM_003560.4:c.1061T>C (p.Leu345Pro).

Figure IV-9. Segregation analysis in Case 1's pedigree

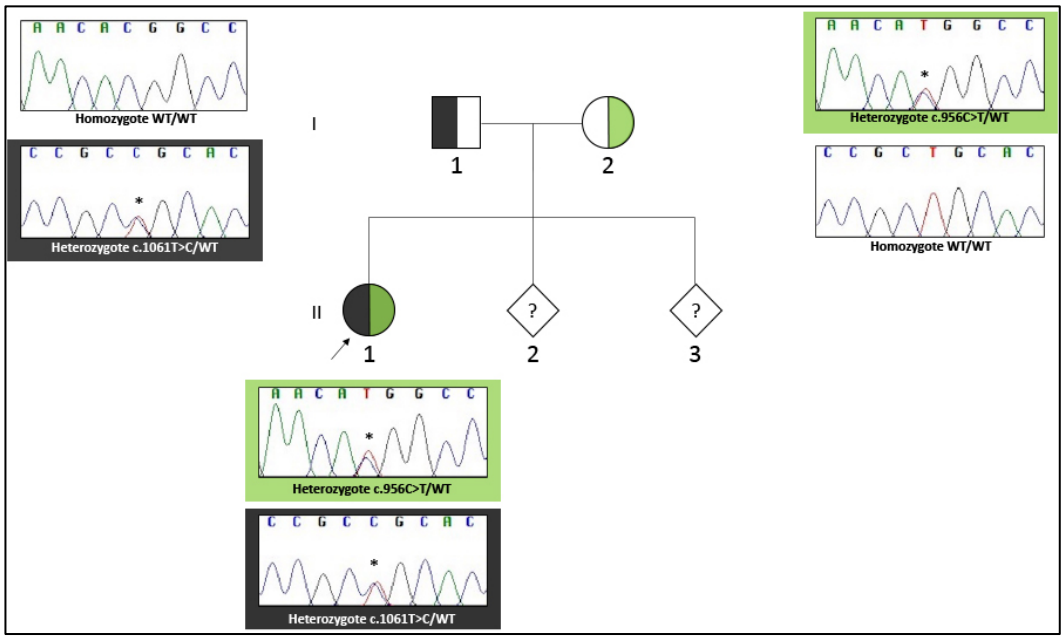

Segregation analysis confirmed the proband (Case 1, II-1) was compound heterozygote for the maternally inherited variant NM_003560.4:c.956C>T (green) and the paternally inherited variant NM_003560.4:c.1061T>C (grey) in the *PLA2G6* gene. The region was amplified using the following primers (5'→3'): F-ctagcgctttccaacatccc, R-agctttgggtgggaagatga, with an amplicon size of 441 base

pairs. Electropherograms were analysed using the Sequencher software package. Arrow = proband; WT = wild type.

The second case was the younger sister of the *PLA2G6* case reported in Chapter III and is extensively discussed in Chapter IV.

SLC2A1

In two individuals with paroxysmal exercise-induced dystonia (PED), I found heterozygous mutations in the *SLC2A1* gene, which is associated with glucose transporter type 1 (Glut1) deficiency syndrome (DS; see also Chapter I). Glut1 DS is a rare treatable neurometabolic disorder caused by monoallelic or, more rarely, biallelic pathogenic variants in the *SLC2A1* gene, which encodes the glucose transporter Glut1. Glut1 is mainly localized in brain capillary endothelial cells and their encircling astrocytic end-feet. Here, it plays a critical role in cerebral glucose delivery, being responsible both for glucose transport from the bloodstream into the extracellular cleft (between the endothelium and astrocyte) and then again for glucose transport from the extracellular cleft into astrocytes. Genetically determined defects in Glut1 result in impaired glucose transport across the blood-brain barrier and into astrocytes, thus causing cerebral energy failure. The classic Glut1 DS phenotype is characterized by infantile-onset chronic encephalopathy with pharmacoresistant epilepsy, developmental delay, acquired microcephaly, spasticity, and movement disorders (ataxia, dystonia, chorea) which may be continuous, paroxysmal, or continual with fluctuations in severity. The clinical spectrum of Glut1 DS also includes milder phenotypes which generally fall into one of three categories: 1) epilepsy; 2) movement disorders, in particular paroxysmal exercise-induced dyskinesia (attacks of chorea and dystonia affecting mainly the lower limbs); and 3) cognitive/behavioral disturbances. These presentations may have onset both in childhood and adulthood and may occur either in isolation or as a mixed syndrome. The diagnosis is established based on one or both of the following criteria:

1) CSF glucose <3.33 mmol/L on fasting lumbar puncture with normal blood glucose (CSF/blood glucose ratio <0.4);
2) monoallelic pathogenic variant (or rarely biallelic pathogenic variants) in the *SLC2A1* gene on molecular genetic testing.
Abnormally low erythrocyte 3-O-methyl-D-glucose uptake assay confirms the clinical diagnosis of Glut1 DS.
CSF lactate is usually low-normal or low.
Ketogenic diet is the treatment of choice since ketone bodies enter the brain by monocarboxylic transporters and are metabolized exclusively within mitochondria, thus representing an alternative fuel to restore cerebral energy.

In one case I detected a previously reported pathogenic *SLC2A1* variant. This is a 41-year-old man with PED presenting with episodes of choreo-dystonia triggered by exercise, but also by stress and anxiety. Usually attacks last for about 10-15 minutes but may occasionally be longer. His history began with a delay in attaining his early milestones. His speech development was also delayed and as a young child he developed attacks where his eyes rolled upwards, and his arms jerked upwards. He had had a sense he would fall off his chair at school and initially, these episodes were diagnosed as being epileptic in nature. The attacks did seem to subside with the administration of sodium valproate. He then developed a different type of attack that would usually occur after exercise such as walking or swimming, where he became floppy and he developed involuntary movements of the legs. During these episodes he was unable to walk. There were occasional isolated movements of the head. The longest attack in the past has been persisted for 5-8 hours, but most last for 10-15 minutes. Food can abort the attacks and they are more common if he is fatigued or has not slept sufficiently. His brain MRI was unremarkable.

Trio WGS revealed the proband carries a *de novo* heterozygous variant c.997C>T (p.Arg333Trp) in the *SLC2A1* gene (Figure IV-10). It is absent in gnomAD and predicted pathogenic by all in silico tools, including a CADD score of 32. The variant is classified as pathogenic/likely pathogenic by ClinVar and has previously been reported in patients with Glut1 deficiency syndrome.

Figure IV-10. Sanger sequencing and biochemical confirmation of Glut1 deficiency

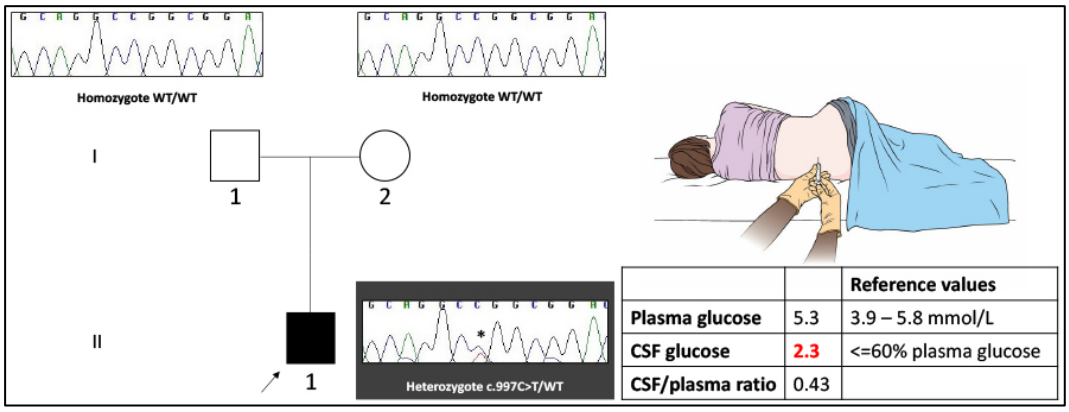

		Reference values
Plasma glucose	5.3	3.9 – 5.8 mmol/L
CSF glucose	2.3	<=60% plasma glucose
CSF/plasma ratio	0.43	

The second case was a 54-year-old lady who presented with paroxysmal exercise-induced dyskinesias with onset at age 6. She was treated with levodopa. Her son was similarly affected, with attacks manifesting with either an ice cold feeling of his body or abnormal posturing of his right foot, which became dorsiflexed and inverted. Attacks usually last for two to three hours and might be triggered by stress. At the age of 27, he died of sudden nocturnal unexpected death, which was considered to be due to epilepsy. There was a family history of epilepsy. Both mother and son were found to carry a previously reported missense variant in *SLC2A1* in the heterozygous state, i.e. ENST00000426263:c.601T>C (p.Cys201Arg). Retrospective review of the proband at the time of first assessment revealed a peculiar pattern of pathological gait. Nearly 90% of patients with Glut1 DS have paroxysmal or constant gait abnormalities, including ataxic, spastic, ataxic-spastic, and dystonic gait. In addition to the present case, we found two unrelated cases of genetically proven Glut1 DS (Figure 2) demonstrating a distinctive paroxysmal gait disorder triggered by exertion or fasting, which we have named “criss-cross gait”. It is characterized by lower-body choreo-dyskinesia causing the legs to intersect repeatedly, producing irregular, random steps combined with some loss of balance. Compensatory upper-body movements help maintain balance. In the appropriate clinical context, the criss-cross gait should prompt evaluation for the treatable Glut1 DS and not be misinterpreted as

functional. Clinico-genetic features of *SLC2A1* mutation carriers with the criss-cross gait among phenotypic characteristics is reported in Table IV-2.

Table IV-2. Summary of identified Glut1 cases presenting with the "criss-cross" gait

	Case 1	Case 2	Case 3
Current age	54	25	24
Sex	Female	Male	Female
Ethnicity	White British	White British	Germanic
Age of onset	6 years	5 years	11 months
Clinical picture	PED (episodes of toe curling, foot dystonia, limb choreoathetosis)	PED (episodes of foot dystonia, jerky choreiform movements in his limbs) Episodes of slurred speech	Motor developmental delay Atypical absence epilepsy PED (episodes of "wobbly gait") Mild intellectual disability
Family history	Father: history of paroxysmal dystonic choreoathetosis, possibly affected (retrospectively); son affected.	Father affected	Negative (de novo mutation)
CSF analysis	Not performed	CSF glucose = 1.9 mmol/L (with blood glucose = 6.8 mmol/L) CSF/blood glucose ratio = 0.28	Not available
Genetic testing *SLC2A1* [ENST00000426263]	Heterozygous variant c.601T>C (p.Cys201Arg)	Heterozygous variant c.278G>A (p.Arg93Gln)	Heterozygous variant c.998G>A (p.Arg333Gln)

These cases and table have been published as a *Video NeuroImage* in *Neurology* (Reference: **Magrinelli F**, Guerreiro R, Bras J, Bhatia KP. "Criss-cross gait": a clue to Glut1 deficiency syndrome

TUBB4A

A 30-year-old White British male clinically diagnosed with the H-ABC syndrome (hypomyelination, atrophy of the basal ganglia and cerebellum) was found to carry the heterozygous pathogenic variant ENST00000264071.2):c.745G>A (p.Asp249Asn) in the *TUBB4A* gene. His family history was unremarkable, and the variant was inherited by the unaffected mother, an occurrence which has been previously reported in the literature.[175] He had a normal birth, with slightly delayed motor milestones. At age 2, his gait, hand control, and standing became worse over a four-week period. After several investigations he was diagnosed with leukodystrophy of unknown cause and has been diagnosed with the H-ABC syndrome together with other patients presenting with the same clinical syndrome

years later. He had severe dysphagia and needed a gastrostomy at age 18. On examination, he has generalized dystonia with bulbar involvement and limb spasticity, which was more pronounced in his legs. His brain MRI showed severe hypomyelination in the cerebral hemispheres as well as basal ganglia and cerebellar atrophy.

Figure IV-10. MRI findings and segregation analysis in the *TUBB4A* case

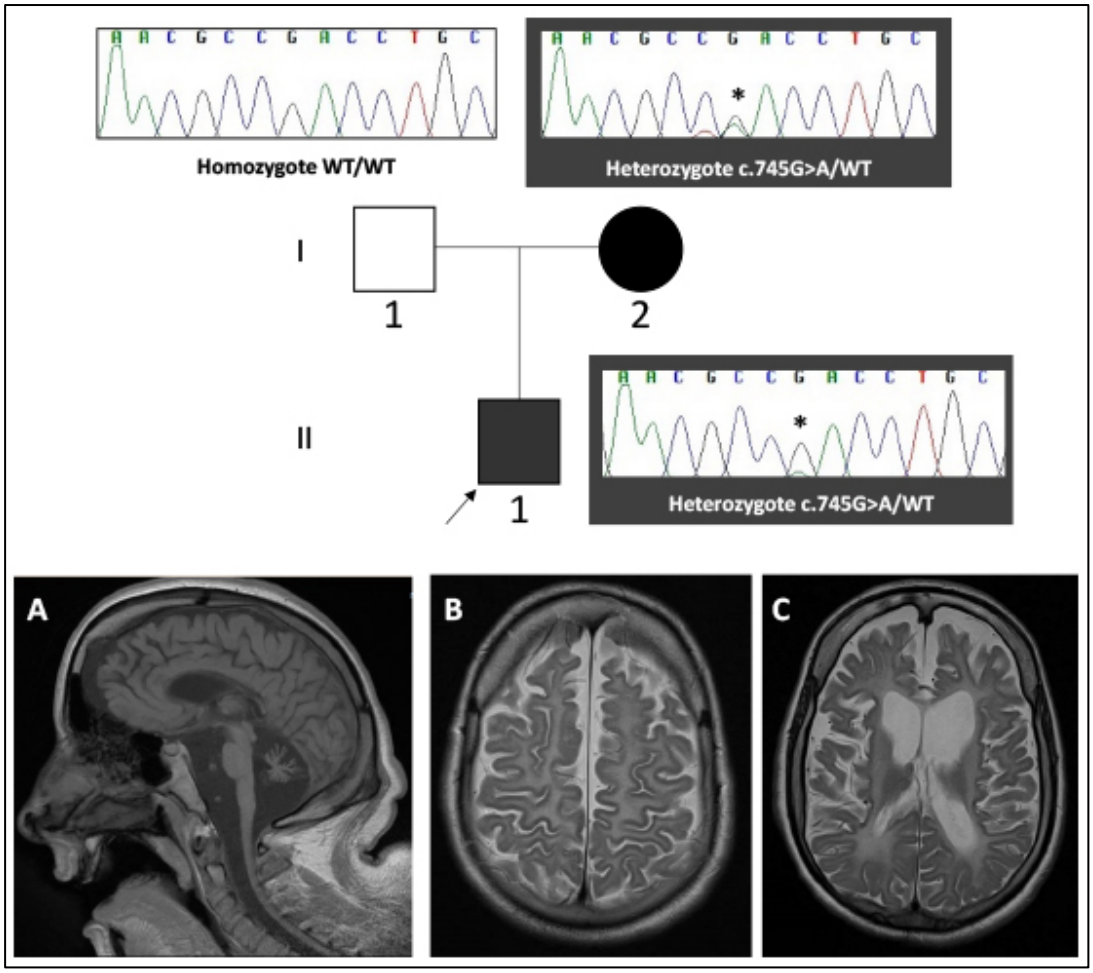

As previously mentioned, the study presented in this chapter has been severely delayed by the COVID-19 pandemic, and only preliminary findings from the first 50 analyzed cases from a cohort of approximately 300 patients with heterogeneous dystonia phenotypes were summarized above. The study is ongoing and will be one of the projects I will work on during my postdoctoral fellowship.

Chapter V

Dissecting the phenotype and genotype of *PLA2G6*-related parkinsonism

1. Preamble

In the study cohorts reported in chapters III and IV, three individuals from two different pedigrees were diagnosed with *PLA2G6*-related parkinsonism. I identified an additional 11 new cases through an in-house review of patients with early-onset dystonia-parkinsonism and a multicentre international collaborative study, which I coordinated. By merging data from these new case series and a systematic literature review, I deeply characterized the phenotype and genotype of *PLA2G6*-related parkinsonism. Parts of this chapter are currently under consideration in a peer-reviewed journal. In addition, I contributed new cases herein presented who are on active follow-up at the National Hospital for Neurology and Neurosurgery, London, UK, to an ongoing natural history study on *PLA2G6*-associated neurodegeneration led by Prof. Manju Kurian.

2. Introduction

Defects in membrane lipid metabolism converging on disruptions of mitochondrial and endo-lysosomal trafficking have increasingly been implicated in the pathophysiology of neurodegenerative disorders, including Parkinson's disease/parkinsonism.[176-179] The calcium-independent phospholipase A2 beta (iPLA2β), encoded by the *PLA2G6* gene, hydrolyzes membrane phospholipids and lysophospholipids, thereby regulating membrane homeostasis and releasing lipid second messengers which act in pathways involved in cell proliferation, $Ca2^{+}$ signaling, mitochondrial dynamics, and apoptosis.[180, 181] iPLA2β is expressed in neuronal and glial cells and enriched in mitochondria and synaptic compartments.[182, 183] Loss of the *Drosophila PLA2G6* homolog (*iPLA-VIA*) impairs

mitochondrial respiratory chain function and ATP synthesis, thus resulting in increased brain lipid peroxidation.[182] It also causes accumulation of ceramide and other sphingolipid intermediates which induces stress in the endo-lysosomal system similar to α-synuclein overexpression, ultimately leading to neuronal dysfunction.[184] Defective Ca^{2+} signaling triggers autophagic dysregulation, loss of dopaminergic neurons and levodopa-sensitive motor impairment in a *PLA2G6* knockout mouse model.[185]

In humans, biallelic pathogenic variants in *PLA2G6* were initially associated with childhood-onset neurodegenerative disorders, including infantile (INAD) and atypical (ANAD) neuroaxonal dystrophy.[186, 187] Children with INAD are asymptomatic at birth and manifest psychomotor regression or delay between 6 and 36 months of age. The clinical picture of INAD encompasses early axial hypotonia progressing to severe spastic tetraparesis, intellectual disability, strabismus, visual impairment secondary to optic atrophy, and axonal sensorimotor neuropathy, with death occurring by age 10 as a consequence of bulbar dysfunction.[186, 188, 189] ANAD usually begins between 1.5 and 6.5 years of age and is characterized by prominent language difficulty and autistic-like traits, as well as a combination of cerebellar, pyramidal and dystonic features. Unlike INAD, ANAD shows a fairly slow progression during early childhood and rapid deterioration at the turn of the first decade.[187] Neuroradiological findings in INAD and ANAD may include cerebellar atrophy, cortical cerebellar MRI-T2 hyperintensities (gliosis), iron deposition in the globus pallidus (GP) and/or substantia nigra (SN), white matter abnormalities, vertically oriented splenium of the corpus callosum, claval hypertrophy, and thinning of the optic pathway.[190] Axonal degeneration with distended axons (spheroid bodies) throughout the central and peripheral nervous system is the pathological hallmark of these disorders.[186, 187, 189]

In 2009 *PLA2G6* was first linked to dystonia-parkinsonism with onset in the second or third decade.[15] Since then, additional phenotypes manifesting later than INAD/ANAD have been described, including parkinsonism either isolated or

combined with other neurological and/or psychiatric features,[191, 192] ataxia,[193, 194] and spastic paraplegia.[195, 196]

Growing evidence suggests that *PLA2G6*-associated neurodegeneration (PLAN) is a phenotypic continuum with overlapping clinico-radiological and pathological characteristics rather than an umbrella term for a number of discrete disorders.[194, 197] In keeping with this, childhood-onset phenotypes and *PLA2G6*-related parkinsonism share Lewy and tau pathology.[198] Equally, there are many unsolved questions about PLAN, particularly late-onset phenotypes. For instance, controversies remain on why mutations in *PLA2G6* account for such a wide phenotypic spectrum, and why the same genetic variant leads to different phenotypes, even in the same pedigree. In addition, little is known about the progression of late-onset PLAN, and ongoing natural history studies mainly focus on INAD.[199, 200] Finally, treatments with disease-modifying potential have not been explored in late-onset PLAN so far.[201] In this regard, some PLAN cases show brain iron deposition, thus raising the option of chelation therapy, as proposed in pantothenate kinase-associated neurodegeneration (PKAN).[202] More promisingly, small molecule therapies are under investigation in cell and murine disease models, and a viral vector-based gene therapy has been explored in the *PLA2G6*-INAD mouse with encouraging results and is approaching completion of pre-clinical studies,[197, 203] as recently reviewed by Iankova et al.[201] The prompt recognition of *PLA2G6*-related phenotypes may therefore have considerable therapeutic implications in the not-too-distant future.

In this chapter, I describe 14 new cases of *PLA2G6*-associated parkinsonism carrying 13 different mutations, four of which are novel. I merge data from this case series and a systematic literature review to provide an in-depth phenotypic and genotypic description of *PLA2G6*-related parkinsonism, highlight clinico-radiological hints for diagnosis and outline its natural history. Finally, I discuss and speculate on some distinct or poorly understood aspects of late-onset PLAN based on the resulting overview.

3. Subjects and methods

New patients with *PLA2G6*-associated parkinsonism diagnosed in six centres (United Kingdom: National Hospital for Neurology and Neurosurgery, London, and Salford Royal NHS Foundation Trust, Manchester; Germany: University Medical Center, Mainz; India: Postgraduate Institute of Medical Education and Research, Chandigarh, Institute of Neurosciences, Kolkata, and Jaslok Hospital and Research Centre, Mumbai) between 2014 and 2020 are reported first.

I then systematically searched PubMed® on 18 March 2021 for records on parkinsonism in genetically confirmed PLAN published since 2006 (disease gene discovery). The search strategy was "PLA2G6" AND "parkins*". There was no language restriction. Additional references from relevant articles were identified and reviewed. Only cases of *PLA2G6*-parkinsonism carrying biallelic gene mutations with individual information were included. Predefined categories for data extraction were sex, ethnicity, age and symptom(s) at onset, age at last assessment, different neurological and psychiatric symptoms/signs, findings from laboratory, neuroimaging and other investigations, family history, genotype, and response to treatment. For previously published cases, neuropathology specimens available at the Queen Square Brain Bank and videos were reviewed. Phenotypic features were recorded as non-missing only if explicitly stated to be present or absent. For genotype analysis, mutated positions in *PLA2G6* were all (re-)annotated in reference to transcript NM_003560.4. The Combined Annotation Dependent Depletion (CADD) tool scores (https://cadd.gs.washington.edu/snv), Polymorphism Phenotyping v2 (PolyPhen-2; http://genetics.bwh.harvard.edu/pph2/), Sorting Intolerant from Tolerant (SIFT; http://sift.bii.a-star.edu.sg), MutationTaster (http://www.mutationtaster.org/), and Protein Variation Effect Analyzer (PROVEAN; http://provean.jcvi.org/index.php) were used to predict the impact of missense mutations on the structure and function of iPLA2β. I used Genomic Evolutionary Rate Profiling (GERP) scores (http://www.ensembl.org/index.html) and/or multiple sequence alignment through Clustal Omega (https://www.ebi.ac.uk/Tools/msa/clustalo/)[152] to assess sequence conservation across species. The Genome Aggregation Database (gnomAD;

https://gnomad.broadinstitute.org/) and the National Center for Biotechnology Information (NCBI) ClinVar database (https://www.ncbi.nlm.nih.gov/clinvar/) were retrieved on 18 March 2021. Variants were finally interpreted according to the guidelines by the American College of Medical Genetics and Genomics (ACMG).[46]

Descriptive statistics were performed using IBM SPSS Statistics for Macintosh (version 21). Results are provided as valid percentages (i.e., counts divided by the total number of non-missing observations) for dichotomous variables and median with interquartile range (IQR, weighted average) for continuous variables.

4. Results

Case Series

Fourteen new cases of *PLA2G6*-parkinsonism, including three European (two British, one German) and 11 Southeast Asian (eight Indian, three Pakistani) patients from 12 families were identified. Their demographic, clinico-radiological and genetic features are summarised in Table V-1.[15, 194, 204] They carried a total of 13 mutations in *PLA2G6*, including four which are novel. Analysis of their genetic variants is provided in Table V-2.[15, 186, 190, 194, 196, 198, 204-219]

Case 1. A 33-year-old white British female presented complaining of her head and trunk pulling backwards. These symptoms appeared over few months during her first cycle of *in vitro* fertilization. Her perinatal and developmental history was unremarkable. She had polycystic ovary syndrome with anovulatory infertility, and an ovarian dermoid cyst removed at age 25 with negative serum anti-NMDAR (N-methyl-D-aspartate receptor) antibody testing. She reported difficulty in holding a pen and a tightening feeling in her right hand (not entirely task-specific) since age 27. There was a history of sleep disturbances suggestive of REM sleep behavior disorder (RBD). Her parents and two youngest siblings were in good health. Dystonia slowly became generalized (facial grimacing, limb involvement). She experienced balance difficulties with occasional falls and developed anxiety and depression with suicidal ideation. On examination at age 36, she showed retrocollis

and extensor truncal dystonia, parkinsonism (rest tremor in her limbs, bradykinesia and rigidity), brisk reflexes, and mild limb dysmetria. She used a walking stick. Laboratory tests and initial brain MRI were unremarkable, and genetic tests of *TOR1A*, *LRRK2*, *PRKN* and *PINK1* negative. Her follow-up brain MRI with susceptibility-weighted imaging (SWI) sequences (Figure V-1A) showed only cerebellar atrophy (Figure V-1B), and a DaTscan detected bilaterally reduced tracer uptake in the striatum (Figure V-1C). Neuropsychological tests at age 37 revealed attentional dysfunction with associated memory difficulty. She had no benefit from trihexyphenidyl and a mild response to ropinirole, whereas low-dose levodopa resulted in worsening of dystonia and tremor as well as early dyskinesias. She had a good, albeit unsustained, response to apomorphine. At age 38, she underwent bilateral deep brain stimulation (DBS) of the GP internus (GPi), with improvement of her truncal dystonia and abrupt cessation of dyskinesias, which allowed to increase her levodopa daily dose. Trio whole-genome sequencing (WGS) and targeted resequencing (Figure V-2) demonstrated she was a compound heterozygote for the maternally inherited variant NM_003560.4:c.956C>T (p.Thr319Met) and the paternally inherited variant NM_003560.4:c.1061T>C (p.Leu345Pro).

Figure V-1. Neuroimages of cases with PLA2G6-parkinsonism (next page)

Case 1: (A) axial susceptibility-weighted imaging (SWI) MRI sequence showing absence of iron deposition in the basal ganglia; (B) sagittal T1-weighted sequence revealing mild cerebellar atrophy on follow-up MRI; (C) DaTscan detecting reduction of tracer uptake in the striatum bilaterally. Case 2: (D) axial SWI MRI sequence showing iron deposition in the basal ganglia. Case 3: (E) Tc-99m TRODAT-1 SPECT/CT detecting bilaterally reduced tracer uptake in the striatum. Case 4: (F) axial T1-weighted sequence revealing cerebral atrophy mainly in the frontotemporal lobes; (G) sagittal T1-weighted MRI sequence showing both cerebral and cerebellar atrophy; (H)18F-fluorodopa PET detecting reduced tracer uptake in the basal ganglia (right>left). Case 8: (I) axial SWI MRI sequence showing mild iron deposition in the basal ganglia. Case 12: (L) sagittal T1-weighted sequence revealing mild cerebellar atrophy; (M) DaTscan detecting reduction of tracer uptake in the striatum bilaterally (right>left). Case 13: (N) sagittal T2-weighted MRI sequence revealing cerebellar atrophy; (O) axial T1-weighted MRI sequence showing frontal and temporal lobe atrophy; (P) axial SWI MRI sequence documenting lack of iron deposition in the basal ganglia. Case 14: (Q) DaTscan detecting bilateral reduction of tracer uptake in the striatum (left>right).

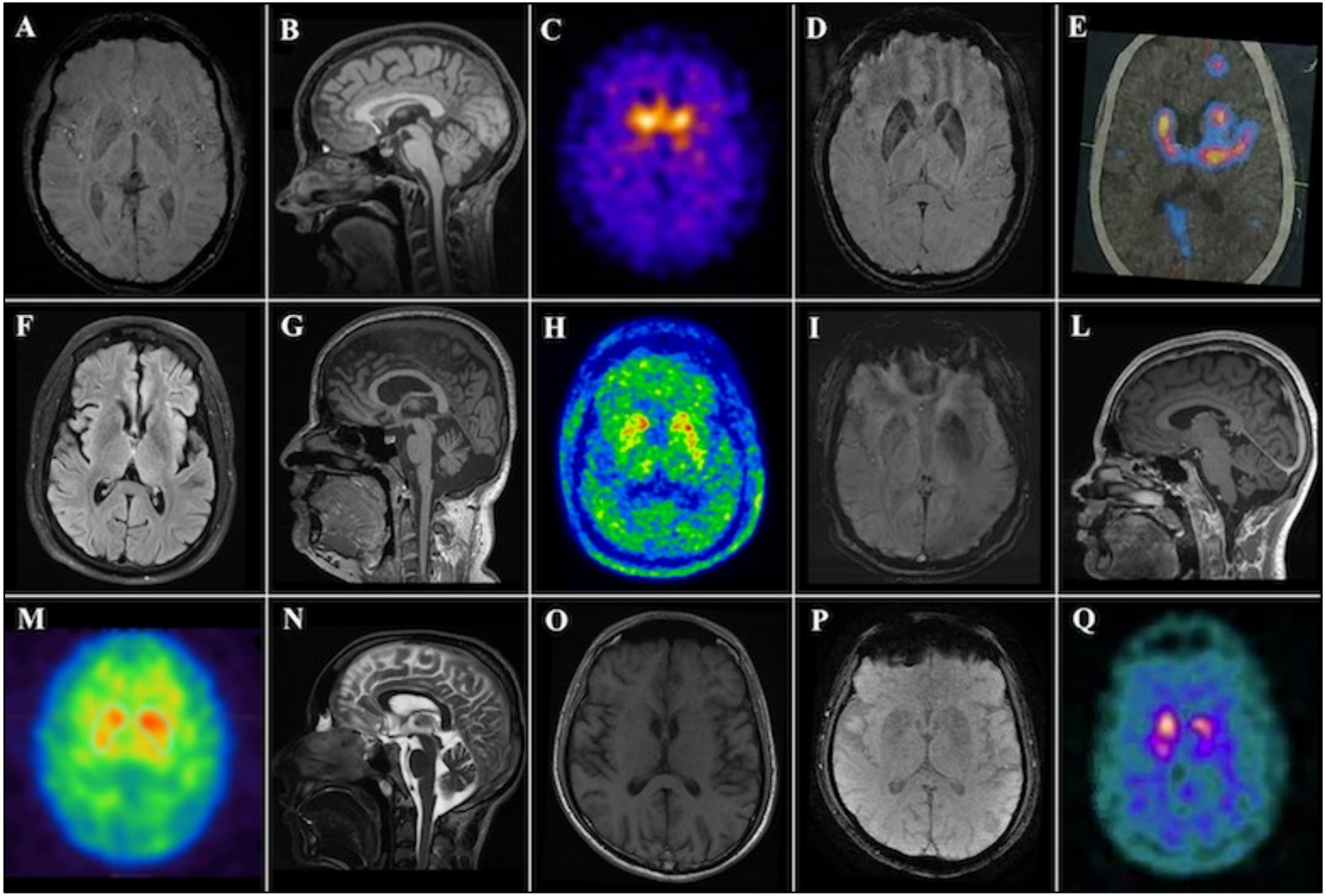
A
B
C
D
E
F
G
H
I
L
M
N
O
P
Q

Figure V-2. Segregation analysis in Case 1's pedigree

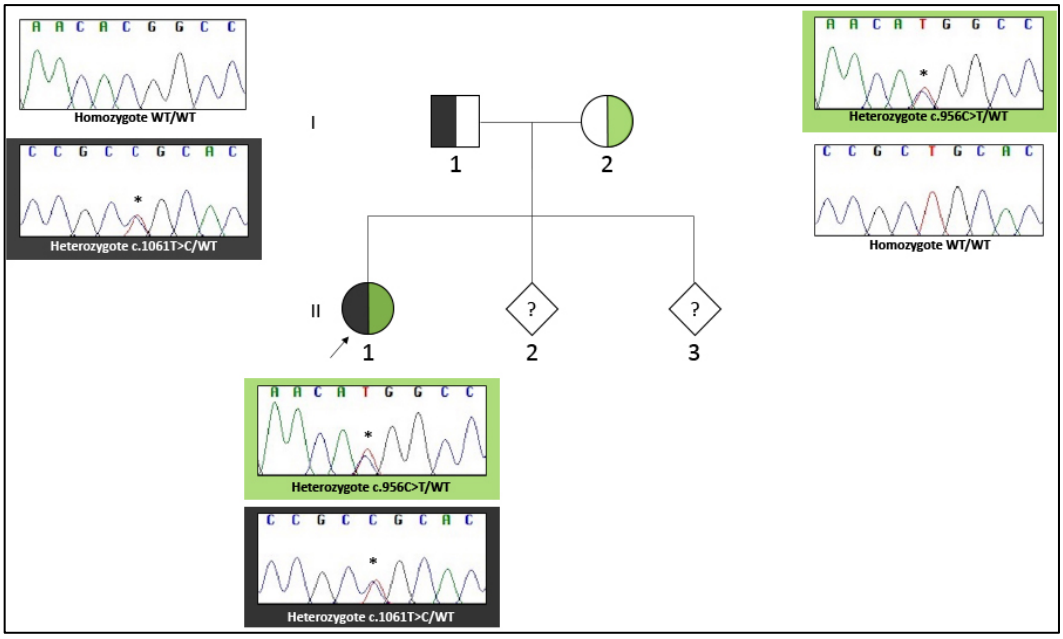

Segregation analysis confirmed the proband (Case 1, II-1) was compound heterozygote for the maternally inherited variant NM_003560.4:c.956C>T (green) and the paternally inherited variant NM_003560.4:c.1061T>C (grey) in the *PLA2G6* gene. The region was amplified using the following primers (5'→3'): F-ctagcgctttccaacatccc, R-agctttgggtgggaagatga, with an amplicon size of 441 base pairs. Electropherograms were analysed using the Sequencher software package. Arrow = proband; WT = wild type.

Case 2. This 36-year-old white British woman was in good health until age 29, when she developed a parkinsonian syndrome with executive dysfunction and personality changes. She became withdrawn, apathetic and emotionally labile, being tearful with relatively little provocation. Her short-term memory was impaired, and she was occasionally disoriented in time and place. She denied sleep disturbances but had a tendency to talk in her sleep. She had nocturia and occasional urinary incontinence. There was no history of hallucinations, disinhibition or hyperorality. Her family history was unremarkable. Brain MRI scan with SWI sequences initially showed subtle iron deposition in the basal ganglia. At age 31 her Montreal Cognitive Assessment (MoCA) score was 25/30, with impairments of verbal fluency, attention and delayed recall; she was rather impulsive during assessment. Genetic tests of *HTT*, *PANK2*, and *WDR45* were negative. She was started on levodopa with quite good response. However, she became pregnant

during the early course of her condition. She therefore discontinued levodopa until 16 weeks, and experienced worsening of her motor function at this time. Levodopa response waned after her uneventful pregnancy, and she developed lower limb dyskinesias with small doses. Since age 33 her gait deteriorated with intoeing, and she manifested balance difficulties with falls typically backwards. On reassessment at age 34, she was mainly wheelchair-bound and showed gaze impersistence with saccadic intrusions on smooth pursuit, twitchy facial movements and chin tremor. Tongue movements were slow, and she had difficulty holding the tongue protruded, as well as moderate dysarthria and occasional facial grimacing. Her trunk appeared stiff with anterocollis. There was action myoclonus of the outstretched hands, which was confirmed of cortical origin on neurophysiology, mild dystonic posturing of her fingers, and inversion of her left foot. There was bradykinesia on finger-tapping bilaterally and brisk reflexes with bilateral ankle clonus. She had an unsteady gait with reduced stride length. Her follow-up MRI revealed stable iron deposition (Figure V-1D) but progressive cerebral and cerebellar atrophy. Trio WGS and subsequent Sanger sequencing revealed she was a compound heterozygote for the maternally inherited variant NM_003560.4:c.238G>A (p.Ala80Thr) and paternally inherited variant NM_003560.4:c.1924A>G (p.Thr642Ala) in *PLA2G6*.

Case 3. This 25-year-old Indian female born to non-consanguineous parents became progressively slow, fearful and depressed since the third month of her first pregnancy at age 21. Her past medical history and family history were unremarkable. Recent sleep disturbances suggestive of RBD were reported. She suffered from urinary urgency with occasional incontinence but denied constipation. She had never experienced hallucinations. On examination, she presented with an asymmetrical akinetic-rigid syndrome with prominent rigidity in her lower limbs and mild gait and limb ataxia. On the 10th day postpartum, her symptoms rapidly deteriorated with diffuse severe rigidity, hypophonia, dysphagia, and psychiatric disturbances. She was initially diagnosed with catatonia and received four cycles of electroconvulsive therapy. On clinical reassessment, she presented with an akinetic rigid syndrome associated with axial and limb dystonia and some cerebellar features. Her mother noticed some deterioration of her short-

term memory. There were no pyramidal signs. Her tandem gait was impaired, and she had mild bilateral ataxia on finger-nose testing. Investigations including routine laboratory testing, iron profile, serum copper and ceruloplasmin, serum vasculitis, paraneoplastic and neuronal antibodies, and CSF analysis were unremarkable. EEG was normal and brain MRI revealed mild cerebellar atrophy but no signs of mineralization on T2-weighted sequences. Tc-99m TRODAT-1 SPECT (Figure V-1E) showed asymmetrical severe decrease in tracer uptake in the striatum (putamen>caudate). A next-generation sequencing (NGS) gene panel for young-onset Parkinson's disease detected the missense variants NM_003560.4:c.673C>T (p.His225Tyr) and NM_003560.4:c.2311G>A (p.Asp771Asn) in *PLA2G6*. The patient was started on levodopa with an optimal response but experienced severe dyskinesias after approximately eight months of treatment.

Case 4. This 22-year-old Indian male was born to non-consanguineous parents and had normal birth and developmental milestones. Since age 15, he developed aggressiveness and disinhibited behaviors, experienced episodes of fear and emotional lability, and showed deterioration of his scholastic performance. He suffered from urinary frequency and urgency, with occasional incontinence, and constipation. There was no history of anosmia, RBD, and orthostatic hypotension. His elder brother manifested psychiatric features, including suicidal ideation, and parkinsonism, since age 17, and died at age 27 without a definite diagnosis. Examination at age 18 revealed an asymmetric akinetic-rigid syndrome (left> right) with impaired postural reflexes. He had bilateral postural tremor in the upper limbs with superimposed myoclonic jerks. Eye movements assessment showed broken pursuits and slow saccades in the horizontal plane. Deep tendon reflexes were brisk with presence of striatal toes. Sensory system and cerebellar examination were unremarkable. Brain MRI with SWI sequences revealed cerebro/cerebellar atrophy (Figure V-1F-1G) and no evidence of iron deposition. ^{18}F-DOPA PET showed asymmetrically decreased tracer uptake (Figure V-1H). He had a modest response to levodopa with early occurrence of dyskinesias predominantly affecting the lower limbs almost a year after starting levodopa with a dose of 100mg three times daily. He also exhibited mild dystonia affecting his left upper limb late into his illness.

Whole exome sequencing (WES) detected the homozygous variant NM_003560.4:c.2222G>A (p.Arg741Gln) in *PLA2G6*.

Case 5. This 20-year-old Indian male, product of consanguineous marriage, presented with a 4-year history of progressive gait disturbance and behavioral issues, including aggressiveness, abusive behaviors, and overreligiosity. His past medical history was unremarkable. There was no history of anosmia, sleep disturbances, and orthostatic hypotension. His sister was similarly affected at age 20 with predominant behavioral features, aggressiveness and obsessive-compulsive disorder. She later developed cervical dystonia and parkinsonism and died by age 23 without formal diagnosis. His examination at age 19 showed spastic paraparesis along with parkinsonian features (bradykinesia and impaired postural reflexes), cranio-cervical dystonia, and motor perseveration. Spasticity, brisk deep tendon reflexes, and bilateral ankle clonus were present. He had extensor plantar response bilaterally. Cerebellar and sensory examination was unremarkable. Saccades were slow in the horizontal plane. He also had occasional myoclonic jerks in the upper limbs on extending his hands. Pull test revealed impaired postural reflexes. His Mini Mental State Examination (MMSE) was 26/30 with subtle impairment in frontal lobe functions and impaired calculation abilities. Brain MRI showed cerebellar atrophy but no iron deposition on SWI sequences. One year into his illness his parkinsonism and postural instability worsened, and he started having episodes of urinary incontinence. ^{18}F-DOPA PET showed moderate-severe reduction in tracer uptake over the caudate and putamen asymmetrically. He was started on levodopa and developed severe dyskinesias three months after treatment initiation at the dose of 300mg daily. Pramipexole was therefore initiated with improvement of dyskinesias. WES detected the homozygous variant NM_003560.4:c.2222G>A (p.Arg741Gln) in *PLA2G6*.

Case 6. This 33-year-old Indian male born to consanguineous parents had a 4-year history of levodopa-responsive asymmetric akinetic-rigid syndrome without rest tremor. He reported falls since two years after the onset of parkinsonian symptoms. His family history was unremarkable. He suffered from anxiety and depression with crying episodes only in the off periods. There were significant sleep problems with

history suggestive of RBD. Other non-motor symptoms included fatigue, pain and urinary issues with occasional incontinence. Anosmia, bowel dysfunction and orthostatic hypotension were not reported. He had mild cognitive impairment (MMSE score 27/30) with apathetic behavior. Eye movement examination revealed square wave jerks and saccadic pursuits. His postural reflexes were impaired. Cerebellar and sensory examination was normal. Brain MRI showed cerebellar atrophy but no iron deposition on SWI sequences. ^{18}F-DOPA PET detected severely reduced tracer uptake in the bilateral striatum (putamen>caudate), asymmetrically. He developed dyskinesias five months after starting levodopa. On NGS gene panel for early-onset parkinsonism, he was found to carry the homozygous variant NM_003560.4:c.1937C>T (p.Pro646Leu) in *PLA2G6*.

Case 7. This 28-year-old Indian female with no history of parental consanguinity manifested asymmetric parkinsonism with rest tremor, postural instability, depressive episodes with suicidal ideation, and emotional lability since age 25. She had urinary disturbances, including frequency, urgency, and occasional incontinence, and constipation. There was no history of anosmia nor elements suggestive of RBD. Her family history was unremarkable. Examination revealed pyramidal signs, including lower limb spasticity (Modified Ashworth score 2) and brisk reflexes. Cerebellar and sensory examination was normal. Eye movement examination revealed normal pursuits with slightly slow saccades. She also exhibited bilateral postural tremor in the hands with superimposed action-induced myoclonic jerks. She had no orthostatic hypotension. Parkinsonism responded to levodopa, but she developed levodopa-induced dyskinesias within 2 months since treatment initiation. Her MMSE score was 26/30 with mild impairment of frontal lobe functions. Brain MRI revealed cerebellar atrophy, with no iron deposition on SWI sequences. ^{18}F-DOPA PET detected asymmetrically reduced uptake in the striatum. WES detected the two variants NM_003560.4:c.2370T>G (p.Tyr790*) and NM_003560.3:c.1511C>T (p.Ser504Leu) in *PLA2G6*.

Case 8. A 21-year-old Indian male born to non-consanguineous parents had normal birth and neurodevelopmental milestones. At age 17, he started developing a progressive akinetic-rigid syndrome with rest tremor in his arms. On examination,

his saccadic movements were slow, and he had upper-limb and axial rigidity as well as spasticity in his lower limbs. There were brisk tendon reflexes and bilateral Babinski sign. Over few years, he also developed gait difficulty, postural instability, and generalized myoclonic jerks. He was wheelchair bound at age 20. There were cognitive and psychiatric issues, including disorientation, attention deficit, apathy, executive dysfunction, progressive reduction in spontaneous speech till mutacism, and emotional lability, as well as urinary incontinence two years into the disease course. Myoclonic jerks appeared few years into the disease course. He had visual hallucinations. A single generalized tonic-clonic seizure was reported. Serum ferritin and ceruloplasmin were unremarkable, and no acanthocytes were detected. EEG showed intermittent generalized epileptiform discharges. Nerve conduction studies (NCS) were unremarkable. On brain MRI, there was evidence of mainly frontotemporal and cerebellar atrophy, with mild iron deposition in the SN, putamen, and GP (Figure V-1I). Brain ^{18}F-fluorodeoxyglucose(FDG)-PET was normal. Parkinsonism was levodopa-responsive, with early appearance of dyskinesias.

Case 9. Case 8's 24-year-old sister also had unremarkable birth and developmental history. At age 22, she presented with behavioral abnormalities (excessive irritability, aggressiveness), emotional lability, generalized bradykinesia, and abnormal posturing of her hands and feet. She had deterioration of her gait and balance over a six-month period and started to fall backwards daily around 18 months after symptom onset. She was not able to sit straight due to truncal dystonia and tendency to retropulsion. On examination, she presented with emotional lability and impairment of her working memory and verbal fluency. There was hypomimia, and eye movement assessment showed square wave jerks and slow saccades. She had truncal dystonia and asymmetric abnormal posturing of the extremities, limb rigidity, and brisk reflexes, with flexor plantar responses. Her gait was characterized by foot dragging and striatal toes. Sensory and cerebellar examination was normal. Serum ceruloplasmin and ferritin were normal, no acanthocytes were detected. Abdominal US excluded organomegaly, and NCS were unremarkable. Brain MRI showed cortical and cerebellar atrophy, as well as mild iron deposition in the bilateral SN, caudate, and putamen. WES detected both siblings (Cases 8-9)

were homozygotes for the variant NM_003560.4(*PLA2G6*):c.2222G>A (p.Arg741Gln). Parkinsonism responded to levodopa.

Case 10. A 26-year-old female, born to consanguineous Pakistani parents, presented with a 2-year-history of anxiety and "unusual emotional states" which started during her first pregnancy. Since approximately the same period, she noticed intermittent tremor of her right hand and then progressively over time a combination of slowing of movement, poor balance, and emotional lability. Brain MRI at age 24 was unremarkable as well as serum copper and ceruloplasmin, slit lamp examination, and CSF analysis. She was initially diagnosed with postpartum depression and a possible functional motor disorder. On examination (age 26), she had facial hypomimia, restriction and slowing of both vertical and horizontal saccades, and difficulty with rapid tongue movements. She had bilateral severe bradykinesia, rest tremor affecting the right arm and stimulus-sensitive action myoclonus, particularly in the legs. Reflexes were pathologically brisk throughout with crossed adductor responses. She walked with a short-stepped gait, having difficulty initiating and stopping movement. She turned with multiple steps and was very unsteady. There were no cerebellar signs. Formal neuropsychometry (age 26) revealed global intellectual underfunctioning. Follow-up brain MRI at age 26 revealed some increase in CSF spaces abnormal for her age. She was started on rotigotine and levodopa but developed dyskinesias within the first three months of treatment. WES detected the homozygous variant NM_003560.4(*PLA2G6*):c.2222G>A (p.Arg741Gln), which was documented in the heterozygous state in her parents (Figure V-3). She was lost to follow-up at age 27 and died of unknown cause at age 36.

Case 11. Case 10's younger sister developed depression and anxiety at age 21, with increasing difficulty in attending university. She was told to be frequently tearful but also to laugh inappropriately at times. On first examination (age 23), she was hypomimic and had slowing of vertical saccades. She had bilateral bradykinesia with action-induced myoclonus in her limbs. She walked with a cautious, short-stepped gait, taking multiple steps on turning. Her postural reflexes were impaired.

Table V-1. Clinical, neuroradiological and genetic features of new cases of *PLA2G6*-related parkinsonism

	Case 1	**Case 2**	**Case 3**	**Case 4**	**Case 5**	**Case 6**	**Case 7**
Sex/Current age (y)	F/43	F/36	F/25	M/22	M/20	M/33	F/28
Ethnicity	White British	White British	Indian	Indian	Indian	Indian	Indian
Parental consanguinity	No	No	No	No	Yes	Yes	No
Family history	Unremarkable	Unremarkable	Unremarkable	Brother similarly affected (no details available)	Sister similarly affected (no details available)	Unremarkable	Unremarkable
Age at onset	27	29	21	15	16	29	25
Symptom at onset	Dystonia right arm	Parkinsonism and executive dysfunction	Parkinsonism and psychiatric features	Psychiatric features (aggressiveness, disinhibition, episodes of fear, emotional lability)	Psychiatric features	Parkinsonism	Parkinsonism
Motor features	Parkinsonism (bradykinesia, rigidity, rest tremor) Dystonia Pyramidal signs (hyperreflexia, crossed adductor response) Cerebellar signs (limb dysmetria) Myoclonus	Parkinsonism (bradykinesia, rigidity) Dystonia Pyramidal signs (hyperreflexia, ankle clonus) Cerebellar signs Myoclonus	Parkinsonism (bradykinesia, rigidity) Dystonia Cerebellar signs (limb dysmetria) Dysphagia	Parkinsonism (bradykinesia, rigidity) Dystonia Pyramidal signs (hyperreflexia) Myoclonus	Parkinsonism (bradykinesia, rigidity) Dystonia Pyramidal signs (hyperreflexia, spasticity LL, ankle clonus) Myoclonus	Parkinsonism (bradykinesia, rigidity)	Parkinsonism (bradykinesia, rigidity, rest tremor) Dystonia Pyramidal signs (hyperreflexia, spasticity LL) Myoclonus
Non-motor features	Postural instability Cognitive impairment Anxiety Depression	Postural instability Cognitive impairment Anxiety Depression Apathy Urinary issues (nocturia, incontinence)	Postural instability Cognitive impairment Anxiety Depression Urinary issues (urgency, urge incontinence)	Postural instability Cognitive impairment Aggressive behaviors Urinary issues (frequency, urgency, incontinence) Constipation	Postural instability Cognitive impairment Aggressive and abusive behaviors Urinary incontinence	Postural instability Cognitive impairment Anxiety Depression Apathy Emotional lability Urinary incontinence	Postural instability Cognitive impairment Depression Emotional lability Urinary issues (frequency, urgency, incontinence) Constipation
Response to LD	Initial good response, then worsening of dystonia Early LD-induced dyskinesias	Initial good response Early LD-induced dyskinesias	Initial optimal response LD-induced dyskinesias after 8 months of treatment	Modest response Early LD-induced dyskinesias	Good response LD-induced dyskinesias after 3 months of treatment	Good response LD-induced dyskinesias after 5 months of treatment	Good response LD-induced dyskinesias after 2 months of treatment
Brain MRI	Unremarkable (no mineralization on SWI); cerebellar atrophy on follow-up MRI	Iron deposition on SWI; cerebral and cerebellar atrophy on follow-up MRI	Cerebral atrophy (FT) Cerebellar atrophy No mineralization on T2*	Cerebellar atrophy No mineralization on T2*	Cerebellar atrophy No mineralization on T2*	Cerebellar atrophy No mineralization on T2*	Cerebellar atrophy No mineralization on T2*
Presynaptic dopaminergic terminal imaging	DaTscan: reduced uptake of tracer throughout the striata bilaterally (>putamen)	N.A.	$^{Tc\text{-}99m}$TRODAT-1 SPECT/CT: reduced tracer uptake in the striatum bilaterally	^{18}F-DOPA PET: Asymmetrical decrease in tracer uptake in the BG	^{18}F-DOPA PET: Asymmetrical decrease in tracer uptake in the BG	^{18}F-DOPA PET: severe decrease in tracer uptake in bilateral putamen more than caudate	^{18}F-DOPA PET: Asymmetrical decrease in tracer uptake
Genetics ***PLA2G6*** (NM_003560.4)	WGS Compound heterozygote c.956C>T p.(Thr319Met); c.1061T>C p.(Leu345Pro)	WGS Compound heterozygote c.238G>A (p.Ala80Thr); c.1924A>G (p.Thr642Ala)	NGS gene panel Compound heterozygote c.673C>T (p.His225Tyr); c.2311G>A (p.Asp771Asn)	WES Homozygote c.2222G>A (p.Arg741Gln)	WES Homozygote c.2222G>A (p.Arg741Gln)	NGS gene panel Homozygote c.1937C>T (p.Pro646Leu)	WES Compound heterozygote c.2370T>G (p.Tyr790*); c.1511C>T (p.Ser504Leu)

Table V-1. Continued

	Case 8	Case 9	Case 10	Case 11	Case 12	Case 13	Case 14
Sex/Current age (y)	M/24	F/24	F/Deceased age 36	F/33	M/24	M/24	M/36
Ethnicity	Indian	Indian	Pakistani	Pakistani	German	Indian	Pakistani
Parental consanguinity	No	No	Yes	Yes	No	Yes	Yes
Family history	Sister affected (case 9)	Brother affected (case 8)	Sister affected (case 11)	Sister affected (case 10)	No	Brother similarly affected (no details available)	Two siblings affected[16,20,32]
Age at onset	17	22	23	21	22	21	31
Symptom at onset	Parkinsonism	Parkinsonism, dystonia and behavioral issues	Psychiatric features (anxiety, unusual emotional states)	Psychiatric features (anxiety, depression)	Balance difficulty, bradykinesia	Psychiatric features (behavioral changes, stubbornness)	Gait and balance difficulties
Motor features	Parkinsonism (bradykinesia, rigidity, rest tremor) Dystonia Pyramidal signs (hyperreflexia, spasticity, Babinski sign) Dysarthria Myoclonus	Parkinsonism (bradykinesia, rigidity) Dystonia Pyramidal Pyramidal signs (hyperreflexia, Hoffman sign) Dysarthria	Parkinsonism (bradykinesia, rigidity) Dystonia Cerebellar signs (gait ataxia) Pyramidal signs (hyperreflexia, crossed adductor response) Dysarthria Myoclonus	Parkinsonism (bradykinesia, rigidity, rest tremor) Pyramidal signs (Babinski sign) Myoclonus	Parkinsonism (bradykinesia, rigidity, rest tremor) Pyramidal signs (hyperreflexia, ankle clonus) Cerebellar signs (limb dysmetria) Dysarthria	Parkinsonism (bradykinesia, rigidity, rest tremor) Pyramidal signs (hyperreflexia) Cerebellar signs (gaze-evoked nystagmus) Dysarthria	Parkinsonism (bradykinesia, rigidity) Dystonia Pyramidal signs (hyperreflexia, spasticity LL, ankle clonus) Cerebellar signs (mild gait ataxia, limb dysmetria, terminal tremor) Myoclonus
Non-motor features	Postural instability Cognitive impairment Apathy Emotional lability Urinary issues Constipation Visual hallucinations	Postural instability Cognitive impairment Apathy Abusive behaviors Emotional lability	Postural instability Cognitive impairment Anxiety Depression Emotional lability Urinary issues (urgency, incontinence)	Postural instability Cognitive impairment Anxiety Depression Emotional lability	Postural instability Cognitive impairment Dysphagia	Cognitive impairment Behavioral issues	Postural instability Cognitive impairment
Response to LD	Good response Early LD-induced dyskinesias	Good response	Good response LD-induced dyskinesias after few months of treatment	Very good response LD-induced dyskinesias after few months of treatment	Optimal response	Good response	Good response Early LD-induced dyskinesias (mainly affecting his jaw)
Brain MRI	Cerebral atrophy Cerebellar atrophy Iron deposition on SWI (SN, putamen, GP)	Cerebral atrophy Cerebellar atrophy Iron deposition on SWI (SN, caudate, putamen)	Mild cerebral atrophy Mild cerebellar atrophy No mineralization on T2*	Mild cerebral (biparietal) atrophy No mineralization on T2*	Mild generalized cerebral atrophy Mild cerebellar atrophy No mineralization on SWI	Cerebral atrophy (FT) Mild cerebellar atrophy No mineralization on T2* and SWI	Mild generalized cerebral atrophy Mild cerebellar atrophy Iron deposition on SWI (SN)
Presynaptic dopaminergic terminal imaging	N.A.	N.A.	N.A.	N.A.	DaTscan: reduced tracer uptake in the striatum bilaterally	N.A.	DaTscan: reduced tracer uptake in the putamen and striatum bilaterally
Genetics ***PLA2G6*** (NM_003560.4)	WES Homozygote c.2222G>A (p.Arg741Gln)	WES Homozygote c.2222G>A (p.Arg741Gln)	WES Homozygote c.2222G>A (p.Arg741Gln)	Sanger sequencing Homozygote c.2222G>A (p.Arg741Gln)	NGS gene panel Compound heterozygote c.1021G>A (p.Ala341Thr); c.1898C>T (p.Ala633Val)	WES Homozygote c.2222G>A (p.Arg741Gln)	Sanger sequencing: Homozygote c.2239C>T (p.Arg747Trp)

Legend: BG = basal ganglia; F = female; FT = frontotemporal; GP = globus pallidus; LD = levodopa; LL = lower limbs; M = male; N.A. = not available; NGS = next-generation sequencing; SN = substantia nigra; SWI = susceptibility-weighted MRI sequence; T2* = T2*-weighted gradient echo MRI sequence; WES = whole-exome sequencing; WGS = whole-genome sequencing; y = years.

She was initially started on ropinirole, with no benefit, and then on rotigotine and levodopa, with very good response. Citalopram was also added for her mood disorder. The patient developed some dyskinetic movements within the first month of treatment with levodopa (150mg daily). Formal psychometry at age 24 was overall suggestive of cortical and subcortical involvement, revealing impaired global memory, cognitive speed and attention. There was also evidence of weak executive function and comprehension. She underwent CSF examination, which was unremarkable except for low homovanillic acid (HVA), 5-hydroxyindoleacetic acid, and tetrahydrobiopterin. Brain MRI showed mild symmetrical biparietal atrophy, but no other abnormalities. Sanger sequencing confirmed she was homozygote for the variant NM_003560.4:c.2222G>A (p.Arg741Gln) in *PLA2G6* (Figure V-3). She was lost to follow-up at age 26 but remained alive at age 33.

Figure V-3. Segregation analysis in the pedigree of Cases 10 and 11

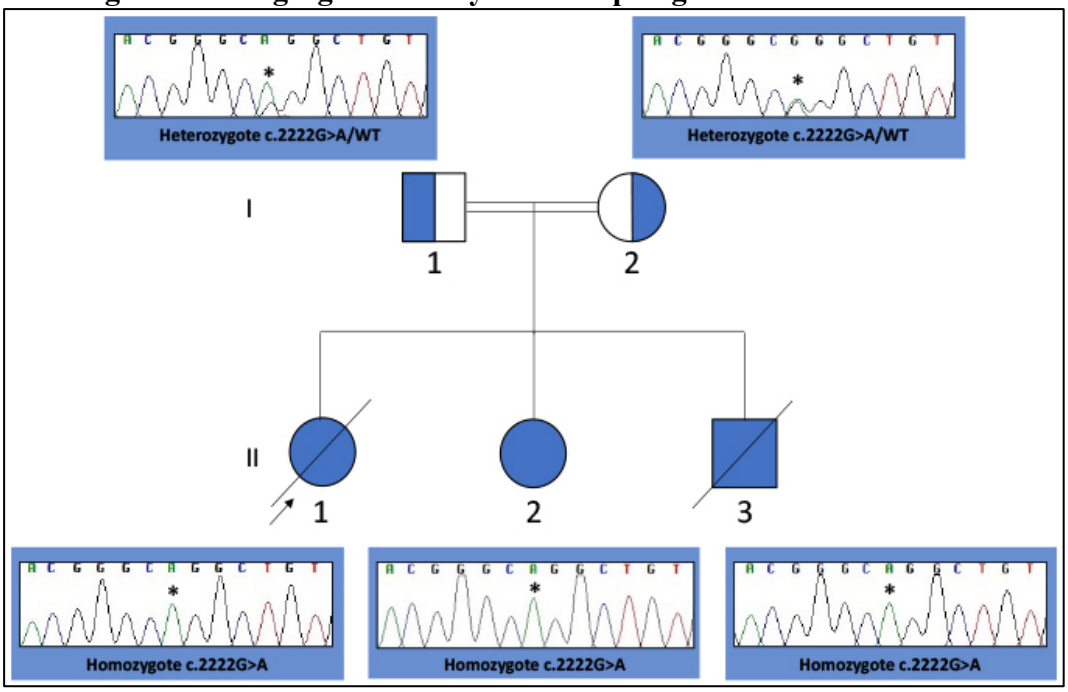

Segregation analysis confirmed the proband (Case 10, II-1) and both her younger sister (Case 11, II-2) and brother (II-3) were homozygotes for the variant NM_003560.4:c.2222G>A (blue) in the *PLA2G6* gene, whereas her parents were heterozygous carriers. The region was amplified using the following primers (5'→3'): F-gctcagcctgactcgaaag, R-aacagagcagacccttggg, with an amplicon size of 315 base pairs. Electropherograms were analysed using the Sequencher software package. Arrow = proband; WT = wild type.

Case 12. This 24-year-old German male with no history of parental consanguinity presented with subjective unsteadiness, slowness of movements and fatigue at age 22. His past medical and family history was unremarkable. The patient did not report any affective symptoms. On examination, he showed asymmetric parkinsonism with marked bradykinesia, rigidity, mild rest tremor and moderate kinetic and postural tremor of the upper limbs. There were mild cerebellar signs with saccades and mild dysmetria. There were no pyramidal signs nor sensory deficits, but mild postural instability. His neuropsychological assessment revealed impairment of attention as well as mnesic and executive functions, with significant fluctuations in his performances during the assessment. Brain MRI showed atrophy of the cerebellum and gyrification exceeding the age limit (Figure V-1L). His DaTscan showed bilaterally reduced tracer uptake in both striata (Figure V-1M). EEG and somatosensory evoked potentials (SEP) were unremarkable. On neurophysiology, he had unilaterally reduced motor evoked potentials (MEP) in lower-limb assessment after cortical stimulation, which reveals subclinical pyramidal dysfunction. He showed optimal response to levodopa, with improvement of gait, bradykinesia and tremor. On an NGS gene panel for early-onset parkinsonism, he was found to carry the variants NM_003560.4:c.1021G>A (p.Ala341Thr) and NM_003560.4:c.1898C>T (p.Ala633Val) in *PLA2G6*, which were detected in the heterozygous state in his father and mother, respectively.

Case 13. This 24-year-old Indian male presented at age 22 with a one-year history of personality changes, including irritability and stubbornness, and a few-month history of gait difficulty and slowness in his daily life activities. His perinatal history and motor developmental milestones were unremarkable. He had mild intellectual disability and poor scholastic performance since childhood. The patient was the youngest of three children born to a consanguineous marriage. His parents and 25-year-old sister were in good health, whereas his eldest brother experienced progressive gait difficulty and global slowness since age 17, became bedridden at age 19, and died at age 25 with no formal diagnosis. On examination, the patient was hypomimic and dysarthric. He had mild blepharospasm and gaze-evoked nystagmus. He had global bradykinesia, with pill-rolling tremor. Muscle strength, sensory and autonomic assessment was normal. He had brisk reflexes throughout.

He scored 24/30 on MMSE. Blood tests, including copper and ceruloplasmin, NCS, EMG, and ophthalmological assessment were normal. Brain MRI showed cerebral atrophy with frontal predominance and mild cerebellar atrophy, with no mineralization of the basal ganglia on T2* and SWI sequences (Figure V-1N-O-P). WES revealed the proband carried the variant NM_003560.4:c.2222G>A (p.Arg741Gln) in *PLA2G6* in the homozygous state, while segregation analysis detected the same variant in the heterozygote state in his parents and sister. Parkinsonism was levodopa-sensitive.

Case 14. This 36-year-old male was born to a first-cousin couple of Pakistani origin. He presented at age 32 with a 6-month history of slowly progressive leg stiffness leading to walking and balance difficulties. Over the first year since symptom onset, he also developed leg tremor and required support for ambulation. He denied swallowing difficulty, bladder and bowel issues, sleep disturbances, and hallucinations. Although he looked quiet and withdrawn, the patient and his family denied recent cognitive and behavioral changes. His past medical history was unremarkable. One of his younger brothers and his younger sister were previously diagnosed with PLAN manifesting as prominent parkinsonian syndrome and ataxic syndrome with mild parkinsonism, respectively.[15, 194] On examination, he had mild facial hypomimia and normal eye movements. On walking, there was mild extension truncal dystonia. He had increased muscle tone in his legs and right arm. He was slow on tapping tasks with his hands but more with his feet. Deep tendon reflexes were markedly brisk throughout, and there was bilateral ankle clonus. Routine blood tests were unremarkable. Brain MRI (age 33) showed mild generalized atrophy in the supra- and infratentorial compartments. On SWI, there was mildly decreased signal in the substantia nigra bilaterally and subtle loss of the appearances of the nigrosome (swallow tail sign). His DaTscan revealed abnormal tracer distribution in the striatum, with relative reduced activity in the putamen bilaterally, worse on the left (Figure V-1Q). Formal cognitive assessment at age 33 revealed marked impairment of processing speed, reduced recognition and recall of visual information, visual constructional difficulty, and reduced executive function, overall indicating marked sub-cortical and milder anterior cognitive compromise with the suggestion of greater right hemisphere involvement. *PLA2G6* targeted

sequencing detected the variant NM_003560.4:c.2239C>T p.(Arg747Trp) in the homozygous state (Figure V-4), as previously detected in his affected siblings. He received baclofen 60mg daily, procyclidine 15mg daily, levodopa 100mg daily, and botulinum toxin injections in his lower limbs. Dyskinesias mainly affecting his jaw were observed few months after starting levodopa.

Figure V-4. Segregation analysis in Case 14's pedigree

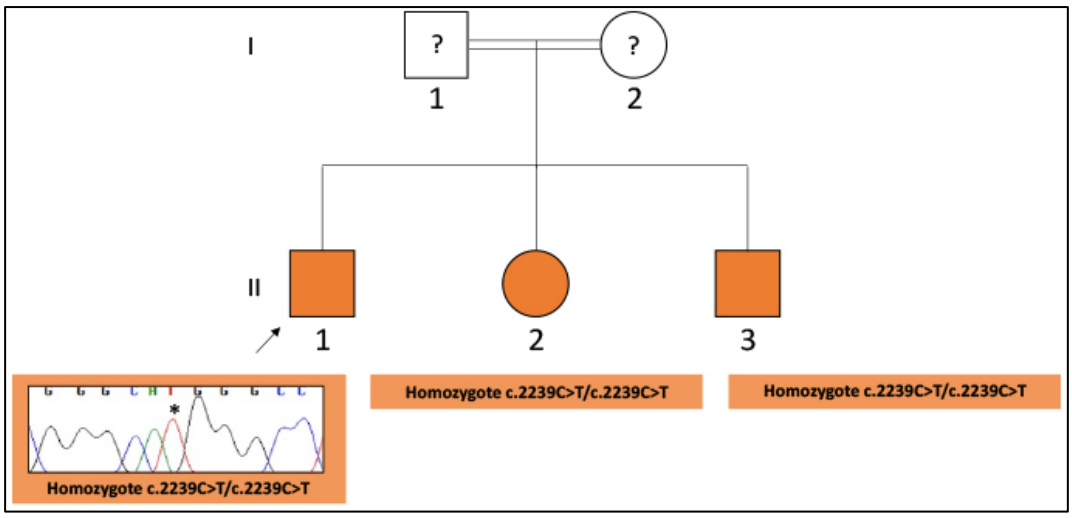

Sanger sequencing confirmed Case 14 (II-1) was homozygote for the variant NM_003560.4:c.2239C>T (orange) in the *PLA2G6* gene, which was previously documented in the homozygous state also in his younger sister and brother. The region was amplified using the following primers (5'→3'): F-actcaccaaggctgcttctc, R-aacagagcagacccttggg, with an amplicon size of 213 base pairs. Electropherograms were analyzed using the Sequencher software package. Arrow = Case 14; WT = wild type.

Table V-2. Analysis of genetic variants in the *PLA2G6* gene detected in 14 new cases with parkinsonism

	Case 1		Case 2		Case 3		Cases 4-5-8-9-10-11-13	Case 6	Case 7		Case 12		Case 14
***PLA2G6* variant** NM_003560.4	c.956C>T p.Thr319Met	c.1061T>C p.Leu354Pro	c.238G>A p.Ala80Thr	c.1924A>G p.Thr642Ala	c.673C>T p.His225Tyr	c.2311G>A p.Asp771Asn	c.2222G>A p.Arg741Gln	c.1937C>T p.Pro646Leu	c.2370T>G p.Tyr790*	c.1511C>T p.Ser504Leu	c.1021G>A p.Ala341Thr	c.1898C>T p.Ala633Val	c.2239C>T p.Arg747Trp
Mutation type	Missense	Missense	Missense	Missense	Missense	Missense	Missense	Missense	Nonsense	Missense	Missense	Missense	Missense
CADD score	23.2	29.8	23.0	26.3	25.5	27.8	25.7	29.6	35.0	23.0	26.4	28.7	29.8
GERP Phred score	2.48	2.48	2.41	2.31	2.62	2.24	2.10	6.43	-4.68	6.51	2.48	2.31	-0.11
PolyPhen-2 (HumDiv score)	Probably damaging (0.997)	Probably damaging (1.000)	Possibly damaging (0.855)	Probably damaging (0.971)	Possibly damaging (0.632)	Probably damaging (0.990)	Probably damaging (1.000)	Probably damaging (0.999)	N.A.	Benign (0.011)	Probably damaging (0.999)	Probably damaging (0.987)	Probably damaging (1.000)
SIFT (score)	Tolerated (0.072)	Damaging (0.001)	Tolerated (0.069)	Damaging (0.007)	Damaging (0.035)	Tolerated (0.147)	Tolerated (0.064)	Damaging (0.004)	N.A.	Tolerated (0.358)	Damaging (0.003)	Tolerated (0.145)	Deleterious (0.000)
PROVEAN (score)	Deleterious (-4.18)	Deleterious (-6.64)	Deleterious (-2.63)	Deleterious (-3.34)	Deleterious (-3-37)	Deleterious (-2.62)	Neutral (-2.06)	Deleterious (-4.63)	N.A.	Neutral (-0.04)	Deleterious (-3.26)	Deleterious (-2.61)	Deleterious (-6.30)
MutationTaster	Disease causing	Disease causing	Disease causing	Disease causing	Disease causing	Disease causing	Disease causing	Disease causing	Disease causing	Disease causing	Disease causing	Disease causing	Disease causing
ClinVar	Uncertain significance (criteria provided, multiple submitters, no conflicts)	Not reported	Uncertain significance (criteria provided, multiple submitters, no conflicts)	Not reported	Pathogenic/Likely pathogenic (criteria provided, multiple submitters, no conflicts)	Not reported	Pathogenic/Likely pathogenic (criteria provided, multiple submitters, no conflicts)	Not reported	Pathogenic/Likely pathogenic/Uncertain significance (criteria provided, conflicting interpretations)	Not reported	Not reported	Not reported	Pathogenic/Likely pathogenic (criteria provided, multiple submitters, no conflicts)
gnomAD v3.1 (allele count/homozygotes)	46/0	1/0	0/0	1/0	0/0	0/0	0/0	0/0	9/0	2/0	0/0	0/0	0/0
Classification (ACMG)	Uncertain significance	Likely Pathogenic	Uncertain significance	Likely Pathogenic	Likely Pathogenic	Uncertain significance	Pathogenic	Likely Pathogenic	Pathogenic	Uncertain significance	Likely Pathogenic	Likely Pathogenic	Pathogenic
References	-	11, 24	11, 33, 34	-	35, 36	-	16, 32, 37-40	-	11, 15, 20, 41, 42	43	11, 44, 45	46	16, 20, 22, 37, 44, 47

Legend: ACMG = American College of Medical Genetics and Genomics; CADD = Combined Annotation Dependent Depletion; GERP = Genomic Evolutionary Rate Profiling; N.A. = not available; PROVEAN = Protein Variation Effect Analyzer; SIFT = Sorting Intolerant From Tolerant.

Systematic literature review

I screened for eligibility 162 references from PubMed® search results (n = 136) and sources cited in the reference lists (Figure V-5). I found 40 references reporting 72 cases of *PLA2G6*-related parkinsonism who belong to 57 pedigrees and carry a total of 46 distinct mutations in *PLA2G6*. Video records and neuropathological specimens were reviewed for 18 and 2 previously published cases, respectively. Predefined data were extracted from previous reports and our case series.[15, 190-192, 194-196, 198, 204, 205, 209-212, 215, 219-243] Detailed information of 86 cases from 68 families contributed to the phenotypic and genotypic description of *PLA2G6*-related parkinsonism reported below.

Figure V-5. PRISMA flow diagram of the systematic review

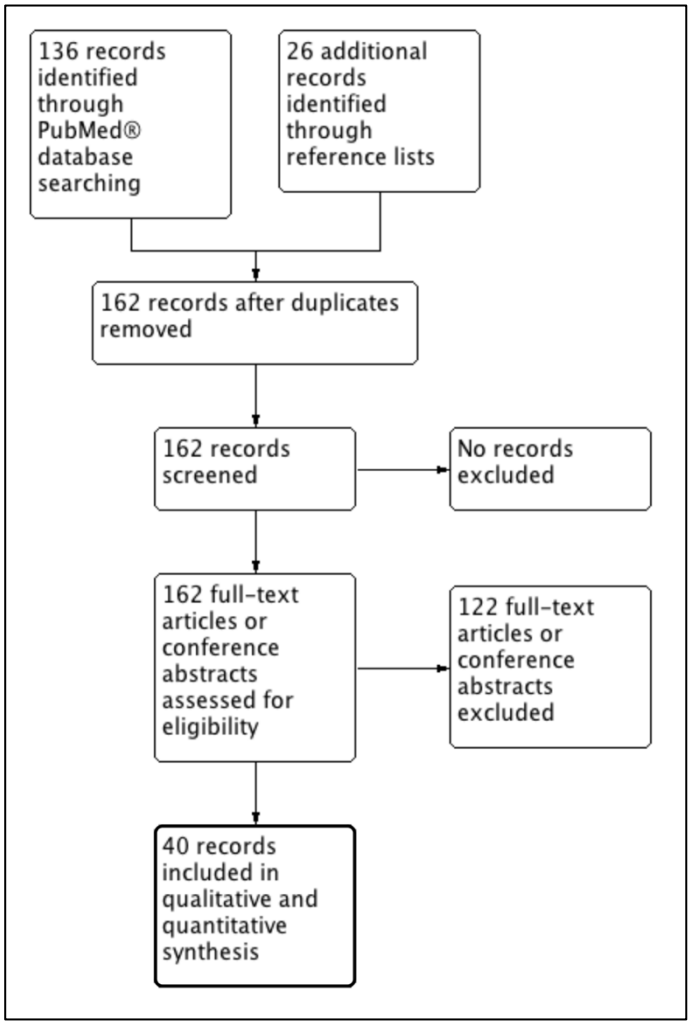

Phenotype

Clinical features

The cohort included 45 females (52.3%) and 41 males (47.7%; Figure V-6A). Ethnicity was traceable in 84/86 (97.7%) patients, with all reported cases having Asian (68/84; 81.0%) or European (16/84, 19.0%) origin (Figure V-6B). Perinatal history and developmental milestones were unremarkable in 42/45 (93.3%) patients, whereas one case experienced long-term toe-walking,[198] one relatively slower development,[221] and one unspecified developmental delay stabilized by therapy.[224] Convergent strabismus was noticed in Case 10 since age 2.

Median age of symptom onset calculated on 81/86 (94.2%) cases was 23.0 years (IQR 11.0; Figure V-6C), with 70/83 (84.3%) patients with presentation before the age of 31. Median age at last assessment determined on 67/86 (77.9%) cases was 31.0 years (IQR 12.0), whereas median disease duration at last assessment in 68/86 (79.1%) cases was 7.0 years (IQR 11.75). Presenting symptoms are summarized in Figure V-6D. Extrapyramidal features (parkinsonism and/or dystonia; 38/79, 48.1%), gait and/or balance disturbance (29/79, 36.7%), and psychiatric and/or cognitive issues (25/79, 31.6%), either alone or combined, were the most common manifestations at onset. Interestingly, psychiatric manifestations (e.g., severe anxiety, major depression, psychosis) were isolated presenting symptoms in 16/79 (20.2%) patients,[192, 198, 205, 209, 224, 237, 239, 240] foot dragging was the solely initial complaint in 8/79 (10.1%) cases,[15, 191, 204, 220, 225, 226, 243] and urinary incontinence was a major symptom at onset in 2/79 (2.5%) cases.[198, 230]

Parkinsonism, either isolated or combined with other neurological and/or psychiatric features (Figure V-6E), started at a median age of 25.0 years (IQR 9.25) and was present at onset or within one year since symptom onset in 45/68 (66.2%) patients. In the remaining 23 cases, the median time interval between symptom onset and onset of parkinsonism was 3.0 years (IQR 9.00). Hypo/anosmia was not reported as a premotor symptom in any of our cases and was only mentioned once in previous literature.[235] Parkinsonism presented as an akinetic-rigid syndrome in nearly half of the cases, whereas 36/67 (53.7%) patients had rest tremor which was

reported to affect the upper limbs in the large majority of cases and/or rarely the lower limbs.[236-238] Parkinsonian signs were described as asymmetric at onset in 40/50 (80.0%) cases. Hallucinations were mentioned in 16/30 cases (53.3%), being reported as visual in 9, visuo-auditory in 4, and auditory in 2. Delusions were present in 11/23 (47.8%). Sleep disturbances, including sleep fragmentation and acting out vivid dreams, were mentioned in 10/16 (62.5%) cases, and polysomnography was only available in Cases 1 and 14, showing prolonged REM phase and sleep apnea, respectively.

Dystonia was present in 50/72 cases (69.4%; Figure V-6E). When specified, dystonia was most often reported to affect the limbs only (17 cases) or to be generalized (8 cases). Cranial dystonia was reported in 11 patients (facial grimacing in 5, overt oromandibular dystonia in 4, blepharospasm in 3). Myoclonus, spontaneous and/or stimulus-sensitive, was reported in 15/23 (65.2%) cases at any point in the disease course but never at onset (Figure V-6E). In Case 2, the cortical origin of myoclonus (EMG bursts duration <50ms, electroencephalographic discharges time-locked to individual myoclonic jerks detected with jerk-locked back averaging) was demonstrated on neurophysiology for the first time (courtesy Dr Anna Latorre). Pyramidal signs were detected in 44/57 subjects (77.2%; Figure V-6E), ranging from hyperreflexia to Babinski sign, spasticity, clonus, crossed adductor response and Hoffmann sign. Reduced muscle strength was mentioned in one case only.[209] Cerebellar signs were present in 29/65 cases (44.6%; Figure V-6E), ranging from mild dysmetria to gait ataxia or gaze-evoked nystagmus. Postural and/or action tremor was mentioned in 10 cases.

Gait abnormalities were constantly present early in the disease course (Figure V-6E). When details were available (39 cases), gait was described as having parkinsonian (46.2% of patients), ataxic (30.8%), pyramidal (23.1%), dystonic (17.9) features, either alone or in combination. Freezing of gait was mentioned in 3 patients. Postural impairment was also constantly reported (Figure V-6E), causing loss of walking independence with a median time interval of 3.0 years (IQR 3.0) after symptom onset.

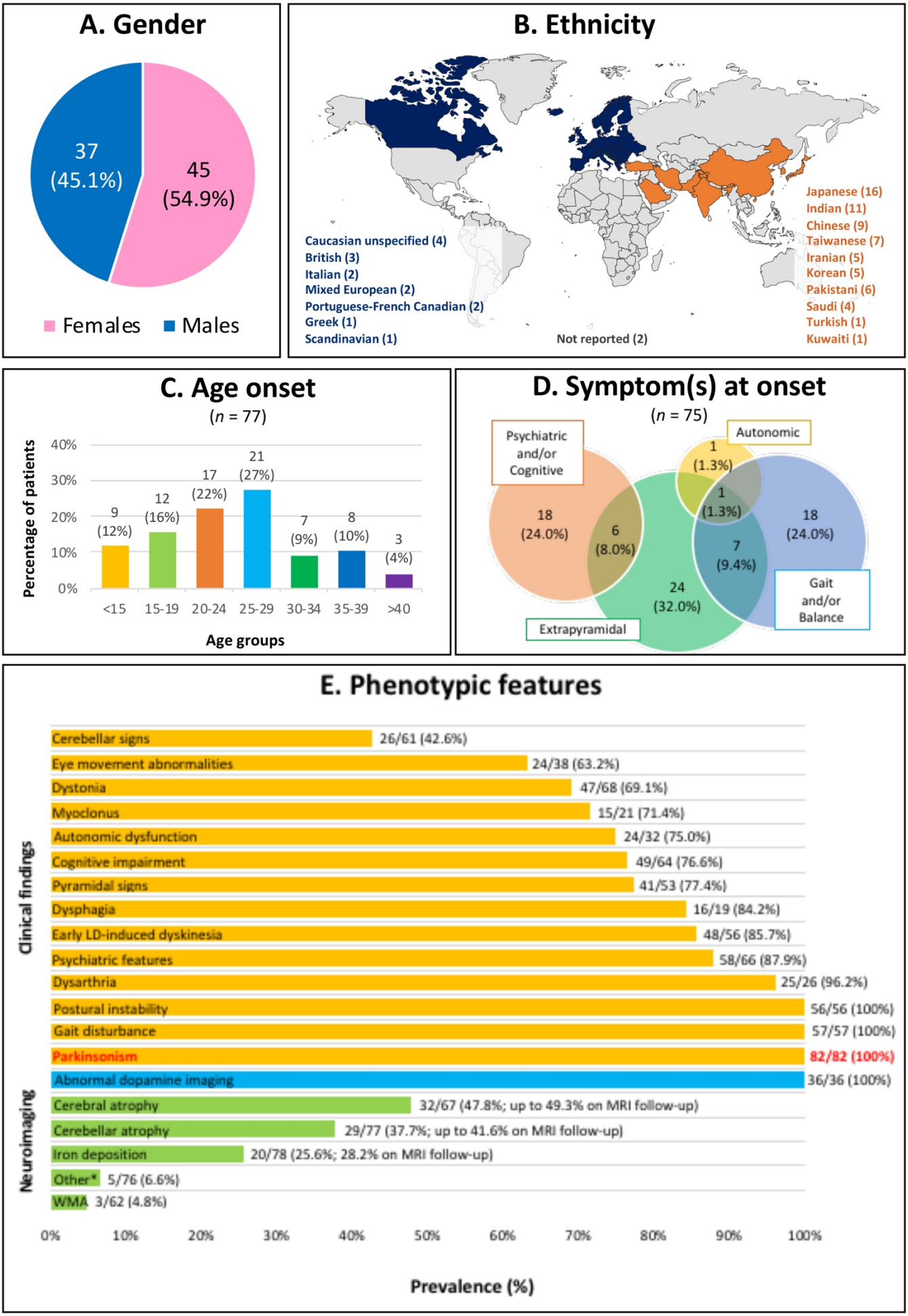
A. Gender
37 (45.1%)
45 (54.9%)
Females
Males
B. Ethnicity
Caucasian unspecified (4)
British (3)
Italian (2)
Mixed European (2)
Portuguese-French Canadian (2)
Greek (1)
Scandinavian (1)
Not reported (2)
Japanese (16)
Indian (11)
Chinese (9)
Taiwanese (7)
Iranian (5)
Korean (5)
Pakistani (6)
Saudi (4)
Turkish (1)
Kuwaiti (1)
C. Age onset
(n = 77)
Percentage of patients
40%
30%
20%
10%
0%
9 (12%)
12 (16%)
17 (22%)
21 (27%)
7 (9%)
8 (10%)
3 (4%)
<15
15-19
20-24
25-29
30-34
35-39
>40
Age groups
D. Symptom(s) at onset
(n = 75)
Psychiatric and/or Cognitive
Autonomic
Gait and/or Balance
Extrapyramidal
18 (24.0%)
1 (1.3%)
1 (1.3%)
18 (24.0%)
6 (8.0%)
7 (9.4%)
24 (32.0%)
E. Phenotypic features
Clinical findings
Neuroimaging
Cerebellar signs 26/61 (42.6%)
Eye movement abnormalities 24/38 (63.2%)
Dystonia 47/68 (69.1%)
Myoclonus 15/21 (71.4%)
Autonomic dysfunction 24/32 (75.0%)
Cognitive impairment 49/64 (76.6%)
Pyramidal signs 41/53 (77.4%)
Dysphagia 16/19 (84.2%)
Early LD-induced dyskinesia 48/56 (85.7%)
Psychiatric features 58/66 (87.9%)
Dysarthria 25/26 (96.2%)
Postural instability 56/56 (100%)
Gait disturbance 57/57 (100%)
Parkinsonism 82/82 (100%)
Abnormal dopamine imaging 36/36 (100%)
Cerebral atrophy 32/67 (47.8%; up to 49.3% on MRI follow-up)
Cerebellar atrophy 29/77 (37.7%; up to 41.6% on MRI follow-up)
Iron deposition 20/78 (25.6%; 28.2% on MRI follow-up)
Other* 5/76 (6.6%)
WMA 3/62 (4.8%)
0% 10% 20% 30% 40% 50% 60% 70% 80% 90% 100%
Prevalence (%)

Figure V-6. Descriptive statistics of the whole cohort with PLA2G6-related parkinsonism, including new and previously published cases (previous page)

The number of cases for which the information was available (non-missing observations) is indicated by "n" in (A-D) and by fractions' denominator in (E). (A) Gender distribution. (B) Ethnicity; number of cases according to ethnicity are reported in brackets. (C) Age at symptom onset according to age group; * = two additional cases with unspecified age of onset of parkinsonism before the age of 31.49(D) Symptom(s) at onset according to major descriptive categories. (E) Phenotypic spectrum of PLA2G6-associated parkinsonism with clinical features (yellow bars), brain MRI findings (green bars), and findings on presynaptic dopaminergic terminal imaging (blue bar); LD = levodopa; WMA = white matter abnormalities.

Dysautonomia was present in 25/35 (71.4%) patients (Figure V-6E), with symptoms of bladder overactivity and/or urinary incontinence reported in 71.9% of cases and constipation in 50%. Orthostatic hypotension was only mentioned in 2 cases.[222, 223] No information about sexual dysfunctions was available, but hypersexuality in response to treatment with dopamine agonists was reported in Case 14.

Cognitive impairment was documented early in the disease course in 51/67 (76.1%) patients (Figure V-6E). Psychiatric comorbidity was present in 61/70 (87.1%) cases (Figure V-6E), including depression (80.0% of cases), anxiety (79.2%), and signs of frontal lobe impairment (87.0%), encompassing, among others, apathy, paranoid thoughts, aggressive behaviors, and emotional lability.

Eye movement abnormalities were reported in 24/41 (58.5%; Figure V-6E) cases, with fragmented pursuit and/or reduced gaze range in the vertical plan being the most frequent. Apraxia of eyelid opening was reported in 6 cases.[15, 204, 205, 235] Dysarthria was described in 29/30 (96.7%; Figure V-6E). Swallowing difficulties were reported in 17/20 (85.0%) patients (Figure V-6E) and, in six cases where details were available,[15, 190, 194, 198, 204, 210, 231] overt dysphagia and/or the need of percutaneous endoscopic gastrostomy occurred a median interval of 10 years (IQR 7) after symptom onset. Sensory signs were reported in only one case.[198] Isolated generalized seizures were reported in five cases some years into the disease

course.[15, 198, 204, 211, 219] Oculogyric crises were reported in four cases.[192, 210, 238] "Paradoxical kinesia" was described in one case.[205]

Five patients died at a median age of 36.0 years (IQR 13.0), showing a median disease duration of 13.0 years (IQR 14.5) since symptom onset.

Response to treatment

Parkinsonism was responsive to levodopa in 71/73 (97.3%) cases, with initial improvement of motor symptoms ranging from minimal to dramatic in different patients. Levodopa-induced dyskinesias were reported in 46/57 (80.7%) cases and appeared within the first year of treatment in the majority of cases with details available, even with very low doses of levodopa. In some cases, levodopa led to behavioral changes with psychotic manifestations or dystonic reactions mainly affecting the oromandibular or cervical region. In 17/18 cases treated with dopamine agonists there was a beneficial response, with some cases experiencing however side effects including psychosis and hypersexuality. Eight out of 11 patients (72.7) had some benefit from anticholinergics, and 13 out of 15 from amantadine. Baclofen was beneficial in two out of three patients. Five patients received botulinum toxin injections for spasticity and/or dystonia, with good response. Four patients underwent bilateral DBS of the subthalamic nucleus (STN) with excellent outcome,[237] and one patient (Case 1) underwent bilateral DBS of the GPi with improvement of trunk dystonia and control of levodopa-induced dyskinesias. One patient underwent unilateral pallidotomy with transient relief of motor fluctuations.[232, 233]

Neuroimaging findings

Brain MRI was available in 82/86 (95.3%) patients. Cerebral atrophy was reported in 34/71 cases (47.9%), being described as mild to moderate in severity, and generalized or mainly involving the frontotemporal lobes (Figure V-1B-F-G-L-O; Figure V-6E). Mild to marked cerebellar atrophy affecting the vermis and/or the hemispheres was observed in 32/81 (39.5%; Figure V-1B-G-L-N; Figure V-6E). In

21/82 (25.6%) cases there was evidence of iron deposition on MRI T2/T2*/SWI sequences (Figure V-1D-I; Figure V-6E). Interestingly, iron deposition was not detected in 15 cases in which dedicated MRI sequences (T2*/SWI) were performed (Figure V-1A-P; Figure V-6E). White matter T2 hyperintensities were reported in three cases,[15, 204, 220, 236] mainly in the frontal lobes. Additional finding on brain MRI (Figure V-6E) were claval hypertrophy in four,[190, 194, 196, 211, 236] vertically oriented corpus callosum in two,[196, 211] and the swallow tail sign in two patients.[241] Follow-up brain MRI scans were available in seven patients, showing progression of cerebral and/or cerebellar atrophy in three cases,[198] as well as appearance of iron deposition in two cases.[15, 204, 231]

Dopamine imaging with presynaptic tracers was available in 37/86 cases (43.0%) and constantly abnormal (Figure V-1C-E-H-M-Q; Figure V-6E). In one patient, ^{11}C-raclopride(RAC)-PET for postsynaptic receptor function revealed increased RAC uptake in the putamen more than in the caudate, thus indicating a largely presynaptic dopaminergic abnormality as seen in idiopathic Parkinson's disease.[205]

In three patients, a CT scan excluded that MRI-T2/SWI hypointensities corresponded to basal ganglia calcification. ^{18}F-FDG-PET was performed in seven cases, showing global hypometabolism of cerebral cortex and cerebellum in one case,[227] hypometabolism in the frontoparietal regions in three cases,[209] hypometabolism in the temporoparietal regions in one case,[219] and hypometabolism in the parieto-occipital lobes in another case.[192] Spine MRI was available in 8 cases showing no signal abnormalities in the spinal cord.

Findings from laboratory tests and other instrumental investigations

No abnormal laboratory findings were identified in routine blood and urine tests in more than one case. CSF analysis were performed in 13 cases and revealed decreased HVA levels in four cases, including Cases 10-11,[15, 204, 209] two of which with subsequent normal phenylalanine loading test.[15, 204]

EEG was described as abnormal in four out of 12 cases in which was reported.[15, 204, 211, 239] In one case (Case 14's brother),[15, 204] EEG was normal early in the disease course and showed diffuse slowing with frequent multifocal epileptiform

abnormalities later in the disease course. This was also reported in the other three cases few years into the disease course. NCS were performed in eight patients, showing signs of distal sensorimotor neuropathy in one (who also showed EMG abnormalities),[190] sensory neuropathy in one,[198] and bilateral tibial neuropathy in one (Case 3). Five patients with pyramidal signs underwent MEP, which showed delayed central motor conduction time in two cases, including Case 1.[230] In one patient (Case 12), MEP was abnormal despite the absence of clinically detectable pyramidal signs.

Ophthalmological assessment excluded pigmentary retinopathy in seven cases.[15, 204, 205, 220, 243] Visual evoked potentials were tested normal in three cases.[15, 204, 209]

Genotype

In the whole cohort, *PLA2G6* mutations were detected by various genetic approaches encompassing genotyping and homozygosity mapping, Sanger sequencing, multiplex ligation-dependent probe amplification, NGS-based gene panels, WES and WGS. Parental consanguinity was reported in 35/64 (54.7%) cases. Overall, 46/86 (53.5%) patients carried homozygous variants in *PLA2G6*, whereas segregation analysis revealed that 40/86 (46.5%) were compound heterozygotes.

The 14 *PLA2G6* new cases I herein report carried 13 distinct *PLA2G6* mutations, including four missense variants (c.956C>T, c.1924A>G, c.2311G>A, c.1937>T) which were novel, four missense variants (c.1061T>C, c.673C>T, c.1021G>A, c.1898C>T) which were previously reported only in *PLA2G6* childhood-onset phenotypes, and one nonsense (c.2370T>G) and three missense variants (c.238G>A, c.2222G>A, c.2239C>T) already detected in both childhood- and late-onset phenotypes (Table V-2). The four novel missense variants I identified were either absent in gnomAD v3.1 (n=2) or exceedingly rare (minor allele frequency (MAF) <0.1%, n=2; gnomAD v3.1), all being highly conserved across species (GERP, visual multiple sequence alignment) and predicted to be pathogenic by at least four of five prediction tools (CADD, PolyPhen-2, SIFT, PROVEAN,

MutationTaster; Table V-2). Among the four variants previously reported only in childhood-onset phenotypes, the first missense variant c.1061T>C was in compound heterozygosity with another missense variant in a case of neurodegeneration with brain iron accumulation (NBIA),[186] with a frameshift variant in an INAD case with iron,[186] and with a nonsense variant in another INAD case.[198] The second missense variant c.238G>A was found in compound heterozygosity with a nonsense variant in a case of NBIA with iron, and in the homozygous state in both a case of ANAD (age onset 8 years)[206] and one case with onset at age 14.[205] The third missense variant c.1021G>A was previously found in compound heterozygosity with a missense variant in two siblings with INAD with brain iron accumulation, whereas the fourth missense c.673C>T was detected in the homozygous state in a childhood-onset case with long history. More intriguingly, among the four variants reported both in childhood- and late-onset phenotypes, the nonsense variant c.2370T>G was in compound heterozygosity with a missense variant in Case 7 (age of onset 25 years), whereas it was found in the homozygous state in a case of INAD reported by Morgan et al.[186] and in compound heterozygosity with another nonsense variant (c.1674del) in two sisters with INAD reported by Blake et al.[213] Overall, these observations suggest a gradient in the age of symptom onset and phenotypes severity reflecting the extent to which variants impact the gene transcript.

When considering all published and the novel mutations herein reported, the number of *PLA2G6* mutations associated with parkinsonism increases to 54 (Table V-2, Figures V-7-8). These included 46 non-truncating (44 missense, two in-frame deletions) and 8 truncating (four splicing, two nonsense, two frameshift) changes, therefore missense variants being the predominant mutation type in *PLA2G6*-related parkinsonism (Figures V-7-8). The majority of *PLA2G6* mutations were present in only one pedigree, whereas 12 mutations occurred in more than one family (c.991G>T, c.2222G>A, c.1904G>A, c.1077G>A, c.2239C>T, c.216C>A, c.109C>T, c.238G>A, c.1547C>T, c.2370T>G, c.1495G>A, c.1427+1G>A). The most frequent variants were c.991G>T (17 pedigrees),[191, 192, 215, 221, 223, 225-227, 239, 242, 244] which has mainly been described in Chinese and Taiwanese pedigrees, c.2222G>A (12 pedigrees),[15, 204, 209-212, 243] which has been reported in Indian,

Pakistani and Saudi families, and c.1904G>A (10 pedigrees),[195, 222, 223, 234, 245] which has hitherto been detected only in Japanese kindreds, which suggests they may be founder mutations, although no haplotype analysis has hitherto been performed.

Mutations in *PLA2G6* linked to parkinsonism are scattered throughout the locus and target different protein domains (Figures V-7-8) rather than being localized in mutational hotspots, as demonstrated in Parkinson's disease genes such as *LRRK2* or *PRKN*. None of these mutations affect the primary structure of iPLA2β functional domains implicated in its enzymatic activities, including the proline-rich motif, glycine-rich nucleotide binding motif, lipase motif, proposed C-terminal Ca2+-dependent calmodulin binding domain, and three putative caspase cleavage sites.[186] All missense mutations determine changes in amino acid residues highly conserved across species. Detailed comparative analysis of the phenotype revealed no apparent genotype-phenotype correlations depending on the mutation type.

Enzymatic activity of the mutant iPLA2β was documented in only one included report.[225] Transfection of cDNA encoding *PLA2G6* carrying the homozygous variant c.991G>T into HEK293T cells revealed about 30% of residual protein activity compared to the wild-type protein.[225]

Figure V-7. Schematic of the *PLA2G6* gene and its product with genetic variants and corresponding protein changes associated with parkinsonism

(next page)

Upper part. Ideogram of chromosome 22 showing the localization of the *PLA2G6* gene. Middle part. Schematic of the *PLA2G6* gene with 54 mutations linked to parkinsonism. Lower part. Schematic of the *PLA2G6* protein product (iPLA2β) with predicted protein changes. The protein structure encompasses seven ankyrin repeats (light blue), a proline-rich motif (yellow), a glycine-rich nucleotide binding motif (light blue), a lipase motif (pink), and a proposed C-terminal calcium-dependent calmodulin binding domain (dark blue).

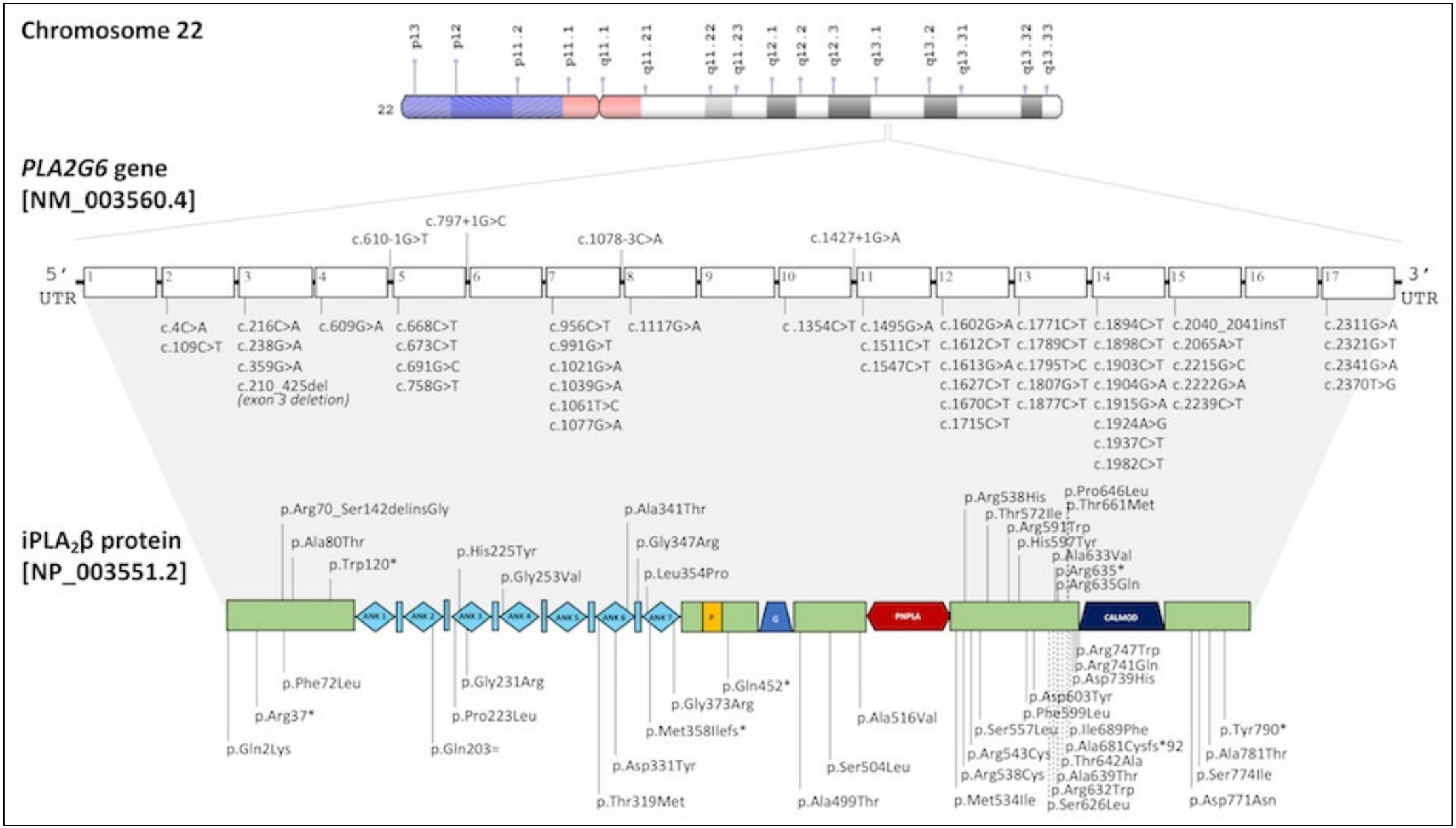
Chromosome 22
p13
p12
p11.2
p11.1
q11.1
q11.21
q11.22
q11.23
q12.1
q12.2
q12.3
q13.1
q13.2
q13.31
q13.32
q13.33
22
PLA2G6 gene
[NM_003560.4]
5′ UTR
3′ UTR
c.610-1G>T
c.797+1G>C
c.1078-3C>A
c.1427+1G>A
c.4C>A
c.109C>T
c.216C>A
c.238G>A
c.359G>A
c.210_425del
(exon 3 deletion)
c.609G>A
c.668C>T
c.673C>T
c.691G>C
c.758G>T
c.956C>T
c.991G>T
c.1021G>A
c.1039G>A
c.1061T>C
c.1077G>A
c.1117G>A
c .1354C>T
c.1495G>A
c.1511C>T
c.1547C>T
c.1602G>A
c.1612C>T
c.1613G>A
c.1627C>T
c.1670C>T
c.1715C>T
c.1771C>T
c.1789C>T
c.1795T>C
c.1807G>T
c.1877C>T
c.1894C>T
c.1898C>T
c.1903C>T
c.1904G>A
c.1915G>A
c.1924A>G
c.1937C>T
c.1982C>T
c.2040_2041insT
c.2065A>T
c.2215G>C
c.2222G>A
c.2239C>T
c.2311G>A
c.2321G>T
c.2341G>A
c.2370T>G
iPLA2β protein
[NP_003551.2]
p.Arg70_Ser142delinsGly
p.Ala80Thr
p.Trp120*
p.His225Tyr
p.Gly253Val
p.Ala341Thr
p.Gly347Arg
p.Leu354Pro
p.Arg538His
p.Thr572Ile
p.Arg591Trp
p.His597Tyr
p.Pro646Leu
p.Thr661Met
p.Ala633Val
p.Arg635*
p.Arg635Gln
ANK 1
ANK 2
ANK 3
ANK 4
ANK 5
ANK 6
ANK 7
P
G
PNPLA
CALMOD
p.Phe72Leu
p.Arg37*
p.Gln2Lys
p.Gly231Arg
p.Pro223Leu
p.Gln203=
p.Asp331Tyr
p.Thr319Met
p.Met358Ilefs*
p.Gly373Arg
p.Gln452*
p.Ala499Thr
p.Ser504Leu
p.Ala516Val
p.Met534Ile
p.Arg543Cys
p.Arg538Cys
p.Ser557Leu
p.Asp603Tyr
p.Phe599Leu
p.Ser626Leu
p.Arg632Trp
p.Ala639Thr
p.Thr642Ala
p.Ala681Cysfs*92
p.Ile689Phe
p.Arg747Trp
p.Arg741Gln
p.Asp739His
p.Asp771Asn
p.Ser774Ile
p.Ala781Thr
p.Tyr790*

Figure V-8. Structural distribution of coding mutations in the *PLA2G6* protein product (iPLA2β)

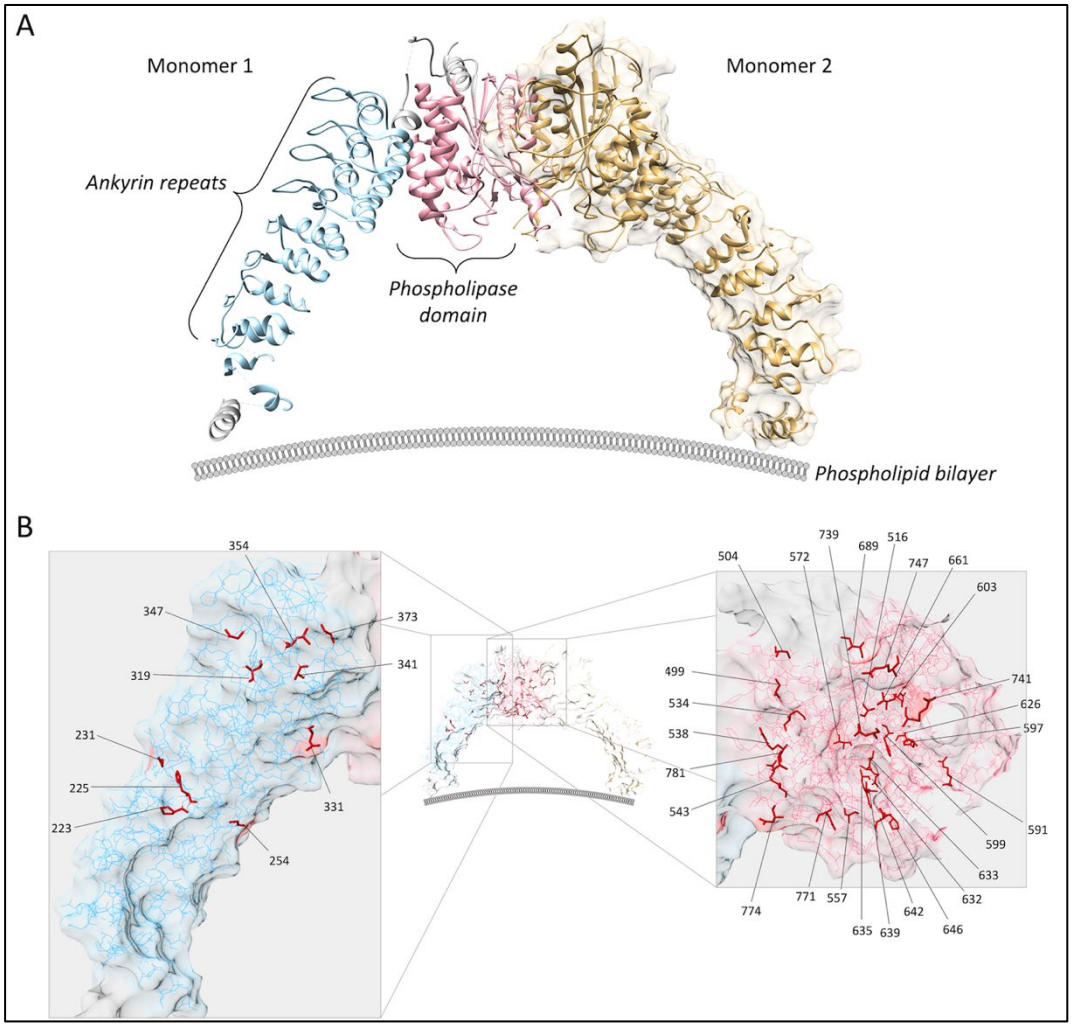

(A) Crystal structure of the dimeric iPLA2β complex, displayed in association with the phospholipid bilayer cell membrane. Monomer 1 shows domain organisation, with the ankyrin repeats coloured light blue, the phospholipase domain coloured pink. (B) Distribution of coding mutations in *PLA2G6* across the functional domains of iPLA2β, showing localization with the ankyrin (left hand inset, blue) and phospholipase domains (right hand inset, pink). Protein co-ordinates derived from Malley et al.,[181] protein database file 6AUN. Images generated using UCSF Chimera.[117]

Pathology

CNS pathology has been reported in three cases.[198, 232, 233 228] In one case, brain autopsy revealed cerebellar cortical atrophy with severe loss of granule cells, prominent gliosis in the molecular layer and to a lesser extent Purkinje cell depletion (cerebellar atrophy in this patient was not detected on brain MRI at symptom onset).[198] Cytoarchitecture of the dentate and inferior olivary nuclei, however, was comparably well preserved. There were occasional neuroaxonal spheroids in the GP, STN, thalamus, ambiguus nucleus, and frequent in the gracile and cuneate nuclei and posterior horns of the spinal cord. There was severe atrophy of the ventral lateral parts of the SN with much better pigmented neuron preservation medially. The locus coeruleus showed only mild depletion and the vagus nerve nucleus in the medulla showed no evidence of severe neuronal loss. Nevertheless, Lewy bodies were present in the brainstem nuclei in the tegmentum and frequently in the less atrophic medial part of the substantia nigra, in the Meynert nucleus, medial temporal lobe and occasionally in the putamen. Lewy pathology was particularly widespread across the deep layers of the neocortex affecting all, including occipital, lobes (Braak stage 6, diffuse neocortical Lewy pathology). There was also very mild tau pathology in the medial temporal lobe with rare neurofibrillary tangles and occasional neuropil threads (Figures V-9).[198] One patient underwent brain biopsy of the frontal cortex which showed severe Lewy pathology and moderate tau pathology (neuropil threads).[198] Post-mortem evaluation in another case showed widespread cortical and limbic structure atrophy, Lewy bodies in the SN and locus coeruleus, Alzheimer's disease-like pathology, mainly in the temporal lobe structures, abundant gliosis detected by glial fibrillary acid protein, and excessive iron accumulation in the reticularis portion of the SN, but also the GP and ventral forebrain.[232, 233]

No cases reported to date had nerve or rectal biopsy available. Muscle biopsy was unremarkable in three cases and showed neurogenic changes and reduced cytochrome oxidase activity (complex IV) in one case.[190, 194, 198] Skin biopsy, which

however did not search for α-synuclein, was unremarkable in three cases.[15, 204] Bone marrow aspiration was normal in two cases.[15, 204]

Figure V-9. Post-mortem findings in the brain and spinal cord of a patient carrying c.109C>T and c.1078-3C>A mutations in *PLA2G6* (previously published;[198] next page**)**

(A) In the cerebellar cortex, there is a severe depletion of granule cells (yellow arrow), prominent gliosis in the molecular layer (red asterisk), and to a lesser extent depletion of the Purkinje cells (blue asterisk), shown on hematoxylin and eosin (H&E) stained section. (B) The dentate nucleus in the cerebellum, demonstrated on H&E-stained section. (C) The inferior olivary nucleus in the medulla (preparation immunostained for non-phosphorylated TDP43) shows only mild gliosis and no significant neuronal loss. (D) The dorsal vagus nerve nucleus, although containing Lewy bodies (not shown), does not demonstrate any severe neuronal depletion. (E) Transverse H&E-stained section of the spinal cord at the lumbar level shows (F) that the posterior nerve roots are much more prominently depleted of myelinated fibers (G) compared to the anterior nerve roots. (H) In the posterior horns, there are frequent, variably large axonal spheroids (green arrow, H&E-stained section), but no apparent Lewy body or tau pathology (not shown). (I) Lewy bodies are particularly numerous in the less atrophic medial part of the substantia nigra, (J) in the CA2 region of the hippocampus and (K) across the deep layers of all the neocortical regions (I and J immunostained for α-synuclein; K immunostained for p62; positive inclusions in K are highlighted with blue arrow). (L) Occasional isolated neuropil threads and (M)very rare tangles are seen in the medial temporal lobe. Scale bar: 300µm in A; 100µm in B, C, D, F, G, H, I, J, L and M; 2.5mm in E; 550µm in K.

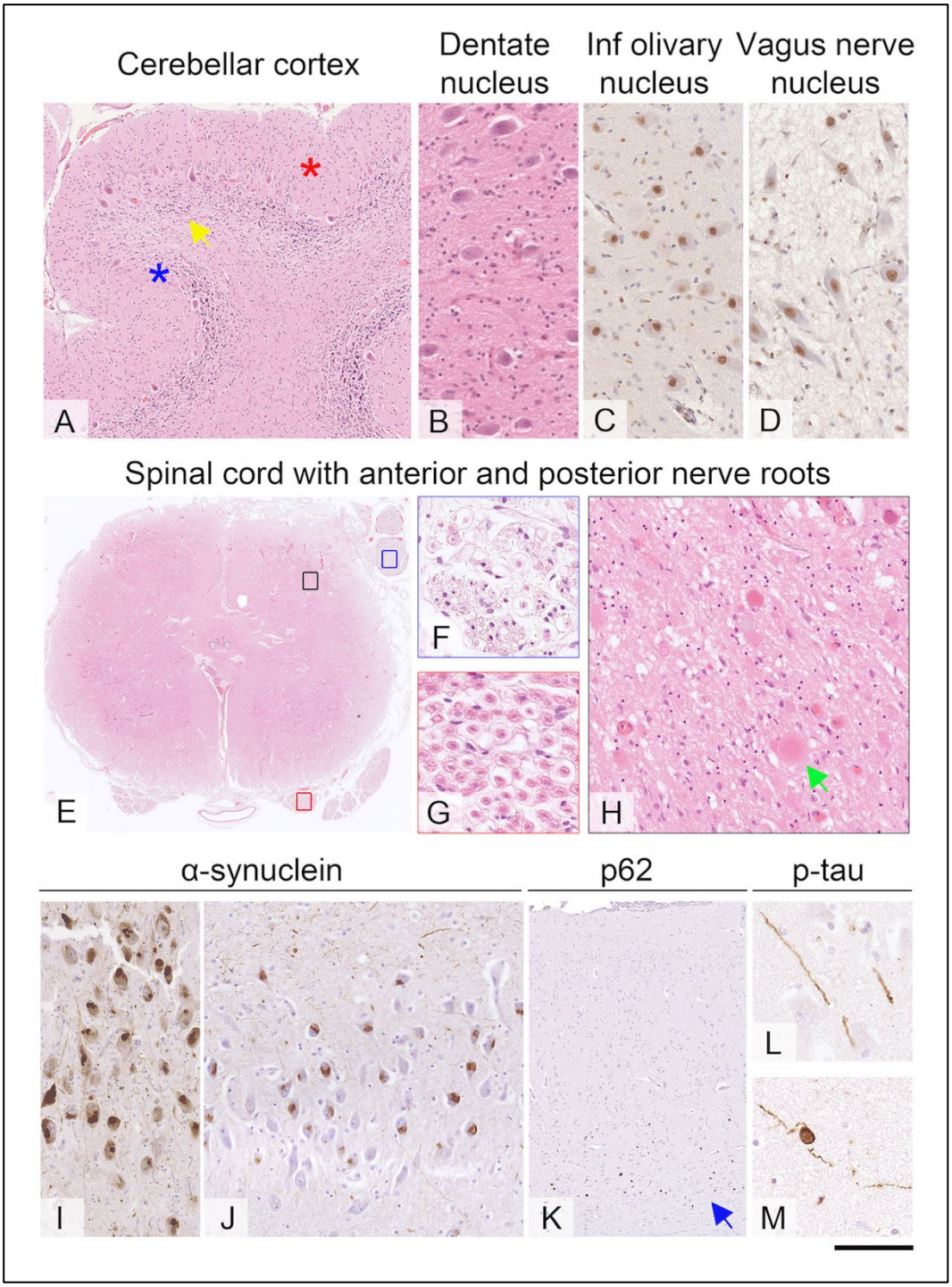
Cerebellar cortex
Dentate nucleus
Inf olivary nucleus
Vagus nerve nucleus
A
B
C
D
Spinal cord with anterior and posterior nerve roots
E
F
G
H
α-synuclein
p62
p-tau
I
J
K
L
M

5. Discussion

This study provided an in-depth phenotypic and genotypic characterization of the largest cohort of *PLA2G6*-related parkinsonism hitherto reported, including 14 new cases. Distinct aspects of this phenotype and corresponding genotypic findings which emerged from this overview are discussed below.

Clinical onset

Although the *age of symptom onset* ranged between the first and the seventh decade, the large majority of cases manifested in the late second and third decades of life. Patients with an earlier onset[190, 194, 236] showed some overlapping clinico-radiological features with previous cases of ANAD but lacked the typical rapid deterioration in late childhood,[187] and instead manifested slower progression of symptoms with parkinsonism from the second decade of life, which supports the notion of PLAN phenotypes as a phenotypic continuum.[194, 197] *Psychiatric features*, including severe depression and/or anxiety and behavioral/personality changes (ranging from withdrawal and apathy to psychosis and aggressiveness), were frequently observed early in the disease course. Psychiatric issues often preceded extrapyramidal manifestations and were the only symptoms at onset in one fifths of the cohort.[192, 198, 205, 209, 210, 224, 239, 240] This evidence should warn clinicians against misdiagnosis of purely psychiatric disorders and the initiation of consistent treatments (i.e., antipsychotics) which can be highly detrimental in the context of an – at least preclinical – extrapyramidal involvement.[209] Interestingly, onset or rapid deterioration of symptoms in *PLA2G6*-related parkinsonism occurred during pregnancy/postpartum (Cases 2-3-11)[210] or in vitro fertilization (Case 1) in five cases. This is in keeping with previous observations of likely hormone-related symptom deterioration during pregnancy and, most often, the peri- and postmenopausal period in idiopathic Parkinson's disease.[246] These observations along with the aforementioned age of onset and high prevalence of psychiatric manifestations suggest that the female population with *PLA2G6*-parkinsonism can be at risk to be misdiagnosed as having pregnancy- or postpartum-related

psychiatric morbidity, autoimmune encephalitis, or functional motor disorders in the early stages of disease.

Motor symptoms

Parkinsonism manifested as an asymmetric akinetic-rigid syndrome, with or without tremor at rest, in the majority of cases. In only few patients parkinsonism was isolated, thus resembling idiopathic Parkinson's disease except for the age of onset.[191, 234] Parkinsonism frequently showed dramatic, albeit unsustained, response to levodopa. Levodopa efficacy was most often limited by the occurrence of severe *levodopa-induced dyskinesias*, as well as exacerbation of psychiatric symptoms usually few weeks/months after treatment initiation, even on small doses (≤300mg/day). I therefore suggest that early-onset levodopa-induced dyskinesias is a tell-tale sign and, in the context of other clinico-radiological "red flags" here discussed, essentially limit the differential diagnosis of *PLA2G6*-related parkinsonism to Kufor-Rakeb syndrome mainly. Five patients underwent bilateral DBS (STN or GPi) with reported good to excellent outcome,[234, 235, 237] thus making DBS a potential treatment option in early stages of disease, especially in cases with intractable complications of levodopa therapy. *Dystonia* was the second most frequent additional motor feature in *PLA2G6*-related parkinsonism after pyramidal signs. Interestingly, isolated foot dragging was reported as the first extrapyramidal feature in nearly 10% of cases,[15, 204, 220, 225] thus suggesting *PRKN*-related parkinsonism in the first instance.[247] I also noticed a high prevalence of extensor truncal dystonia in our cases and previous literature, thus confirming dystonic opisthotonus as a hint for clinicians to suspect the historically so-called NBIA syndromes. Oculogyric crises were observed in five cases,[192, 210, 238] thus expanding the spectrum of disorders encompassing these paroxysmal dystonic manifestations in their clinical picture.[248, 249] Finally, the prevalence of oromandibular dystonia seemed lower than observed in PKAN,[249] and the presence of facial grimacing or jaw dystonia, at least in our cases, was mainly secondary to levodopa treatment initiation. While the presence of *pyramidal features* is not particularly diriment in the context of early-onset parkinsonian, pallidopyramidal or NBIA syndromes, the

detection of (even subtle) *cerebellar signs* could strongly point towards *PLA2G6*. Finally, I found a high prevalence of *myoclonus* few years into the disease course. Myoclonus was poorly characterized in previous reports, but I first proved its cortical origin on neurophysiology in one of our cases (Case 2).

Non-motor symptoms

Information on non-motor symptoms commonly associated with idiopathic Parkinson's disease (e.g., anosmia, constipation, RBD, orthostatic hypotension, sexual dysfunction) were most often scarce or missing in previous reports on *PLA2G6*-parkinsonism. Interestingly, none of our 12 patients reported *anosmia* as prodromal symptom. In addition, half of patients reporting hallucinations experienced auditory hallucinations either alone or associated with *visual hallucinations* throughout the follow-up period, and we speculated that this might be due to a different pattern of Lewy pathology progression compared to idiopathic Parkinson's disease. In addition to the high prevalence of *psychiatric comorbidity*, *cognitive impairment* was described as being often present early in the disease course. However, formal neuropsychometry was limited to the MMSE in most reports. *Urinary dysfunction*, mainly consisting in bladder overactivity, was the most well recognized autonomic feature in *PLA2G6*-parkinsonism. *Sleep disturbances* were reported in 10 cases, but most of them lacked polysomnography. Two patients in our new series underwent a sleep study few years into the disease course, one showing periodic limb movements and prolonged REM phase (Case 1) and the other showing sleep apnea only (Case 8). Isolated generalized tonic-clonic *seizures* were reported in only four cases some years into the disease course, thus suggesting that epilepsy is not a major feature of late-onset PLAN, even in advanced stages.

Neuroradiological findings

Mild to marked *cerebellar atrophy* was detected in above 40% of all brain MRI, either alone or as part of *global brain volume loss*. Although this neuroimaging finding is a hallmark of INAD/ANAD,[250] its frequency in late-onset PLAN was not equally highlighted in previous literature. Genetic ablation of *PLA2G6* in mice ($iPLA_2\beta^{-/-}$) was documented to cause cerebellar atrophy, with loss of Purkinje cells, reactive astrogliosis, microglia activation, and up-regulation of the proinflammatory cytokines. I speculate that the less frequent and, in most cases, less severe, grade of cerebellar atrophy in late-onset PLAN reflects a higher level of residual activity of $iPLA_2\beta$. In addition, this could correlate with the disease duration, given that I documented the presence of cerebellar atrophy on follow-up MRI in three cases in which it was not present on early MRI. *Iron deposition* was found in around 28% of the whole cohort and, interestingly, was often not documented even on dedicated MRI sequences (T2*/SWI). This observation claims for an extensive revision of the nomenclature of the historically so-called NBIA syndromes. When available, *dopamine imaging* invariably documented signs of nigrostriatal degeneration. It is noteworthy that in one patient, ^{11}C- RAC-PET for postsynaptic receptor function revealed increased RAC uptake in the putamen more than in the caudate, thus indicating a largely presynaptic dopaminergic abnormality as seen in idiopathic Parkinson's disease.[205]

Genetic and functional aspects

The crystal structure of $iPLA_2\beta$, reported in 2018, revealed a dimeric holoprotein complex in which the active site of each subunit is proposed to adopt an open conformation for phospholipids to access the catalytic regions in the absence of membrane interaction. The dimer consists of catalytic domains, which firmly interact through an extensive interface, and ankyrin domains, which are oriented outwards from the catalytic core and anchor the protein to the membrane in its inactive state.[181] Pathogenic mutations in *PLA2G6* which are associated with different PLAN phenotypes are spread throughout all protein domains, and may therefore impair iPLA2β function through a spectrum of loss-of-function mechanisms, affecting either $iPLA_2\beta$ enzymatic activity, its regulation, or its

interactions at the macromolecular level. Our review documents that the large majority of mutations hitherto linked to *PLA2G6*-parkinsonism are non-truncating, and therefore more likely to result in less detrimental effects compared to truncating variants, which are found more frequently in INAD/ANAD cases. As previously suggested, different mutation sites in the domains of iPLA2β can lead, directly or indirectly, to different changes in its enzymatic activity, which might be a critical factor in the phenotypic heterogeneity of PLAN.[251] This is supported by the previous observation that all individuals with two null alleles manifest with INAD, while most patients with ANAD or late-onset phenotypes carry two missense *PLA2G6* mutations.[250] In addition, this is consistent with scarce biochemical and enzymatic studies on *PLA2G6* mutations available. Engel et al.[251] demonstrated *in vitro* that mutations associated with different *PLA2G6* phenotypes have different impact on its catalytic activity. Mutations associated with INAD/NBIA cause loss of enzyme activity, with mutant proteins exhibiting less than 20% of wild-type enzymatic activity in both lysophospholipase and phospholipase assays. In contrast, three mutations associated with dystonia-parkinsonism (c.1894C>T, c.2222G>A, c.2239C>T) do not impair phospholipase nor lysophospholipase catalytic activity.[251] Shi et al.[225] documented that the *PLA2G6* variant c.991G>T is associated with approximately 30% residual protein activity compared to the wild-type iPLA2β.[225] Finally, Zhou et al.[185] found defective activation of endogenous store-operated Ca^{2+} and iPLA2β activation in cells from patient with familial Parkinson's disease carrying the c.2239C>T mutation in *PLA2G6*.[185] Functional studies of the tertiary and quaternary structure of the mutant iPLA2β as well as its residual enzymatic activity and defective regulation are needed to further explore the aforementioned phenotype-genotype correlations.

I acknowledge some limitations of this review mainly due to its retrospective nature. Among others, frequencies of predefined clinico-radiological variables were calculated as valid percentages, and this - as well as any alternative imputation - is not exempt from risk of under- and overestimation of their prevalence. In addition, information on the natural history of disease was limited by the lack of a precise timeline for the onset of different symptoms/signs in the majority of published

cases, which mainly reported on the clinico-radiological picture at onset/diagnosis and missed follow-up assessments. Nevertheless, based on this systematic review, I am confident this is the most comprehensive analysis of the largest population with *PLA2G6*-related parkinsonism hitherto reported.

In conclusion, homozygous or compound heterozygous mutations in *PLA2G6* cause a distinct early-onset parkinsonism with various combinations of dystonia, pyramidal and cerebellar signs, myoclonus, and early cognitive decline. Psychiatric manifestations are often present, being isolated presenting symptoms in one fifth of cases. Early signs of bladder overactivity are also frequently reported. Against this background, irrespective of whether iron deposition is present on brain MRI, the detection of cerebellar atrophy points towards *PLA2G6* among other genetic causes of early-onset parkinsonian, pallidopyramidal and NBIA syndromes. Early occurrence of severe levodopa-induced dyskinesias with low doses represents a tell-tale sign. The prompt recognition of patients with these clinico-radiological features should prompt *PLA2G6* mutation analysis, even in the absence of parental consanguinity or a positive family history. This should also prevent clinicians from initiating treatments (antipsychotic medications) which are detrimental in the context of an - at least prospective – extrapyramidal involvement. In addition, it should make neurologists cautious in titrating levodopa in these patients. Finally, it might have considerable therapeutic implications in the near future, given the promising preclinical development of disease-modifying strategies.[201]

Chapter VI

Final remarks and future directions

The present thesis summarizes the 18-month clinical and research experience of the PhD candidate in a hub center for the diagnosis and treatment of movement disorders (National Hospital for Neurology and Neurosurgery) and its neurogenetic research laboratory (UCL Queen Square Institute of Neurology) in the United Kingdom. Over this period, the PhD candidate had the opportunity to deepen her clinical knowledge in movement disorders and to be initiated to wet lab activities and analytical skills to explore the genetic underpinnings of movement disorders and neurodegeneration. She had an active role in clinicogenetic correlations.

This PhD split between "deep phenotyping" and genetics of complex movement disorders has taken forward detailed clinical data from a large cohort of patients with combined and complex dystonia phenotypes, including neurodegeneration with brain iron accumulation (NBIA) syndromes, and explored their genetic underpinnings through next-generation sequencing (NGS) techniques, i.e. whole-exome (WES) and whole-genome sequencing (WGS), and ancillary tests (e.g., Sanger sequencing, homozygosity mapping and, in few cases, functional tests). It has investigated the role of variants in genes associated with dystonia and, more broadly, neurodegeneration in previously unexplored cohorts of dystonia patients in order to establish genetic diagnoses in probands/families, assist genetic counselling, broaden/refine the phenotypic and genotypic spectrum of known genetic disorders, and explore new clinicogenetic correlations. It has discovered novel mutations in various genes, novel genotype-phenotype descriptions in the fields of hereditary movement disorders, and at least one possible new dystonia-related gene (ongoing validation).

Main findings from the previous chapters are summarized below.

Chapter III

In this study, I retrospectively reviewed clinical data and re-analysed exome data from a large historical cohort of patients with complex movement disorders, enriched in combined and complex dystonia phenotypes, including neurodegeneration with brain iron accumulation (NBIA) syndromes, in order to absorb the most recent updates in genetics of dystonia and bioinformatic pipelines. This study has revealed a final diagnostic yield for WES of 27.6%. Besides expanding the phenotypic and genotypic spectrum of several genetic dystonic syndromes, this study has replicated the association between the *DRD2* gene and a choreo-dystonia phenotype and identified one recently confirmed dystonia-associated gene (*TSPOAP1*) and one new candidate gene (*ENSG00000165714*), for which further research is ongoing. Further work will be required to prove pathogenicity in unclear cases, and where DNA from family members and further biomaterial from the patients was unavailable at least overexpression studies in cell or animal models would need to be performed to study functional consequences. Further variants in known and novel disease associated genes remain to be identified in the cohort. Given the limitations of the chosen approach of WES (reduced coverage for some areas of the exome increase the risk of missing disease-causing variants; insensitivity of this technique towards large deletions/insertions, repeats, copy number variants present), the unsolved cases of this cohort could be re-examined with WES and/or be submitted for WGS and CGH arrays or genotyping methods to rule out disease causing copy number variants. Finally, the exome data will be constantly re-analyzed in view of novel annotation and bioinformatic tools under development.

Chapter IV

In chapter IV, I presented preliminary findings of an ongoing study on the screening of a large cohort of patients with heterogeneous dystonia phenotypes through WGS in the context of the 100,000 UK Genomes Project. This study has been severely delayed by the COVID-19 pandemic, and only validated findings from the first 30 analyzed cases from a cohort of approximately 300 patients were herein summarized. Besides discovering new variants in a number of known dystonia-associated genes, including, among others, *ATP13A2*, *SLC2A1*, *DDC*, *TUBB4A*, I first reported on a new phenotype associated with the peroxisomal disorder alpha-methylacyl-CoA racemase deficiency, which is adult-onset generalized dystonia with prominent upper limb involvement. This new phenotype was replicated in a

second family, and genetic and functional tests overall confirmed the pathogenicity of all three novel *AMACR* variants herein reported. Overall, this evidence confirmed that peroxisomal functions might represent a new biological pathway to explore in the pathogenesis of dystonia, as previously suggested by the single case of sterol carrier protein X (SCPx) deficiency hitherto reported. Finally, I first described a peculiar paroxysmal gait pattern, herein named "criss-cross gait", associated with heterozygous variants in the *SLC2A1* gene (glucose transporter type 1 deficiency syndrome) in three unrelated cases.

Chapter V

In this chapter, I deeply characterized, both phenotypically and genotypically, *PLA2G6*-related parkinsonism in the largest cohort ever reported, highlighted clinico-radiological hints for diagnosis, and outlined its natural history. Biallelic mutations in the *PLA2G6* gene were initially recognized to cause childhood-onset neuroaxonal dystrophies and have then been linked to late-onset phenotypes, the most common being complex parkinsonism. The prompt recognition of patients with early-onset parkinsonism requiring *PLA2G6* mutation analysis may have considerable therapeutic implications in the near future, given promising preclinical disease-modifying strategy development. I described 14 unpublished cases of *PLA2G6*-related parkinsonism and examined a further 72 cases from a systematic review of PubMed® records (search terms: "PLA2G6" AND "parkins*"; time interval: 01/01/2006-18/03/2021) and their reference lists for predefined phenotypic and genotypic data. Neuropathology specimens available at the Queen Square Brain Bank were reviewed. In these 86 cases (52.3% female), belonging to 68 families, median age at onset was 23.0 years (interquartile range, IQR 11.0). Extrapyramidal disturbances (parkinsonism/dystonia), gait/balance issues, and psychiatric and/or cognitive symptoms were common presenting features. Parkinsonism started at a median age of 25.0 years (IQR 9.25). Pyramidal signs occurred in 77.2%, dystonia in 69.4%, myoclonus in 65.2% and cerebellar signs in 44.6% of cases. Loss of independent ambulation occurred after a median disease duration of 3.0 years (IQR 3.0). Early bladder overactivity was present in nearly

three-quarters of cases. Cognitive impairment was reported in 76.1% of cases and psychiatric features in 87.1%, the latter being an isolated presenting feature in 20.1%. Parkinsonism was nearly always levodopa-responsive, and frequently complicated by early severe dyskinesias. Five patients benefited from deep brain stimulation. Brain MRI findings included cerebral atrophy (49.3%), cerebellar atrophy (43.2%) and basal ganglia and/or substantia nigra iron deposition (28.1%). Presynaptic dopaminergic terminal imaging was anormal in all cases where performed. Fifty-four *PLA2G6* mutations have hitherto been associated with parkinsonism, including four novel variants herein reported. These mainly determine non-truncating changes and always spare the primary structure of functional domains of the PLA2G6 protein product, which may partly explain phenotypic differences between *PLA2G6*-related parkinsonism and childhood-onset neuroaxonal dystrophies. In five deceased patients, median disease duration was 13.0 years (IQR 14.5). Brain pathology in three cases showed mixed Lewy and tau pathology. In conclusion, biallelic mutations in *PLA2G6* cause early-onset parkinsonism associated with various combinations of dystonia, pyramidal and cerebellar signs, myoclonus, and cognitive impairment. Early psychiatric manifestations and bladder overactivity are common. Cerebro/cerebellar atrophy are frequent MRI features, whereas brain iron deposition is not. Early, severe levodopa-induced dyskinesias is a tell-tale sign.

Within its discussed restraints, in particular delays and limitations due to the COVID-19 pandemic, the 18-month period of my PhD spent at the National Hospital for Neurology and Neurosurgery and the UCL Queen Square Institute of Neurology allowed me to deepen my clinical knowledge in movement disorders, to acquire technical and analytic skills for genetic diagnostics and research, and to lay the foundations to continue my clinical and research experience at the same institutions as a postdoctoral fellow.

Publications/Book Chapters (during my PhD period only)

Articles in international peer reviewed journals (reverse chronological order)

1. Mencacci NE, Steel D, **Magrinelli F**, Hsu J, Keller Sarmiento IJ, Troncoso Schifferli M, Munoz D, Stefanis L, Lubbe SJ, Wood NW, Kurian MA, Stamelou M. Childhood-Onset Chorea Caused By A Recurrent De Novo DRD2 Variant. *Mov Disord.* 2021 (accepted in March 2021).
2. Mulroy E, Baschieri F, **Magrinelli F**, Latorre A, Cortelli P, Bhatia KP. Movement Disorders and Liver Disease. *Mov Disord Clin Pract.* 2021 May 11 (online first).
3. Currò R, Salvalaggio A, Tozza S, Gemelli C, Dominik N, Galassi Deforie V, **Magrinelli F**, [...], Houlden H, Reilly MM, Mandich P, Schenone A, Manganelli F, Briani C, Cortese A. RFC1 expansions are a common cause of idiopathic sensory neuropathy. *Brain* 2021 May 9; awab072 (online first).
4. Di Lazzaro G, **Magrinelli F**, Estevez-Fraga C, Valente EM, Pisani A, Bhatia KP. X-linked parkinsonism: phenotypic and genetic heterogeneity. *Mov Disord.* 2021 May 7 (online first).
5. Estevez-Fraga C, **Magrinelli F**, Hensman Moss D, Mulroy E, Di Lazzaro G, Latorre A, Mackenzie M, Houlden H, Tabrizi SJ, Bhatia KP. Expanding the Spectrum of Movement Disorders Associated With C9orf72 Hexanucleotide Expansions. *Neurol Genet* 2021; 7:e575.
6. Mulroy E, Ilinca A, Gonzalez-Robles C, **Magrinelli F**, Puschmann A, Bhatia KP. Throat-clearing vocalisations in primary brain calcification syndromes. *Parkinsonism Relat Disord*. 2021; 8:627-630.
7. **Magrinelli F**, Balint B, Bhatia KP. Challenges in Clinicogenetic Correlations. One gene - Many phenotypes. *Mov Disord Clin Pract.* 2021; 8:299-310.
8. Mulroy E, **Magrinelli F**, Mohd Fauzi NA, Koya Kutty S, Latorre A, Bhatia KP. Paroxysmal, exercise-induced, diurnally fluctuating dystonia: expanding the phenotype of SPG8. *Parkinsonism Relat Disord*. 2021; 85:26-28.

9. Koya Kutty S, Mulroy E, **Magrinelli F**, Di Lazzaro G, Latorre A, Bhatia KP. Huntington disease-like phenotype in a patient with ANO3 mutations. *Parkinsonism Relat Disord*. 2021; S1353-8020(21)00071-7.
10. Koya Kutty S, Di Lazzaro G, **Magrinelli F**, Mulroy E, Latorre A, Bhatia KP. Late-onset chorea in JAK2-associated essential thrombocythemia. *Mov Disord Clin Pract.* 2020; 8:145-148.
11. Di Lazzaro G*, **Magrinelli F***, Ganos C, Bhatia KP. The need to tic. *Mov Disord Clin Pract.* 2020; 7:863-864. **[* Co-first authorship, order not changed]**
12. **Magrinelli F**, Tinazzi M, Bhatia KP. Toward an Early Real-Time Quaking-Induced Conversion–Based Diagnostic Biomarker for Lewy Body–Related Synucleinopathies. *Mov Disord Clin Pract.* 2020; 7:780-781.
13. Balint B, Damasio J, **Magrinelli F**, Guerreiro R, Bras J, Bhatia KP. Psychiatric manifestation of ATP13A2 mutations. *Mov Disord Clin Pract.* 2020; 7:838-841.
14. Latorre A, Rocchi L, **Magrinelli F**, Mulroy E, Berardelli A, Rothwell JC, Bhatia KP. Reply to: Cortical tremor: a tantalizing conundrum between cortex and cerebellum and Pentameric repeat expansions: cortical myoclonus or cortical tremor? *Brain* 2020 Oct 4: awaa261.
15. Belvisi D, Pellicciari R, Fabbrini A, Costanzo M, Pietracupa, De Lucia M, Modugno N, **Magrinelli F**, et al. Risk factors of Parkinson's disease: Simultaneous assessment, interactions and etiological subtypes. *Neurology* 2020; 95:e2500-e2508.
16. Boscolo-Galazzo I*, **Magrinelli F***, Pizzini FB, Storti SF, Agosta F, Filippi M, Marotta A, Mansueto G, Menegaz G, Tinazzi M. Voxel-based morphometry and task functional magnetic resonance imaging in essential tremor: evidence for a disrupted brain network. *Scientific Reports* 2020; 10:15061. **[* Co-first authorship, order not changed]**
17. Estevez-Fraga C*, **Magrinelli F***, Latorre A, Cordivari C, Houlden H, Tinazzi M, Hemingway C, Tabrizi SJ, Bhatia KP. A new family with GLRB-related hyperekplexia showing chorea in homo- and heterozygous variant

carriers. *Parkinsonism Relat Disord*. 2020; 79:97-99. **[* Co-first authorship, order not changed]**

18. **Magrinelli F**, Mulroy E, Schneider S, Latorre A, Di Lazzaro G, Hennig A, Grunewald S, De Vivo D, Bhatia KP. The "criss-cross gait": A clue to glucose transporter type 1 deficiency syndrome. *Neurology* 2020; 95:500-501.
19. **Magrinelli F**, Latorre A, Balint B, Mackenzie M, Mulroy E, Stamelou M, Tinazzi M, Bhatia KP. Isolated and combined genetic tremor syndromes: a critical appraisal based on the 2018 MDS criteria. *Parkinsonism Relat Disord*. 2020; 77:121-140.
20. **Magrinelli F**, Fabrizi GM, Santoro L, Manganelli F, Zanette G, Cavallaro T, Tamburin S. Pharmacological treatment for familial amyloid polyneuropathy. *Cochrane Database of Systematic Reviews* 2020, Issue 4. Art. No.: CD012395.
21. Latorre A, Rocchi L, **Magrinelli F**, Mulroy E, Berardelli A, Rothwell JC, Bhatia KP. Unravelling the enigma of cortical tremor and other forms of cortical myoclonus. *Brain* 2020 May 17:awaa.
22. Mulroy E, Latorre A, Menozzi E, Teh PC, **Magrinelli F**, Bhatia KP. Huntington disease like 2 (HDL-2) with parkinsonism and abnormal DAT-SPECT – A novel observation. *Parkinsonism Relat Disord*. 2020; 71:46-48.
23. **Magrinelli F**, Geroin C, Squintani G, Gandolfi M, Rizzo G, Barillari M, Vattemi G, Morgante F, Tinazzi M. Upper camptocormia in Parkinson's disease: neurophysiological and imaging findings of both central and peripheral pathophysiological mechanisms. *Parkinsonism Relat Disord*. 2020; 71:28-34.
24. Mulroy E, Latorre A, **Magrinelli F**, Bhatia KP. Ciliary dysfunction: the hairy explanation of normal pressure hydrocephalus? *Mov Disord Clin Pract.* 2020; 7:30-31.
25. Gandolfi M, Tinazzi M, **Magrinelli F**, Busselli G, Dimitrova E, Polo N, Manganotti P, Fasano A, Smania N, Geroin C. Four-week trunk-specific exercise program decreases forward trunk flexion in Parkinson's disease: a single-blinded, randomized controlled trial. *Parkinsonism Relat Disord*. 2019; 64:268-274.

26. **Magrinelli F**, Bacchin R, Tinazzi M, Gambarin M. Twelve-year follow-up of a large Italian family with atypical phenotypes of DYT1-dystonia. *Mov Disord Clin Pract.* 2018; Mov Disord Clin Pract. 2018; 6:166-170.
27. Erro R, Bacchin R, **Magrinelli F**, Tomei P, Geroin C, Squintani G, Lupo A, Zaza G, Tinazzi M. Tremor induced by Calcineurin inhibitor immunosuppression: a single-centre observational study in kidney transplanted patients. *J Neurol.* 2018; 265:1676-1683.
28. Fabrizi GM, Tamburin S, Cavallaro T, Cabrini I, Ferrarini M, Taioli F, **Magrinelli F**, Zanette G. The spectrum of Charcot-Marie-Tooth disease due to myelin protein zero: an electrodiagnostic, nerve ultrasound and histological study. *Clinical Neurophysiol.* 2018; 129:21-32.

Book chapter

1. Tinazzi M, **Magrinelli F**, Baldacci F, Bonuccelli U. Capitolo 5: Dolore neuropatico e nevralgie. In: Manuale di Neurologia Clinica. Eds: Idelson Gnocchi 1908 (in press).

Acknowledgements

I would like to thank my supervisor Professor Michele Tinazzi for teaching me to always think big and forward, and for encouraging my wish to turn an immature passion for movement disorders and neurogenetics into an expertise. This implied spending the majority of my PhD abroad, which would not have been possible without his open-mindedness and constant support.

I am most grateful to my mentor Professor Kailash Bhatia for his enthusiastic and illuminating clinical supervision and support, for sharing and inciting brilliant research ideas, and for introducing me to his amazing networking. I will always be proud to be a "KB's fellow".

I am indebted to Professor Henry Houlden for his excellent supervision and unconditional support, laboratory environment and patient mentorship. I look forward to working hard on our ongoing and future lab projects.

Special thanks to Dr Anna Latorre, Dr Giulia Di Lazzaro, Dr Anna Vera Milner, Dr Eoin Mulroy, and Dr Carlos Estevez-Fraga for being the most wonderful clinical collaborators, adventure mates, and friends.

Special thanks also to my marvellous lab collaborators Dr Stephanie Efthymiou, Dr Sarah Wiethoff, Dr Niccolo Mencacci, Dr Andrea Cortese, Natalia Dominik, Dr Elisa Cali, Clarissa Rocca, Alice Gennari, Dr Rauan Kaiyrzhanov, Dr Reza Maroofian, Valentina Galassi Deforie, Alkyoni Athanasiou-Fragkouli, Dr Benjamin O'Callaghan, Dr Arianna Tucci, Hallgeir Jonvik, David Murphy, Dr Jana Vandrovcova, Prasanth Sivakumar, Mark Gaskin, for introducing me to neurogenetics, bioinformatics, and wet lab activities and for never leaving me alone in my evolution by trial and error.

Thanks to our patients and their families for providing their time, patience, and material as well as to our external collaborators around the world who contributed with excellent clinical cases.

I would like to thank the *European Commission for Erasmus+ projects*, the *European Academy of Neurology*, Mrs Emma Gianesini, and *UniCredit Foundation* for providing the financial support behind my fellowship in the UK.

I am endlessly grateful to my parents, who gave me wings and roots without which I would not be both a global citizen and my most authentic self wherever I am in the world, and to my sweet and strong sister Eleonora for always being on my side.

This thesis is dedicated to my beloved family, to all patients suffering from rare neurogenetic conditions I have met on my path and, in loving memory, to Prof. Giovanna Barozzi.

Bibliography

1. Magrinelli F, Balint B, Bhatia KP. Challenges in Clinicogenetic Correlations: One Gene - Many Phenotypes. Mov Disord Clin Pract 2021;8:299-310.
2. Strachan T, Goodship J, Chinnery P. Genetics and genomics in medicine. New York; London: GS, Garland Science, 2015.
3. Abdo WF, van de Warrenburg BP, Burn DJ, Quinn NP, Bloem BR. The clinical approach to movement disorders. Nat Rev Neurol 2010;6:29-37.
4. Fahn S, Jankovic J. Principles and practice of movement disorders. Philadelphia: Saunders, 2011.
5. Fahn S. Classification of movement disorders. Mov Disord 2011;26:947-957.
6. Donaldson IM. Marsden's book of movement disorders. Oxford: Oxford University Press, 2012.
7. Ganos C, Neumann WJ, Muller-Vahl KR, et al. The Phenomenon of Exquisite Motor Control in Tic Disorders and its Pathophysiological Implications. Mov Disord 2021.
8. Gusella JF, Wexler NS, Conneally PM, et al. A polymorphic DNA marker genetically linked to Huntington's disease. Nature 1983;306:234-238.
9. MacDonald ME, Ambrose CM, Duyao MP, et al. A novel gene containing a trinucleotide repeat that is expanded and unstable on Huntington's disease chromosomes. The Huntington's Disease Collaborative Research Group. Cell 1993;72:971-983.
10. Bull PC, Thomas GR, Rommens JM, Forbes JR, Cox DW. The Wilson disease gene is a putative copper transporting P-type ATPase similar to the Menkes gene. Nat Genet 1993;5:327-337.
11. Ezquerra M, Compta Y, Marti MJ. Identifying the genetic components underlying the pathophysiology of movement disorders. Appl Clin Genet 2011;4:81-92.
12. Paisan-Ruiz C, Jain S, Evans EW, et al. Cloning of the gene containing mutations that cause PARK8-linked Parkinson's disease. Neuron 2004;44:595-600.
13. Paisan-Ruiz C, Saenz A, Lopez de Munain A, et al. Familial Parkinson's disease: clinical and genetic analysis of four Basque families. Ann Neurol 2005;57:365-372.
14. Hartig MB, Iuso A, Haack T, et al. Absence of an orphan mitochondrial protein, c19orf12, causes a distinct clinical subtype of neurodegeneration with brain iron accumulation. Am J Hum Genet 2011;89:543-550.
15. Paisan-Ruiz C, Bhatia KP, Li A, et al. Characterization of PLA2G6 as a locus for dystonia-parkinsonism. Ann Neurol 2009;65:19-23.
16. Ramirez A, Heimbach A, Grundemann J, et al. Hereditary parkinsonism with dementia is caused by mutations in ATP13A2, encoding a lysosomal type 5 P-type ATPase. Nat Genet 2006;38:1184-1191.

17. Bonifati V, Rizzu P, van Baren MJ, et al. Mutations in the DJ-1 gene associated with autosomal recessive early-onset parkinsonism. Science 2003;299:256-259.
18. Ezquerra M, Pastor P, Gaig C, et al. Different MAPT haplotypes are associated with Parkinson's disease and progressive supranuclear palsy. Neurobiol Aging 2011;32:547 e511-546.
19. Shojaee S, Sina F, Banihosseini SS, et al. Genome-wide linkage analysis of a Parkinsonian-pyramidal syndrome pedigree by 500 K SNP arrays. Am J Hum Genet 2008;82:1375-1384.
20. Nalls MA, Blauwendraat C, Vallerga CL, et al. Identification of novel risk loci, causal insights, and heritable risk for Parkinson's disease: a meta-analysis of genome-wide association studies. Lancet Neurol 2019;18:1091-1102.
21. Genetic Modifiers of Huntington's Disease C. Identification of Genetic Factors that Modify Clinical Onset of Huntington's Disease. Cell 2015;162:516-526.
22. Krebs CE, Paisan-Ruiz C. The use of next-generation sequencing in movement disorders. Front Genet 2012;3:75.
23. Olgiati S, Quadri M, Bonifati V. Genetics of movement disorders in the next-generation sequencing era. Mov Disord 2016;31:458-470.
24. Levy SE, Myers RM. Advancements in Next-Generation Sequencing. Annu Rev Genomics Hum Genet 2016;17:95-115.
25. Marras C, Lang A, van de Warrenburg BP, et al. Nomenclature of genetic movement disorders: Recommendations of the international Parkinson and movement disorder society task force. Mov Disord 2016;31:436-457.
26. Gannamani R, van der Veen S, van Egmond M, de Koning TJ, Tijssen MAJ. Challenges in Clinicogenetic Correlations: One Phenotype - Many Genes. Mov Disord Clin Pract 2021;8:311-321.
27. Mantere T, Kersten S, Hoischen A. Long-Read Sequencing Emerging in Medical Genetics. Frontiers in genetics 2019;10:426.
28. Midha MK, Wu M, Chiu KP. Long-read sequencing in deciphering human genetics to a greater depth. Hum Genet 2019;138:1201-1215.
29. Amarasinghe SL, Su S, Dong X, Zappia L, Ritchie ME, Gouil Q. Opportunities and challenges in long-read sequencing data analysis. Genome Biol 2020;21:30.
30. Logsdon GA, Vollger MR, Eichler EE. Long-read human genome sequencing and its applications. Nat Rev Genet 2020;21:597-614.
31. Bragg DC, Mangkalaphiban K, Vaine CA, et al. Disease onset in X-linked dystonia-parkinsonism correlates with expansion of a hexameric repeat within an SVA retrotransposon in

TAF1. Proceedings of the National Academy of Sciences of the United States of America 2017;114:E11020-E11028.
32. Westenberger A, Reyes CJ, Saranza G, et al. A hexanucleotide repeat modifies expressivity of X-linked dystonia parkinsonism. Ann Neurol 2019;85:812-822.
33. Ishiura H, Doi K, Mitsui J, et al. Expansions of intronic TTTCA and TTTTA repeats in benign adult familial myoclonic epilepsy. Nat Genet 2018;50:581-590.

34. Corbett MA, Kroes T, Veneziano L, et al. Intronic ATTTC repeat expansions in STARD7 in familial adult myoclonic epilepsy linked to chromosome 2. Nat Commun 2019;10:4920.
35. Florian RT, Kraft F, Leitao E, et al. Unstable TTTTA/TTTCA expansions in MARCH6 are associated with Familial Adult Myoclonic Epilepsy type 3. Nat Commun 2019;10:4919.
36. Yeetong P, Pongpanich M, Srichomthong C, et al. TTTCA repeat insertions in an intron of YEATS2 in benign adult familial myoclonic epilepsy type 4. Brain 2019;142:3360-3366.
37. Sone J, Mitsuhashi S, Fujita A, et al. Long-read sequencing identifies GGC repeat expansions in NOTCH2NLC associated with neuronal intranuclear inclusion disease. Nature genetics 2019;51:1215-1221.
38. Seaby EG, Pengelly RJ, Ennis S. Exome sequencing explained: a practical guide to its clinical application. Brief Funct Genomics 2016;15:374-384.
39. Jalali Sefid Dashti M, Gamieldien J. A practical guide to filtering and prioritizing genetic variants. Biotechniques 2017;62:18-30.
40. Carson AR, Smith EN, Matsui H, et al. Effective filtering strategies to improve data quality from population-based whole exome sequencing studies. BMC Bioinformatics 2014;15:125.
41. Efthymiou S, Manole A, Houlden H. Next-generation sequencing in neuromuscular diseases. Curr Opin Neurol 2016;29:527-536.
42. Tanaka N, Takahara A, Hagio T, et al. Sequencing artifacts derived from a library preparation method using enzymatic fragmentation. PLoS One 2020;15:e0227427.
43. Mencacci NE, Carecchio M. Recent advances in genetics of chorea. Curr Opin Neurol 2016;29:486-495.
44. Erro R, Bhatia KP. Unravelling of the paroxysmal dyskinesias. J Neurol Neurosurg Psychiatry 2019;90:227-234.
45. Balint B, Thomas R. Hereditary Hyperekplexia Overview. In: Adam MP, Ardinger HH, Pagon RA, et al., eds. GeneReviews((R)). Seattle (WA)1993.
46. Richards S, Aziz N, Bale S, et al. Standards and guidelines for the interpretation of sequence variants: a joint consensus recommendation of the American College of Medical Genetics and Genomics and the Association for Molecular Pathology. Genet Med 2015;17:405-424.
47. Robinson PN. Deep phenotyping for precision medicine. Human mutation 2012;33:777-780.
48. Albanese A, Bhatia K, Bressman SB, et al. Phenomenology and classification of dystonia: a consensus update. Mov Disord 2013;28:863-873.
49. Balint B, Mencacci NE, Valente EM, et al. Dystonia. Nat Rev Dis Primers 2018;4:25.
50. Albanese A, Di Giovanni M, Lalli S. Dystonia: diagnosis and management. Eur J Neurol 2019;26:5-17.
51. Grutz K, Klein C. Dystonia updates: definition, nomenclature, clinical classification, and etiology. J Neural Transm (Vienna) 2021;128:395-404.

52. Domingo A, Yadav R, Ozelius LJ. Isolated dystonia: clinical and genetic updates. J Neural Transm (Vienna) 2021;128:405-416.
53. Weissbach A, Saranza G, Domingo A. Combined dystonias: clinical and genetic updates. J Neural Transm (Vienna) 2021;128:417-429.
54. Magrinelli F, Mulroy E, Schneider SA, et al. Criss-cross gait: A clue to glucose transporter type 1 deficiency syndrome. Neurology 2020;95:500-501.
55. Magrinelli F, Latorre A, Balint B, et al. Isolated and combined genetic tremor syndromes: a critical appraisal based on the 2018 MDS criteria. Parkinsonism Relat Disord 2020;77:121-140.
56. Kaji R, Bhatia K, Graybiel AM. Pathogenesis of dystonia: is it of cerebellar or basal ganglia origin? J Neurol Neurosurg Psychiatry 2018;89:488-492.
57. Breakefield XO, Blood AJ, Li Y, Hallett M, Hanson PI, Standaert DG. The pathophysiological basis of dystonias. Nat Rev Neurosci 2008;9:222-234.
58. Ichinose H, Ohye T, Takahashi E, et al. Hereditary progressive dystonia with marked diurnal fluctuation caused by mutations in the GTP cyclohydrolase I gene. Nat Genet 1994;8:236-242.
59. Ozelius LJ, Hewett JW, Page CE, et al. The early-onset torsion dystonia gene (DYT1) encodes an ATP-binding protein. Nat Genet 1997;17:40-48.
60. Lungu C, Ozelius L, Standaert D, et al. Defining research priorities in dystonia. Neurology 2020;94:526-537.
61. Charlesworth G, Bhatia KP, Wood NW. The genetics of dystonia: new twists in an old tale. Brain 2013;136:2017-2037.
62. Balint B, Bhatia KP. Isolated and combined dystonia syndromes - an update on new genes and their phenotypes. Eur J Neurol 2015;22:610-617.
63. Lohmann K, Klein C. Update on the Genetics of Dystonia. Curr Neurol Neurosci Rep 2017;17:26.
64. Gonzalez-Latapi P, Marotta N, Mencacci NE. Emerging and converging molecular mechanisms in dystonia. J Neural Transm (Vienna) 2021;128:483-498.
65. Houlden H, Schneider SA, Paudel R, et al. THAP1 mutations (DYT6) are an additional cause of early-onset dystonia. Neurology 2010;74:846-850.
66. Jinnah HA, Berardelli A, Comella C, et al. The focal dystonias: current views and challenges for future research. Mov Disord 2013;28:926-943.
67. Jankovic J, Leder S, Warner D, Schwartz K. Cervical dystonia: clinical findings and associated movement disorders. Neurology 1991;41:1088-1091.
68. Defazio G, Martino D, Aniello MS, et al. A family study on primary blepharospasm. J Neurol Neurosurg Psychiatry 2006;77:252-254.
69. Peckham EL, Lopez G, Shamim EA, et al. Clinical features of patients with blepharospasm: a report of 240 patients. Eur J Neurol 2011;18:382-386.
70. Jinnah HA, Sun YV. Dystonia genes and their biological pathways. Neurobiol Dis 2019;129:159-168.
71. Wijemanne S, Jankovic J. Dopa-responsive dystonia--clinical and genetic heterogeneity. Nat Rev Neurol 2015;11:414-424.
72. Ludecke B, Dworniczak B, Bartholome K. A point mutation in the tyrosine hydroxylase gene associated with Segawa's syndrome. Hum Genet 1995;95:123-125.

73. Bonafe L, Thony B, Penzien JM, Czarnecki B, Blau N. Mutations in the sepiapterin reductase gene cause a novel tetrahydrobiopterin-dependent monoamine-neurotransmitter deficiency without hyperphenylalaninemia. Am J Hum Genet 2001;69:269-277.
74. Leuzzi V, Carducci CA, Carducci CL, et al. Phenotypic variability, neurological outcome and genetics background of 6-pyruvoyl-tetrahydropterin synthase deficiency. Clin Genet 2010;77:249-257.
75. Wassenberg T, Molero-Luis M, Jeltsch K, et al. Consensus guideline for the diagnosis and treatment of aromatic l-amino acid decarboxylase (AADC) deficiency. Orphanet J Rare Dis 2017;12:12.
76. Rilstone JJ, Alkhater RA, Minassian BA. Brain dopamine-serotonin vesicular transport disease and its treatment. N Engl J Med 2013;368:543-550.
77. Kurian MA, Zhen J, Cheng SY, et al. Homozygous loss-of-function mutations in the gene encoding the dopamine transporter are associated with infantile parkinsonism-dystonia. J Clin Invest 2009;119:1595-1603.
78. Carbon M, Niethammer M, Peng S, et al. Abnormal striatal and thalamic dopamine neurotransmission: Genotype-related features of dystonia. Neurology 2009;72:2097-2103.
79. Meyer E, Carss KJ, Rankin J, et al. Mutations in the histone methyltransferase gene KMT2B cause complex early-onset dystonia. Nat Genet 2017;49:223-237.
80. Deutschlander AB, Wszolek ZK. Dyt-Gnal. In: Adam MP, Ardinger HH, Pagon RA, et al., eds. GeneReviews((R)). Seattle (WA)1993.
81. Carapito R, Paul N, Untrau M, et al. A de novo ADCY5 mutation causes early-onset autosomal dominant chorea and dystonia. Mov Disord 2015;30:423-427.
82. Mencacci NE, Rubio-Agusti I, Zdebik A, et al. A missense mutation in KCTD17 causes autosomal dominant myoclonus-dystonia. Am J Hum Genet 2015;96:938-947.
83. Mencacci NE, Bruggemann N. KCTD17 is a confirmed new gene for dystonia, but is it responsible for SGCE-negative myoclonus-dystonia? Parkinsonism Relat Disord 2019;61:1-3.
84. Charlesworth G, Angelova PR, Bartolome-Robledo F, et al. Mutations in HPCA cause autosomal-recessive primary isolated dystonia. Am J Hum Genet 2015;96:657-665.
85. Balint B, Charlesworth G, Erro R, Wood NW, Bhatia KP. Delineating the phenotype of autosomal-recessive HPCA mutations: Not only isolated dystonia! Mov Disord 2019;34:589-592.
86. Gardiner AR, Bhatia KP, Stamelou M, et al. PRRT2 gene mutations: from paroxysmal dyskinesia to episodic ataxia and hemiplegic migraine. Neurology 2012;79:2115-2121.
87. Coleman J, Jouannot O, Ramakrishnan SK, et al. PRRT2 Regulates Synaptic Fusion by Directly Modulating SNARE Complex Assembly. Cell Rep 2018;22:820-831.

88. Valente P, Castroflorio E, Rossi P, et al. PRRT2 Is a Key Component of the Ca(2+)-Dependent Neurotransmitter Release Machinery. Cell Rep 2016;15:117-131.
89. Fruscione F, Valente P, Sterlini B, et al. PRRT2 controls neuronal excitability by negatively modulating Na+ channel 1.2/1.6 activity. Brain 2018;141:1000-1016.
90. Zhang G, Gibson RA, McDonald M, et al. A Gain-of-Function Mutation in KCNMA1 Causes Dystonia Spells Controlled With Stimulant Therapy. Mov Disord 2020;35:1868-1873.
91. Gardiner AR, Jaffer F, Dale RC, et al. The clinical and genetic heterogeneity of paroxysmal dyskinesias. Brain 2015;138:3567-3580.
92. Sadnicka A, Hoffland BS, Bhatia KP, van de Warrenburg BP, Edwards MJ. The cerebellum in dystonia - help or hindrance? Clin Neurophysiol 2012;123:65-70.
93. Finsterer J. Leigh and Leigh-like syndrome in children and adults. Pediatr Neurol 2008;39:223-235.
94. Lake NJ, Compton AG, Rahman S, Thorburn DR. Leigh syndrome: One disorder, more than 75 monogenic causes. Ann Neurol 2016;79:190-203.
95. Schubert Baldo M, Vilarinho L. Molecular basis of Leigh syndrome: a current look. Orphanet J Rare Dis 2020;15:31.
96. Nikoskelainen EK, Marttila RJ, Huoponen K, et al. Leber's "plus": neurological abnormalities in patients with Leber's hereditary optic neuropathy. J Neurol Neurosurg Psychiatry 1995;59:160-164.
97. Balck A, Schaake S, Margolesky J, Domingo A, Klein C, Westenberger A. Reviewing the clinical and mutational spectrum of SLC20A2, PDGFB, PDGFRB, XPR1 and MYORG mutations in Primary Familial Brain Calcification (PFBC) for MDSGene. Movement Disord 2019;34:S166-S167.
98. Kobayashi T, Suzuki K. Chronic GM1 gangliosidosis presenting as dystonia: II. Biochemical studies. Ann Neurol 1981;9:476-483.
99. Goldman JE, Katz D, Rapin I, Purpura DP, Suzuki K. Chronic GM1 gangliosidosis presenting as dystonia: I. Clinical and pathological features. Ann Neurol 1981;9:465-475.
100. Pillai SH, Sundaram S, Zafer SM, Rajan R. Expanding the phenotypic spectrum of type III GM1 gangliosidosis: Progressive dystonia with auditory startle. Neurol India 2018;66:S149-S150.
101. Gordon BA, Gordon KE, Seo HC, Yang M, DiCioccio RA, O'Brien JS. Fucosidosis with dystonia. Neuropediatrics 1995;26:325-327.
102. Gautschi M, Merlini L, Calza AM, Hayflick S, Nuoffer JM, Fluss J. Late diagnosis of fucosidosis in a child with progressive fixed dystonia, bilateral pallidal lesions and red spots on the skin. Eur J Paediatr Neurol 2014;18:516-519.
103. Wali G, Wali GM, Sue CM, Kumar KR. A Novel Homozygous Mutation in the FUCA1 Gene Highlighting Fucosidosis as a Cause of Dystonia: Case Report and Literature Review. Neuropediatrics 2019;50:248-252.
104. Koens LH, Kuiper A, Coenen MA, et al. Ataxia, dystonia and myoclonus in adult patients with Niemann-Pick type C. Orphanet J Rare Dis 2016;11:121.

105. Steel D, Zech M, Zhao C, et al. Loss-of-Function Variants in HOPS Complex Genes VPS16 and VPS41 Cause Early Onset Dystonia Associated with Lysosomal Abnormalities. Ann Neurol 2020;88:867-877.
106. Sanderson LE, Lanko K, Alsagob M, et al. Bi-allelic variants in HOPS complex subunit VPS41 cause cerebellar ataxia and abnormal membrane trafficking. Brain 2021;144:769-780.
107. Haack TB, Ignatius E, Calvo-Garrido J, et al. Absence of the Autophagy Adaptor SQSTM1/p62 Causes Childhood-Onset Neurodegeneration with Ataxia, Dystonia, and Gaze Palsy. Am J Hum Genet 2016;99:735-743.
108. Marcogliese PC, Shashi V, Spillmann RC, et al. IRF2BPL Is Associated with Neurological Phenotypes. Am J Hum Genet 2018;103:456.
109. Ganos C, Zittel S, Hidding U, Funke C, Biskup S, Bhatia KP. IRF2BPL mutations cause autosomal dominant dystonia with anarthria, slow saccades and seizures. Parkinsonism Relat Disord 2019;68:57-59.
110. Prilop L, Buchert R, Woerz S, Gerloff C, Haack TB, Zittel S. IRF2BPL mutation causes nigrostriatal degeneration presenting with dystonia, spasticity and keratoconus. Parkinsonism Relat Disord 2020.
111. Ginevrino M, Battini R, Nuovo S, et al. A novel IRF2BPL truncating variant is associated with endolysosomal storage. Mol Biol Rep 2020;47:711-714.
112. Batla A, Tai XY, Schottlaender L, Erro R, Balint B, Bhatia KP. Deconstructing Fahr's disease/syndrome of brain calcification in the era of new genes. Parkinsonism Relat D 2017;37:1-10.
113. Chelban V, Carecchio M, Rea G, et al. MYORG-related disease is associated with central pontine calcifications and atypical parkinsonism. Neurol-Genet 2020;6.
114. Gregory A, Hayflick S. Neurodegeneration with Brain Iron Accumulation Disorders Overview. In: Adam MP, Ardinger HH, Pagon RA, et al., eds. GeneReviews((R)). Seattle (WA)1993.
115. Di Meo I, Tiranti V. Classification and molecular pathogenesis of NBIA syndromes. Eur J Paediatr Neurol 2018;22:272-284.
116. Schneider SA, Hardy J, Bhatia KP. Syndromes of neurodegeneration with brain iron accumulation (NBIA): an update on clinical presentations, histological and genetic underpinnings, and treatment considerations. Mov Disord 2012;27:42-53.
117. Pettersen EF, Goddard TD, Huang CC, et al. UCSF Chimera--a visualization system for exploratory research and analysis. J Comput Chem 2004;25:1605-1612.
118. Quadri M, Federico A, Zhao T, et al. Mutations in SLC30A10 cause parkinsonism and dystonia with hypermanganesemia, polycythemia, and chronic liver disease. Am J Hum Genet 2012;90:467-477.
119. Tuschl K, Clayton PT, Gospe SM, Jr., et al. Syndrome of hepatic cirrhosis, dystonia, polycythemia, and hypermanganesemia caused by mutations in SLC30A10, a manganese transporter in man. Am J Hum Genet 2012;90:457-466.
120. Tuschl K, Meyer E, Valdivia LE, et al. Mutations in SLC39A14 disrupt manganese homeostasis and cause childhood-onset parkinsonism-dystonia. Nat Commun 2016;7:11601.

121. Riley LG, Cowley MJ, Gayevskiy V, et al. A SLC39A8 variant causes manganese deficiency, and glycosylation and mitochondrial disorders. J Inherit Metab Dis 2017;40:261-269.
122. Wirth T, Tranchant C, Drouot N, et al. Increased diagnostic yield in complex dystonia through exome sequencing. Parkinsonism Relat Disord 2020;74:50-56.
123. van Egmond ME, Lugtenberg CHA, Brouwer OF, et al. A post hoc study on gene panel analysis for the diagnosis of dystonia. Mov Disord 2017;32:569-575.
124. Ma J, Wang L, Yang YM, Wan XH. Targeted gene capture sequencing in diagnosis of dystonia patients. J Neurol Sci 2018;390:36-41.
125. Powis Z, Towne MC, Hagman KDF, et al. Clinical diagnostic exome sequencing in dystonia: Genetic testing challenges for complex conditions. Clin Genet 2020;97:305-311.
126. Carecchio M, Invernizzi F, Gonzalez-Latapi P, et al. Frequency and phenotypic spectrum of KMT2B dystonia in childhood: A single-center cohort study. Mov Disord 2019;34:1516-1527.
127. Zech M, Boesch S, Jochim A, et al. Clinical exome sequencing in early-onset generalized dystonia and large-scale resequencing follow-up. Mov Disord 2017;32:549-559.
128. Zech M, Jech R, Wagner M, et al. Molecular diversity of combined and complex dystonia: insights from diagnostic exome sequencing. Neurogenetics 2017;18:195-205.
129. Montaut S, Tranchant C, Drouot N, et al. Assessment of a Targeted Gene Panel for Identification of Genes Associated With Movement Disorders. JAMA Neurol 2018;75:1234-1245.
130. Reale C, Panteghini C, Carecchio M, Garavaglia B. The relevance of gene panels in movement disorders diagnosis: A lab perspective. Eur J Paediatr Neurol 2018;22:285-291.
131. Kumar KR, Davis RL, Tchan MC, et al. Whole genome sequencing for the genetic diagnosis of heterogenous dystonia phenotypes. Parkinsonism Relat Disord 2019;69:111-118.
132. Li H, Durbin R. Fast and accurate short read alignment with Burrows-Wheeler transform. Bioinformatics 2009;25:1754-1760.
133. Van der Auwera GA, Carneiro MO, Hartl C, et al. From FastQ data to high confidence variant calls: the Genome Analysis Toolkit best practices pipeline. Curr Protoc Bioinformatics 2013;43:11 10 11-11 10 33.
134. McLaren W, Gil L, Hunt SE, et al. The Ensembl Variant Effect Predictor. Genome Biol 2016;17:122.
135. Koressaar T, Remm M. Enhancements and modifications of primer design program Primer3. Bioinformatics 2007;23:1289-1291.
136. Ye J, Coulouris G, Zaretskaya I, Cutcutache I, Rozen S, Madden TL. Primer-BLAST: a tool to design target-specific primers for polymerase chain reaction. BMC Bioinformatics 2012;13:134.
137. Auwera GAVD, O'Connor BD. GENOMICS IN THE CLOUD : using docker, gatk, and wdl in terra;using docker, gatk, and wdl in terra. [Place of publication not identified: O'REILLY MEDIA, INCORPORA, 2020.

138. Gregory A, Lotia M, Jeong SY, et al. Autosomal dominant mitochondrial membrane protein-associated neurodegeneration (MPAN). Mol Genet Genomic Med 2019;7:e00736.
139. Casey HL, Gomez CM. Spinocerebellar Ataxia Type 6. In: Adam MP, Ardinger HH, Pagon RA, et al., eds. GeneReviews((R)). Seattle (WA)1993.
140. Spacey S. Episodic Ataxia Type 2. In: Adam MP, Ardinger HH, Pagon RA, et al., eds. GeneReviews((R)). Seattle (WA)1993.
141. Jen JC. Familial Hemiplegic Migraine. In: Adam MP, Ardinger HH, Pagon RA, et al., eds. GeneReviews((R)). Seattle (WA)1993.
142. Giffin NJ, Benton S, Goadsby PJ. Benign paroxysmal torticollis of infancy: four new cases and linkage to CACNA1A mutation. Dev Med Child Neurol 2002;44:490-493.
143. Jiang X, Raju PK, D'Avanzo N, et al. Both gain-of-function and loss-of-function de novo CACNA1A mutations cause severe developmental epileptic encephalopathies in the spectrum of Lennox-Gastaut syndrome. Epilepsia 2019;60:1881-1894.
144. Molloy A, Kimmich O, Martindale J, Moore H, Hutchinson M, O'Riordan S. A novel CACNA1A mutation associated with adult-onset, paroxysmal head tremor. Movement disorders : official journal of the Movement Disorder Society 2013;28:842-843.
145. Wszolek Z, Konno T. Perry Syndrome. In: Adam MP, Ardinger HH, Pagon RA, et al., eds. GeneReviews((R)). Seattle (WA)1993.
146. Farrer MJ, Hulihan MM, Kachergus JM, et al. DCTN1 mutations in Perry syndrome. Nat Genet 2009;41:163-165.
147. Newsway V, Fish M, Rohrer JD, et al. Perry syndrome due to the DCTN1 G71R mutation: a distinctive levodopa responsive disorder with behavioral syndrome, vertical gaze palsy, and respiratory failure. Mov Disord 2010;25:767-770.
148. Mishima T, Fujioka S, Tomiyama H, et al. Establishing diagnostic criteria for Perry syndrome. J Neurol Neurosurg Psychiatry 2018;89:482-487.
149. Tacik P, Fiesel FC, Fujioka S, et al. Three families with Perry syndrome from distinct parts of the world. Parkinsonism Relat Disord 2014;20:884-888.
150. Grandy DK, Marchionni MA, Makam H, et al. Cloning of the cDNA and gene for a human D2 dopamine receptor. Proc Natl Acad Sci U S A 1989;86:9762-9766.
151. van der Weijden MCM, Rodriguez-Contreras D, Delnooz CCS, et al. A Gain-of-Function Variant in Dopamine D2 Receptor and Progressive Chorea and Dystonia Phenotype. Mov Disord 2021;36:729-739.
152. Madeira F, Park YM, Lee J, et al. The EMBL-EBI search and sequence analysis tools APIs in 2019. Nucleic Acids Res 2019;47:W636-W641.
153. Yin J, Chen KM, Clark MJ, et al. Structure of a D2 dopamine receptor-G-protein complex in a lipid membrane. Nature 2020;584:125-129.
154. Pu J, Schindler C, Jia R, Jarnik M, Backlund P, Bonifacino JS. BORC, a multisubunit complex that regulates lysosome positioning. Dev Cell 2015;33:176-188.

155. Rattay TW, Lindig T, Baets J, et al. FAHN/SPG35: a narrow phenotypic spectrum across disease classifications. Brain 2019;142:1561-1572.
156. Curtis AR, Fey C, Morris CM, et al. Mutation in the gene encoding ferritin light polypeptide causes dominant adult-onset basal ganglia disease. Nat Genet 2001;28:350-354.
157. Batla A, Adams ME, Erro R, et al. Cortical pencil lining in neuroferritinopathy: a diagnostic clue. Neurology 2015;84:1816-1818.
158. Ohta E, Takiyama Y. MRI findings in neuroferritinopathy. Neurol Res Int 2012;2012:197438.
159. Stepien KM, Ciara E, Jezela-Stanek A. Fucosidosis-Clinical Manifestation, Long-Term Outcomes, and Genetic Profile-Review and Case Series. Genes (Basel) 2020;11.
160. Henneke M, Combes P, Diekmann S, et al. GJA12 mutations are a rare cause of Pelizaeus-Merzbacher-like disease. Neurology 2008;70:748-754.
161. Yoshida K, Oshima A, Shimmoto M, et al. Human beta-galactosidase gene mutations in GM1-gangliosidosis: a common mutation among Japanese adult/chronic cases. Am J Hum Genet 1991;49:435-442.
162. Yoshida K, Oshima A, Sakuraba H, et al. GM1 gangliosidosis in adults: clinical and molecular analysis of 16 Japanese patients. Ann Neurol 1992;31:328-332.
163. Caciotti A, Garman SC, Rivera-Colon Y, et al. GM1 gangliosidosis and Morquio B disease: an update on genetic alterations and clinical findings. Biochim Biophys Acta 2011;1812:782-790.
164. Cif L, Demailly D, Lin JP, et al. KMT2B-related disorders: expansion of the phenotypic spectrum and long-term efficacy of deep brain stimulation. Brain 2020;143:3242-3261.
165. Bartsakoulia M, Pyle A, Troncoso-Chandia D, et al. A novel mechanism causing imbalance of mitochondrial fusion and fission in human myopathies. Hum Mol Genet 2018;27:1186-1195.
166. Rak M, Rustin P. Supernumerary subunits NDUFA3, NDUFA5 and NDUFA12 are required for the formation of the extramembrane arm of human mitochondrial complex I. FEBS Lett 2014;588:1832-1838.
167. Ostergaard E, Rodenburg RJ, van den Brand M, et al. Respiratory chain complex I deficiency due to NDUFA12 mutations as a new cause of Leigh syndrome. J Med Genet 2011;48:737-740.
168. Torraco A, Nasca A, Verrigni D, et al. Novel NDUFA12 variants are associated with isolated complex I defect and variable clinical manifestation. Hum Mutat 2021.
169. Speer RR, Ezeanya UC, Beaudoin SJ, Glass KM, Oji-Mmuo CN. Term Neonate Presenting with the Combined Occurrence of Mucolipidosis Type II and Leigh Syndrome. J Pediatr Genet 2020;9:137-141.
170. Mencacci NE, Brockmann MM, Dai J, et al. Biallelic variants in TSPOAP1, encoding the active-zone protein RIMBP1, cause autosomal recessive dystonia. J Clin Invest 2021;131.

171. Di Lazzaro G, Magrinelli F, Estevez-Fraga C, Valente EM, Pisani A, Bhatia KP. X-Linked Parkinsonism: Phenotypic and Genetic Heterogeneity. Mov Disord 2021.
172. Ferdinandusse S, Denis S, Clayton PT, et al. Mutations in the gene encoding peroxisomal alpha-methylacyl-CoA racemase cause adult-onset sensory motor neuropathy. Nat Genet 2000;24:188-191.
173. Ferdinandusse S, Kostopoulos P, Denis S, et al. Mutations in the gene encoding peroxisomal sterol carrier protein X (SCPx) cause leukencephalopathy with dystonia and motor neuropathy. Am J Hum Genet 2006;78:1046-1052.
174. Balint B, Damasio J, Magrinelli F, Guerreiro R, Bras J, Bhatia KP. Psychiatric Manifestations of ATP13A2 Mutations. Mov Disord Clin Pract 2020;7:838-841.
175. Ferreira C, Poretti A, Cohen J, Hamosh A, Naidu S. Novel TUBB4A mutations and expansion of the neuroimaging phenotype of hypomyelination with atrophy of the basal ganglia and cerebellum (H-ABC). Am J Med Genet A 2014;164A:1802-1807.
176. Alessenko AV, Albi E. Exploring Sphingolipid Implications in Neurodegeneration. Front Neurol 2020;11:437.
177. Plotegher N, Bubacco L, Greggio E, Civiero L. Ceramides in Parkinson's Disease: From Recent Evidence to New Hypotheses. Front Neurosci 2019;13:330.
178. Alecu I, Bennett SAL. Dysregulated Lipid Metabolism and Its Role in α-Synucleinopathy in Parkinson's Disease. Front Neurosci 2019;13:328.
179. Fanning S, Selkoe D, Dettmer U. Parkinson's disease: proteinopathy or lipidopathy? NPJ Parkinsons Dis 2020;6:3.
180. Burke JE, Dennis EA. Phospholipase A2 structure/function, mechanism, and signaling. J Lipid Res 2009;50 Suppl:S237-242.
181. Malley KR, Koroleva O, Miller I, et al. The structure of iPLA(2)β reveals dimeric active sites and suggests mechanisms of regulation and localization. Nat Commun 2018;9:765.
182. Kinghorn KJ, Castillo-Quan JI, Bartolome F, et al. Loss of PLA2G6 leads to elevated mitochondrial lipid peroxidation and mitochondrial dysfunction. Brain 2015;138:1801-1816.
183. Ong WY, Yeo JF, Ling SF, Farooqui AA. Distribution of calcium-independent phospholipase A2 (iPLA 2) in monkey brain. J Neurocytol 2005;34:447-458.
184. Lin G, Wang L, Marcogliese PC, Bellen HJ. Sphingolipids in the Pathogenesis of Parkinson's Disease and Parkinsonism. Trends Endocrinol Metab 2019;30:106-117.
185. Zhou Q, Yen A, Rymarczyk G, et al. Impairment of PARK14-dependent Ca(2+) signalling is a novel determinant of Parkinson's disease. Nat Commun 2016;7:10332.
186. Morgan NV, Westaway SK, Morton JE, et al. PLA2G6, encoding a phospholipase A2, is mutated in neurodegenerative disorders with high brain iron. Nat Genet 2006;38:752-754.
187. Gregory A, Westaway SK, Holm IE, et al. Neurodegeneration associated with genetic defects in phospholipase A(2). Neurology 2008;71:1402-1409.
188. Khateeb S, Flusser H, Ofir R, et al. PLA2G6 mutation underlies infantile neuroaxonal dystrophy. Am J Hum Genet 2006;79:942-948.

189. Kurian MA, Morgan NV, MacPherson L, et al. Phenotypic spectrum of neurodegeneration associated with mutations in the PLA2G6 gene (PLAN). Neurology 2008;70:1623-1629.
190. Illingworth MA, Meyer E, Chong WK, et al. PLA2G6-associated neurodegeneration (PLAN): further expansion of the clinical, radiological and mutation spectrum associated with infantile and atypical childhood-onset disease. Mol Genet Metab 2014;112:183-189.
191. Xie F, Cen Z, Ouyang Z, Wu S, Xiao J, Luo W. Homozygous p.D331Y mutation in PLA2G6 in two patients with pure autosomal-recessive early-onset parkinsonism: further evidence of a fourth phenotype of PLA2G6-associated neurodegeneration. Parkinsonism Relat Disord 2015;21:420-422.
192. Chu YT, Lin HY, Chen PL, Lin CH. Genotype-phenotype correlations of adult-onset PLA2G6-associated Neurodegeneration: case series and literature review. BMC Neurol 2020;20:101.
193. Ji Y, Li Y, Shi C, et al. Identification of a novel mutation in PLA2G6 gene and phenotypic heterogeneity analysis of PLA2G6-related neurodegeneration. Parkinsonism Relat Disord 2019;65:159-164.
194. Erro R, Balint B, Kurian MA, et al. Early Ataxia and Subsequent Parkinsonism: PLA2G6 Mutations Cause a Continuum Rather Than Three Discrete Phenotypes. Mov Disord Clin Pract 2017;4:125-128.
195. Koh K, Ichinose Y, Ishiura H, et al. PLA2G6-associated neurodegeneration presenting as a complicated form of hereditary spastic paraplegia. J Hum Genet 2019;64:55-59.
196. Park JK, Youn J, Cho JW. Intrafamilial variability and clinical heterogeneity in a family with PLA2G6-associated neurodegeneration. Precis Future Med 2019;3:135-138.
197. Gregory A, Kurian MA, Maher ER, Hogarth P, Hayflick SJ. PLA2G6-Associated Neurodegeneration. In: Adam MP, Ardinger HH, Pagon RA, et al., eds. GeneReviews((R)). Seattle (WA)1993.
198. Paisán-Ruiz C, Li A, Schneider SA, et al. Widespread Lewy body and tau accumulation in childhood and adult onset dystonia-parkinsonism cases with PLA2G6 mutations. Neurobiol Aging 2012;33:814-823.
199. Natural History of Infantile Neuroaxonal Dystrophy.
200. A Natural History Study of Infantile Neuroaxonal Dystrophy.
201. Iankova IK, I.; Klopstock, T.; Schneider, S.A. Emerging disease-modifying therapies in Neurodegeneration with Brain Iron Accumulation (NBIA) disorders. . Frontiers in Neurology In press.
202. Klopstock T, Tricta F, Neumayr L, et al. Safety and efficacy of deferiprone for pantothenate kinase-associated neurodegeneration: a randomised, double-blind, controlled trial and an open-label extension study. Lancet Neurol 2019;18:631-642.
203. Whaler S. Novel strategies in NBIA: a gene therapy approach for PLA2G6-associated neurodegeneration: University College London, Department of Pharmacology, 2018.

204. Paisán-Ruiz C, Guevara R, Federoff M, et al. Early-onset L-dopa-responsive parkinsonism with pyramidal signs due to ATP13A2, PLA2G6, FBXO7 and spatacsin mutations. Mov Disord 2010;25:1791-1800.
205. Agarwal P, Hogarth P, Hayflick S, et al. Imaging striatal dopaminergic function in phospholipase A2 group VI-related parkinsonism. Mov Disord 2012;27:1698-1699.
206. Kapoor S, Shah MH, Singh N, et al. Genetic Analysis of PLA2G6 in 22 Indian Families with Infantile Neuroaxonal Dystrophy, Atypical Late-Onset Neuroaxonal Dystrophy and Dystonia Parkinsonism Complex. PLoS One 2016;11:e0155605.
207. Salih MA, Mundwiller E, Khan AO, et al. New findings in a global approach to dissect the whole phenotype of PLA2G6 gene mutations. PLoS One 2013;8:e76831.
208. Khan AO, AlDrees A, Elmalik SA, et al. Ophthalmic features of PLA2G6-related paediatric neurodegeneration with brain iron accumulation. Br J Ophthalmol 2014;98:889-893.
209. Bohlega SA, Al-Mubarak BR, Alyemni EA, et al. Clinical heterogeneity of PLA2G6-related Parkinsonism: analysis of two Saudi families. BMC Res Notes 2016;9:295.
210. Virmani T, Thenganatt MA, Goldman JS, Kubisch C, Greene PE, Alcalay RN. Oculogyric crises induced by levodopa in PLA2G6 parkinsonism-dystonia. Parkinsonism Relat Disord 2014;20:245-247.
211. Karkheiran S, Shahidi GA, Walker RH, Paisán-Ruiz C. PLA2G6-associated Dystonia-Parkinsonism: Case Report and Literature Review. Tremor Other Hyperkinet Mov (N Y) 2015;5:317.
212. Davids M, Kane MS, He M, et al. Disruption of Golgi morphology and altered protein glycosylation in PLA2G6-associated neurodegeneration. J Med Genet 2016;53:180-189.
213. Blake RB, Gilbert DL, Schapiro MB. Child Neurology: Two sisters with dystonia and regression: PLA2G6-associated neurodegeneration. Neurology 2016;87:e1-3.
214. Darling A, Aguilera-Albesa S, Tello CA, et al. PLA2G6-associated neurodegeneration: New insights into brain abnormalities and disease progression. Parkinsonism Relat Disord 2019;61:179-186.
215. Chen YJ, Chen YC, Dong HL, et al. Novel PLA2G6 mutations and clinical heterogeneity in Chinese cases with phospholipase A2-associated neurodegeneration. Parkinsonism Relat Disord 2018;49:88-94.
216. Jansen AC-dG, C.; Vanderhasselt, T.; Seneca, S.; Stouffs, K.; De Meirleir, L. OP10 – 2707: Childhood-onset ataxic gait solved by muscle biopsy. European Journal of Paediatric Neurology 2015;19:S4.
217. Hoogwijs I. Diagnosing neurodegeneration with brain iron accumulation before iron starts to accumulate. Journal of the International Child Neurology Association 2019;1.
218. Ozes B, Karagoz N, Schüle R, et al. PLA2G6 mutations associated with a continuous clinical spectrum from neuroaxonal dystrophy to hereditary spastic paraplegia. Clin Genet 2017;92:534-539.

219. Giri A, Guven G, Hanagasi H, et al. PLA2G6 Mutations Related to Distinct Phenotypes: A New Case with Early-onset Parkinsonism. Tremor Other Hyperkinet Mov (N Y) 2016;6:363.
220. Sina F, Shojaee S, Elahi E, Paisán-Ruiz C. R632W mutation in PLA2G6 segregates with dystonia-parkinsonism in a consanguineous Iranian family. Eur J Neurol 2009;16:101-104.
221. Wu-Chou YHL, C. P3.153 PLA2G6 mutations in a Taiwanese cohort of early onset

parkinsonism. Parkinsonism Relat Disord 2009;15:1.
222. Yoshino H, Tomiyama H, Tachibana N, et al. Phenotypic spectrum of patients with PLA2G6 mutation and PARK14-linked parkinsonism. Neurology 2010;75:1356-1361.
223. Daida K, Nishioka K, Li Y, et al. PLA2G6 variants associated with the number of affected alleles in Parkinson's disease in Japan. Neurobiol Aging 2020.
224. Bower MA, Bushara K, Dempsey MA, Das S, Tuite PJ. Novel mutations in siblings with later-onset PLA2G6-associated neurodegeneration (PLAN). Mov Disord 2011;26:1768-1769.
225. Shi CH, Tang BS, Wang L, et al. PLA2G6 gene mutation in autosomal recessive early-onset parkinsonism in a Chinese cohort. Neurology 2011;77:75-81.
226. Yan XG, J.; Shi, C.; B. Tang. Novel PLA2G6 gene mutation is associated with autosomal recessive early-onset parkinsonism. Parkinsonism and Related Disorders 2012;18:S188.
227. Lu CS, Lai SC, Wu RM, et al. PLA2G6 mutations in PARK14-linked young-onset parkinsonism and sporadic Parkinson's disease. Am J Med Genet B Neuropsychiatr Genet 2012;159b:183-191.
228. Tofaris GK, Revesz T, Jacques TS, Papacostas S, Chataway J. Adult-onset neurodegeneration with brain iron accumulation and cortical alpha-synuclein and tau pathology: a distinct clinicopathological entity. Arch Neurol 2007;64:280-282.
229. Zhang P, Gao Z, Jiang Y, et al. Follow-up study of 25 Chinese children with PLA2G6-associated neurodegeneration. Eur J Neurol 2013;20:322-330.
230. Malaguti MC, Melzi V, Di Giacopo R, et al. A novel homozygous PLA2G6 mutation causes dystonia-parkinsonism. Parkinsonism Relat Disord 2015;21:337-339.
231. Kim YJ, Lyoo CH, Hong S, Kim NY, Lee MS. Neuroimaging studies and whole exome sequencing of PLA2G6-associated neurodegeneration in a family with intrafamilial phenotypic heterogeneity. Parkinsonism Relat Disord 2015;21:402-406.
232. Klein C, Lochte T, Delamonte SM, et al. PLA2G6 mutations and Parkinsonism: Long-term follow-up of clinical features and neuropathology. Mov Disord 2016;31:1927-1929.
233. Tabamo RE, Fernandez HH, Friedman JH, Simon DK. Young-onset Parkinson's disease: a clinical pathologic description of two siblings. Mov Disord 2000;15:744-746.
234. Choi AN. NOVEL COMPOUND HETEROZYGOUS MUTATIONS OF PLA2G6 IN A

KOREAN PEDIGREE OF YOUNG-ONSET PARKINSON'S DISEASE: A

STUDY OF WHOLE GENOME SEQUENCING.
235. Yamashita C, Funayama M, Li Y, et al. Mutation screening of PLA2G6 in Japanese patients with early onset dystonia-parkinsonism. J Neural Transm (Vienna) 2017;124:431-435.
236. Michelis JP, Hattingen E, Gaertner FC, et al. Expanded phenotype and hippocampal involvement in a novel compound heterozygosity of adult PLA2G6 associated neurodegeneration (PARK14). Parkinsonism Relat Disord 2017;37:111-113.
237. Wirth T, Weibel S, Montaut S, et al. Severe early-onset impulsive compulsive behavior and psychosis in PLA2G6-related juvenile Parkinson's disease. Parkinsonism Relat Disord 2017;41:127-129.
238. Rohani M, Shahidi G, Vali F, et al. Oculogyric crises in PLA2G6 associated neurodegeneration. Parkinsonism Relat Disord 2018;52:111-112.
239. Huang MH, Chiu YC, Tsai CF. Aripiprazole in a Patient of PLA2G6-Associated Neurodegeneration With Psychosis. Clin Neuropharmacol 2018;41:136-137.
240. Kamel WA, Al-Hashel JY, Abdulsalam AJ, Damier P, Al-Mejalhem AY. PLA2G6-related parkinsonism presenting as adolescent behavior. Acta Neurol Belg 2019;119:621-622.
241. Shen T, Hu J, Jiang Y, et al. Early-Onset Parkinson's Disease Caused by PLA2G6 Compound Heterozygous Mutation, a Case Report and Literature Review. Front Neurol 2019;10:915.
242. Lin CH, Chen PL, Tai CH, et al. A clinical and genetic study of early-onset and familial parkinsonism in taiwan: An integrated approach combining gene dosage analysis and next-generation sequencing. Mov Disord 2019;34:506-515.
243. Sachan D, Yadav A, Yadav D. PLA2G6-Associated Dystonia Parkinsonism. Indian Pediatr 2021;58:77-78.
244. Shen T, Pu J, Lai HY, et al. Genetic analysis of ATP13A2, PLA2G6 and FBXO7 in a cohort of Chinese patients with early-onset Parkinson's disease. Sci Rep 2018;8:14028.
245. Koh K, Ichinose Y, Ishiura H, et al. PLA2G6-associated neurodegeneration presenting as a complicated form of hereditary spastic paraplegia. J Hum Genet 2019;64:55-59.
246. Olivola S, Xodo S, Olivola E, Cecchini F, Londero AP, Driul L. Parkinson's Disease in Pregnancy: A Case Report and Review of the Literature. Front Neurol 2019;10:1349.
247. Elia AE, Del Sorbo F, Romito LM, Barzaghi C, Garavaglia B, Albanese A. Isolated limb dystonia as presenting feature of Parkin disease. Journal of neurology, neurosurgery, and psychiatry 2014;85:827-828.
248. Barow E, Schneider SA, Bhatia KP, Ganos C. Oculogyric crises: Etiology, pathophysiology and therapeutic approaches. Parkinsonism Relat Disord 2017;36:3-9.
249. Darling A, Tello C, Marti MJ, et al. Clinical rating scale for pantothenate kinase-associated neurodegeneration: A pilot study. Movement disorders : official journal of the Movement Disorder Society 2017;32:1620-1630.

250. Gregory A, Kurian MA, Maher ER, Hogarth P, Hayflick SJ. PLA2G6-Associated Neurodegeneration. In: Adam MP, Ardinger HH, Pagon RA, et al., eds. GeneReviews(®). Seattle (WA): University of Washington, Seattle

251. Engel LA, Jing Z, O'Brien DE, Sun M, Kotzbauer PT. Catalytic function of PLA2G6 is impaired by mutations associated with infantile neuroaxonal dystrophy but not dystonia-parkinsonism. PLoS One 2010;5:e12897.